GEOLOGICAL SETTING OF THE HEDLEY GOLD SKARN CAMP WITH SPECIFIC REFERENCE TO THE FRENCH MINE, SOUTH-CENTRAL BRITISH COLUMBIA

by

GARNET LINN DAWSON

B.Sc., The University of Manitoba, 1981

A THESIS SUBMITTED IN PARTIAL FULFILLMENT OF

THE REQUIREMENTS FOR THE DEGREE OF

MASTER OF SCIENCE

in

THE FACULTY OF GRADUATE STUDIES

(Department of Geological Sciences)

We accept this thesis as conforming

to the required standard:

THE UNIVERSITY OF BRITISH COLUMBIA

July 1994

In presenting this thesis in partial fulfillment of the requirements for an advanced degree at the University of British Columbia, I agree that the Library shall make it freely available for reference and study. I further agree that permission for extensive copying of this thesis for scholarly purposes may be granted by the head of my department or by his or her representatives. It is understood that copying or publication of this thesis for financial gain shall not be allowed without my written permission.

(Signature)

Department of Geological Sciences

The University of British Columbia
Vancouver, Canada

Date September 21, 1994

ABSTRACT

The Hedley gold skarn camp in south-central British Columbia is the second largest gold producer in the province. From the period 1902 to 1955 about 51 million grams (1.6 million ounces) of gold were produced from four gold bearing skarn deposits; over 95% of this came from the Nickel Plate and Mascot mines that mined underground a large skarn deposit centered on Nickel Plate Mountain. The Nickel Plate deposit was reopened in 1987 as a large tonnage, low grade open pit deposit; from 1987 to the end of 1993, 18.6 million grams (0.54 million ounces) of gold were recovered from 7 236 430 tonnes milled. The French mine produced 1.36 million grams of gold from 69 508 tonnes of ore during the periods 1950 to 1955, 1957 to 1961, and in 1983.

The camp is underlain predominantly by the sedimentary facies of the Late Triassic Nicola Group that unconformably overlies more deformed oceanic rocks of the middle to late Paleozoic Apex Mountain complex. The sedimentary facies of the Nicola Group is subdivided into four sedimentary and one volcaniclastic formation that were deposited in a north trending, westward deepening, fault controlled basin along the eastern margin of the main Nicola arc in Quesnellia. They are represented by: (i) siltstones and thick limestones as the shallow water Hedley formation, (ii) siltstones and thin limestones as the intermediate depth Chuchuwayha formation, and (iii) argillite and rare limestone as the deeper water Stemwinder formation. Collapse of this basin is marked by deposition of the Copperfield breccia, which separates the Hedley, Chuchuwayha and Stemwinder formations from the overlying volcaniclastics of the Whistle formation. The Copperfield breccia is a limestone breccia that represents a catastrophic massive gravity slide deposit derived from uplifted and faulted reef material with a provenance to the east. The overlying Whistle formation forms an extensive unit that grades from thinly laminated tuffaceous siltstones at its base to massive alkalic and subalkalic intermediate to mafic ash. Three periods of calcalkaline intrusive activity and associated mineralization recognized are: (i) Late Triassic Hedley intrusions (gold skarn), (ii) Early Jurassic Bromley batholith - Mount Riordan stock (minor W-Cu and industrial garnet skarns), and (iii) Middle Jurassic Cahill Creek pluton (minor W-Mo porphyry and skarn), Lookout Ridge pluton and rhyolite porphyry dykes.

Hedley intrusions form a texturally diverse suite of intermediate to mafic calcalkaline dykes, sills and stocks that are spatially and temporally associated with gold skarn mineralization. Features such as wavy sill contacts, destruction of sedimentary structures, peperite, quench textures, sedimentary dykes, and preliminary U-Pb zircon dates suggest that they preferentially intruded unconsolidated to poorly consolidated siltstone between beds of lithified limestone in the Hedley formation. Implications of this synsedimentary sill interpretation are: (i) contemporaneous sedimentation and intrusive volcanism, (ii) an extensional setting, and (iii) a shallow depth of intrusion and associated skarn formation. In addition, this interpretation helps to explain and integrate the lithologic, stratigraphic and structural controls to gold skarn mineralization in the camp.

At the French mine gold-arsenopyrite-telluride mineralization is associated with skarn zones on both sides of limestone - biotitic aphyric intrusion contacts. The skarn displays consistent mineralogical zoning from (i) biotitic aphyric intrusion, (ii) orthoclase (endoskarn), (iii) Mg-rich clinopyroxene (endoskarn), (iv) Fe-rich clinopyroxene (endoskarn and exoskarn spanning the aphyric - limestone contact) and (vi) Fe-rich garnet (exoskarn). Quartz, calcite, vesuvianite, scapolite, arsenopyrite, Cu and Fe sulphides, tellurides and associated gold occur in microfractures and vugs between the iron-rich garnet $\pm$ pyroxene skarn. This mineralogical zoning is complicated locally by crosscutting hydrothermal overprinting. Late stage, retrograde alteration is limited, and is represented by minor replacement of garnet and clinopyroxene by chlorite $\pm$ actinolite $\pm$ titanite $\pm$ epidote.

TABLE OF CONTENTS

LIST OF TABLES

Page

LIST OF FIGURES

Page

LIST OF PLATES

Page

ACKNOWLEDGMENTS

I would like to thank those from the Department of Geological Sciences, The University of British Columbia (UBC), from the British Columbia Geological Survey Branch (BCGS) of the B.C. Ministry of Energy, Mines and Petroleum Resources and from industry that I have come in contact with over the last few years who have generously shared their ideas and time with me. In particular, I would like to thank Dr. Gerry Ray (BCGS) and Dr. Colin Godwin (UBC). Much of the data and many of the ideas presented here were a result of a regional mapping program I had the opportunity to work on with Gerry. Colin supervised, edited and re-edited my thesis and put up with my antics over the too long period it took to finish this project. I would also like to thank Anne Pickering and Ian Webster for help in and out of the field, Janet Gabites, Peter van der Hayden and Don Murphy for the U-Pb zircon analyses, and Matti Raudsepp for the electron microprobe analyses. My friends Craig, Andy, Wendy and Tracy are thanked for offering welcome diversions and getting me through those angst ridden times. Finally, I would like to thank my parents for their unconditional support and encouragement.

Field and financial support for this study was generously provided by International Corona Corporation (now Homestake Canada Inc.), British Columbia Geological Survey Branch of the B.C. Ministry of Energy, Mines and Petroleum Resources, A.E. Aho Scholarship and a G.R.E.A.T Award from the Science Counsil of B.C. Cambria Geological Ltd. provide a place from which to work and use of software and plotting equipment during writing.

GEOLOGICAL SETTING OF THE HEDLEY GOLD SKARN CAMP WITH SPECIFIC REFERENCE TO THE FRENCH MINE, SOUTH-CENTRAL BRITISH COLUMBIA

CHAPTER 1.0 INTRODUCTION

Hedley gold camp in south-central British Columbia is 240 km east of Vancouver and 40 km southeast of Princeton (inset, Fig. 1.1; NTS Maps 92H/8E and 82E/5W; centered near 49^{o} 21' N, 120^{o} 05' W). Access is by a number of gravel roads off Highway 3, which passes through the middle of the study area.

The camp is the second largest gold producer in the province and the largest gold skarn in Canada. From the period 1902 to 1955 about 51 million grams of gold were produced from four gold bearing skarn deposits (Table 1.1, Fig. 1.1). Over 95% of this came from the Nickel Plate and Mascot mines, which worked a large skarn deposit centered on Nickel Plate mountain. Early studies of these deposits include: Camsell (1910), Warren and Cummings (1936), Warren and Peacock (1945), Billingsley and Hume (1941), Dolmage and Brown (1945), Lee (1951) and Lamb *et al.* (1957). Bostock (1930, 1940a, 1940b) completed the first regional mapping of the camp.

Renewed interest in the Nickel Plate deposit took place in the early 1980's following increased gold prices (Simpson and Ray, 1986). The Nickel Plate mine was reopened by Mascot Gold Mines Limited (now Corona Corporation) in August 1987 as a large tonnage low grade open pit gold deposit. Metals recovered from 1987 to 1990 total 7 145 kg of gold and 7 168 kg of silver (Table 1.1). Ettlinger *et al.* (1992) examined skarn evolution and hydrothermal characteristics of the Nickel Plate deposit.

The geology, geochemistry and structural setting of the Hedley gold skarns were recently examined by the British Colombia Geological Survey Branch (Ray *et al.*, 1986, 1987, 1988, 1993; Ray and Dawson, 1994). This work is summarized in Chapter 3.0.

Table 1.1: Production of gold, silver and copper from skarn deposits, Hedley area, south-central British Columbia

Deposit	Ore milled (tonnes)	Gold (kg)	Silver (kg)	Copper (tonnes)	Reference[1]
Nickel Plate 1904-1963	2 983 900	41 706	4 161	981	a
Nickel Plate 1987-1993	7 236 358	18 571	NA	NA	b
Hedley Mascot 1936-1949	619 019	6 937	1 707	NA	a
Nickel Plate total	10 839 277	67 214	5 868	981	a, b
French 1950-1955	29 450	786	NA	NA	a
French 1957-1961	35 620	550	45	NA	a
French 1982-1983	4 438	26	135	20	a
French total	69 508	1 362	180	20	a

1. References: a = BCEMPR MINFILE; b = Homestake Canada Inc. (Greg Lang, written communication, 1994); c = National Mineral Inventory (NMI 92H/8-Au3).

Table 1.1: Production of gold, silver and copper from skarn deposits, Hedley area, south-central British Columbia (continued)....

Deposit	Ore milled (tonnes)	Gold (kg)	Silver (kg)	Copper (tonnes)	Reference[1]
Canty 1939-41	1 493	16	NA	NA	a
Good Hope 1946-1948	4 241	89	NA	NA	c
Good Hope 1982	6 847	77	119	0.6	a
Good Hope total	11 115	166	119	0.6	a, c
TOTAL:	**10 921 393**	**68 758**	**6 167**	**1 001.6**	**a, b, c**

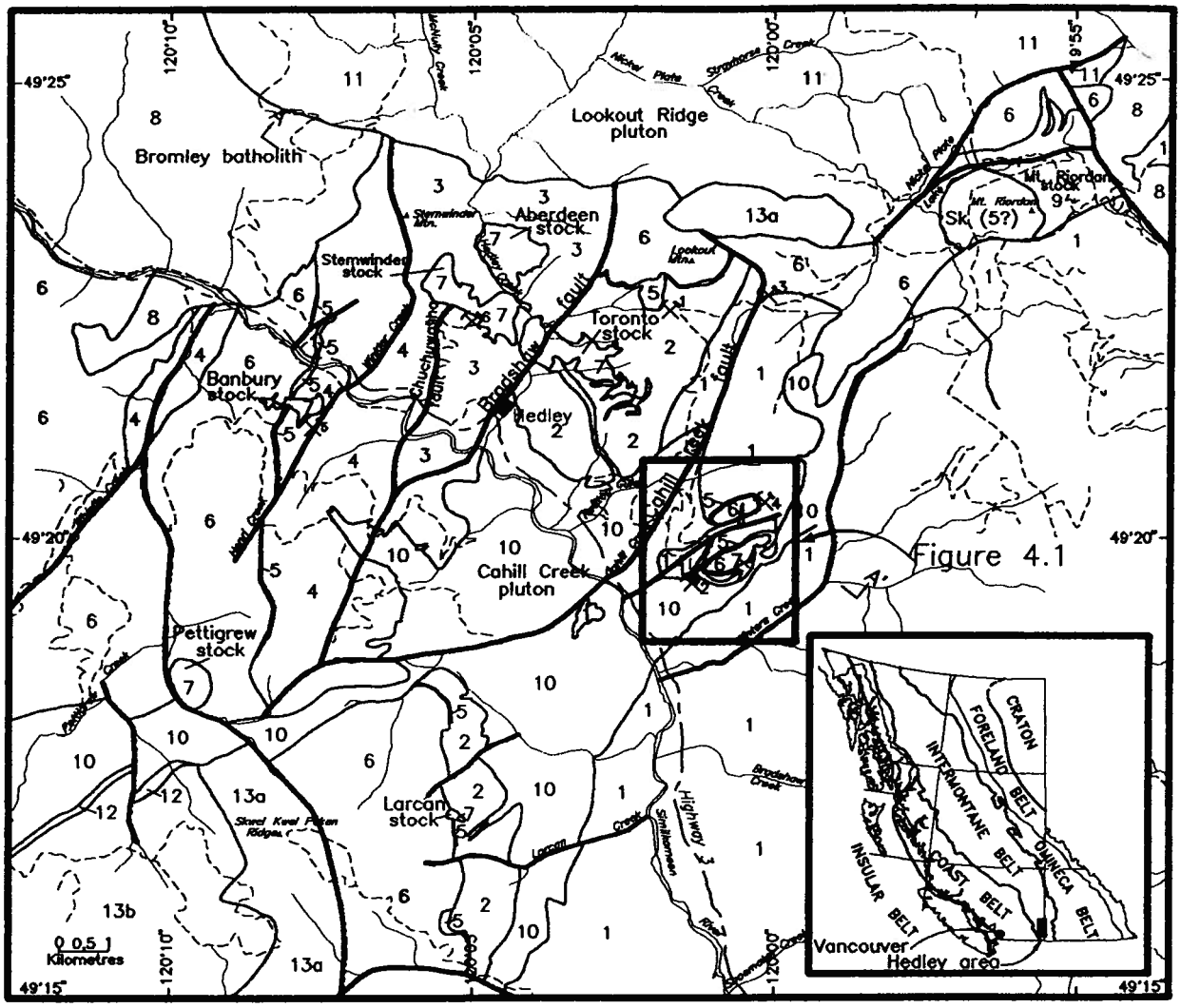

Figure 1.1: Regional geology of the Hedley gold skarn camp, south-central British Columbia (modified from Ray *et al.*, 1988). Sills and dykes are not shown at this scale. Inset map shows Hedley camp to be in the Intermontane Belt (Monger *et al.*, 1982). Map units are: 1 = Apex Mountain complex, 2 = Hedley formation, 3 = Chuchuwayha formation, 4 = Stemwinder formation, 5 = Copperfield breccia, 6 = Whistle formation, 7 = Hedley intrusions, 8 = Bromley batholith, 9 = Mount Riordan stock, 10 = Cahill Creek pluton, 11 = Lookout Ridge pluton, 12 = Rhyolite porphyry, 13a = Skwel Peken formation (lower felsic unit), 13b = Skwel Peken formation (upper intermediate unit). Mineral deposits (crossed shovel and pick) are: 1 = Nickel Plate mine, 2 = French mine, 3 = Canty mine, 4 = Good Hope mine, 5 = Banbury mine, 6 = Peggy mine. Line types are: thick continuous = faults, medium continuous = geological contacts, thin continuous = rivers, long-short dash = Highway 3, short dash = gravel roads.

CHAPTER 2.0 REGIONAL GEOLOGY

Hedley gold camp lies within Quesnellia in the Intermontane Belt of the Canadian Cordillera (inset, Fig. 1.1). Quesnellia, an accreted terrane, comprises Paleozoic to Jurassic marine volcanic and sedimentary rocks, and comagmatic intrusions formed in island arc and marginal basin environments (Monger *et al.*, 1982). In southern British Columbia, the Late Triassic Nicola Group lies west of, and rests with depositional unconformity on, the deformed Paleozoic Harper Ranch Group (Monger, 1985). The Harper Ranch Group is correlative with the Apex Mountain complex in the Hedley area (Milford, 1984).

Late Triassic subduction of the Pennsylvanian to Triassic Cache Creek Group resulted in initiation of the Nicola arc (Monger, 1985). Rocks of this arc are dominantly Late Triassic Nicola Group, which has been divided into three volcanic facies and one sedimentary facies (Preto, 1979; Monger, 1985, 1989; Mortimer, 1987).

The sedimentary facies in the Hedley area, however, probably formed in a back-arc basin east of this arc (Monger, 1985). Sedimentary rocks consist of Upper Triassic Carnian to Norian clastic sediments, limestone and tuff. They are intruded by synsedimentary sills, dykes and stocks.

CHAPTER 3.0 GEOLOGY OF THE HEDLEY GOLD SKARN CAMP

3.1 Introduction

Hedley gold camp is underlain by middle to late Paleozoic Apex Mountain complex, sedimentary facies of the Late Triassic Nicola Group, and Middle Jurassic Skwel Peken formation. Late Triassic to Tertiary intrusive rocks ranging from gabbro to rhyolite have intruded the above section (Fig. 1.1). Table 3.1 outlines the stratigraphic names used here. These names are related to those in Ray and Dawson (1994).

Whole rock compositions (53 samples) of intrusive and extrusive rocks were measured to classify them chemically and compare their trends to those in known tectonic settings. Tables C.1 and C.2 presents major, minor and trace element chemistry along with their calculated CIPW (Cross, Iddings, Pirsson and Washington) normative mineralogy. Sample locations are plotted on Figure 3.1.

Conodonts extracted from limestone units in the Nicola Group and the underlying Apex Mountain complex constrain the age of the various sedimentary units. Samples, located on Figure 3.1, were identified by M.J. Orchard and E.C. Prosh (written communications, 1988), Geological Survey of Canada (Table A.1).

U-Pb analyses of zircons from four intrusive rocks and one volcanic rock (Table B.1; located in Fig. 3.1), and previously published K-Ar (biotite, hornblende and amphibole) and U-Pb (zircon) analyses (Table B.2; located in Fig. 3.1) constrain the timing of magmatic events in the Hedley area. U-Pb data in Table B.1 are plotted on concordia diagrams (Fig. 3.10).

Lead isotope analyses of galena from three samples within the Nickel Plate open pit are in Table B.3 and plotted on conventional Pb-isotope diagrams in Figure 3.16. These data, compared to three samples from the Copper Mountain copper-gold porphyry gold deposit, help constrain the origin of hydrothermal fluids responsible for gold skarn mineralization.

Table 3.1: Table of formations relating the different useage of lithologic and formational names in the Hedley area, south-central British Columbia. Fossil ages and radiometric dates are listed and referenced in Tables A.1, B.1 and B.2.

	Ray and Dawson (1994) (Bulletin 87)	This paper (see Fig. 1.1)	Date [1] or Age[2]
Middle Jurassic (163 - 187 Ma)	Unit 15: Skwel Peken formation	Unit 13: Skwel Peken formation	< 187 ± 9 Ma[z] (Fig. 3.10f) - Allenian or younger
		----------Intrusive Contact----------	
	Unit 14: Quartz porphyry	Unit 12: Rhyolite porphyry	154.5 + 8/-43 Ma[z] (Fig. 3.10e) - Kimmeridgian
	Unit 13: Lookout Ridge pluton	Unit 11: Lookout Ridge pluton	164.5 ± 4.8 Ma[b] (Table B.2) - Callovian
	Unit 12: Cahill Creek pluton	Unit 10: Cahill Creek pluton	168.8 ± 9.3 Ma[z] (Fig. 3.10d) - Bathonian 159.9 ± 2.9 to 174.5 ± 5.2 Ma[h] (Table B.2) - Oxfordian to Bathonian 153.4 ± 4.6 to 161.3 ± 3.4 Ma[b] (Table B.2) - Kimmeridgian to Oxfordian
		----------Intrusive Contact----------	
Early Jurassic (187 - 208 Ma)	Unit 11: Mount Riordan stock	Unit 9: Mount Riordan stock	194.6 ± 1.2 Ma[z] (Fig. 3.10c) - Pliensbachian
	Unit 10: Bromley batholith	Unit 8: Bromley batholith	193.0 ± 1.0 Ma[z] (Table B.2) - Toarcian to Pliensbachian 185.7 ± 2.8 to 188.1 ± 5.8 Ma[h] (Table B.2) - Allenian to Toarcian 173.4 ± 4.7 to 180.9 ± 5.4 Ma[b] (Table B.2) - Batholnian to Bajocian
		----------Intrusive Contact----------	
Late Triassic (208-230 Ma)	Unit 9: Hedley intrusions	Unit 7: Hedley intrusions	< 215.4 ± 4 Ma[z] (Fig. 3.10b) - Norian or younger 175.0 ± 5.4 to 195.0 ± 9.0 Ma[a] (Table B.2) - Batholnian to Pliensbachian
		----------Intrusive Contact----------	

1. [z] = U-Pb zircon analysis; [h] = K-Ar hornblende analysis; [b] = K-Ar biotite analysis; [a] = K-Ar amphibole analysis; [f] = fossil.
2. Time scale used is after Armstrong *et al.*, 1988.

Table 3.1: Table of formations relating the different useage of lithologic and formational names in the Hedley area, south-central British Columbia (continued)....

	Ray and Dawson (1994) (Bulletin 87)	This paper (see Fig. 1.1)	Date [1] or Age[2]
	Unit 7: Whistle formation	Unit 6: Whistle formation	
	Unit 3: French Mine formation	Unit 5: Copperfield breccia	Late Carnian to Early Norian[f] (Table A.1)
	Unit 5: Stemwinder formation	Unit 4: Stemwinder formation	Late Carnian to Late Norian[f] (Table A.1)
	Unit 6: Chuchuwayha formation	Unit 3: Chuchuwayha formation	Early to Middle Norian[f] (Table A.1)
	Unit 4: Hedley formation	Unit 2: Hedley formation	Early to Middle Norian[f] (Table A.1)
		----------Unconformity ?----------	
Middle to Late Paleozoic	Unit 8: Uncertain position	Unit 1: Apex Mountain complex	Ordovician, Early to Late Devonian, Middle to Late Triassic[f] (Table A.1)
	Unit 2: Oregon Claims formation		
	Unit 1: Apex Mountain complex		

3.2 Apex Mountain complex (unit 1)

The Middle to Late Paleozoic Apex Mountain complex rocks (unit 1: Table 3.1) are the oldest and most strongly deformed in the Hedley area. They crop out (Fig. 1.1) along and east of Cahill Creek north of the Similkameen River, east of the Cahill Creek pluton south of the Similkameen River, and in a small fault slice west of the Bradshaw fault. The complex consists of: (i) mafic volcaniclastic rocks, (ii) thin bedded siltstone, (iii) limestone, (iv) argillite, (v) chert, and (vi) greenstone.

Mafic volcaniclastic rocks are exposed (Fig. 1.1) east of the Nickel Plate mine along Cahill Creek, in the vicinity of the Good Hope and French mines, and in a small exposure west of the Bradshaw fault. This unit consists of massive to weakly laminated dark green to black ash tuff with lesser amounts of lapilli tuff. In areas of poor exposure, these tuffs are difficult to distinguish from tuffs in the younger Whistle formation. However, tuffs in the Apex Mountain complex are darker, and contain rare grains of mosaic quartz and local interbeds of chert pebble conglomerate. The tuffs have a crystal assemblage of hornblende (<10 mm), augite (<1 mm) and plagioclase (<4 mm) within an ash matrix. Lapilli are mainly homolithic, but rare clasts of limestone and chert occur.

Thin bedded siltstone is associated with minor argillite and rare chert pebble conglomerate. It crop out (Fig. 1.1) northwest of Winters Creek and west of the Similkameen River. The siltstones consist of broken and rounded grains of mosaic quartz and feldspar, with minor clay, sericite, chlorite, titanite and opaque minerals. Near the contact of the Cahill Creek pluton these sedimentary rocks are locally hornfelsed to biotite + cordierite + muscovite + garnet. Subparallel alignment of red biotite and muscovite in argillaceous layers impart a moderate foliation.

Limestone is relatively rare but widespread throughout the Apex Mountain complex. It occurs as disrupted blocks or as thin horizons within mafic volcaniclastic rocks west of the French mine (Fig. 1.1). The disrupted blocks are <10 m in diameter and probably olistoliths. Bedding in the fine grained mafic volcaniclastic rocks that surround these blocks is often contorted; this suggests the tuffs were unconsolidated when the limestone blocks were deposited. Thicker limestone units occur north of the mouth of Winters Creek, and between Larcan and Paul Creek south of the Similkameen River. The

limestone north of Winters Creek forms a large cliff that is recrystallized to marble, locally contains skarn and is malachite stained. South of the Similkameen River the limestone, also recrystallized to marble, is up to 60 m thick and traceable for over 1 km along strike. Fossils from limestone beds throughout the stratigraphy [based on limited sampling during this study (Table A.1, Fig. 3.1) and previous work (Milford, 1984)] were Ordovician, Early to Late Devonian, Carboniferous and Middle to Late Triassic. Rocks in the western part of the complex are younger, but structurally underlie older rocks in the east (Milford, 1984).

Argillite is massive to weakly foliated. It crops out east of Winters creek. This unit contains minor interbeds of siltstone and rare beds of chert.

Chert occurs predominantly south of Bradshaw Creek where it is interbedded with greenstone. In thin section it consists of fine grained quartz with minor tremolite-actinolite, chlorite, biotite, epidote, titanite, carbonate, plagioclase and opaques.

Greenstone forms discontinuous units up to 100 m thick throughout the complex, and as thicker bodies at the headwaters of Bradshaw Creek where they are intimately associated with coarse grained hornblende gabbro and diorite. From thin sections, the hornblende phenocrysts (<1 cm) are partially replaced by chlorite, tremolite-actinolite and minor biotite. The altered matrix consists of plagioclase, chlorite, epidote, biotite, sericite, carbonate, titanite, rutile and opaque minerals.

3.3 Nicola Group (units 2 to 6)

Sedimentary facies of the Late Triassic Nicola Group can be divided informally into four sedimentary units--Hedley formation, Chuchuwayha formation, Stemwinder formation and Copperfield breccia--and the volcaniclastic Whistle formation. The shallow water Hedley formation, the intermediate depth Chuchuwayha formation and the deep water Stemwinder formation are facies equivalents, representing deposition across a westerly sloping and fault controlled basin margin. Nicola Group unconformably overlies the Apex Mountain complex elsewhere in southern British Columbia. However, in

the Hedley area the relationship at this contact is not everywhere clear as it is commonly faulted, intruded by the Cahill Creek pluton, or poorly exposed. Collapse of the basin in Late Triassic time is marked by deposition of the Copperfield breccia followed by volcaniclastic and pyroclastic deposits of the Whistle formation.

Hedley formation (unit 2) is best exposed north of the Similkameen River, between the Bradshaw and Cahill Creek faults, where it is at least 500 m thick (Fig. 1.1). East of the Cahill Creek fault, the unit abruptly thins to less than 50 m thick where it is preserved at the Good Hope and French mines. South of the Similkameen River, the unit is bounded by the Bradshaw fault or overlain by the Whistle formation (western map area of Fig. 1.1), and intruded by the Cahill Creek pluton (eastern map area).

The formation comprises a mixed sequence of clastic sedimentary rocks and limestone. Finely laminated white to beige siltstones are interbedded with minor black argillite that locally display graded beds, scour and fill structures, and flames and cross-bedding that indicate deposition by westerly directed paleocurrents. Laminated to massive beds of white to grey limestone are generally <10 m thick and form both continuous and discontinuous horizons within the siltstones. Some beds, such as the Sunnyside limestone described by Bostock (1930), are up to 75 m thick and can be followed along strike for over 1 km. Diagenesis and metamorphism have destroyed many of the primary textures and structures in the limestones making interpretation of their depositional environment difficult. Some beds locally contain crinoid ossicles, solitary corals, bivalve fragments and belemnites. Conodonts from limestones in this unit are Late Triassic and Early to Middle Norian (Table A.1, Fig. 3.1). Interbedded polymictic conglomerate, grit and limestone crop out near the base of the Hedley formation along the southeast slope of Nickel Plate mountain. This conglomerate has a maximum thickness of 100 m and can be followed along strike for 1 km. It contains subrounded, pebble sized clasts of grey to cream coloured chert and minor limestone, volcanic, argillite and siltstone within a silty calcareous matrix. This unit may represent a fan deposit developed along the edge of the Cahill Creek normal fault. Tuffaceous horizons occur near the top of the formation close to the contact with the overlying Whistle formation.

Chuchuwayha formation (unit 3) forms a wedge shaped unit bounded by the Chuchuwayha fault to the west and the Bradshaw fault to the east (Fig. 1.1). The northern part of this unit is intruded by the Lookout Ridge pluton. The unit is a minimum of 1 500 m thick.

This formation consists of thin bedded, pale calcareous siltstone, minor black argillite and grey impure limestone, and rare chert pebble conglomerate. The formation resembles Hedley formation, but lacks thick and extensive limestone beds. Limestone beds in the Chuchuwayha formation are generally less than 5 m thick and often have graded beds containing chert clasts, broken bivalve shells and crinoid ossicles. Conodonts from these limestone beds are Late Triassic and range from Early to Middle Norian (Table A.1, Fig. 3.1).

Stemwinder formation (unit 4) is bounded by the Chuchuwayha fault to the east, intruded by the Bromley batholith and Lookout Ridge pluton to the north, and by a tongue of the Cahill Creek pluton to the south (Fig. 1.1). Western exposures are overlain by the Whistle formation. The bottom of the Stemwinder formation is not exposed, however the unit is a minimum of 1 500 m thick.

The formation consists of thinly bedded black calcareous argillite, lesser amounts of pale calcareous siltstone, and minor dark grey to black impure limestone. A number of sedimentary structures--such as overturned flames, cross-bedding and scour and fill textures preserved in the finely laminated sediments--indicate deposition by westerly directed paleocurrents. Rare limestone beds, up to 3 m in thickness, often contain graded chert pebbles. Conodonts from these limestone beds are Late Triassic and range from Late Carnian to Late Norian (Table A.1, Fig. 3.1). Rare andesite ash tuff occurs near the top of formation close to the contact with the overlying Whistle formation.

Copperfield breccia (unit 5) often forms a coherent but discontinuous stratigraphic unit. Locally it forms several horizons separated by tuffaceous sediments. The unit varies from less than 15 to 200 m in thickness. It is well exposed 4.3 km west of Hedley, south of the Larcan stock, and in the vicinity of the Nickel Plate, Good Hope and French mines (Fig. 1.1). This unit was first described by Bostock (1930) and thought to be a tectonic breccia related to a subsidiary splay of the nearby Bradshaw thrust fault (Billingsley and Hume, 1941).

Limestone clasts within a calcareous tuffaceous matrix characterize the Copperfield breccia (Plate 3.1). The clasts are angular to rounded, poorly sorted, boulder to pebble sized, and mainly limestone. Bivalves and conodonts from a limestone clast were Late Triassic and range from Late Carnian to Early Norian (Table A.1, Fig. 3.1). Minor clasts include: argillite, siltstone, chert, and felsic to intermediate volcanic and intrusive rocks. The matrix consists of fine grained carbonate, chert, limestone, siltstone and tuff.

Whistle formation (unit 6) is widespread throughout the Hedley map area (Fig. 1.1). It consists of thinly bedded tuffaceous siltstone and argillite near its base, but grades up section into massive green andesitic ash and lapilli tuff, and minor breccia. The unit is a minimum of 1 000 m thick and usually is separated from underlying formations--Hedley, Chuchuwayha and Stemwinder--by the Copperfield breccia.

Thin bedded tuffaceous siltstone and argillite overly the Copperfield breccia. Individual beds are often graded with sharp feldspar rich bases and diffuse argillaceous tops. Rare cross-bedding and oblique flame structures indicate initial sedimentation in the Whistle formation was by westerly directed turbidity currents, similar to the underlying formations. Higher in the stratigraphy, the thin bedded tuffaceous sediment are intercalated with massive to weakly bedded ash tuff. These units gradually grade upwards into ash, lapilli and tuff breccia, which probably represent water settled pyroclastic fall deposits (Cas and Wright, 1987).

Most of these ash tuffs contain a crystal assemblage of plagioclase (An_{40}), augite and rare hornblende within a fine grained tuffaceous matrix (Plate 3.2). Plagioclase crystals (<2 mm) are subhedral to euhedral and display reverse oscillatory zoning. Augite crystals are subhedral to euhedral (<1 mm). Accessory and trace minerals include quartz, chlorite, carbonate, epidote, titanite and opaque minerals.

Lapilli tuff and minor tuff breccia form extensive, massive units (Plate 3.3). Clasts are mostly rounded to angular and andesite to basalt in composition. Rare clasts of dacite, siltstone and limestone occur.

Whole rock analyses of ash tuff from the Whistle formation are mainly basalt with some bordering the andesite fields of the TAS (total alkalis *vs.* silica) diagram in Figure 3.2 (Cox *et al.*, 1979).

Plate 3.1: Copperfield breccia of angular to rounded clasts of limestone in a limey-tuffaceous matrix (unit 5: Fig. 1.1). Outcrop is along Whistle Creek road, 4 km west of Hedley township.

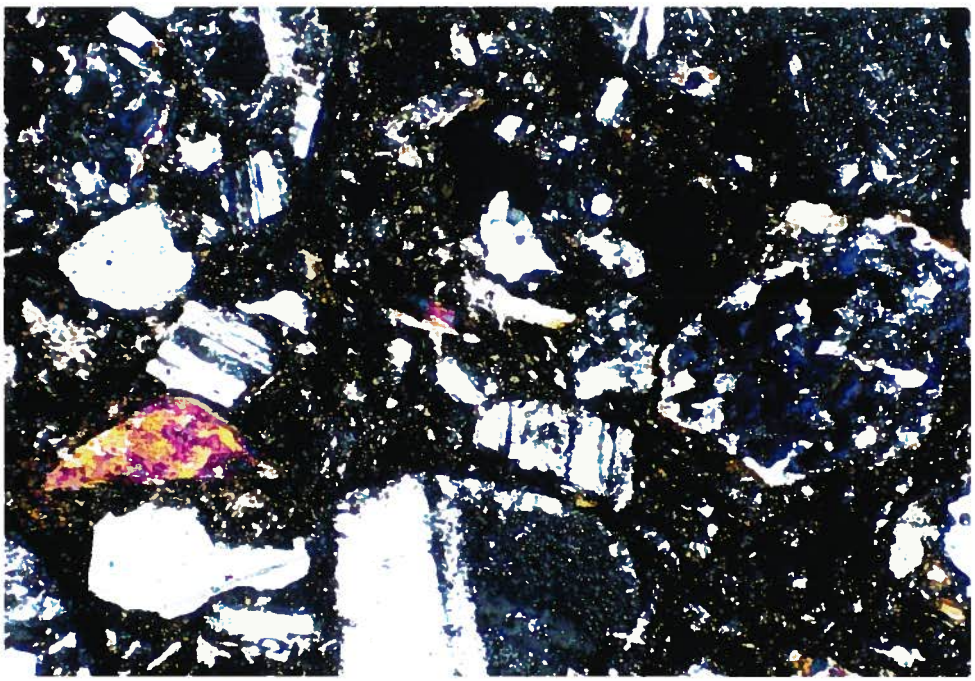

Plate 3.2: Photomicrograph (transmitted light, crossed polars, field of view = 1.25 mm) of plagioclase-augite phyric andesite tuff, Whistle formation (unit 6: Fig. 1.1).

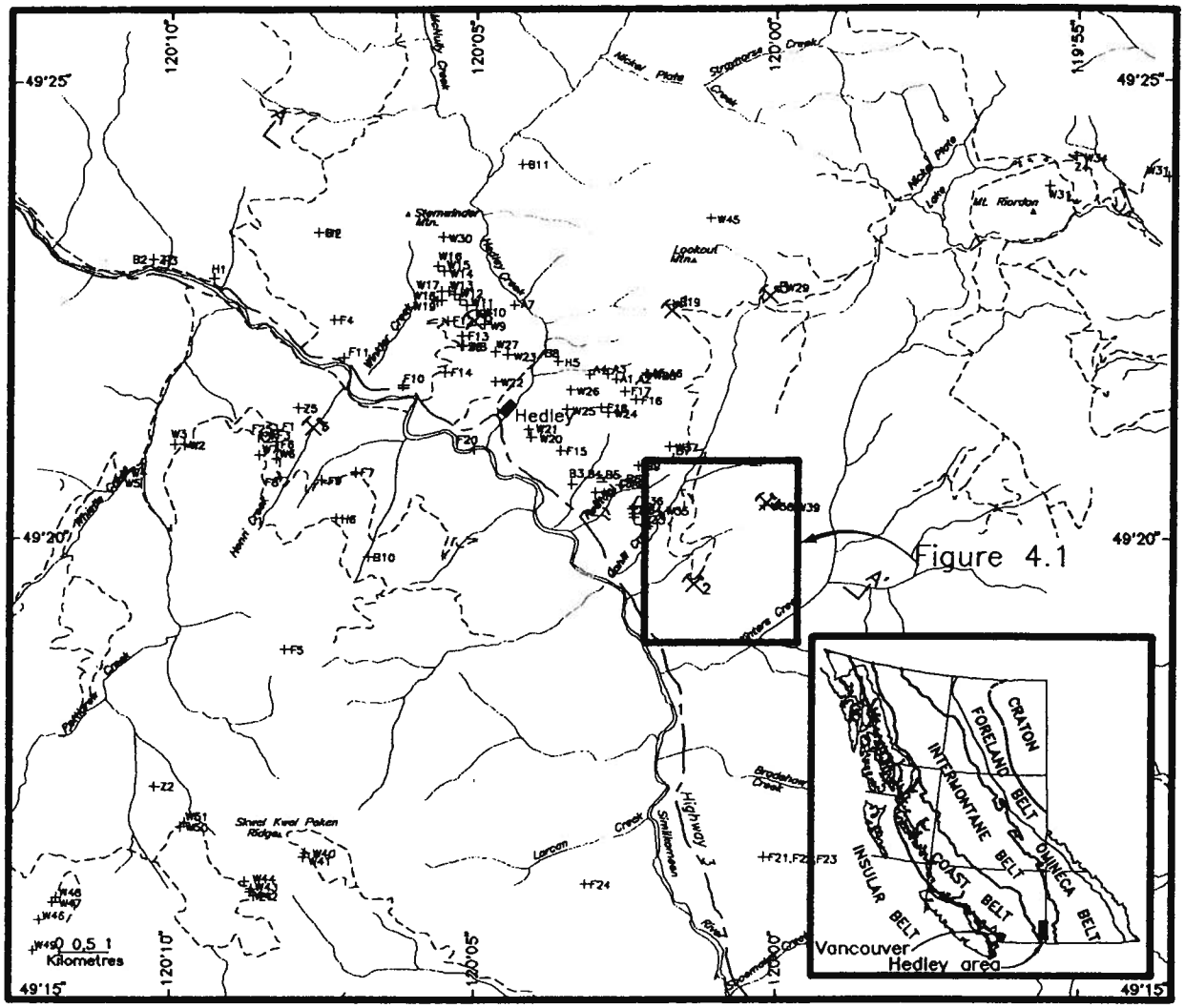

Figure 3.1: Sample locations are plotted for: whole rock chemical analyses (W: Table C.1 and C.2), microfossils (F: Table A.1), zircon U-Pb dates (Z: Table B.1, Fig. 3.10), biotite K-Ar dates (B: Table B.2), hornblende K-Ar dates (H: Table B.2), amphibole K-Ar dates (A: Table B.2), and mineral deposits (crossed shovel and pick: 1 = Nickel Plate mine, 2 = French mine, 3 = Canty mine, 4 = Good Hope mine, 5 = Banbury mine, 6 = Peggy mine). Line types are: thin continuous = rivers, long-short dash = Highway 3, short dash = gravel roads.

Plate 3.3: Whistle formation andesite lapilli tuff containing clasts of hornblende phyric andesite-basalt (unit 6: Fig. 1.1). Outcrop is along the Whistle Creek road, 4 km west of Hedley township.

Plate 3.4: Photomicrograph (transmitted light, crossed polars, field of view = 5.0 mm) of plagioclase-hornblende phyric quartz diorite of the Stemwinder pluton. Plagioclase and poikolitic hornblende crystals are strongly zoned (unit 7: Fig. 1.1).

They span the alkalic and subalkalic boundary on the TAS diagram in Figure 3.3 (Irvine and Baragar, 1971). The subalkalic samples plot in the calcalkaline field on a AFM (total alkali, total iron, magnesium) diagram in Figure 3.4 (Irvine and Baragar, 1971).

Relatively immobile trace element plots do not clearly define the tectonic environment of these rocks. On the Ti/100 - Zr - Y*3 diagram in Figure 3.5 (Pearce and Cann, 1973) the samples plot mainly in the IAB (island arc basalt) field. On the Nb*2 - Zr/4 - Y diagram of Figure 3.6 (Meschede, 1986) the samples plot mainly in the N- MORB (mid-ocean ridge basalt, normal-type) field; one analysis plots on the border of the P-MORB field (mid-ocean ridge basalt, plume-type). However, the rocks are enriched in LILE (large ion lithophile elements: Sr, K, Rb, Ba and Th) similar to modern calcalkaline island arcs (Fig. 3.7: Pearce, 1983). This LILE enrichment can reflect contributions from the subduction zone to the mantle wedge during magma generation (Wilson, 1989). Most of the immobile elements (*e.g.* Nb, Zr, Ti and Y) have low values of about 1 that consequently parallel MORB trends. This indicates that the immobile elements were not markedly modified by subduction processes.

3.4 Hedley intrusions (unit 7)

Hedley intrusions (unit 7) form dykes, sills and stocks that intrude the Nicola Group and the underlying Apex Mountain complex. The Aberdeen, Stemwinder, Toronto, Banbury, Pettigrew and Larcan stocks (Fig. 1.1) form elongate to round bodies that follow east-west to northwest trending fractures. The stocks, equigranular in texture, are quartz diorite to gabbro in composition. They are hornblende, plagioclase and rarely augite phyric in a fine grained quartzo-feldspathic groundmass. Dykes and sills have a similar composition to the stocks, but are markedly porphyritic. Dykes, rare compared to sills, mostly follow west-northwest fractures (similar to the stocks). Sills are best developed within the Hedley formation and are spatially and temporally associated with gold skarn mineralization. The Stemwinder and Toronto stocks, and the associated sill complex exposed on Nickel Plate mountain, are described below.

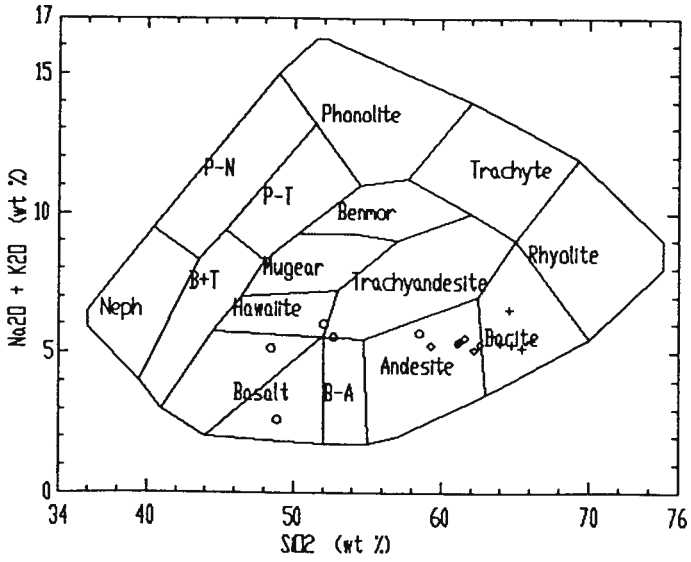

Figure 3.2: Total alkali *vs.* silica diagram (TAS: compositional fields defined by Cox *et al.*, 1979) with plot of volcanic rocks from the Hedley area, south-central British Columbia. Circles = Whistle formation tuffs (mainly basalt); crosses = Skwel Peken formation (lower unit tuffs: dacite); diamonds = Skwel Peken formation (upper unit tuffs: andesite).

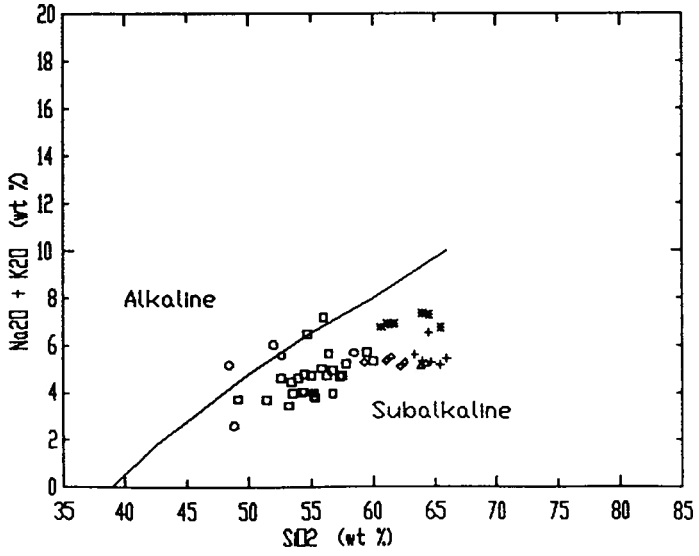

Figure 3.3: Total alkali *vs.* silica plot (TAS: Irvine and Baragar, 1971) of rocks from the Hedley area, south-central British Columbia. Circles = Whistle formation tuffs; squares = Hedley intrusions; triangles = Mount Riordan stock; asterisks = Cahill Creek pluton; crosses = Skwel Peken formation (lower unit tuffs); diamonds = Skwel Peken formation (upper unit tuffs). Samples are dominantly subalkaline.

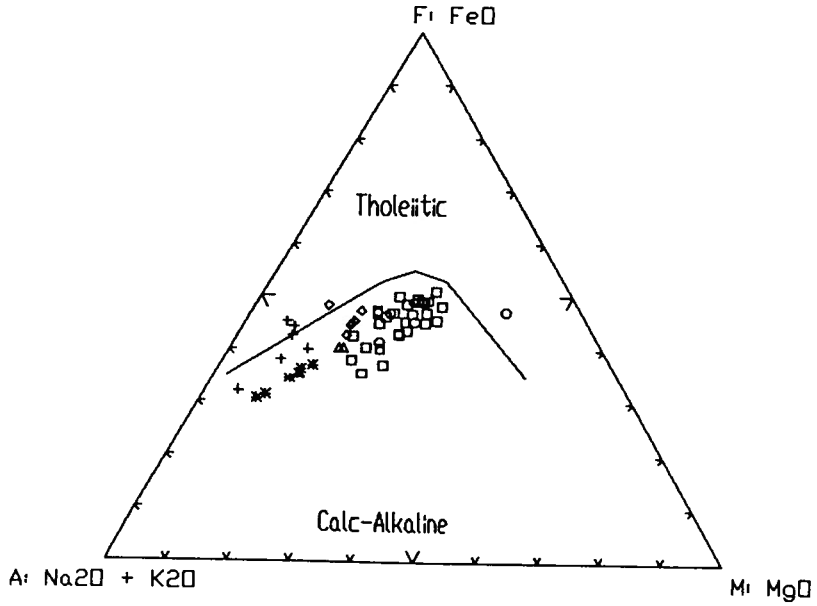

Figure 3.4: Total alkali, total iron, magnesium diagram (AFM: Irvine and Baragar, 1971) of subalkalic rocks from the Hedley area, south-central British Columbia. Circles = Whistle formation tuffs; squares = Hedley intrusions; triangles = Mount Riordan stock; asterisks = Cahill Creek pluton; crosses = Skwel Peken formation (lower unit tuffs); diamonds = Skwel Peken formation (upper unit tuffs). Samples are dominantly calcalkaline.

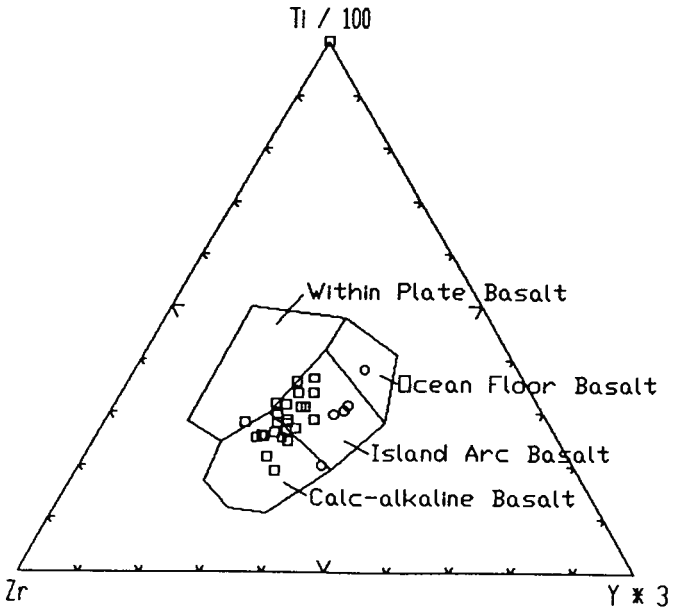

Figure 3.5: Titanium, zirconium, yttrium diagram (Pearce and Cann, 1973) of rocks from the Hedley area, south-central British Columbia. Circles = Whistle formation tuffs; squares = Hedley intrusions. Most analyses are compatible with an origin within an island arc. One sample of Whistle formation plots within an ocean floor environment, indicating that it may be more 'primitive'.

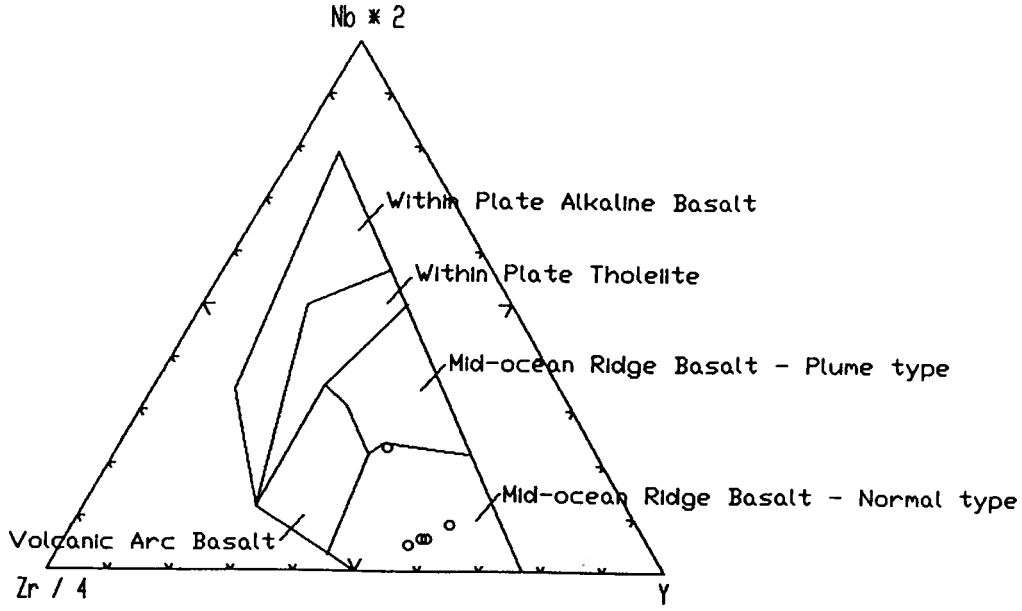

Figure 3.6: Niobium, zirconium, yttrium plot (Nb*2 - Zr/4 - Y: Meschede, 1986) of rocks from the Hedley area, south-central British Columbia. Circles = Whistle formation tuffs. The primitive 'nature' of Whistle formation noted in Figure 3.5, is clear by its plotted position within the field for mid-ocean ridge basalt of the normal type. Note that on this diagram it does not look like it has volcanic arc characteristics. Thus, it may have a marginal basin affinity.

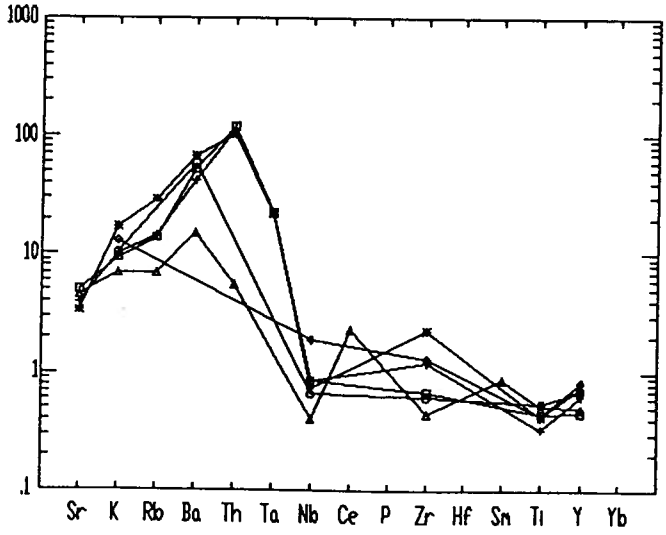

Figure 3.7: MORB normalized (see Pearce, 1983, for normalizing factors) trace element plot of rocks from the Hedley area, south-central British Columbia compared to modern day calcalkaline island-arc basalts (triangle = data from Sun, 1980). Circles = Whistle formation tuffs; squares = Hedley intrusions; asterisks = Cahill Creek pluton; crosses = Skwel Peken formation (lower unit tuffs); diamonds = Skwel Peken formation (upper unit tuffs). Note common enrichment in LILE (large ion lithophile elements: Sr to Th).

Stemwinder stock, about 2 km north of Hedley township (Fig. 1.1), forms a subhorizontal body 2 km long by <1 km wide that is elongate in a west-northwest direction. The mainly quartz diorite stock is massive, medium grained and equigranular to weakly porphyritic. It consists of plagioclase (An_{35}), hornblende, microcline, orthoclase, quartz and minor augite (Plate 3.4). Plagioclase crystals are subhedral to euhedral (<4 mm) and show normal and reverse oscillatory zoning. The poikilitic hornblende crystals are subhedral to euhedral (<3 mm). Rare augite phenocrysts are anhedral to subhedral (<1 mm) and are partly replaced by hornblende. Accessory minerals include titanite, apatite, zircon and opaque minerals.

Toronto stock, about 2 km northeast of Hedley township (Fig. 1.1), forms a subhorizontal body 1.5 km long by 500 m wide that is elongate in a west-northwest direction. It is not known whether the stock is: (i) a composite body comprised of numerous dykes that fed the nearby sills, or (ii) one large body with numerous apophyses that formed sills in the adjacent sediments. The former interpretation is preferred. Limited access to the area around the Toronto stock (because of active mining) prevented detailed mapping, however Bostock (1929) traced several sills back to their source in the stock.

The stock is a massive, medium grained, equigranular quartz diorite. It consists of hornblende, plagioclase (An_{40}), orthoclase, quartz and rarely augite. Hornblende crystals are euhedral (<5 mm) and poikilitic. Plagioclase crystals are subhedral to euhedral (<4 mm) and show reverse oscillatory zoning. Accessory and trace minerals include: biotite, zircon, apatite, titanite and opaques.

A colour, compositional and textural zoning in the stock was recognized by Dolmage and Brown (1945). The lower exposed part of the stock consists of dark equigranular quartz diorite. An intermediate zone consists of augite diorite, and an upper zone is a pale hornblende porphyritic gabbroic phase. However, the pale colour and porphyritic nature of the upper part of the stock is a result of groundmass replacement by fine grained orthoclase, albite and quartz during skarn alteration (Plate 3.5). In addition, much of the pyroxene in the upper part of the stock appears to be secondary replacement of hornblende.

Plate 3.5: Bleached hornblende phyric quartz diorite cut by fractures with calcite + garnet + pyroxene envelopes (unit 7: Toronto stock, Fig 1.1). Outcrop is along Princeton portal road, Nickel Plate mountain.

Plate 3.6: Nickel Plate sill complex (unit 7) intruding limestones and siltstones of the Hedley formation (unit 2: Fig. 1.1). Note that the sills (brown) are thin where the limestones and siltstones (grey) are thinly bedded (middle-right of photograph) and thick where the limestones and siltstones are thickly bedded (middle of photograph). Photograph was taken looking north from Highway 3, one kilometre east of Hedley township.

Nickel Plate sill complex is exposed over a vertical distance of 1 000 m on the cliffs 1 km east of Hedley township (Fig. 1.1, Plate 3.6). At this locality, the sills vary from <1 to 75 m in thickness, are traceable along strike for over 2 km and comprise up to 40% of the stratigraphy. Because of its banded appearance the mountain was called 'kyish-ming' (banded) by the natives and 'Striped Mountain' by Dawson (1877). The striped appearance is caused by rusty weathering dark brown sills separated by grey limestones and siliciclastics. In thinly bedded mixed limestone and siltstone sections, the sills are generally numerous and thin (1 to 5 m). In thicker limestone units they are less frequent and much thicker (>50 m). Individual sills vary from flat planar sheets to bodies that pinch, swell and bifurcate. They often thicken where they step across (probably up) stratigraphy. Sill contacts vary from straight to irregular (Plate 3.7), gradational and are brecciated rarely (Plate 3.8). Dolmage and Brown (1945) describe some gabbro contacts as gradational because it is locally difficult to define a precise contact between the intrusion and sediment. They attributed the gabbro composition and gradational contacts to assimilation of limey sediments by quartz diorite. Brecciated contacts are infrequent, but were observed by most of the earlier workers. Camsell (1910) describes short intervals along intrusion margins where the intrusion and siliciclastics are mixed or gradational making it difficult to place a contact over a few metres. Similar gradational contacts, described by Billingsley and Hume (1941), underlie the base of the 'Upper Purple' ore in the Nickel Plate mine. They described quartz diorite porphyry underlying the southern part of the ore zone that grades into a fine grained breccia in the central part. The breccia consists of fine grained chert (siliciclastics) in a groundmass of fine grained secondary quartz that is intrusive in nature, sending off numerous apophyses across and along bedding. These gradational contacts, described by the above previous workers, are interpreted to be related to synsedimentary sill intrusion (see peperitic margins below). A brecciated contact observed along the Princeton portal road (this study) consists of rusty weathering quartz diorite clasts (< 1 to 50 cm) hosted in siltstones of the Hedley formation up to 2 m from the sill contact. This brecciated contact and those described by previous workers are interpreted as peperite (see Section 4.3.3). Cooling joints perpendicular to sill contacts locally are developed within the sills (Plate 3.9).

Plate 3.7: Hedley quartz diorite sill (unit 7) intruded into limestone of the Hedley formation (unit 2: Fig. 1.1). Note irregular wavy contact of sill. Outcrop is along the Princeton portal road, Nickel Plate mountain.

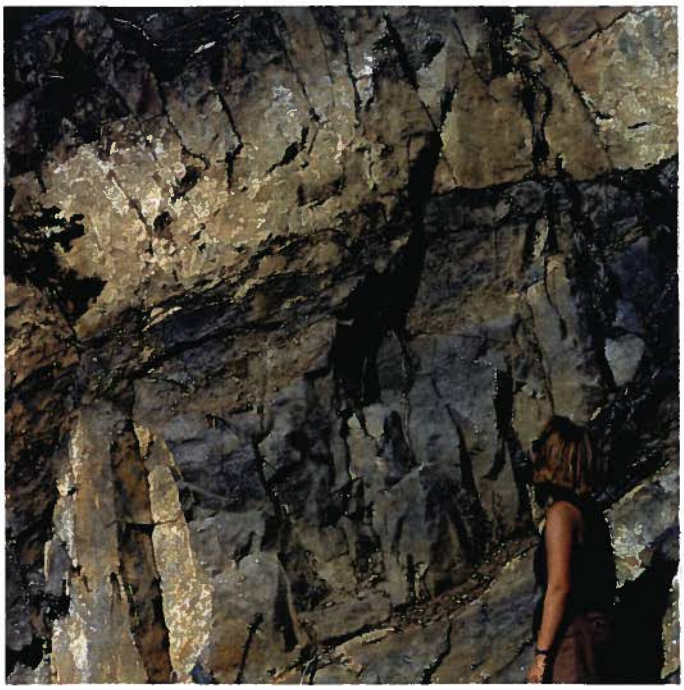

Plate 3.8: Hedley quartz diorite sill (unit 7) in siltstones and limestone of the Hedley formation (unit 2: Fig. 1.1). Note the bleached white clasts of Hedley quartz diorite (globular peperite) within grey limestone near the sill contact. Outcrop is along the Princeton portal road, Nickel Plate mountain.

Plate 3.9: Hedley quartz diorite sill (unit 7) in siltstone and limestone of the Hedley formation (unit 2, Fig. 1.1). Cooling joints perpendicular to sill contacts are prominent. Outcrop is along the Princeton portal road, Nickel Plate mountain.

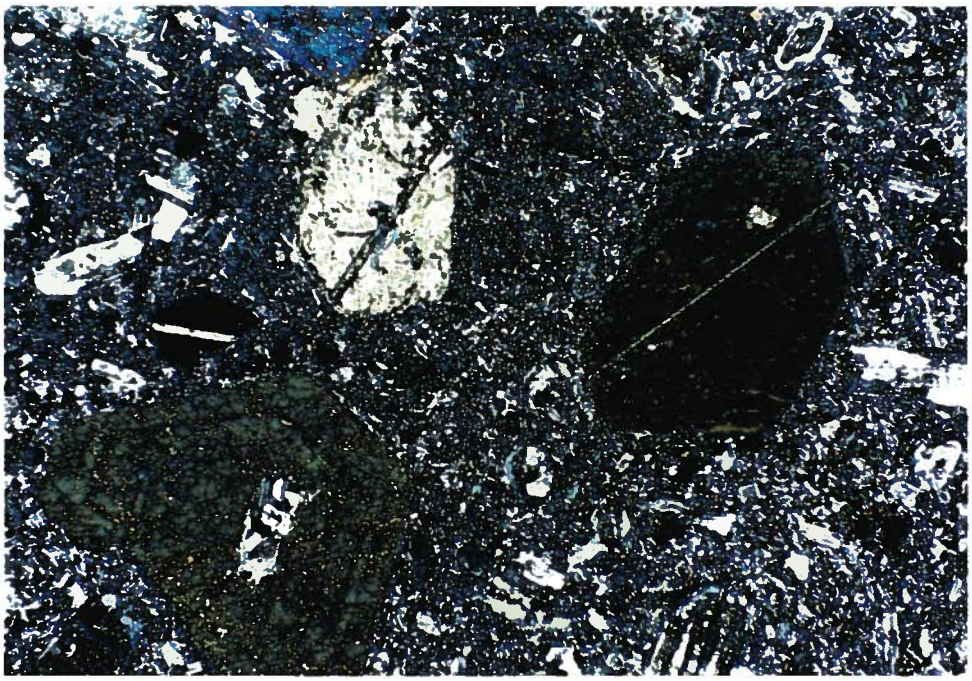

Plate 3.10: Photomicrograph (transmitted light, crossed polars, field of view = 5.0 mm) of hornblende porphyritic Hedley diorite sill (unit 7: Fig. 1.1). Hornblende crystals are zoned.

The sills consist of hornblende (± augite) and plagioclase porphyritic quartz diorite. The poikilitic hornblende crystals are euhedral (<5 mm) and zoned (Plate 3.10). The plagioclase (An_{40}) is subhedral to euhedral (<3 mm) and normally zoned. Rare augite crystals are <2 mm in diameter. The groundmass consists of a fine grained intergrowth of plagioclase with minor quartz, microcline and orthoclase. Accessory minerals include titanite, carbonate and opaques. Opaque minerals include pyrite, ilmenite, magnetite, pyrrhotite and arsenopyrite.

Samples from the Hedley intrusions on a normative mineralogy diagram (Fig. 3.8: Streckeisen and Lemaitre, 1979) vary from quartz diorite to gabbro. They also plot mainly in the quartz diorite field on a TAS diagram (Fig. 3.9: Middlemost, 1985) and are generally subalkalic, although two samples plotted in the alkaline field (Fig. 3.3). The subalkalic samples, all calcalkaline when plotted on a AFM diagram, show a depletion in iron typical of calcalkaline differentiation (Fig. 3.4).

Subvolcanic rocks are plotted on tectonic discrimination diagrams constructed for volcanic rocks in Figures 3.5 and 3.7. On Figure 3.5 (Ti/100 - Zr - Y*3) the data plots in both the island arc basalt and calcalkaline basalt fields. These rocks are similar to those from modern day calcalkaline island arcs when plotted on a spiderdiagram plot (Fig. 3.7; Sun, 1980).

U-Pb analysis of zircon from the Hedley intrusive suite (Fig. 3.1: sample Hd-81 and Hd-273; Table B.1) gave inconclusive ages due to lead loss and lead inheritance. One sample collected from the Toronto stock contained insufficient zircon for analysis. Four fractions obtained from the Stemwinder stock (sample Hd-81) were inconclusive due to combined lead loss and inheritance of Paleozoic or older zircon (Table B.1, Fig. 3.10a). If the intrusion is Triassic or younger, a three stage lead evolution is implied by the old $^{207}Pb/^{206}Pb$ ages. The intrusion is most likely between 175 ± 0.6 Ma (youngest $^{206}Pb/^{238}U$ age) and 219 ± 11 Ma ($^{207}Pb/^{206}Pb$ age of most concordant fraction). Sample Hd-273 from the relatively mafic quartz diorite phase of the Banbury stock gave a maximum age of 215.4 ± 4.0 Ma (J. Gabites, written communication, 1993) based on five fractions. This age is given by the upper intercept of an isochron (least squares regression) that passed through zero and the two non-magnetic fractions ('a' and 'b') that show the least inheritance (Table B.1, Fig. 3.10b). Two fine magnetic fractions ('d' and 'e') plot below concordia indicating inheritance of Cambrian or older zircon as well as lead loss. This suite

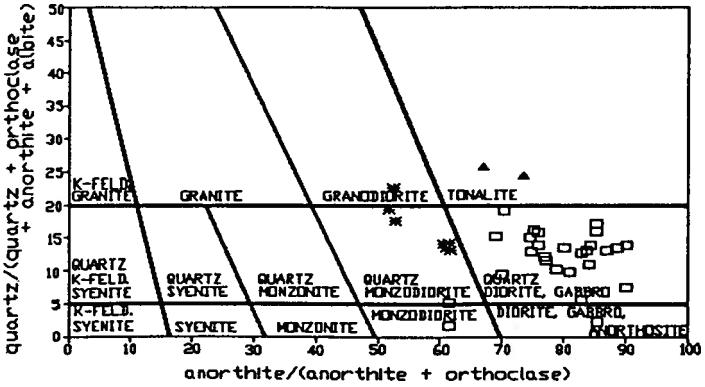

Figure 3.8: Chemical composition of intrusive rocks from the Hedley area, south-central British Columbia plotted on normative diagram (Streckeisen and Lemaitre, 1979). Squares = Hedley intrusions; triangles = Mount Riordan stock; asterisks = Cahill Creek pluton.

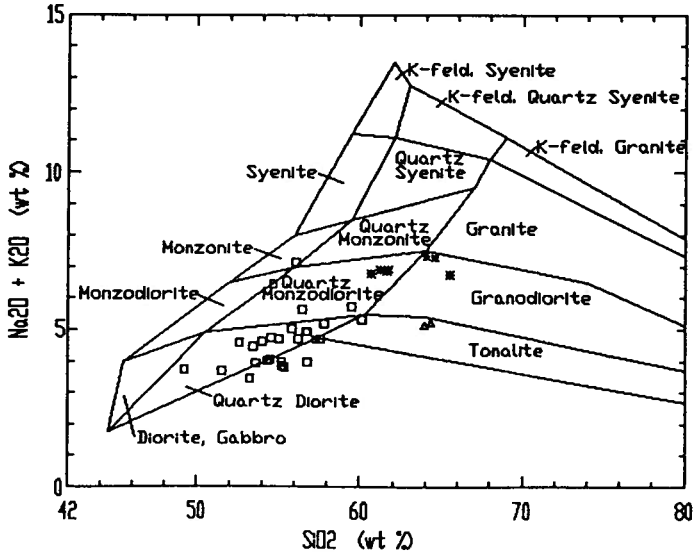

Figure 3.9: Total alkali *vs.* silica diagram (compositional fields defined by Middlemost, 1985) of intrusive rocks from the Hedley area, south-central British Columbia. Squares = Hedley intrusions; triangles = Mount Riordan stock; asterisks = Cahill Creek pluton.

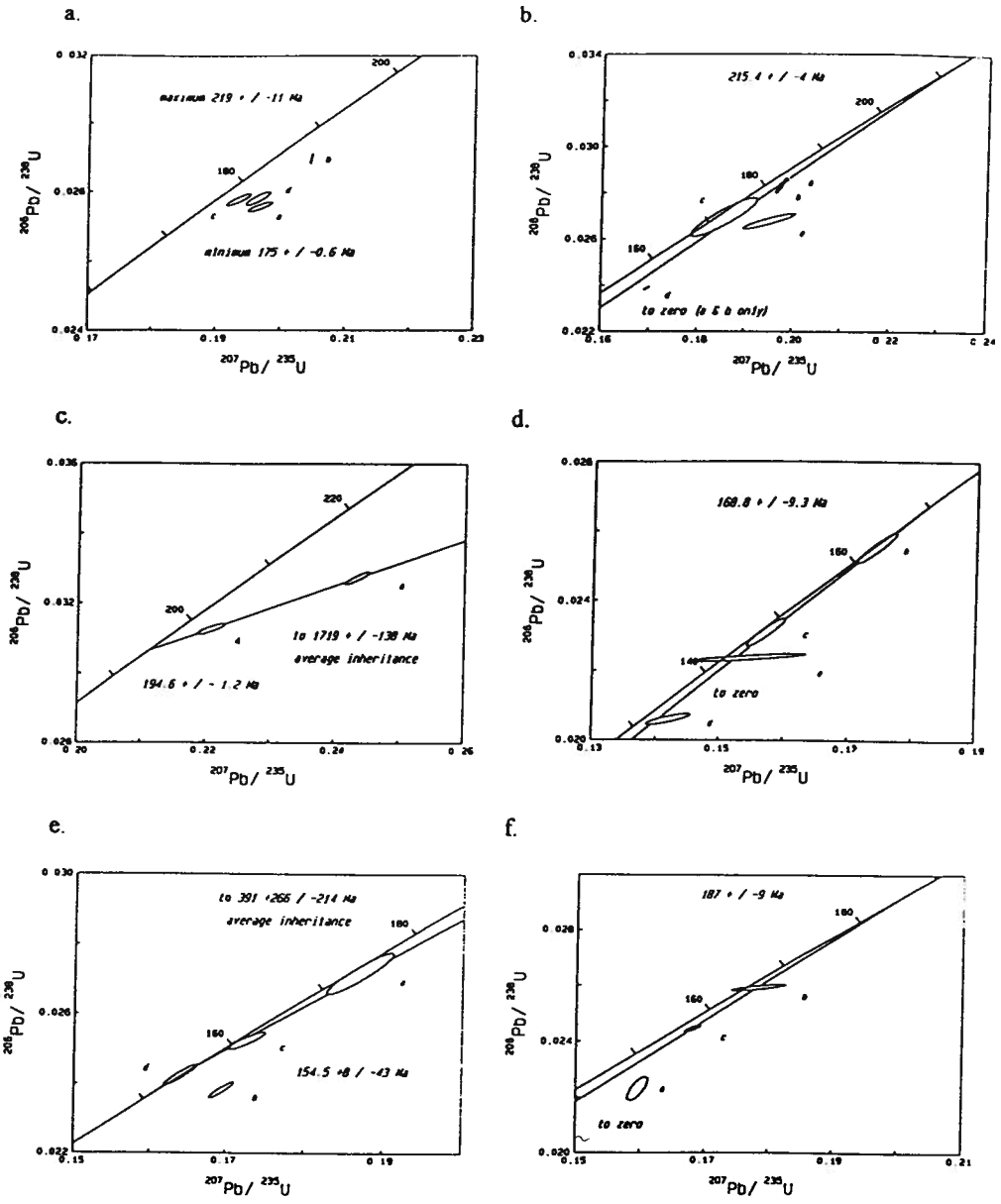

Figure 3.10: U-Pb concordia diagrams for analyses of zircons (J. Gabites, written communication, 1993), from intrusive and extrusive rocks in the Hedley area, south-central British Columbia. Samples are located on Figure 3.1; zircon analyses are in Table B.1. (a) Zircons are from quartz diorite, Stemwinder stock (unit 7, sample Hd-81). A minimum date of 175 $\pm$ 0.6 Ma is indicated. (b) Zircons are from quartz diorite, Banbury stock (unit 7, sample Hd-273). By extrapolation to zero a 215 $\pm$ 4 Ma age is indicated. (c) Zircons are from granodiorite, Mount Riordan stock (unit 9, sample Hd-406). An age of 194.6 $\pm$ 1.2 Ma with inheritance of 1719 $\pm$ 138 Ma is implied. (d) Zircons are from granodiorite, Cahill Creek pluton (unit 10, sample Hd-80). An age of 168.8 $\pm$ 9.3 Ma is indicated. (e) Zircons are from quartz rhyolite porphyry (unit 12, sample Hd-272). A date of 154.5 + 8/-43 Ma with inheritance of 391 + 266/-214 Ma is indicated. (f) Zircons are from quartz-feldspar dacite tuff, lower unit of Skwel Peken formation (unit 13a, sample Hd-271). An age of 187 $\pm$ 9 Ma is indicated.

does not cross-cut the Bromley batholith which has a minimum age of 193 ± 1 Ma (Table B.2). Previously published K-Ar (amphibole) analyses from the Hedley intrusive suite (Toronto stock, 4 samples; Stemwinder stock, 1 sample) yielded dates that range from 175.0 ± 5.4 to 195.0 ± 6.0 Ma (Table B.2).

3.5 Bromley batholith (unit 8)

Bromley batholith (unit 8) forms a large body that intrudes the Nicola Group in the northwest corner of the map area (Fig. 1.1). It consists of pale pink to grey, medium to coarse grained, equigranular granodiorite. The crystal assemblage consists of hornblende, biotite, plagioclase (An_{30}), orthoclase and quartz. Accessory minerals include sericite, apatite, epidote, carbonate and opaque minerals. The margin of the batholith, generally granodiorite, is locally diorite to quartz diorite in composition. Country rocks surrounding the batholith are biotite hornfelsed up to 1 000 m from the contact.

Previously published dates (Table B.2) from the Bromley batholith are 173.4 ± 4.7 to 180.9 ± 5.4 Ma (two K-Ar biotite analyses), 185.7 ± 2.8 to 188.1 ± 5.8 Ma (two K-Ar hornblende analyses) and 193.0 ± 1.0 Ma (U-Pb zircon analysis). The 20 Ma difference between the minimum K-Ar (biotite) and U-Pb (zircon) date likely represents partial resetting by the Cahill Creek pluton. Rocks of the Bromley batholith are similar in texture and composition to those of the Mt. Riordan stock. The later has an equivalent U-Pb zircon date of 194.6 ± 1.2 Ma.

3.6 Mount Riordan stock (unit 9)

Mount Riordan stock (unit 9) forms a small body in a area of poor exposure in the northeast corner of the map area (Fig. 1.1). It is predominantly a medium to coarse grained, equigranular granodiorite to tonalite that contains rare mafic xenoliths. The phenocrystic assemblage consists of: hornblende, biotite, plagioclase (An_{30}), orthoclase and quartz. Accessory minerals include: carbonate,

sericite, epidote, chlorite, titanite, apatite, zircon and opaques. The stock is spatially related to tungsten-copper skarn mineralization and the Crystal Peak industrial garnet skarn at Mt. Riordan (Ray *et al.*, 1992).

Whole rock analysis of samples from the Mount Riordan stock plot in the tonalite field in Figures 3.8 and 3.9. They are subalkalic (Fig. 3.3) and calcalkaline (Fig. 3.4).

U-Pb anaylsis of zircon from the stock (Fig. 3.1: sample Hd-406) gave an age of 194.6 $\pm$ 1.2 Ma (J. Gabites, written communication, 1993). This age is defined by the lower intercept of an isochron passing through an abraded magnetic and non-magnetic fraction (Table B.1, Fig. 3.10c). The fractions contain inherited old zircon with an average age of 1719 $\pm$ 138 Ma.

3.7 Cahill Creek pluton (unit 10)

Cahill Creek pluton (unit 10) forms a large irregular body in the center of Figure 1.1. It has a laccolith like shape in cross-section and commonly occupies the contact between the Apex Mountain complex and the overlying Nicola Group. It is a massive, medium to coarse grained, equigranular granodiorite to quartz monzodiorite that is characterized by about 5% mafic xenoliths up to 30 cm in diameter. Aplite forms irregular bodies along the upper contact of the pluton as well as small dykes in adjacent country rocks. The main body consists of: plagioclase (An_{20}), orthoclase, quartz, hornblende and biotite. Plagioclase crystals have both normal and reverse oscillatory zoning. Accessory and trace minerals include: carbonate, sericite, chlorite, epidote, titanite, apatite, zircon and opaques. Locally, minor molybdenum-tungsten-quartz mineralization occurs as microveins and veins within aplite and adjacent country rocks.

Samples plot in the quartz monzodiorite and granodiorite fields on the normative mineralogy diagram of Figure 3.8. They also plot in the quartz monzodiorite to granodiorite fields on the TAS diagram of Figure 3.9. The pluton is subalkalic (Fig. 3.3) and calcalkaline (Fig. 3.4).

U-Pb analysis of zircon from the pluton (Fig. 3.1, Table B.1: sample Hd-80) gave an age of 168.8 $\pm$ 9.3 Ma (J. Gabites, written communication, 1993). This age is the upper intercept of an isochron (least squares regression) passing through zero and four fractions (Table B.1, Fig. 3.10d). Three of the four fractions have lost lead, however the rock does not appear to contain inherited zircon. Previously published K-Ar dates (Table B.2) for this body are 153.4 $\pm$ 4.6 to 161.3 $\pm$ 3.4 (eight K-Ar biotite analyses) and 159.9 $\pm$ 2.9 to 174.5 $\pm$ 5.2 (three K-Ar hornblende analyses).

3.8 Lookout Ridge pluton (unit 11)

Lookout Ridge pluton (unit 11) forms an elongate body in an area of poor exposure in the northern part of Figure 1.1. It is an isolated body related to the Osprey Lake batholith that occurs 10 km to the north. The pluton consists mainly of massive, medium to coarse grained, orthoclase porphyritic quartz monzonite. The phenocrystic assemblage consists of orthoclase (<30 mm), microcline, perthite, quartz and biotite. Accessory minerals include carbonate, sericite, chlorite, apatite, zircon and opaque minerals. The pluton is locally bordered by a thin unit of coarse grained hornblende-biotite diorite that may represent a marginal phase.

3.9 Rhyolite porphyry (unit 12)

Rhyolite porphyry (unit 12) occurs as rare isolated dykes throughout the map area. The dykes are typically less that 3 m thick. However, immediately west of Skwel Kwel Peken Hill, a 100-200 m thick body occurs along the upper contact of the Cahill Creek pluton for 3.3 km (Fig. 1.1). It is pale pink to buff in outcrop, leucocratic, fine grained to aphanitic and is quartz-feldspar$\pm$biotite phyric. Quartz phenocrysts are anhedral to subhedral (<4 mm) and often have embayed rims (Plate 3.11). Plagioclase (An_{20}) phenocrysts are subhedral to euhedral (<4 mm).

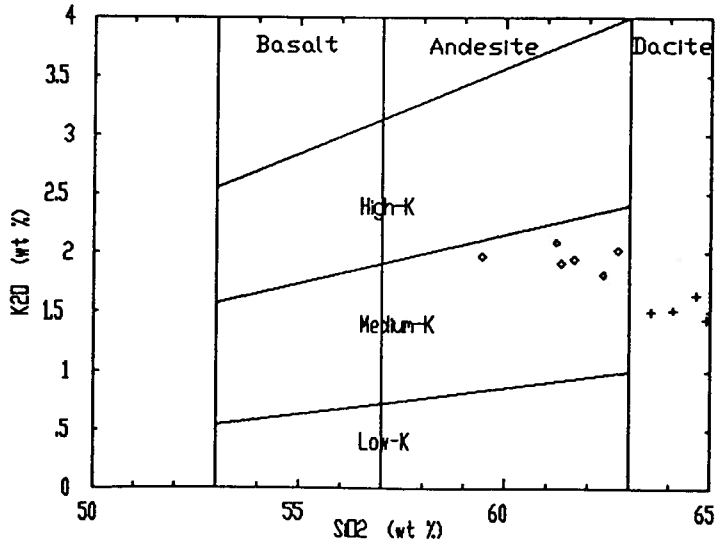

Figure 3.11: K_2O *vs.* SiO_2 diagram (Gill, 1981) for the Skwel Peken formation, Hedley area, south-central British Columbia. Crosses (unit 13a) plot as dacite; diamonds (unit 13b) plot as medium-K andesite.

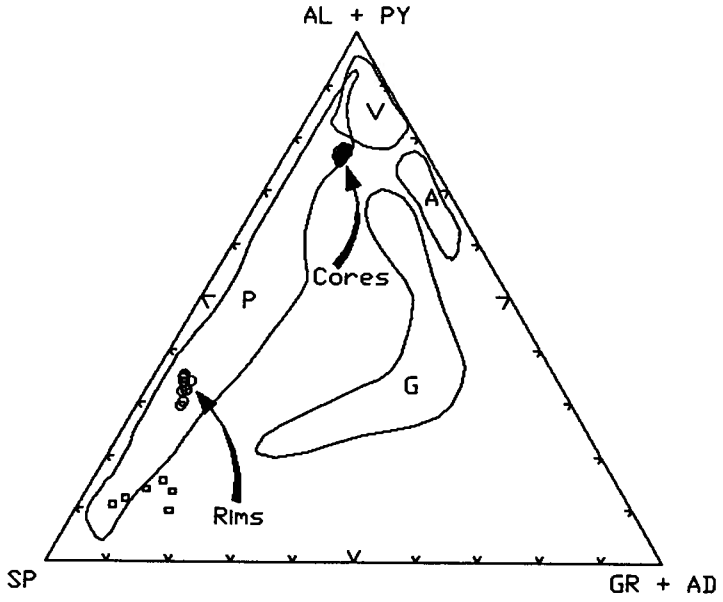

Figure 3.12: Compositions of garnet expressed as the end members: AL (almandine) + PY (pyrope), SP (spessartine), and GR (grossularite) + AD (andradite) from a rhyolite dyke near Skwel Peken Ridge, Hedley area, south-central British Columbia. Data is from Table D.1. These garnets(circles: cores and rims) are compared to garnets from the Upper Cretaceous Capoose rhyolite (boxes) and to garnet fields from a number of other geological settings (Andrew, 1988 and references therein). Rims are relatively spessartine rich (Mn) compared to cores. P = plutonic field; V = volcanic field; G = greenschist field; A = amphibolite field.

Rare flakes of biotite (<3 mm) are partially altered to chlorite. The groundmass consists of an intergrowth of quartz and feldspar. Accessory minerals include zircon and opaque minerals.

U-Pb zircon analysis of zircon from the intrusion (Fig. 3.1, Table B.1: sample Hd-272) gives a date of 154.5 + 8/-43 Ma (J. Gabites, written communication, 1993). This age is the lower intercept of the isochron (least squares regression) passing through three fractions (Table B.1, Fig. 3.10e). The average age of inherited zircon in fractions 'a', 'c' and 'd' is 391 + 266/-214 Ma. Fraction 'b' that plots well below concordia suggest it contains inherited zircon of a much older age than the other fractions.

3.10 Skwel Peken formation (unit 13)

Skwel Peken formation (unit 13) occurs in two separate outliers centered on Lookout Ridge and Skwel Kwel Peken Ridge (Fig. 1.1). It is a Middle Jurassic felsic to intermediate volcaniclastic unit that overlies the Whistle formation. Two distinct stratigraphic units, a lower and upper one, are recognized.

The lower stratigraphic unit (unit 13a), about 1 500 m thick, consists of massive, grey to maroon, feldspar-quartz phyric dacitic ash and lapilli tuff, and minor bedded tuffaceous siltstone, dust tuff and crystal tuff. The ash tuff (Plate 3.12) contains a crystal assemblage of quartz (<2 mm), orthoclase (<3 mm) and plagioclase (<2 mm: An_{20}). The groundmass is a fine grained intergrowth of feldspar, quartz, devitrified glass, chlorite, epidote and opaque minerals. Contact with the underlying Nicola Group was not observed.

The upper stratigraphic unit (unit 13b) occurs in the southern outlier, immediately west of Skwel Kwel Peken Ridge. About 200 m thick and overlying the lower unit, it consists of massive dark green plagioclase phyric andesite to basaltic crystal ash tuff and lapilli tuff. The plagioclase phenocrysts (<5 mm: An_{20}) exhibit normal and reverse oscillatory zoning (Plate 3.13). The matrix consists of a fine grained intergrowth of quartz, orthoclase, plagioclase, devitrified glass, chlorite and opaque minerals.

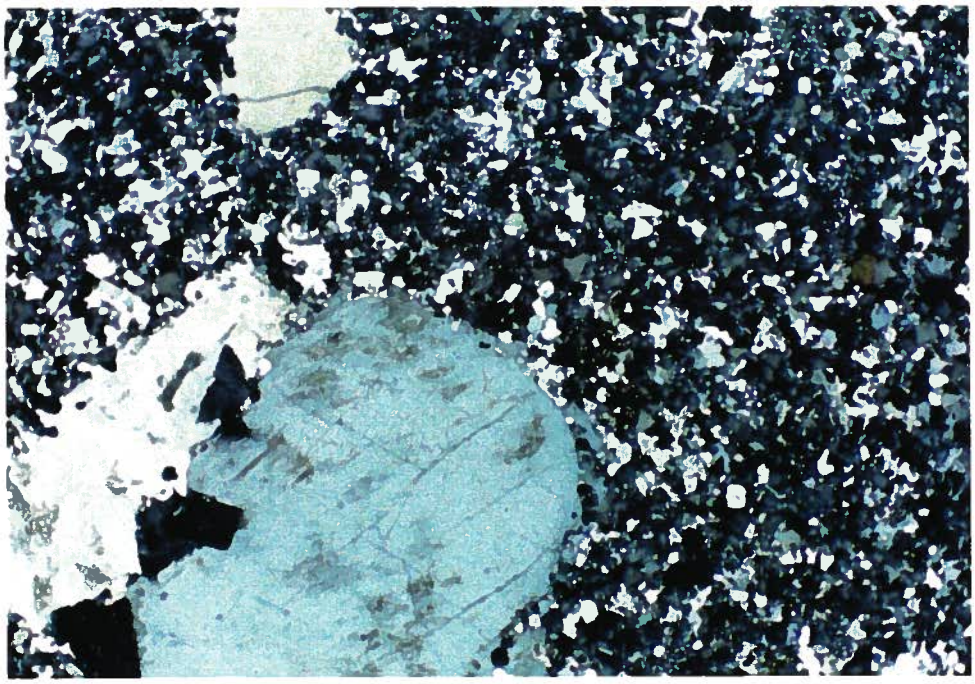

Plate 3.11: Photomicrograph (transmitted light, crossed polars, field of view = 5.0 mm) of quartz porphyry (unit 12: Fig. 1.1). Embayed quartz phenocrysts occur in a fine grained quartzo-feldspathic matrix.

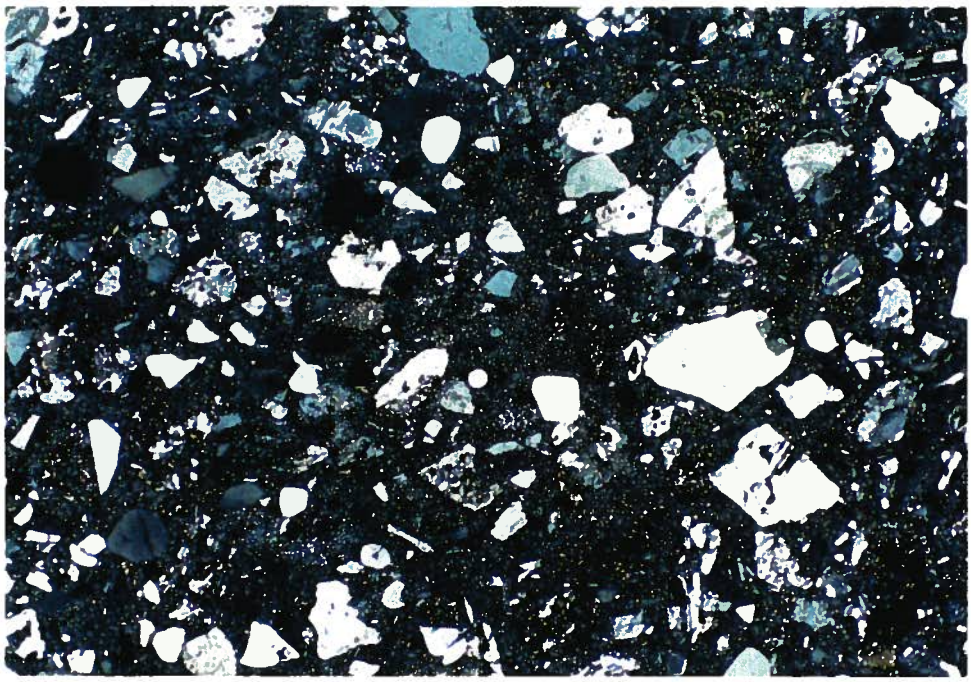

Plate 3.12: Photomicrograph (transmitted light, crossed polars, field of view = 5.0 mm) of dacitic ash tuff from lower unit of the Skwel Peken formation (unit 13a: Fig. 1.1).

Whole rock analysis of samples from the felsic lower unit of this formation plot in the dacite field on the TAS diagram of Figure 3.2. The intermediate upper unit of this formation plots in the andesite field on Figure 3.2. The formation is subalkalic (Fig. 3.3) and calcalkaline (Fig. 3.4).

On a tectonic discrimination diagram constructed for intermediate rocks (Gill, 1981), both units of the Skwel Peken formation plot in the medium-K calcalkaline field (Fig. 3.11); the lower unit is medium-K dacite and the upper unit is andesite. Incompatible element patterns of the Skwel Peken formation (lower and upper unit) are similar to modern day calcalkaline island arcs (Figure 3.7).

U-Pb analysis of zircon from the Skwel Peken formation-lower unit (Fig. 3.1, Table B.1: sample Hd-271) gave a maximum date of 187 $\pm$ 9 Ma (J. Gabites, written communication, 1993). This estimate of age is the upper intercept of an isochron passing through zero, the fine magnetic fraction, and the abraded coarse non-magnetic fraction (Table B.1, Fig. 3.10f). The non-magnetic fraction 'a' contains inherited zircon of Paleozoic or older age and has lost lead. The formation is probably the extrusive equivalent of a suite of Middle Jurassic intrusions that include the rhyolite porphyry, and the Cahill Creek and Lookout Ridge plutons. Mineralogically and texturally these volcanic rocks resemble the rhyolite porphyry that is 154.5 + 8/-43 Ma (Table B.1, Fig. 3.10e).

3.11 Minor intrusions

Minor, narrow dykes less than 5 m thick are exposed throughout the map area (Fig. 1.1). Their compositions range from basalt to rhyodacite.

Several dark green andesite to basalt dykes in the vicinity of the Nickel Plate mine were emplaced along north to northeast trending fractures. Characterized by chilled margins and carbonate amygdules, they probably represent feeder-dykes to the Tertiary Marron volcanics that locally crop out in the area. Phenocrysts consist of sub-parallel twinned plagioclase (An_{40}) and minor chloritized hornblende in a fine grained groundmass of feldspar and opaque minerals. Trace to accessory minerals include titanite, rutile, epidote, ilmenite, apatite and clinozoisite.

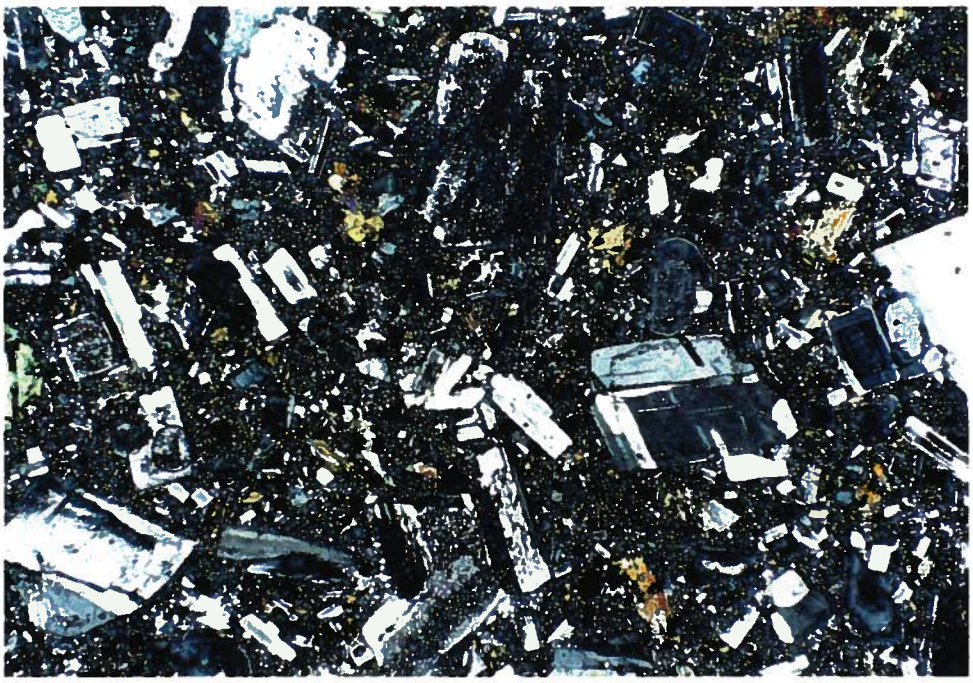

Plate 3.13: Photomicrograph (transmitted light, crossed polars, field of view = 5.0 mm) of andesite crystal tuff from the upper unit of the Skwel Peken formation (unit 13b: Fig. 1.1).

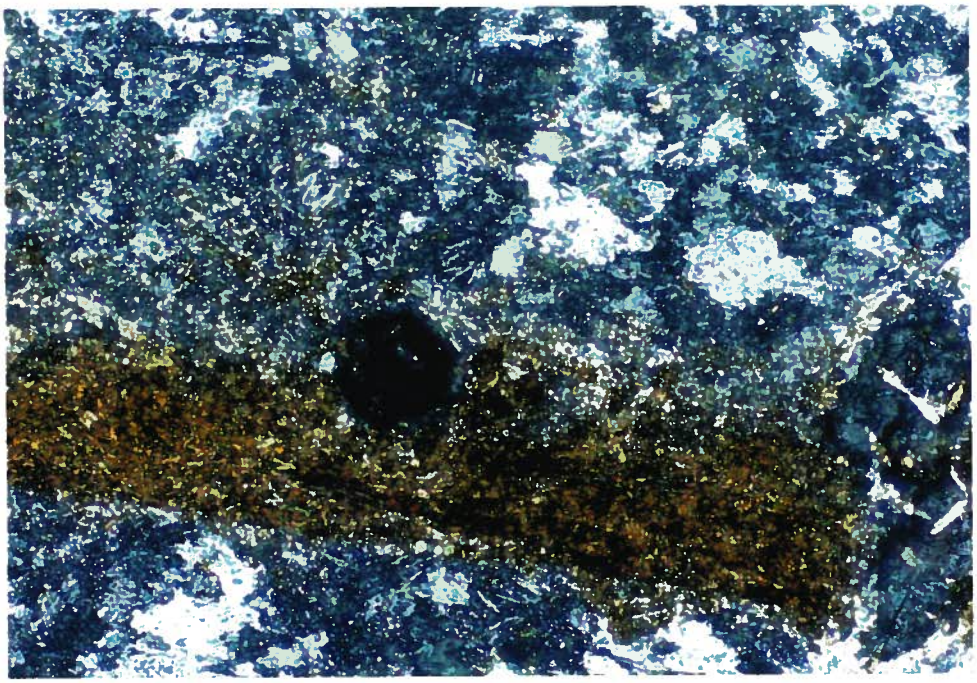

Plate 3.14: Photomicrograph (transmitted light, crossed polars, field of view = 0.625 mm) of an igneous garnet from a rhyolite intrusion near Skwel Kwell Peken Ridge.

A grey, fine grained to aphanitic, leucocratic rhyolite dyke that contains rare garnet crystals crops out on Skwel Kwel Peken Ridge. This unit is spatially related to the Skwel Peken formation. The eastern contact of this body south of Skwel Kwel Peken Ridge is irregular and marked by weak flow banding that dips moderately westward. The phenocryst assemblage of: orthoclase (<3 mm), biotite (<2 mm) and garnet (<2 mm) is in a altered groundmass of fine grained: quartz, plagioclase (An_{10}), orthoclase, muscovite, chlorite, epidote, zircon and opaque minerals. Altered orthoclase phenocrysts are often sericitized. The pink, anhedral to euhedral, isotropic garnet crystals are commonly fractured and have corroded margins (Plate 3.14). Microprobe analysis from core to rim across several crystals (Table D.1, Fig. 3.12) indicate that some have almandine (iron and magnesium rich) cores and spessartine (manganese rich) rims, a zonation typical for igneous garnets (Green, 1977). Some crystals were unzoned almandine. The chemistry of these garnets are compared to garnets from the Upper Cretaceous Capoose rhyolite and garnets from a number of other geological settings (Andrew, 1988) in Figure 3.12. They fall within the plutonic field as defined by Andrew (1988) and references therein, but show a greater range in end member composition (about 45%) from core to rim as compared to garnets from the Capoose rhyolite (<5%). Progressive enrichment in manganese from core to rim may be a result of crystal fractionation, because apart from garnet, manganese is not a principal constituent of other igneous silicates (Miller and Stoddard, 1981 in Andrew, 1988).

3.12 Structure

Apex Mountain complex, not examined in detail during this study, exhibits several features not observed in the overlying Nicola Group rocks. The greenschist metamorphic grade is higher than in Nicola rocks (Monger, 1985). Polyphase deformation is indicated by tight to isoclinal folds with northeast striking, steeply dipping axial planes and subhorizontal fold axes that are overprinted by broad open folds with steeply dipping, northerly striking axial planes (Milford, 1984).

Nicola Group records Late Triassic extension and a Lower Jurassic to Cretaceous(?) compressional history. The overlying Skwel Peken formation was also affected by the Mesozoic compression. Features related to Tertiary extension were not recognized in the Hedley area. Such features in the Okanagan area to the east are manifested as low angle detachment and high angle normal faults that preserve Tertiary volcanic and epiclastic rocks (Tempelman-Kluit and Parkinson, 1986).

The Late Triassic extensional event produced northeasterly striking normal faults and west-northwesterly striking fracture zones. The major normal faults from east to west are the Cahill Creek, Bradshaw and Chuchuwayha faults (Figs. 1.1 and 3.13). These are deep crustal faults that are rooted in the Apex Mountain complex. They mark the eastern edge of a westerly sloping basin margin. Displacement on these faults during Late Triassic sedimentation, Carnian to Norian, formed a stepped seafloor of successively westward down dropped blocks. This is reflected in the deepening facies changes represented by the sequence of formations: Hedley to Chuchuwayha to Stemwinder. The vertical to subvertical west-northwesterly striking faults controlled emplacement of some Hedley intrusions.

Small upright 'crumples' with a wavelength of 30 m and amplitude of 3-5 m plunge 20-30^{o} to the northwest (Dolmage and Brown, 1945). Hedley sills and adjacent sediment commonly are folded by these 'crumples'; rarely dykes at a low angle to bedding crosscut these folds (Billingsley and Hume, 1941). Such structures are economically important because many of the Nickel Plate orebodies form along their axes. The origin of these crumples is uncertain, however they may form by local compression associated with sill injection.

Lower Jurassic to Cretaceous(?) compression produced a number of structures. Major ones include a district wide asymmetric anticline called the Hedley anticline (Billingsley and Hume, 1941), asymmetric minor folds, reverse faults and easterly directed thrust faults (Fig. 3.14).

The axial plane of the Hedley anticline dips steeply west. Its trace lies along Cahill Creek east of the Nickel Plate mine (Fig. 1.1). Bedding dips are: moderately to steeply west in the western portion of the map area, subhorizontal in the central part of the map area around Nickel Plate mine, and vertical to steeply overturned east of Cahill Creek. Poles to bedding in the Nicola Group (stereoplot: Fig. 3.15) indicate a subhorizontal fold axis with a moderate to steeply west dipping axial plane that strike 202^{o}

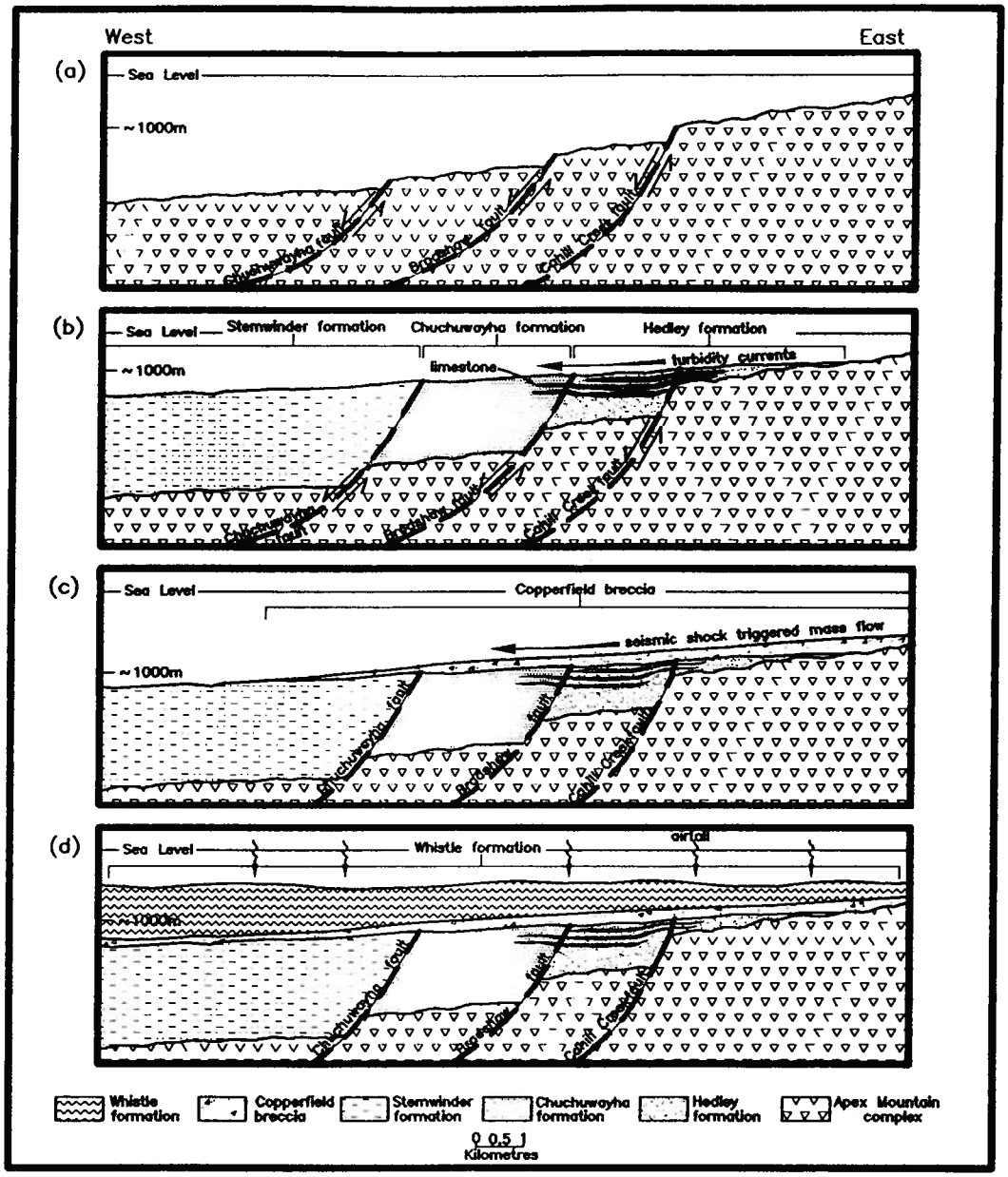

Figure 3.13: Schematic cross-sections of the eastern rifted margin of the Nicola basin during formation of major units in the Hedley area, south-central British Columbia. (a) Extensional faults related to rifting associated with the Late Triassic Nicola arc. (b) Westerly directed paleocurrents produced a number of facies changes represented by the shallow water Hedley formation (siltstone and thick limestone), the intermediate Chuchuwayha formation (siltstone and thin limestone), and the deeper water Stemwinder formation (argillite and rare thin limestone) during Late Triassic, Carnian to Norian, time. (c) Copperfield breccia (limestone breccia) formed a thin laterally extensive unit that separated the overlying volcaniclastics from the underlying sedimentary facies. Seismic shock related to earthquakes associated with volcanism may have triggered the breakup of reefal material to form this mass flow deposit. (d) Whistle formation (intermediate volcaniclastics) mark the gradual change from westerly directed clastic sedimentation to airfall deposits where facies changes are not recognized.

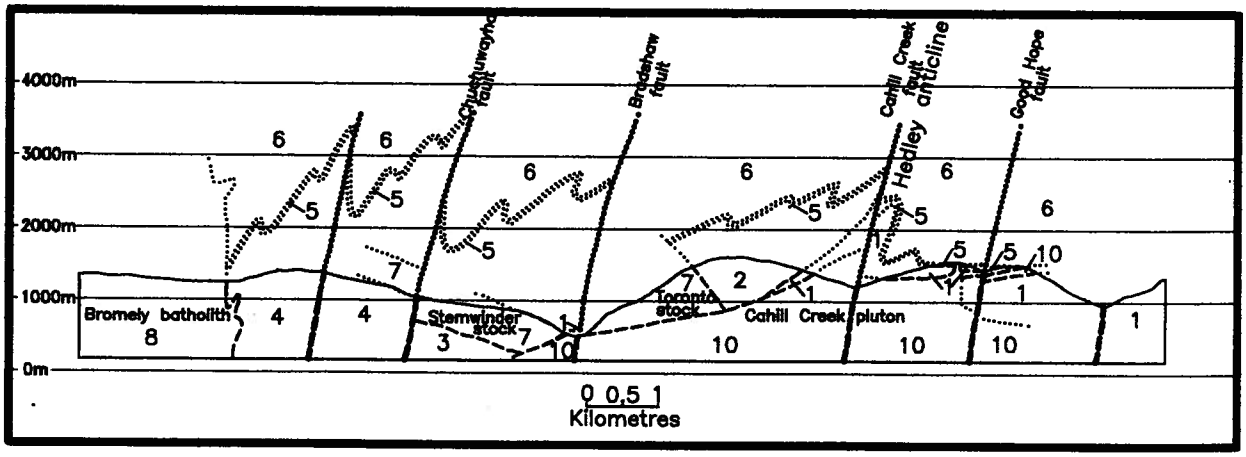

Figure 3.14: Cross-section A-A' through Stemwinder and Nickel Plate Mountain (see Fig. 1.1 for section location) showing Hedley anticline and reverse faults related to Lower Jurassic to Cretaceous (?) compression. Map units are: 1 = Apex Mountain complex, 2 = Hedley formation, 3 = Chuchuwayha formation, 4 = Stemwinder formation, 5 = Copperfield breccia, 6 = Whistle formation, 7 = Hedley intrusions, 8 = Bromley batholith, 10 = Cahill Creek pluton. Line types are: dots = stratigraphy, medium dash = geological contacts.

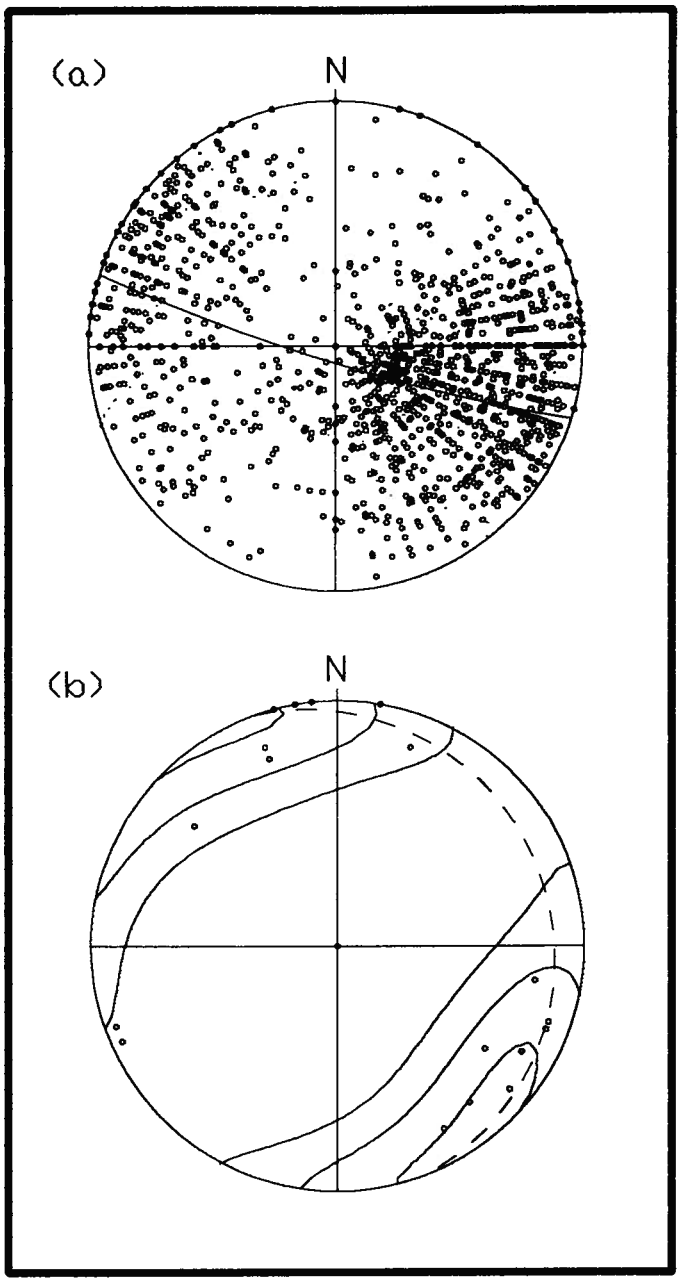

Figure 3.15: Stereoplots of structural measurements from the Nicola Group, Hedley area, south-central British Columbia. (a) Poles to bedding (1414 measurements). (b) Poles to axial planar cleavage (18 measurements). The average of these axial planar cleavage measurements strikes 232° and dips 78° northwest.

(average of 1414 measurements). Axial planar cleavage associated with this fold is poorly developed; it strikes 232^{0} and dips 78^{0} west (average of 18 measurements). Asymmetric minor folds (Plate 3.15) are rare but widespread. Their orientations mimic the district wide Hedley anticline.

Reverse faults mark compressional reactivation of many of the Late Triassic normal faults. For example, uplift on the west side of the Bradshaw fault may be up to 200 m based on the displacement of the contact of the Cahill Creek pluton and the Nicola Group (Fig. 3.14).

Westerly dipping, easterly directed thrust faults have been identified underground at the Nickel Plate and French mine, but are not observed on surface. Duplex like structures (Plate 3.16), observed on cliffs northwest of Hedley township, may be related to thrust faulting.

3.13 Galena lead isotopes

Galena lead isotope ratios from the Nickel Plate gold skarn and the Copper Mountain copper-gold porphyry deposit are presented in Table B.3. The data (provided by C.I. Godwin, Department of Geological Sciences, The University of British Columbia, written communication, 1994), are plotted on conventional lead-lead diagrams in Figure 3.16. These two deposits are compared because they both: (i) represent large deposits of gold, (ii) are of similar Jurassic age, (iii) were formed by intrusive activity, and (iv) were generated within Quesnellia.

Generally, the galena lead isotope data for these two deposits are similar. The data plot between upper crustal lead characterized by the shale curve (Fig. 3.16, SH: Godwin and Sinclair, 1982) and mantle lead (MN: Zartman and Doe, 1981). This is characteristic of lead mixed between reservoirs in an orogene or island arc setting. (Straight lines joining the present day ends of the mantle model and the shale curve models approximate the mixing trends involved in orogene lead.) The average composition of galena lead from Copper Mountain and Hedley is a good representation of Late Triassic to Lower Jurassic (*ca.* 208 Ma) lead on an orogene like growth curve for Quesnellia.

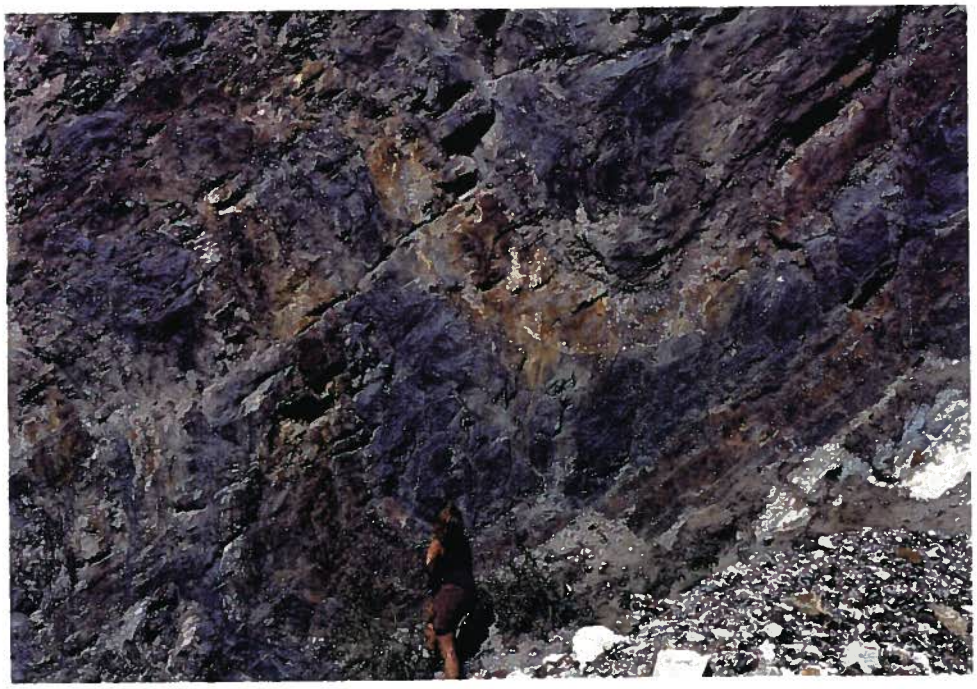

Plate 3.15: Asymmetric minor fold within thinly bedded siltstones of the Hedley formation (unit 2: Fig. 1.1). The axial plane strikes northeast and dips steeply west. Photograph was taken looking north, approximately 1 km north of Hedley township along Bradshaw creek.

Plate 3.16: Duplex like structures within Chuchuwayha formation (unit 3: Fig. 1.1) probably related to Lower Jurassic thrust faults. Photograph was taken looking north from Highway 3 at Hedley township.

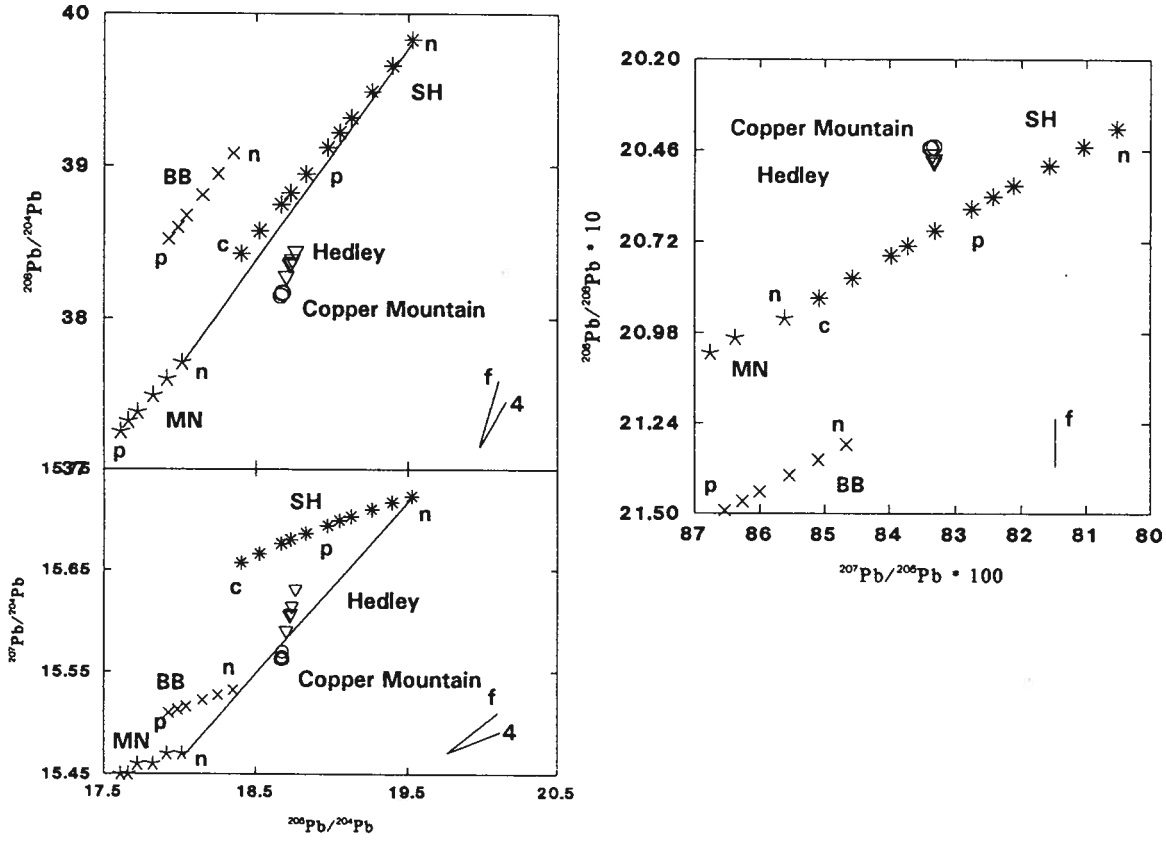

Figure 3.16: Galena lead isotopes (Table B.3) from the Nickel Plate gold skarn and Copper Mountain copper-gold porphyry deposit, south-central British Columbia. Generally, the isotope data plot as orogene lead characterized as a mixture between upper crustal lead represented by the shale curve (SH: Godwin and Sinclair, 1982) and mantle lead (MN: Zartman and Doe, 1981). Straight lines joining the present day ends (n = now or 0 Ga) of the mantle models and the shale curve models approximate the mixing involved in orogene or island arc lead. The probably lower crustal Bluebell curve model (BB: Andrew *et al.*, 1984) does not appear to characterize the lead from the deposits. n = now, 0.0 Ga. p = base of Permian, 0.29 Ga. c = base of Cambrian, 0.57 Ga. 4 = 204 error is much less than 0.1% 2σ error.

Neither the shale curve model (SH) or mantle model (MN) are likely to relate very closely or directly to the plumbotectonic environment (Doe and Zartman, 1979) of Quesnellia. Consequently, the age of the deposit can not be even approximately estimated from the framework models. In addition, the probably lower crustal Bluebell curve model (BB: Andrew *et al.*, 1984) does not appear to characterize the lead.

The Copper Mountain lead is slightly more primitive that the Nickel Plate data; that is, it appears to have a slightly greater mantle component. This suggests that the large alkalic porphyry system at Copper Mountain had relatively limited access to upper crustal components. On the other hand, the sediments involved in skarn mineralization at Hedley might have contributed the slightly more pronounced upper crustal components.

3.14 Discussion

The Middle to Late Paleozoic Apex Mountain complex (unit 1) consists of mafic volcanic, chert, limestone and siliciclastic rocks, and forms the lowest stratigraphic unit in the Hedley area (Table 3.2). East of Winters Creek (Fig. 1.1), Milford (1984) interprets the complex to be an accretionary prism formed above an eastward dipping subduction zone. In this area, individual structural units in the Apex Mountain complex young to the east. However, the overall package of rocks youngs westward (Milford, 1984). Progressive eastwardly directed underthrusting and accretion of younger slices of ocean crust is responsible for the northeastly striking shallowly dipping isoclinal folds (Milford, 1984). West of Winters Creek, the complex forms the eastern rifted basin margin on which sediments of the Nicola Group were deposited.

Late Triassic Nicola Group forms a north trending belt of rocks in southern British Columbia that represents an island arc succession formed above an easterly dipping subduction zone (Monger, 1985; Mortimer, 1987). East of the main volcanic arc, a back-arc basin developed and is characterized by clastic sedimentary rocks, limestone and synsedimentary intrusions (Table 3.2: units 2 to 7). The Hedley area

Table 3.2: Summary of stratigraphy, chemistry and tectonic setting of the Hedley area, south-central British Columbia.

Name/ Formation	Unit:	Date[1]/Age	Field Rock Name	Chemical Rock Name	Magma Series	Discrimination Diagrams	Remarks
Skwel Peken formation (upper unit)	13b		andesite ash to lapilli tuff	andesite (Fig. 3.2)	subalkalic, calcalkaline (Figs. 3.3 and 3.4)	continental arc ? (Fig. 3.7)	- subaerial deposition
Skwel Peken formation (lower unit)	13a	< 187 ± 9 Ma[z]	dacite ash to lapilli tuff	dacite (Fig. 3.2)	subalkalic, calcalkaline (Figs. 3.3 and 3.4)	continental arc ? (Fig. 3.7)	- subaqueous to subaerial deposition - extrusive equivalent of quartz rhyolite porphyry ?
Rhyolite porphyry	12	154.5 + 8/-43 Ma[z]	quartz porphyry	---	---	---	- intrusive equivalent of Skwel Peken formation ?
Lookout Ridge pluton	11	164.5 ± 4.8 Ma[b]	quartz monzonite	---	---	---	- satelite body to Osprey Lake batholith 10 km to the north
Cahill Creek pluton	10	168.8.0 ± 9.3 Ma[z]	granodiorite	granodiorite (Figs. 3.8 and 3.9)	subalkalic, calcalkaline (Figs. 3.3 and 3.4)	continental arc ? (Fig. 3.7)	- laccolith-like body intruded near Apex Mountain complex -Nicola Group unconformity
Mount Riordan stock	9	194.6 ± 1.2 Ma[z]	granodiorite	tonalite (Figs. 3.8 and 3.9)	subalkalic, calcalkaline (Figs. 3.3 and 3.4)	island arc (Fig. 3.7)	- satelite body to Bromley batholith

1. [z] = U-Pb zircon analysis, [b] = K-Ar biotite analysis, [f] = fossil.

Table 3.2: Summary of stratigraphy, chemistry and tectonic setting of the Hedley area, south-central British Columbia (continued)...

Name/ Formation	Unit:	Date[1]/Age	Field Rock Name	Chemical Rock Name	Magma Series	Discrimination Diagrams	Remarks
Bromley batholith	8	193 ± 1 Ma[z]	granodiorite	---	---	---	
Hedley intrusions	7	193 ± 1 to 215.4 ± 4 Ma[z]	quartz diorite, gabbro	quartz diorite (Figs. 3.8 and 3.9)	subalkalic, calcalkaline (Figs. 3.3 and 3.4)	island arc (Figs. 3.5 and 3.7)	- sill complex and stocks, minor dykes; sills contemporaneous with sedimentation
Whistle formation		---	andesite tuff and siltstone	andesite (Fig. 3.2)	alkalic to subalkalic (Fig. 3.3)	island arc (Figs. 3.5, 3.6 and 3.7)	source (Nicola Group: eastern volcanic facies)
Copperfield breccia	5	Late Carnian - Early Norian[f] (*circa.* 225 Ma)	limestone breccia	---	---	---	- seismically triggered (?) mass flow derived from limestone reef to the east (Apex Mountain complex)
Stemwinder formation	4	Late Carnian - Late Norian[f] (circa. 220 Ma)	argillite ± siltstone, limestone	---	---	---	- deposited by westerly directed paleocurrents (deeper water facies)
Chuchuwayha formation	3	Early - Middle Norian[f] (circa. 220 Ma)	siltstone ± argillite, limestone	---	---	---	- deposited by westerly directed paleocurrents (intermediate water facies)

Table 3.2: Summary of stratigraphy, chemistry and tectonic setting of the Hedley area, south-central British Columbia (continued)....

Name/ Formation	Unit:	Date[1]/Age	Field Rock Name	Chemical Rock Name	Magma Series	Discrimination Diagrams	Remarks
Hedley formation	2	Early - Middle Norian[f] (*circa.* 220 Ma)	siltstone ± limestone, argillite	---	---	---	- deposited by westerly directed paleocurrents (shallow water facies); hosts economic gold skarns
Apex Mountain complex	1	Ordovician, Devonian, Carboniferous, Middle - Late Triassic[f]	mafic tuff, siltstone, limestone, argillite, chert, greenstone	---	---	---	- ophiolite complex, accretionary prism

represents the eastern rifted margin of this basin. West of Hedley, much of this basin has been obscured by Jurassic and Cretaceous intrusions (Table 3.2: units 8 to 13).

The westward dipping basin margin apparently was controlled by normal faults such as the Cahill Creek, Bradshaw and Chuchuwayha faults (Fig. 3.13). Displacement on these faults influenced sedimentation during Carnian to Norian times (Fig. 3.17). Westerly directed turbidity currents deposited: (i) siltstones and thick limestones as the shallower water Hedley formation (unit 2), (ii) siltstones and thin limestones as the intermediate Chuchuwayha formation (unit 3), and (iii) argillite and rare limestones as the deeper water Stemwinder formation (unit 4). Continued uplift and nondeposition or erosion is suggested by the thin, poorly preserved Hedley formation east of the Cahill Creek fault. The clastic sediments and limestone were probably derived from uplifted chert beds and limestone reefs in the Apex Mountain complex along the basin margin to the east.

Collapse of this Late Triassic basin is marked by deposition of the Copperfield breccia (unit 5) which separates the Hedley, Chuchuwayha and Stemwinder formations from the overlying volcaniclastics of the Whistle formation. It occurs as a nearly continuous unit and appears to be a catastrophic massive gravity slide deposit derived from uplifted and faulted brittle reef material that has a provenance to the east. Seismic shocks related to earthquakes associated with the start of volcanism may have contributed to the generation of this unit. The relatively short lived basin (<20 Ma based on the range of conodont ages, Fig. 3.17) is similar to modern back-arc basins (Molnar and Atwater, 1978). Similar limestone breccias are recorded in the Carboniferous to Permian Akiyoshi terrane of southwestern Japan (Kanmera and Sano, 1991) and in Tertiary basins off the Nicaraguan Rise in the western Caribbean Sea (Hine *et al.*, 1992). In the Nicaraguan basin, one limestone breccia is approximately 120 m thick, extends 27 km along slope and approximately 16 km out into the basin--similar to dimensions of the Copperfield breccia.

The overlying Whistle formation (unit 6) tuffs are alkaline to subalkaline and have an island arc trace element signature similar to the eastern volcanic facies (Mortimer, 1987) of the Nicola Group. The finely laminated tuffaceous siltstone rapidly grades upwards into massive ash and lapilli tuff. The tuffs were derived from airfall through water. Absence of major variations in facies and limestone units in the

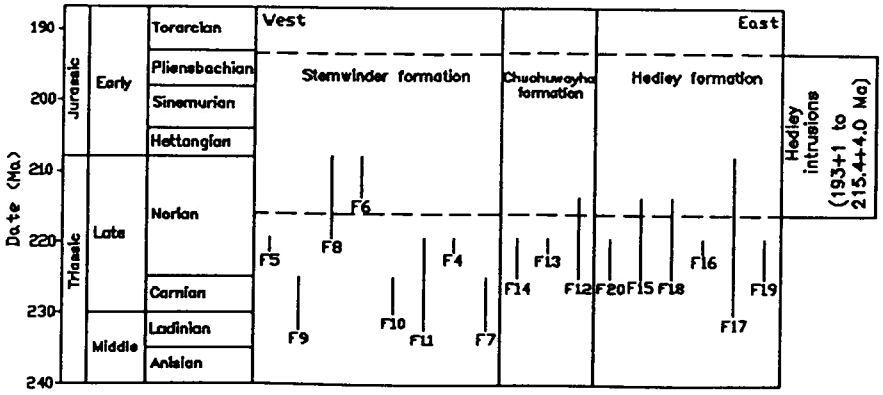

Figure 3.17: Conodont ages from sedimentary formations in the Nicola Group, Hedley area, south-central British Columbia. Data are from Table A.1. Sample locations are shown on Figure 1.1. Note that the age range for the Hedley intrusions--based on a maximum age determined by U-Pb zircon dating and a minimum age determined by contact relationships--is permissible with its intrusion into unconsolidated Nicola Group sediments.

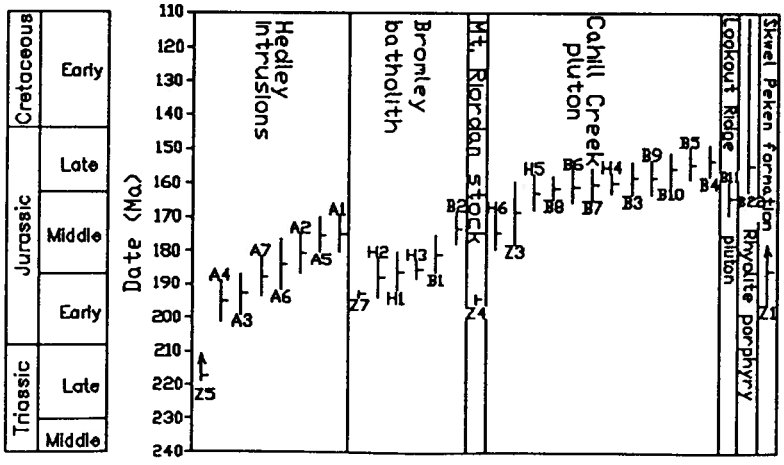

Figure 3.18: U-Pb and K-Ar dates for intrusive and extrusive rocks in the Hedley area, south-central British Columbia. Horizontal tick and vertical bar represents date and error of analysis, respectively. Data are from Table B.1 and B.2. Locations are plotted on Figure 3.1.

Whistle formation tuffs suggests sea floor topography changed from a fault bounded basin to a relatively smooth featureless surface after deposition of the Copperfield breccia.

Late Triassic to possibly Early Jurassic calcalkaline quartz diorite to gabbro Hedley intrusions (unit 7) form porphyritic sills and dykes, and equigranular stocks. Many of the larger dykes and stocks (*e.g.* Stemwinder and Toronto stocks) were emplaced along east-west to northwest fractures that are perpendicular to northeast striking normal faults. These structures may reflect transform faults associated with Late Triassic rifting.

Sills are best developed in the shallow water Hedley formation where they comprise up to 40% of the stratigraphic section, and are spatially and temporally associated with gold skarn mineralization on Nickel Plate mountain. Sills are commonly <2 m thick in the thinly bedded siltstone and limestone. However, in the thick bedded limestone the sills are up to 75 m thick. Individual sill contacts vary from planar to highly irregular; they rarely are gradational or brecciated (peperite).

The above morphological features and the indicated Late Triassic age of the sills, based on preliminary U-Pb zircon dates (Fig. 3.18), suggest the sills were synsedimentary and emplaced into unconsolidated to poorly consolidated sediment. The apparent lithological control on sill thickness and frequency in the Hedley formation may result from exclusion of sills from those limestone units that diagenetically lithified quickly after deposition. Lithification of limestone on the seafloor is geologically instantaneous, involving time spans on the order of 10 to 10 000 years (Choquette and James, 1987). The sills, therefore, preferentially invaded the wet unconsolidated to poorly consolidated siltstone. The preponderance of sills over dykes is additional evidence that the sediments were not completely lithified during sill intrusion (Lee, 1951). Lithified sediments fracture as a result of deformation associated with magma emplacement; thus dykes are as likely to form as sills. Lack of sills in the Stemwinder formation may be related to the increased lithostatic and hydrostatic pressure associated with the thicker sedimentary pile and deeper water environment (*cf.* Kokelaar, 1982).

The Early Jurassic Bromley batholith (unit 8) and Mount Riordan stock (unit 9) are calcalkaline granodiorite to tonalite. They crop out along the northern boundary of the map area. The Mount Riordan

stock is spatially and temporally related to Cu-W mineralization and industrial garnet skarn on Mount Riordan (Ray *et al.*, 1992).

The age and calcalkaline chemistry of the Bromley batholith and Mount Riordan stock in the Hedley area may be explained by a change from moderate or steep to shallow east dipping subduction in the Early Jurassic (Parrish and Monger, 1991). This would result in an eastward widening of the arc. The Early Jurassic calcalkaline low-K magmatism (*i.e.* Bromley batholith and Mount Riordan stock) in the Hedley area and the high-K magmatism (*i.e.* Rossland volcanics) in southeastern British Columbia may represent parallel belts equivalent to the magmatic belts documented by Mortimer (1987) in the Late Triassic Nicola Group farther west (Parrish and Monger, 1991). A similar interpretation of shallowing subduction may be valid in explaining the juxtaposition of the slightly younger, probably Late Triassic, calcalkaline Hedley intrusions in a back-arc extensional setting.

Middle to Late Jurassic calcalkaline magmatism is represented by the Cahill Creek pluton (unit 10), Lookout Ridge pluton (unit 11), rhyolite porphyry (unit 12) and their extrusive equivalent--Skwel Peken formation (unit 13). The Cahill Creek pluton is quartz monzonite to granodiorite and has a laccolith like shape in cross-section. This shape suggests it rose diapirically to the unconformity between the Apex Mountain complex and the Nicola Group. At this horizon it intruded laterally. Aplite phases at the top of the stock and rhyolite porphyry dykes in the nearby country rocks formed as the main body crystallized. Minor W-Mo porphyry style mineralization is spatially and temporally associated with the aplite and overprints earlier gold skarn mineralization. Rhyolite porphyry dykes are texturally and mineralogically similar to the lower unit of the Skwel Peken formation. They presumably represent subvolcanic feeder dykes between the Skwel Peken volcanics and the deeper level Cahill Creek pluton. The consanguineous relationship among the granodiorite, aplite and rhyolite porphyry dykes was first noted by Camsell (1911).

Skwel Peken formation consists of a lower unit of massive to bedded tuffaceous siltstone and dacitic tuff that is overlain by an upper unit of massive feldspar phyric andesite tuff. The formation was deposited in a nonmarine, shallow water to subaerial environment, which in part may explain its lack of

preservation. It represents the first example of mid-Jurassic volcanism recognized in south-central British Columbia--although plutonism of this age is common and widespread in the Canadian Cordillera.

Early to Middle Jurassic magmatism coincides with a change from extensional to compressional tectonics as Quesnellia became accreted to North America. By about 185 Ma there was more than 200 km of tectonic overlap such that, based on Nd-Sr isotopic data (Ghosh, 1990), the eastern margin of North America reached at least to the Okanagan valley. Structures related to this compressional event include the Hedley anticline and associated minor folds, reverse faults (reactivated normal faults) and thrust faults.

CHAPTER 4.0 GEOLOGY OF THE FRENCH MINE GOLD SKARN

4.1 Introduction

The abandoned French mine, 1 km southeast of the Nickel Plate mine, is the second largest gold producer in the Hedley camp. It is located 240 km east of Vancouver and 40 km southeast of Princeton in south-central British Columbia (inset, Fig. 1.1; NTS Maps 92H/8E and 82E/5W; centered near 49^{o} 19'30" N and 120^{o} 01' W).

The original showing, discovered in 1905 by F.H. French, consisted of bornite + chalcopyrite mineralization at the western extremity of a skarn zone in close proximity to a fault (French fault). Development work up to 1917 included an 11 metre adit and a 2.5 metre cross-cut and two lower adits, which failed to intersect mineralization. The property lay dormant until 1949 at which time it was optioned by the Kelowna Exploration Company who operated the nearby Nickel Plate mine (Billingsley *et al.*, 1949). Diamond drilling was completed in 1949 and underground development and production began in 1950. Seasonal production totaled 27-36 tonnes per day and was hauled to the company mill in Hedley. Mining ceased in 1955 when the nearby Nickel Plate mine and mill shut down (Hedley, 1955; Lamb, 1957); underground development up to this time included 310 m of drifting, 30 m of raising and 1 500 m of diamond drilling. Cariboo Gold Quartz Mining Company acquired the controlling interest in the property in 1956 and formed French Mines Ltd. to operate it. They completed underground development and mining up to 1961 and also constructed a 45 tonne/day 'cyanide' mill at Hedley. Development work during this period included 910 m of drifting, 235 m of crosscutting, 275 m of raising and 4 400 m of diamond drilling. Grove Explorations Limited optioned the property in 1976 and completed geological mapping and rock sampling (Sharp, 1976; Westervelt, 1978a, 1978b; Stacey and Goldsmith, 1980), geophysical (electromagnetic and induced polarization) surveys (White, 1976) and diamond drilling (Stacey and Goldsmith, 1981). A potential reserve of 8 731 tonnes grading 5.1 g/t gold, 102.9 g/t silver and 2% copper that could be mined by open cuts and shallow underground workings was outlined (Sharp, 1976). In 1983 some 1 497 tonnes of this ore was mined and milled at the Dankoe mill 64 km to the east (Godfrey, 1983). In 1988, Corona Corporation (formerly Mascot Gold Mines Ltd.) completed property

scale geological mapping, soil geochemistry and diamond drilling (Hammack, 1988; D. Bordin, personal communication, 1988, 1989). Production figures between 1950 and 1961, and in 1983 are incomplete, however British Columbia Geological Survey Branch MINFILE data indicates 1 362 kg of gold, 180 kg of silver and 20 tonnes of copper were recovered from approximately 69 508 tonnes of ore (Table 1.1).

Gold skarn mineralization at the French Mine is spatially and temporally related to aphyric basalt sills (Hedley intrusions) hosted within shallow water siltstone and limestone of the Late Triassic Hedley formation. The significant difference between the geology of the French mine and the nearby Nickel Plate mine is that gold skarn mineralization is associated with quartz diorite porphyry sills (Hedley intrusions) at Nickel Plate mine. Morphological features of the phyric and aphyric sills, and preliminary U-Pb zircon dates of the phyric intrusions support a model whereby the sills intruded Hedley formation sediments soon after deposition while poorly consolidated (Dawson *et al.*, 1990a and 1990b). This interpretation has important implications with respect to the physical and chemical conditions during gold skarn formation. This chapter focuses on emplacement and chemistry of the sill complex, and zoning of calc-silicate alteration and associated gold mineralization about these sills. Data is from surface mapping, core logging, petrographic studies, and whole rock and electron microprobe analysis.

4.2 Geology of the French - Good Hope mine area

The French - Good Hope mine area occurs along the eastern rifted margin of the north trending elongate Nicola back-arc basin (Monger 1985). This basin is underlain by oceanic rocks of the Middle to Late Paleozoic Apex Mountain complex on which sediments, sills and dykes of the Late Triassic Nicola Group were deposited (Figs. 4.1 and 4.2). Post Nicola intrusive rocks occur as plutons and dykes. Late faulting and folding is minor.

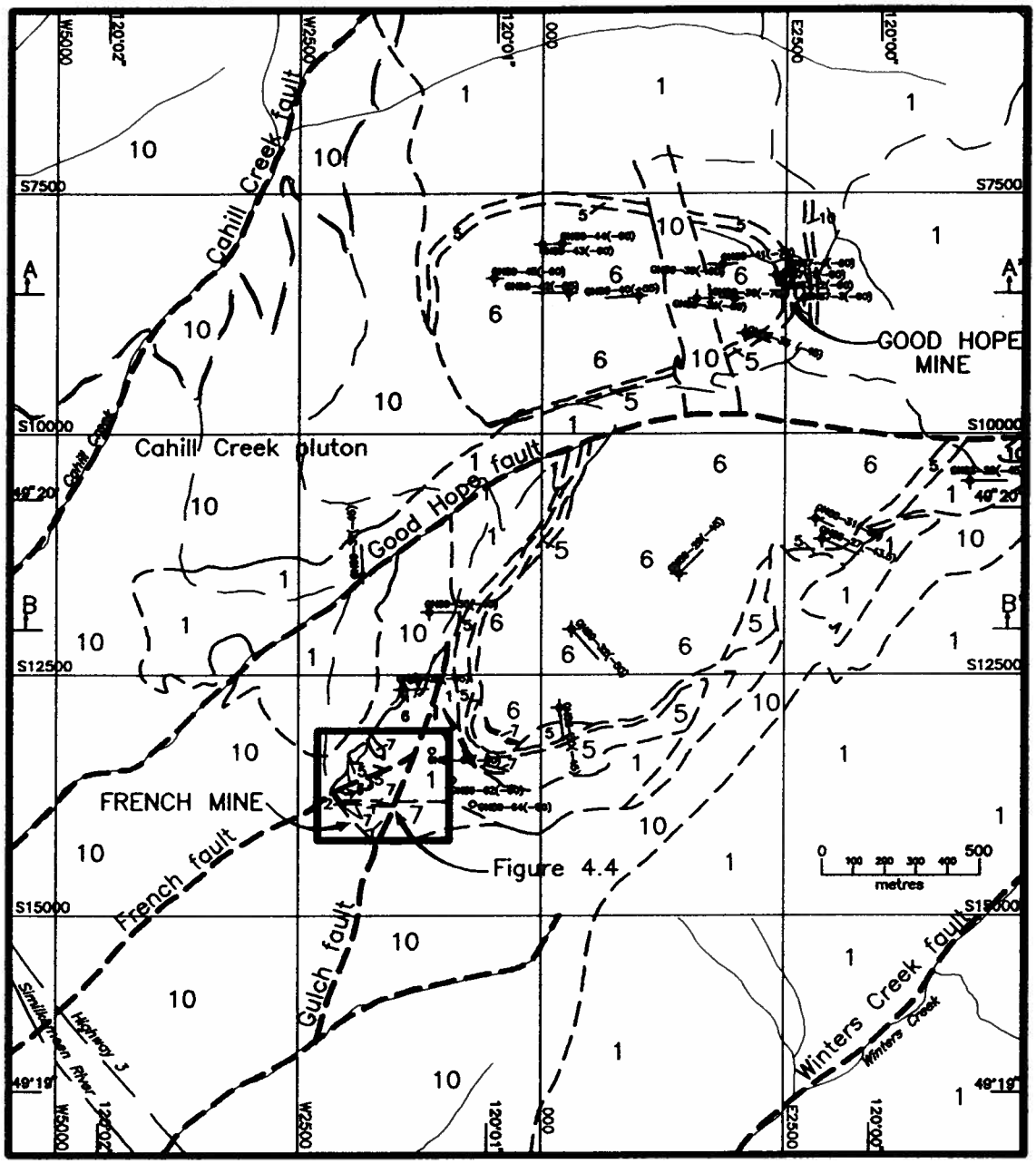

Figure 4.1: Local Geology of the French - Good Hope mine area, south-central British Columbia. Map units are: 1 = Apex Mountain complex, 2 = Hedley formation, 5 = Copperfield breccia, 6 = Whistle formation, 7 = Hedley intrusions, 10 = Cahill Creek pluton. Line types are: thick dash = faults, medium dash = geological contacts, thin dash = gravel roads, thin continuous = rivers. Diamond drill holes, drilled in 1987-1989 by Corona Corporation are located and labeled. Cross-sections A-A' and B-B' are in Figure 4.2. French mine is detailed in Figure 4.4.

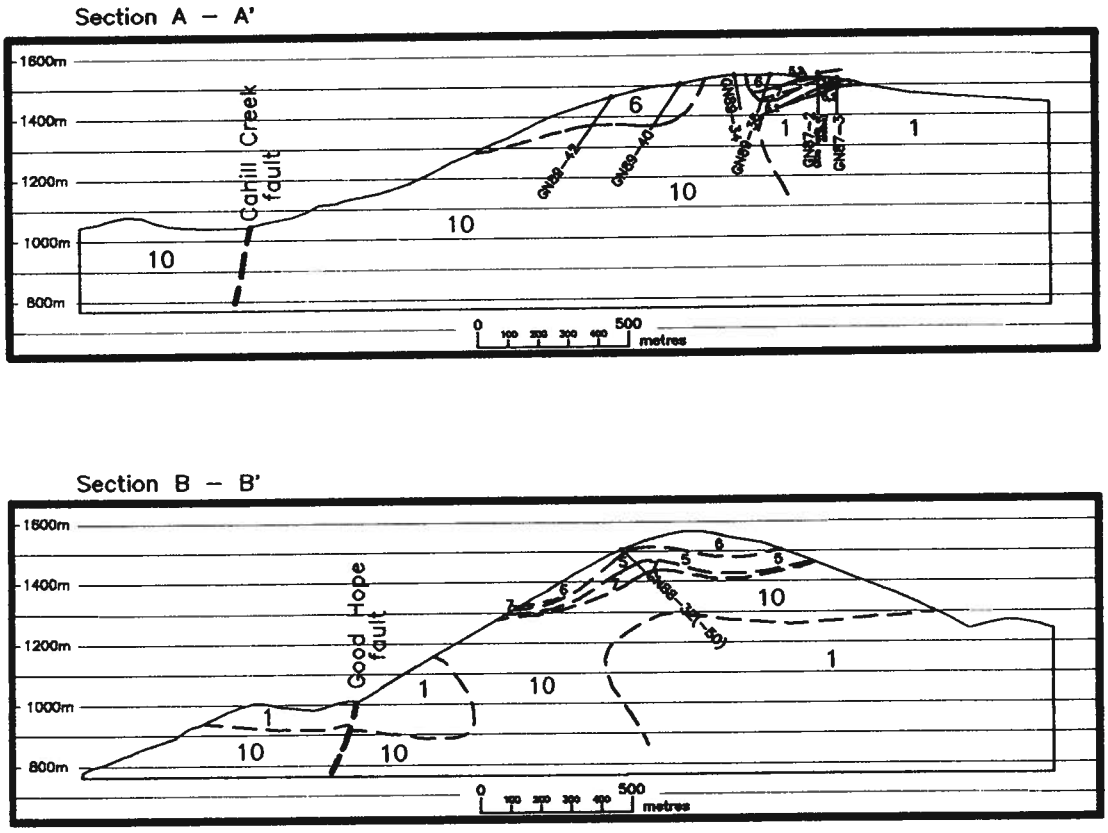

Figure 4.2: East - west cross sections A-A' and B-B' (see Fig. 4.1 for section locations) through the French - Good Hope mine area, south-central British Columbia. Map units are: 1 = Apex Mountain complex, 2 = Hedley formation, 5 = Copperfield breccia, 6 = Whistle formation, 7 = Hedley intrusions, 10 = Cahill Creek pluton. Line types are: thick dash = faults, medium dash = geological contacts. Diamond drill holes drilled in 1987-1989 by Corona Corporation are identified.

4.2.1 Apex Mountain complex (unit 1)

Apex Mountain complex (unit 1) consists of: (i) siliciclastic rocks, (ii) andesitic to basaltic volcanic rocks (greenstone), and minor (iii) chert pebble conglomerate, (iv) chert, (v) limestone, and (vi) ultramafic rock. The oceanic character is defined locally by the presence of mafic pillowed flows and chert (Milford, 1985). These units are detailed below and in Figures 4.1 and 4.2.

Siliciclastic rocks crop out northwest of Winters Creek and southeast of the Cahill Creek pluton where they form a northeast striking, moderately dipping, west facing unit. Siltstone and argillite consist of mosaic quartz and minor plagioclase, apatite, white mica, clays, organic material and opaque minerals. Irregular veinlets (<1 mm) of mosaic quartz (<0.1 mm) may represent dewatering structures formed during compaction and diagenesis of the sediment (Plate 4.1). These units were probably derived from uplifted and eroded older portions of the Apex Mountain complex. They were deposited as turbidites along the west sloping basin margin.

A metamorphic assemblage of biotite + cordierite + garnet overprints these rocks between the lower contact of the Cahill Creek pluton and Winters Creek. Biotite (<0.03 mm) forms pervasive randomly oriented reddish brown flakes that are best developed in fine grained argillaceous layers (Plate 4.2). Cordierite (<0.5 mm) occurs as weakly aligned anhedral to subhedral grains that contain numerous inclusions of biotite, quartz and rarely garnet (Plate 4.3). Garnet (<0.3 mm) forms rare anhedral to subhedral pale pink grains surrounded by biotite and quartz (Plate 4.4). The distribution of metamorphic cordierite + garnet in siliciclastic units below the Cahill Creek pluton indicates that these rocks underwent higher grade metamorphism associated with a deeper structural level than rocks overlying the pluton.

Andesitic to basaltic volcanic rocks (greenstone) are associated with minor siltstone, limestone, chert and ultramafic rock, and form a heterogeneous sequence that underlies the French - Good Hope mine area. Road exposures west of the French mine consist of massive to weakly layered brown biotitic volcanic rock that contain phenocrysts of hornblende, and rarely, plagioclase. These units, interpreted to be mainly tuffs with lesser flows or shallow sills, are occasionally separated by interflow lenses of limestone or siltstone. Some units are similar to aphyric basalt sills (Hedley intrusions) hosted within

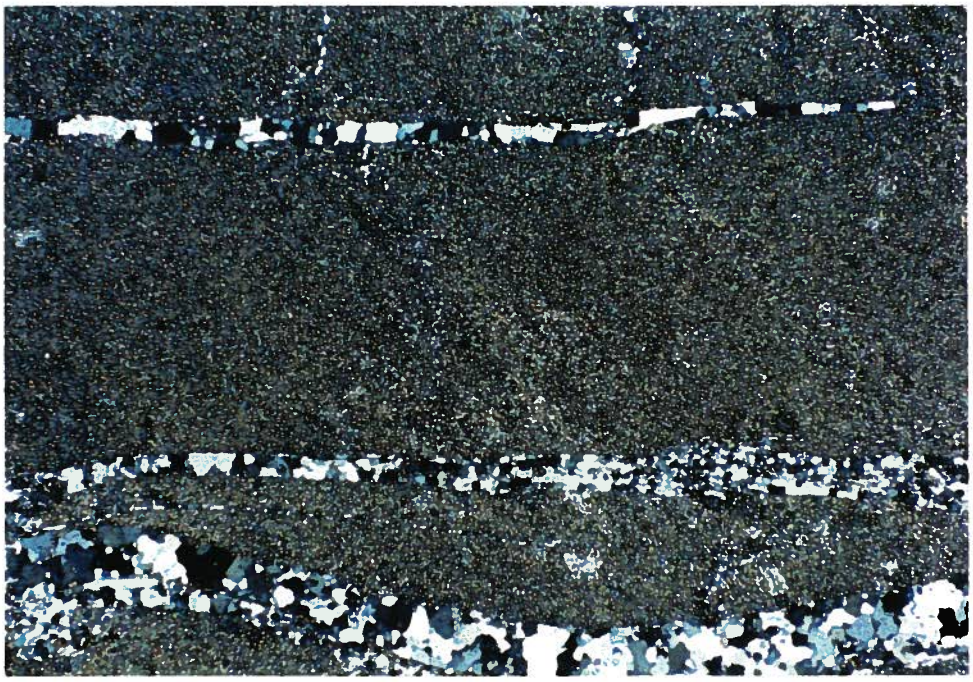

Plate 4.1: Photomicrograph (transmitted light, crossed polars, field of view = 5.0 mm) of siltstone from the Apex Mountain complex cut by irregular veinlets of mosaic quartz (unit 1: Fig. 4.1). Veinlets may represent dewatering structures formed during sediment compaction and diagenesis.

Plate 4.2: Photomicrograph (transmitted light, crossed polars, field of view = 5.0 mm) of biotite + cordierite altered argillite and siltstone from the Apex Mountain complex (unit 1: Fig. 4.1).

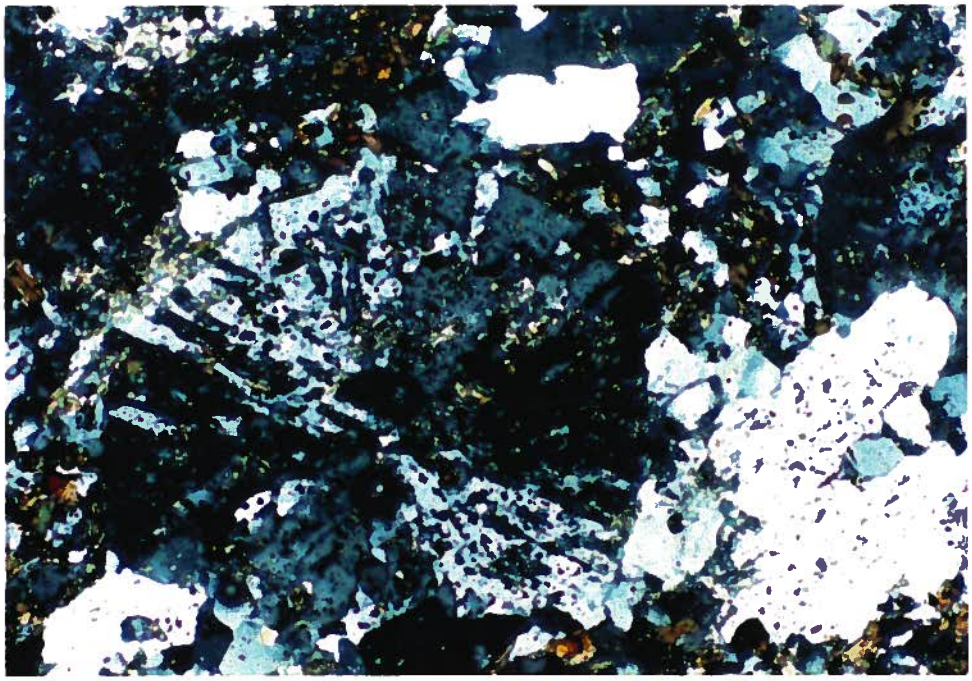

Plate 4.3: Photomicrograph (transmitted light, crossed polars, field of view = 1.25 mm) of cordeirite porphyroblasts in siltstones of the Apex Mountain complex (unit 1: Fig. 4.1). Cordierite is anhedral to subhedral and contains numerous inclusions of biotite, quartz and rarely garnet; some grains exhibit sector twinning.

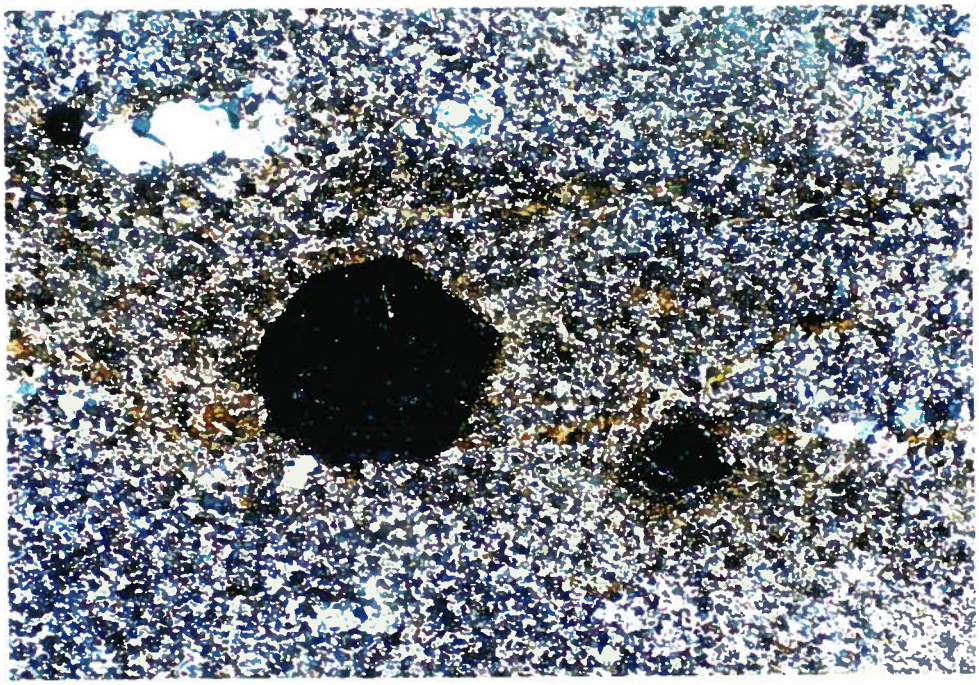

Plate 4.4: Photomicrograph (transmitted light, crossed polars, field of view = 1.25 mm, field of view = 5.0 mm) of clear to pink subhedral garnet crystals in siltstone from the Apex Mountain complex (unit 1: Fig. 4.1). Garnet is surrounded by biotite and quartz.

Hedley formation at the French mine, however their distribution in the Apex Mountain complex is poorly understood because of poor exposure and pervasive biotite alteration associated with contact metamorphism by the Cahill Creek pluton. Poorly bedded units that contain volcanic clasts may be hyaloclastites derived from the associated volcanic units. From thin section, the volcanic rocks consist of hornblende and minor plagioclase phenocrysts in a fine grained plagioclase - glass matrix. Hornblende (<10 mm) is euhedral and partially to completely replaced by brown biotite and ilmenite (Plate 4.5). Plagioclase (<2 mm: An_{40}) is subhedral and partly altered to fine grained clay minerals. The matrix consists of acicular feldspar microlites and glass overprinted by fine grained biotite and white mica. Accessory minerals include clinopyroxene, ilmenite and opaque minerals.

Chert pebble conglomerate forms rare, resistant, discontinuous beds throughout the section. The beds are generally <3 m thick and can be followed along strike for up to 50 m. Clasts (<1 cm) of fine grained mosaic quartz are subangular and matrix supported (Plate 4.6). The matrix consists of microcrystalline quartz and feldspar that is overprinted by brown biotite, acicular actinolite-tremolite, white mica (muscovite), chlorite and opaque minerals. These deposits may represent coarse grained debris flows that filled channels that mark pathways where sediments were discharged from an uplifted and eroded Apex Mountain complex. The sediments were discharged toward the west into the deeper basin.

Chert occurs as rare, thin discontinuous grey to white beds within laminated siltstones. Beds are <2 m thick and traceable along strike for up to 10 m. They consist of microcrystalline quartz, rare feldspar, and opaque minerals, and are overprinted by fine grained brown biotite. Locally, spherical mosaic quartz clasts (<3 mm) are preserved in fine grained laminae. These laminae show the least evidence of recrystallization and the contained round clasts likely represent radiolarian tests (Plate 4.7). The chert represents rare periods of quiescence when chemical precipitation occurred without being diluted by siliciclastics.

Limestone recrystallized to marble occurs as rare disrupted blocks and thin beds within andesitic to basaltic rocks immediately west of the French mine. The disrupted blocks (<5 m) are interpreted to be

Plate 4.5: Photomicrograph (transmitted light, crossed polars, field of view = 5.0 mm) of hornblende phyric andesite to basaltic volcanic rock from the Apex Mountain complex (unit 1: Fig. 4.1). Hornblende phenocrysts are partly altered to brown biotite and ilmenite.

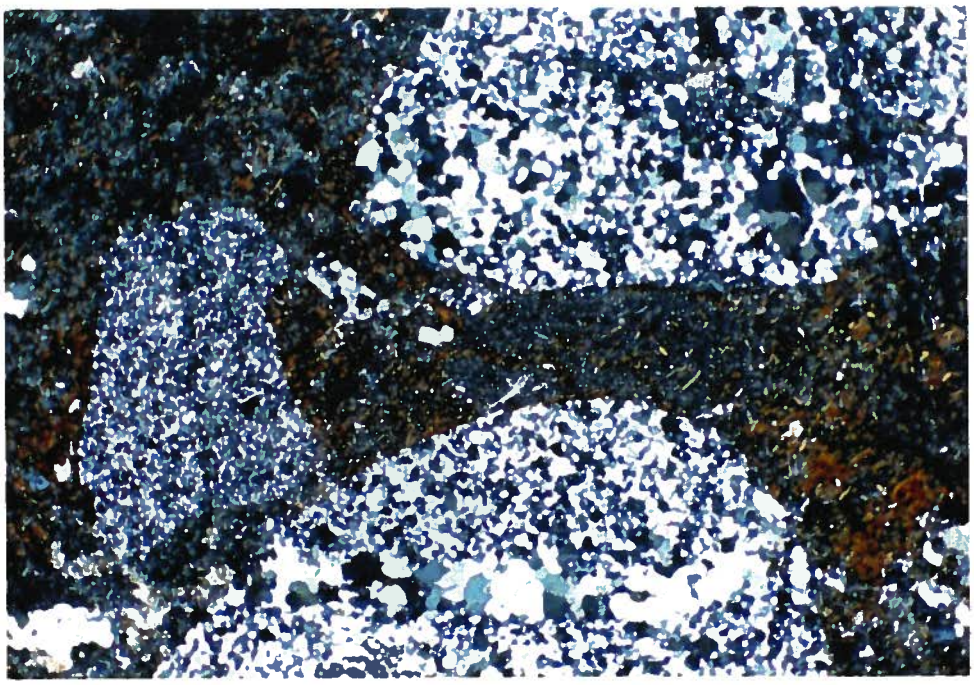

Plate 4.6: Photomicrograph (transmitted light, crossed polars, field of view = 5.0 mm) of chert pebble conglomerate from the Apex Mountain complex (unit 1: Fig. 4.1). Recrystallized chert clast is in a fine grained matrix of quartz, feldspar, biotite, tremolite-actinolite, muscovite, chlorite and opaque minerals.

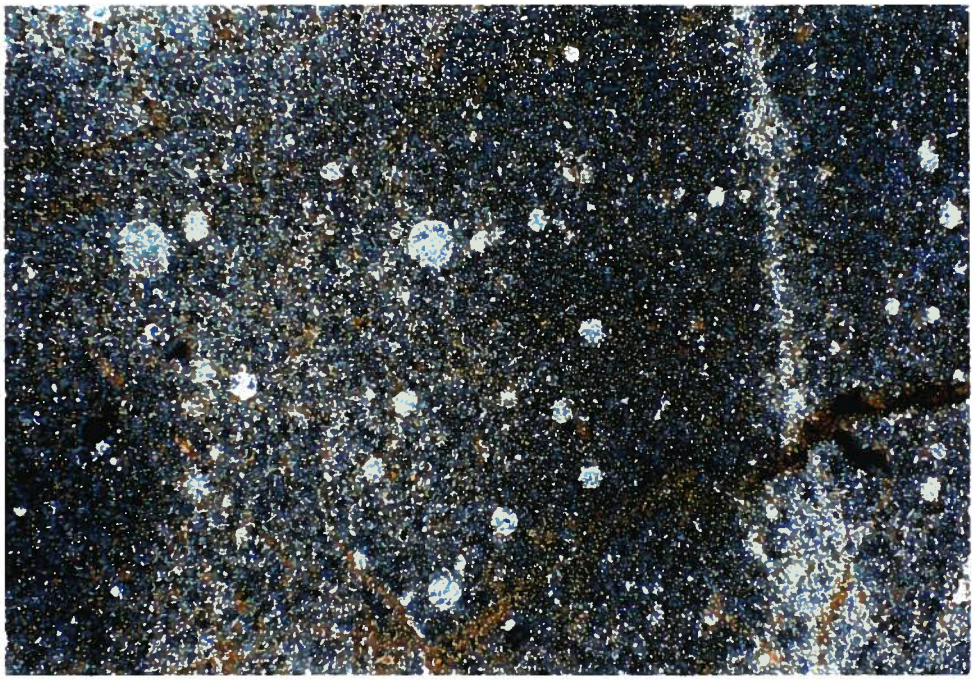

Plate 4.7: Photomicrograph (transmitted light, crossed polars, field of view = 5.0 mm) of chert from the Apex Mountain complex (unit 1: Fig. 4.1). Spherical microcrystalline quartz grain (<3 mm) may represent radiolarian tests.

Plate 4.8: Photomicrograph (transmitted light, crossed polars, field of view = 5.0 mm) of serpentinized ultramafic (dunite) from the Apex Mountain complex (unit 1: Fig. 4.1). Sheared and fractured olivine is altered to chrysotile and magnetite.

olistoliths derived from carbonate reefs somewhere to the east. Bedding in the tuffs underlying the blocks is locally disrupted. Thin discontinuous limestone beds separate some of the volcanic horizons. Such beds are <3 m thick, traceable for up to 50 m, and often contain graded chert clasts and broken shell fragments.

Ultramafic rock was intersected from 49.4 to 55.4 m in drill hole GN89-62 collared 200 m northeast of the French mine (Fig. 4.1). It occurs as fine grained to aphanitic black and white boudinaged bands <5 mm thick in hand sample. From thin section, the rock, originally probably dunite, consists mainly of sheared and fractured olivine altered to chrysotile and magnetite (Plate 4.8). This rock-type was not identified during surface mapping, and therefore, the extent of this minor unit is unknown.

4.2.2 Nicola Group (units 2-6)

Nicola Group (units 2-6: Section 3.3) forms a westerly, shallow dipping unit that unconformably overlies the Apex Mountain complex (Figs. 4.1 and 4.2). In the French - Good Hope mine area, it consists of the Hedley formation (unit 2), Copperfield breccia (unit 5) and Whistle formation (unit 6). These units are detailed below.

Hedley formation (unit 2) forms a thin discontinuous unit <50 m thick of interbedded siltstone, limestone and minor argillite. Siltstones are white and consist of recrystallized microcyrstalline quartz. Limestone forms massive to weakly bedded units that are recrystallized to marble. The unit is preserved in paleotopographic lows around the French and Good Hope mine along the westerly sloping basin edge. West of the Cahill Creek fault this unit dramatically thickens to over 500 m where it hosts gold skarn mineralization at the Nickel Plate deposit.

Copperfield breccia (unit 5) overlies the Hedley formation and Apex Mountain complex. It varies from <10 m to 100 m in thickness. The unit consists of massive to bedded limestone breccia and conglomerate with minor interbeds of thinly laminated limestone. Limestone makes up 95% of the clasts; they are <5 to 50 cm in diameter, subangular to subrounded, and both clast and matrix supported. Rare clasts of tuff, argillite and aphyric basalt occur within this unit. In the vicinity of the Good Hope - French

mine area, the limey tuffaceous matrix is altered to brown garnet ± clinopyroxene reaction (or bimetasomatic diffusion) skarn (Rose and Burt, 1979); the limestone clasts and beds are altered to white marble and wollastonite (Plate 4.9). This reaction skarn, is likely caused by the Cahill Creek pluton, which underlies much of the French - Good Hope mine area. It was previously called the Pinto formation and was thought to be a tectonic breccia related to thrust faulting (Hedley, 1955). A similar tectonic origin, related to the Bradshaw thrust fault (Billingsley and Hume, 1941) was given for the limestone breccia (Copperfield breccia) overlying the Nickel Plate deposit. However, mapping by Ray *et al.* (1986) interpret this unit to be a massive gravity slide deposit formed by breakup of reefal material with a provenance to the east. It marks the change from westerly directed clastic sedimentation (units 2-4) to volcaniclastic and pyroclastic rocks of the Whistle formation (unit 6). Seismic activity (*i.e.* earthquakes) related to the onset of volcanism may have been responsible for basin collapse and deposition of this unit.

Whistle formation (unit 6) conformably overlays the Copperfield breccia. The unit has a maximum thickness of about 200 m in the French - Good Hope mine area. It consists of thin bedded tuffaceous siltstone that grades upward into massive andesitic to basaltic ash and lapilli tuff. The lower part of the unit is markedly epiclastic and exhibits features that indicate the unit is right-way-up (*e.g.* graded beds, flame textures and load casts). Paleocurrent directions are predominantly from the east. Biotite + potassium feldspar + clinopyroxene hornfels is common in the lower sedimentary section of this unit where it is in close proximity to the Cahill Creek pluton.

4.2.3 Intrusive units (units 7-12)

Hedley intrusions (unit 7), Cahill Creek pluton (unit 10), and rhyolite porphyry (unit 12) occur in the French - Good Hope area. These units are described below and in Figures 4.1 and 4.2. Units 8, 9 and 11 were not noted in the French - Good Hope area, but occur regionally (see Sections 3.5, 3.6 and 3.8, respectively).

Plate 4.9: Photograph of Copperfield breccia at the French mine (unit 5: Fig. 4.1). The limey tuffaceous matrix is altered to garnet and the limestone clasts are altered to marble and/or wollastonite. This skarn apparently is a metamorphic reaction skarn formed by the intrusion of the adjacent Cahill Creek pluton (unit 10).

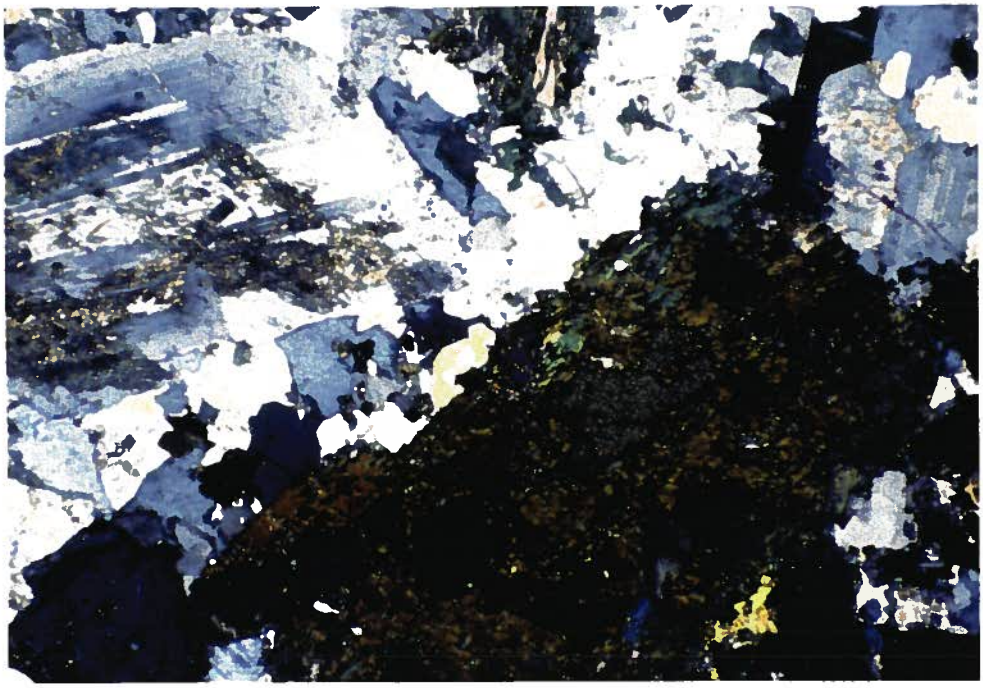

Plate 4.10: Photomicrograph (transmitted light, crossed polars) of hornblende granodiorite from the Cahill Creek pluton (unit 10: Fig. 4.1). Hornblende crystals are altered to brown biotite, chlorite, carbonate and sphene.

Hedley intrusions (unit 7) form phyric and aphyric dykes, sills and stock like bodies that are spatially and temporally associated with gold skarn mineralization in the French - Good Hope mine area (Fig. 4.1). The phyric intrusions vary from equigranular quartz diorite to hornblende porphyries. Aphyric intrusions form thin sills, dykes or margins to hornblende phyric intrusions. Both the hornblende phyric and aphyric intrusions are similar to units in the Apex Mountain complex described in Section 4.1.

Cahill Creek pluton (unit 10) forms a large body that occupies the western portion of the map area. Flat lying to shallow dipping tongues from this body intrude along or close to the contact between the Apex Mountain complex and the overlying Nicola Group in the eastern part of the map area (Figs. 4.1 and 4.2). Siliciclastics of the Apex Mountain complex below and to the east of the intrusion are biotite + cordierite + garnet hornfelsed. Tuffaceous siltstones (Whistle formation) and limestone breccia (Copperfield breccia) of the Nicola Group, above and to the west of the intrusion, are altered to calc-silicate reaction skarn. The pluton is medium grained, equigranular, biotite-hornblende granodiorite to monzodiorite. It consists of: plagioclase (An_{20}), orthoclase, quartz, biotite and hornblende. Accessory minerals include apatite, zircon and opaque minerals. Plagioclase crystals exhibit normal and reverse zoning; their cores are preferentially altered to sericite. Hornblende crystals are pseudomorphed by brown biotite, which is altered to chlorite + carbonate + titanite (Plate 4.10).

Aplite occurs as discrete lenses along the upper contact of the pluton, and as isolated dykes in the surrounding country rocks. It consists of fine grained quartz, plagioclase (An_{10}) and orthoclase. Accessory minerals include: muscovite, chlorite, apatite, titanite, zircon and opaque minerals. W-Mo mineralization is spatially and temporally related to this intrusion. It occurs as disseminations and veins of quartz $\pm$ actinolite, epidote, molybdenite and scheelite in the aplite and adjacent country rocks (Plate 4.11). At the French and Good Hope mines, the close proximity to the upper contact of the Cahill Creek pluton has caused the earlier gold skarn to be overprinted by this mineralization. Rock chip samples from a drift and incline above the Granby adit near the French fault returned 36 m grading 0.68% WO_3 and 15 m grading 0.58% WO_3, respectively (Westervelt, 1978a).

Rhyolite porphyry (unit 12) occurs as isolated thin dykes (<3 m thick) throughout the map area. They are white to beige, massive and have phenocrysts of quartz, plagioclase and orthoclase (Plate 4.12).

Plate 4.11: Quartz + actinolite + epidote ± molybdenite ± scheelite veins related to the aplite phase of the Cahill Creek pluton (unit 10: Fig. 4.1). Veins cross-cut garnet skarn related to intrusion of the older Hedley intrusions (unit 7); the protolith to the garnet skarn is Hedley formation limestones (unit 2). Photograph is from the southern end of the Good Hope open pit.

Plate 4.12: Rhyolite porphyry (unit 12: Fig. 4.4) containing phenocrysts of quartz, plagioclase and orthoclase in an aphanitic groundmass. Photograph is along the upper haulage track west of the 3920 Level adit.

Quartz phenocrysts (<3 mm) are anhedral to subhedral and occasionally have resorbed rims. Plagioclase (<2 mm: An_{10}) and orthoclase (<2 mm) phenocrysts are subhedral and partially altered to clay and carbonate. Groundmass consists mainly of fine grained myrmekite (Plate 4.13). Accessory minerals include: biotite, titanite, zircon, carbonate, clays, chlorite and opaques. These dykes are interpreted to be feeders between the Cahill Creek pluton and the overlying Skwel Peken formation volcanics that crop out on Lookout Mountain 7 km north of the French mine.

4.2.4 Structure

Structural elements identified (Figs. 4.1 and 4.2) include: (i) northeast striking steeply dipping faults, (ii) northeast striking moderately west dipping faults, and (iii) minor open folds. These are detailed below.

Northeast striking steeply dipping faults include the Cahill Creek, Good Hope, French and Gulch faults. The Cahill Creek fault is a northeast striking, steeply dipping normal fault related to Late Triassic extensional tectonics. This fault influenced sedimentation during Carnian to Norian time. Hedley formation, less than 50 metres thick east of this fault, dramatically thickens to over 500 metres west of the fault. Other northeast striking faults such as the Good Hope, French and Gulch faults are poorly defined. The Good Hope fault forms a strong linear depression that strikes northeast to east and separates the Good Hope mine area in the north from the French Mine area to the south. The fault was not observed in outcrop, however a topographic trace of the fault indicates it is steeply dipping to the south. Movement on the fault appears to be right lateral, mainly strike-slip, and in the order of 1 000 m based on the displacement of a Cahill Creek granodiorite dyke that outcrops west of the French and Good Hope mines (Figs. 4.1 and 4.2). The French fault is mapped in roadcuts at the French mine where it strikes 055^{o} and dips 75^{o} southeast; in a small crosscut north of the Granby adit it strikes 055^{o} and dips 60^{o} southeast. The fault has approximately 1 m of clay gouge and separates aphyric Hedley intrusion (unit 7) from skarn altered limestones and siltstones (unit 2); displacement across the fault is uncertain, but appears to be

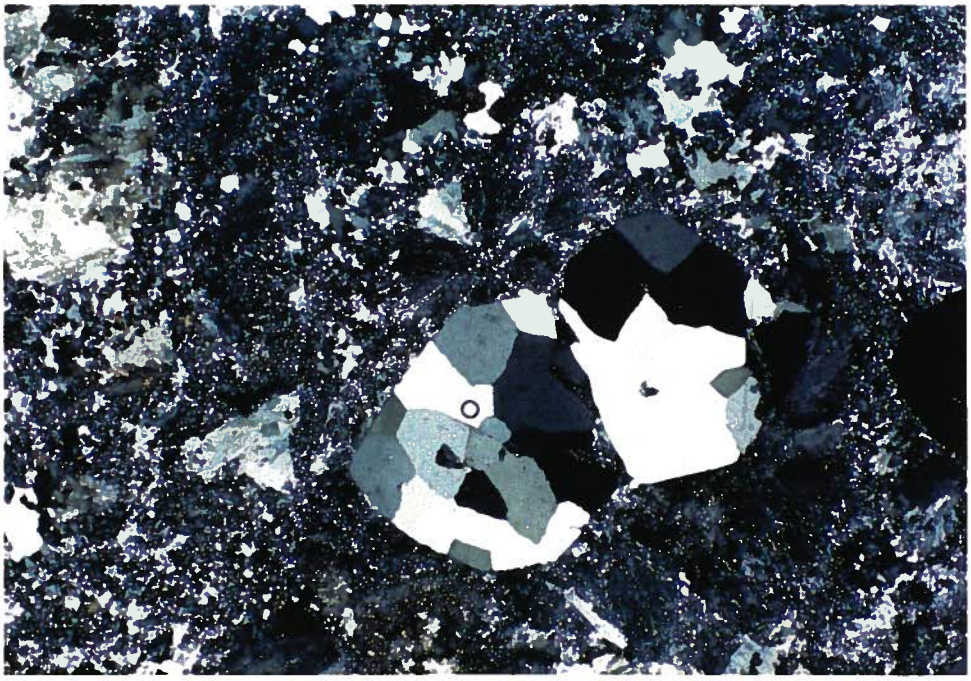

Plate 4.13: Photomicrograph (transmitted light, crossed polars, field of view = 5.0 mm) of quartz rhyolite porphyry (unit 12: Fig. 4.4).

Plate 4.14: Quartz diorite of the Hedley intrusions contains numerous mafic xenoliths and forms a stock like body at the French mine (unit 7: Fig. 4.4). Photograph is of outcrop along road 50 m northwest of the Cariboo adit, French mine.

minor. The Gulch fault was not observed in outcrop, however, it forms a linear depression on surface that trends north-northeast. Underground the fault was mapped in the Cariboo adit and the lower stope where it strikes 028° and dips 80° east (Fig. 4.4). It forms a two metre thick sheared and brecciated zone with up to 1.0 m of clay gouge. A 1 m thick intermediate to mafic dyke infills the fault and has been hydrothermally altered to clay. Displacement across the fault is uncertain.

Northeast striking moderately west dipping faults are represented by the Cariboo fault (200°/40° west). It was intersected in a small drift east of the Cariboo adit (Fig. 4.4), but was neither identified on surface nor were linears identified on aerial photographs where the fault would project to surface. Underground the fault has slickensides that indicate mainly dip slip movement. It separates skarn altered Hedley formation sediments from the underlying Apex Mountain complex. An underground drill program (1 000 m in 7 drill holes) to test the panel below the Cariboo thrust failed to intersect skarn altered Hedley formation sediments (Stacey and Goldsmith, 1981). All holes encountered chlorite + serpentinite altered mafic volcanics and sediments, and minor limestone--presumably of the Apex Mountain complex. Most holes terminated in the Cahill Creek granodiorite.

Minor open folds occur throughout the Nicola Group in the French - Good Hope mine area (Figs. 4.1 and 4.2). Overall the Nicola Group forms a northeast striking and shallowly westward dipping unit that unconformably overlies more structurally deformed Apex Mountain complex. This general relationship of shallowly dipping units above the Cahill Creek pluton and steeply dipping units below the pluton was noted by Hedley (1955). Stereoplot of poles to bedding (Fig. 4.3a) in the Nicola Group indicate that the unit strikes 226° and dips 18° northwest (average of 68 measurements). Locally, in the French mine area (Fig. 4.4), Nicola Group bedding strikes east-northeast and dips shallowly about 30° to the northwest. Fold axes are subhorizontal and strike northeast. Stereoplots of poles to bedding (Fig. 4.3b) in the Apex Mountain complex indicate that the unit strikes northeast and dips moderately to steeply east and west. The best fit girdle of the poles to bedding strikes 313° and dips 82° northeast suggesting shallow northeast plunging folds. Thus folding in the Apex Mountain complex and the Nicola Group are similar in strike of axial planes. However, folding in the Nicola Group is more open.

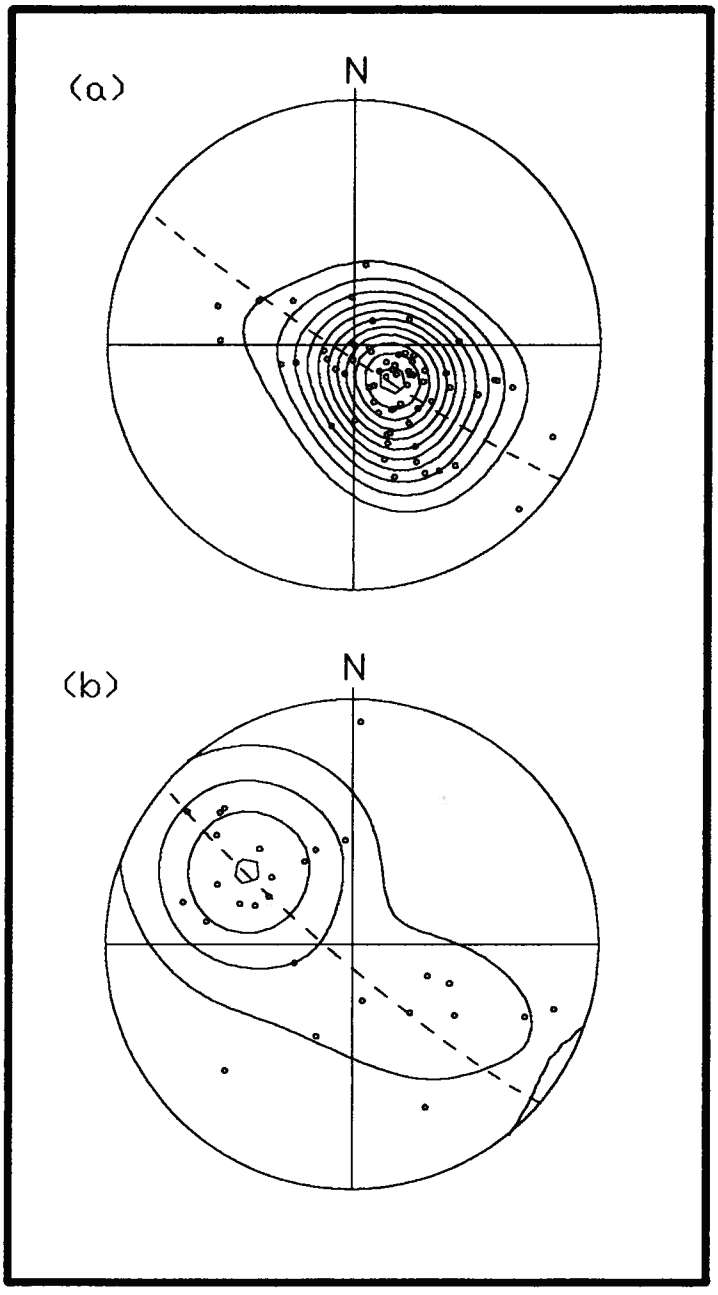

Figure 4.3: Stereoplots of structural measurements from the French - Good Hope mine area, south-central British Columbia: (a) poles to bedding (68 measurements) from the Nicola Group; (b) poles to bedding (27 measurements) from the Apex Mountain complex.

4.3 Phyric and aphyric Hedley intrusions (unit 7)

4.3.1 Detailed description

Hedley intrusions (unit 7) form sills, dykes and irregular stock like bodies in the French - Good Hope mine area (Fig. 4.1). They vary from: (i) fine to medium grained quartz diorite to (ii) hornblende phyric tachylitic basalt to (iii) aphyric tachylitic basalt. The hornblende phyric and aphyric intrusions are unique to the French Mine area, whereas quartz diorite occurs throughout the district.

Fine to medium grained quartz diorite forms a large sill (<50 m thick) that intrudes along or near the contact of the Copperfield breccia and Whistle formation northeast of the French mine. At the French mine, it forms a stock like body containing numerous mafic xenoliths (Plate 4.14), and a number of smaller dykes and sills (Figs. 4.4 and 4.5). It consists of hornblende (<3 mm) and plagioclase (<2 mm: An_{40}) phenocrysts in a fine grained matrix of plagioclase, orthoclase and quartz. Accessory minerals include biotite, zircon, apatite, titanite and opaque minerals. A sample collected from the quartz diorite stock like body for U-Pb zircon dating contained insufficient zircon for analysis.

Hornblende phyric tachylitic basalt occurs as sills and dykes within the Hedley formation at the French mine (Figs. 4.4 and 4.5). Euhedral hornblende (<1 cm) and rare plagioclase crystals (<3 mm) occur in a fine grained matrix of feldspar microlites, glass and opaque minerals (Plate 4.15). The hornblende phenocrysts are partly to completely pseudomorphed by fine grained brown biotite.

Aphyric tachylitic basalt occurs as thin brown sills, dykes or as margins to phyric sills (Plate 4.16) and stock like bodies within the Hedley formation at the French mine. Stock like bodies exposed in underground stopes may be composite bodies consisting of numerous dykes that fed the adjacent sills (Fig. 4.16a). Thin beds of structureless Hedley formation siltstone and limestone separate the sills; these beds vary from <0.5 to 3 m thick (Plate 4.17). The sills are <2 cm to a few metres in thickness. Irregular upper and lower contacts with pronounced lobes, fingers and stringers commonly thicken, thin, twist and turn over distances of <1 m. Along one sill contact, spherical clasts of basalt are surrounded by Hedley formation sediment (Plate 4.18). These admixtures of igneous clasts enclosed within sediment and up to 20 cm from the sill contact are interpreted to be globular peperite (see Section 4.3.3).

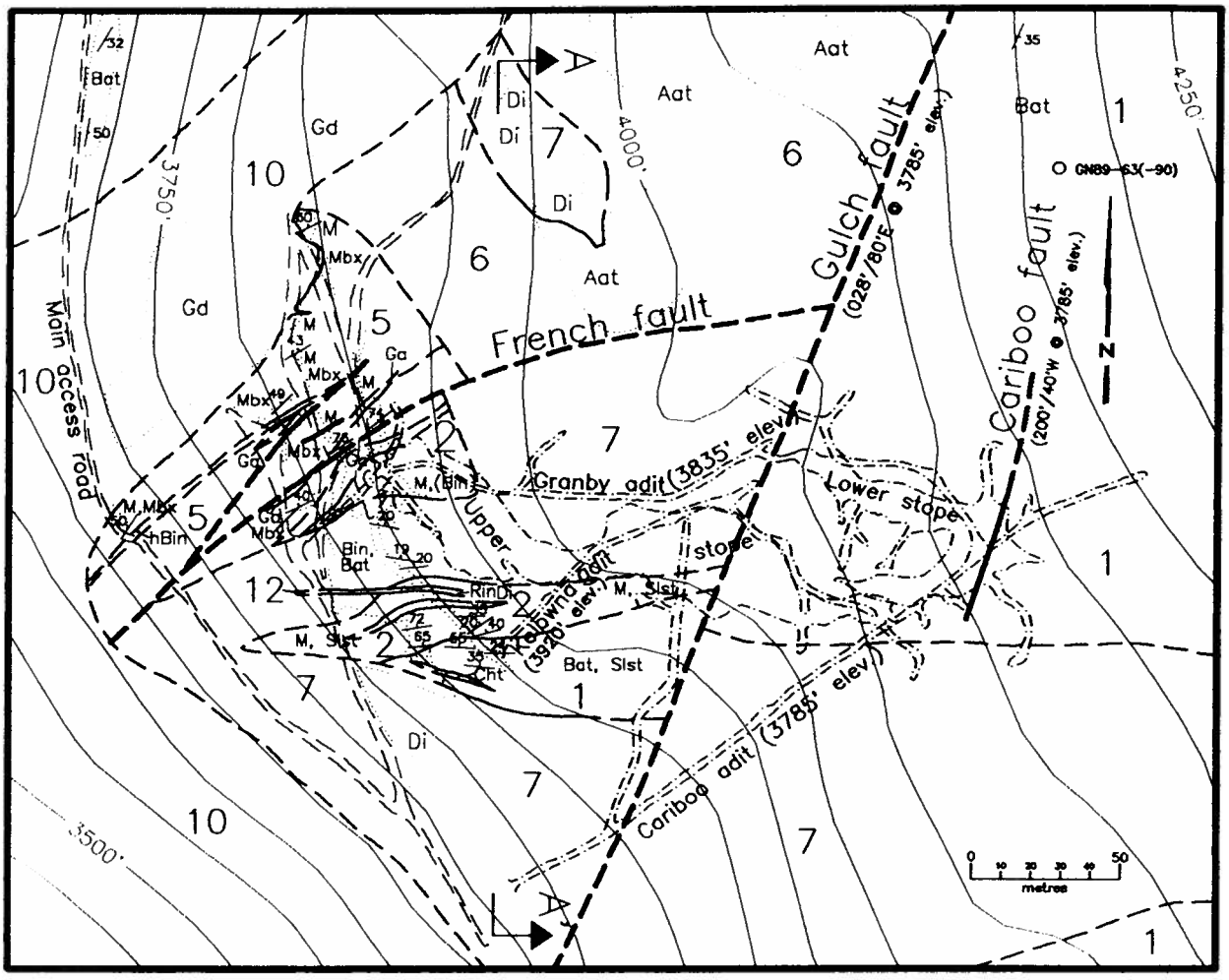

Figure 4.4: Detailed geology of the French Mine, south-central British Columbia. Map units are: 1 = Apex Mountain complex, 2 = Hedley formation, 5 = Copperfield breccia, 6 = Whistle formation, 7 = Hedley intrusions, 10 = Cahill Creek pluton. Rock abbreviations are: M = marble, Mbx = marble breccia, Slst = siltstone, Bat = mafic ash tuff, Cht = chert, Bin = aphyric mafic intrusion, hBin = hornblende phyric mafic intrusion, Aat = intermediated ash tuff, Ga = garnetite skarn, Di = diorite, Gd = granodiorite. Line types are: thick dash = faults, medium dash = geological contacts, thin dash = gravel roads, dash-dot = underground workings. The collar of diamond drill hole GN89-63 is marked. Contours are in feet above sea level.

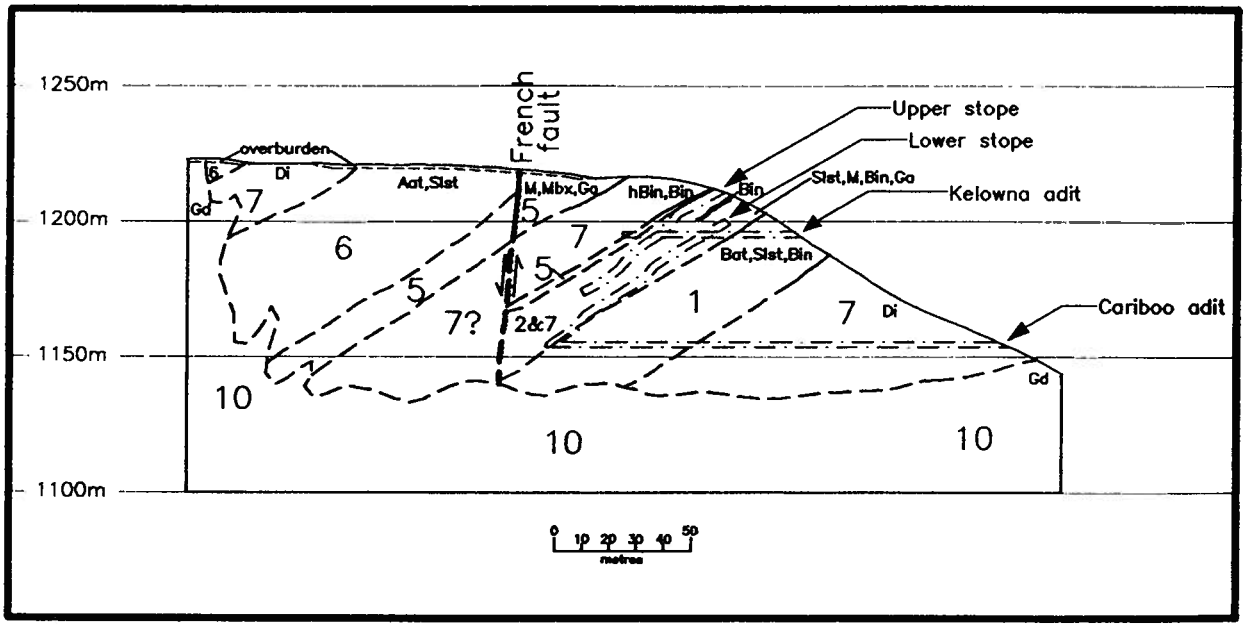

Figure 4.5: North - south cross-section A-A' (see Fig. 4.3 for section location) through the French mine, south-central British Columbia. Map units are: 1 = Apex Mountain complex, 2 = Hedley formation, 5 = Copperfield breccia, 6 = Whistle formation, 7 = Hedley intrusions, 10 = Cahill Creek pluton. Rock abbreviations are: M = marble, Mbx = marble breccia, Slst = siltstone, Bat = mafic ash tuff, Cht = chert, Bin = aphyric mafic intrusion, hBin = hornblende phyric mafic intrusion, Aat = intermediated ash tuff, Ga = garnetite skarn, Di = diorite, Gd = granodiorite. Line types are: thick dash = faults, medium dash = geological contacts, dash-dot = underground workings.

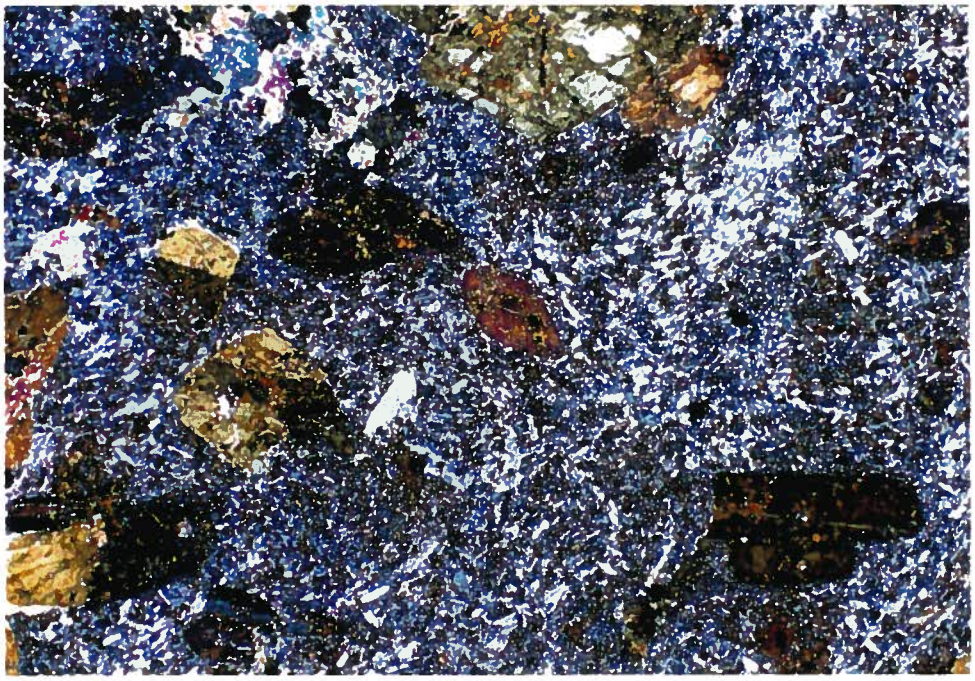

Plate 4.15: Photomicrograph (transmitted light, crossed polars, field of view = 5.0 mm) of hornblende phyric Hedley intrusion (unit 7: Fig. 4.4). Euhedral hornblende crystals are partly replaced by fine grained biotite.

Plate 4.16: Photograph across aphyric - hornblende phyric contact (dashed lines), Hedley intrusion (unit 7: Fig. 4.4). Contact is gradational over 10's of centimetres. Outcrop is along upper haulage track immediately east of the "open" stopes.

Plate 4.17: Aphyric Hedley sills (unit 7: Fig. 4.4) enveloped by a 1cm rim of structureless Hedley formation siltstone (unit 2). Note the irregular wavy sill contact. Outcrop is along upper haulage track immediately west of the 3920 Level adit.

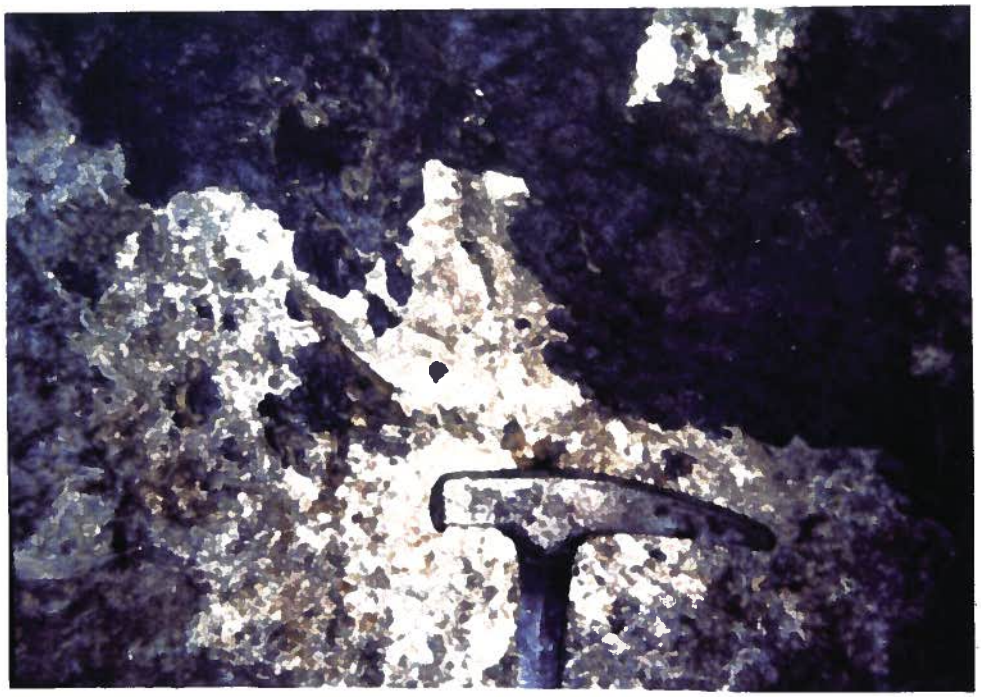

Plate 4.18: Possible globular peperite along contact of Hedley formation siltstone (unit 2: Fig. 4.4) and aphyric Hedley sill (unit 7). Exposure is on the back of the Granby adit, approximately 75 metres from the portal.

Aphyric intrusions vary in texture from altered glass to randomly oriented microlites of plagioclase and ilmenite in an altered glass matrix. The glass can be flow banded and folded (Plate 4.19), or massive with well developed perlitic cracks (Plate 4.20). Plagioclase (<1 mm) forms radiating splays of acicular crystals that have a common nucleation point (bow-tie texture [Lofgren, 1974]: Plate 4.21). These crystals in cross-section (belt-buckle texture [Bryan]: Plate 4.22) have cores of altered glass. Ilmenite occurs as acicular crystals (<1 mm) and as a fine grained dusting throughout the matrix. In some thin sections, vesicles and irregular microveinlets of mosaic quartz cut the altered glass matrix (Plate 4.23). These irregular structures, interpreted as sedimentary dykelets, formed as a result of siltstone or silica rich fluids infilling fractures created by quenching of the basalt during intrusion.

4.3.2 Petrochemistry

Sixteen samples of Hedley intrusion were analyzed and are used to: (i) compare the composition of the phyric and aphyric bodies, (ii) chemically classify the rocks, and (iii) compare their compositions with those of known tectonic settings. Most of the phyric intrusions are overprinted by biotite; glass in the aphyric intrusions has been replaced by biotite, chlorite, actinolite-tremolite, clays and unknown fine grained minerals. Alteration likely affected the major element chemistry; therefore classification schemes using these elements may be suspect. Immobile trace elements, relatively unaffected by hydrothermal and low grade metamorphic processes, are used in some of the diagrams below. Tables C.3 and C.4 presents major element chemistry along with their calculated Cross, Iddings, Pearson and Washington (CIPW) normative mineralogy, and trace element chemistry, respectively. Sample locations are plotted on Figure 4.6.

Quartz diorite (field name, unit 7, Fig. 4.1 and Map1) plots in the quartz diorite field on a normative mineralogy diagram (Fig. 4.7: Streckeisen and Lemaitre, 1979). On a total alkali *vs.* silica (TAS) diagram (Fig. 4.8: Middlemost, 1985) it plots in the monzodiorite, quartz monzodiorite and quartz diorite fields. These samples have higher Na_2O values (average of fourteen analyses = 4.5%) compared to

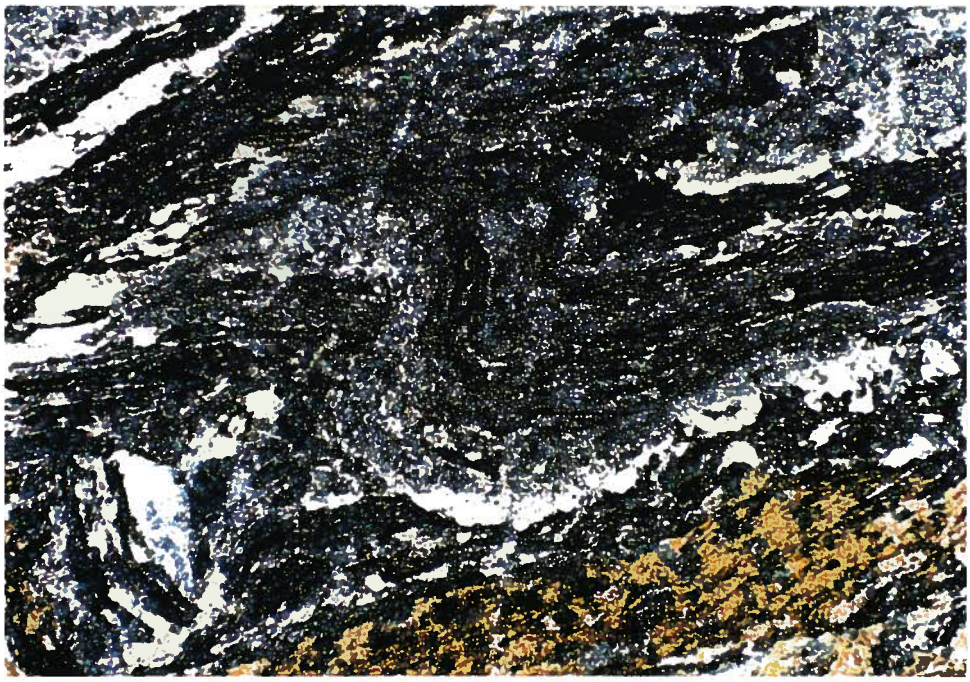

Plate 4.19: Photomicrograph (transmitted light, crossed polars, field of view = 5.0 mm) of flow banded aphyric Hedley sill (unit 7: Fig. 4.4). Sample is from lower stope of the French mine.

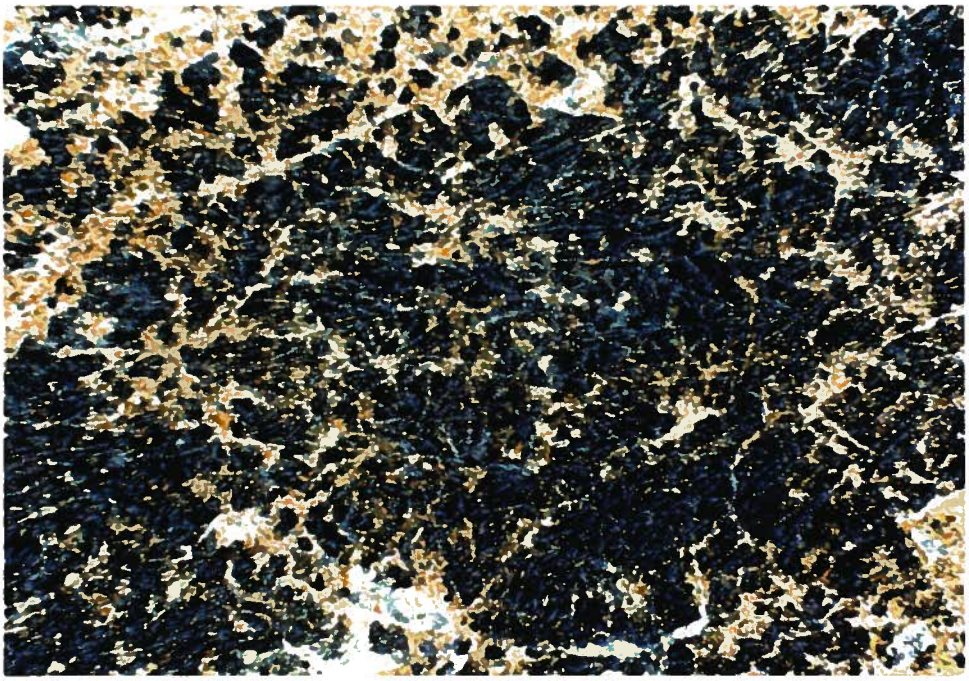

Plate 4.20: Photomicrograph (transmitted light, crossed polars, field of view = 5.0 mm) of quenched, glassy, aphyric Hedley sill (unit 7: Fig 4.4) with well developed perlitic cracks. Sample is from lower stope, French mine.

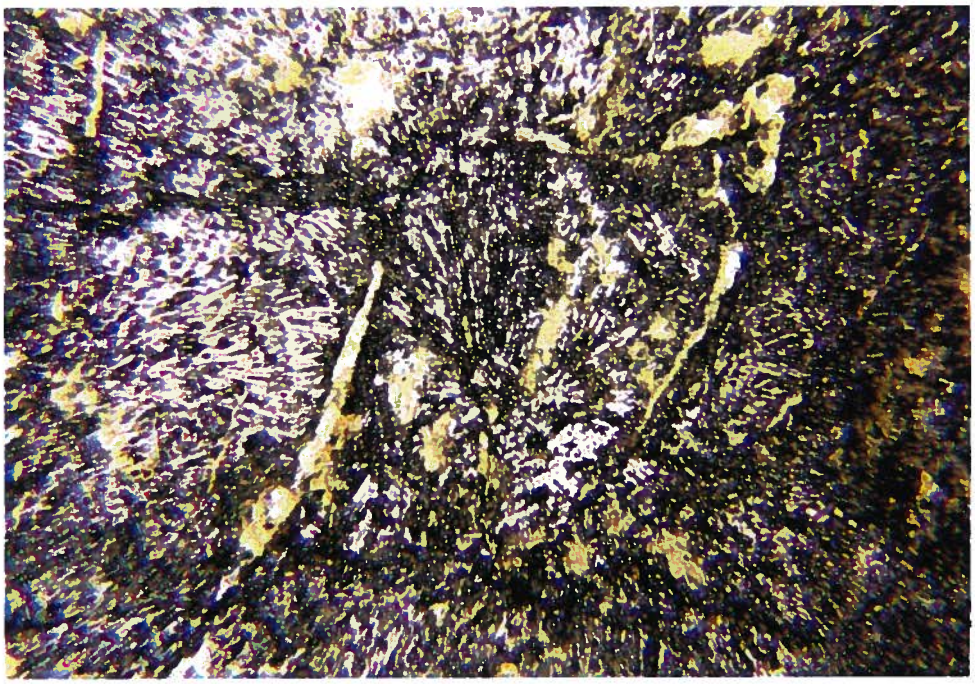

Plate 4.21: Photomicrograph (transmitted light, crossed polars, field of view = 5.0 mm) of quenched aphyric Hedley sill (unit 7: Fig. 4.4). These radiating splays of acicular plagioclase crystals with a common nucleation point are called "bow-tie" texture (Lofgren, 1974). Sample is from lower stope, French mine.

Plate 4.22: Photomicrograph (transmitted light, crossed polars, field of view = 5.0 mm) of aphyric Hedley sill (unit 7: Fig. 4.4). Plagioclase crystals have altered glass cores. Such textures are described as "belt-buckle" texture (Bryan, 1972). Sample is from lower stope, French mine.

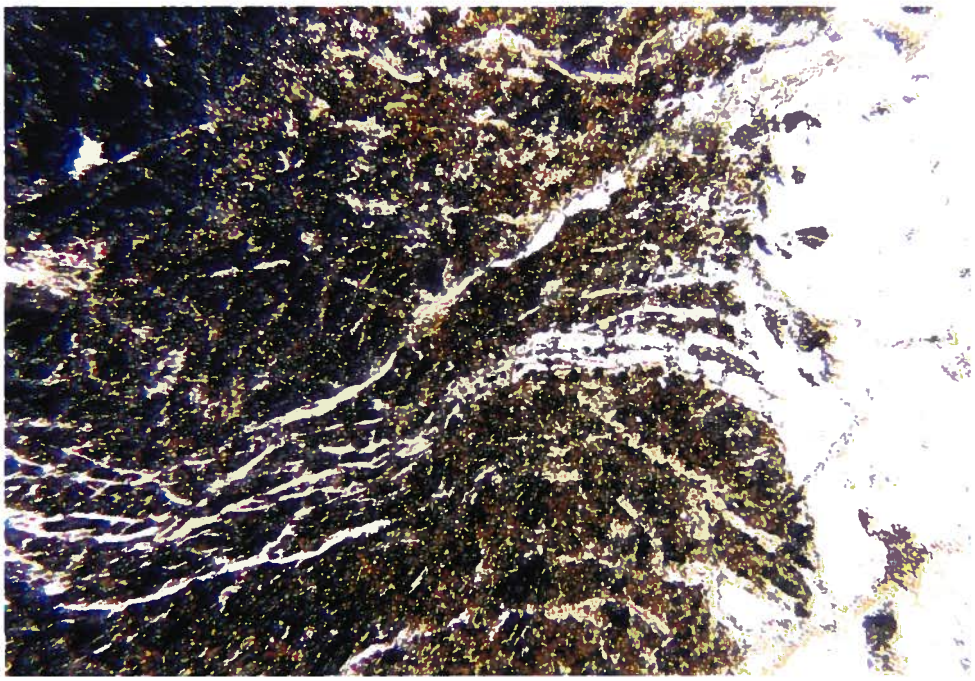

Plate 4.23: Photomicrograph (transmitted light, crossed polars, field of view = 1.25 mm) of mosaic quartz vesicles and microveinlets (on right) in aphyric Hedley sill (on left: unit 7, Fig. 4.4). Sample is from lower stope, French mine.

Plate 4.24: Thin centimetre scale aphyric basalt sill (unit 7: Fig. 4.4) within structureless Hedley formation siltstone (unit 2). Photograph is from lower stope in the French mine.

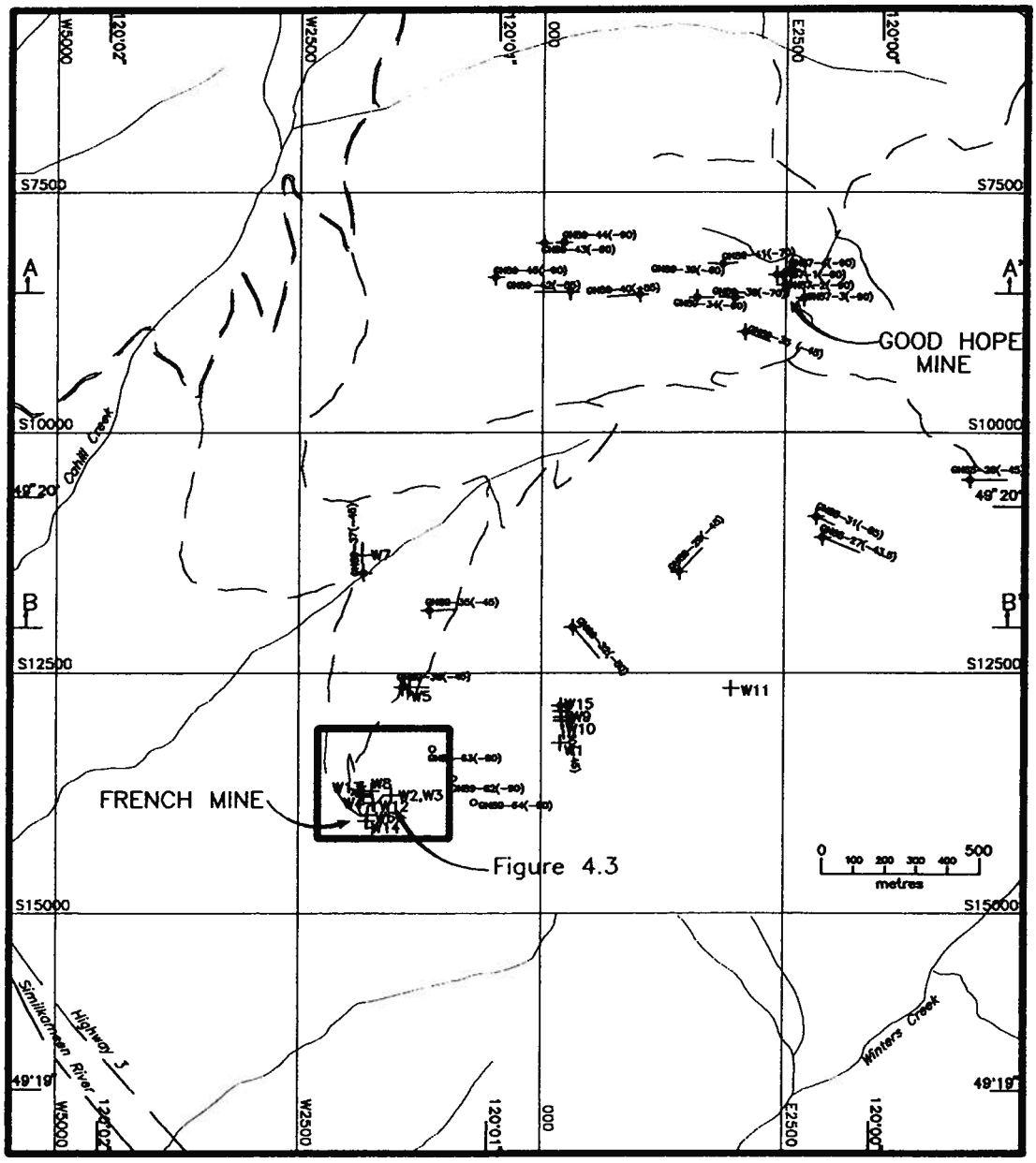

Figure 4.6: Plot of sample locations for whole rock chemical analysis (W: Tables C.3 and C.4).

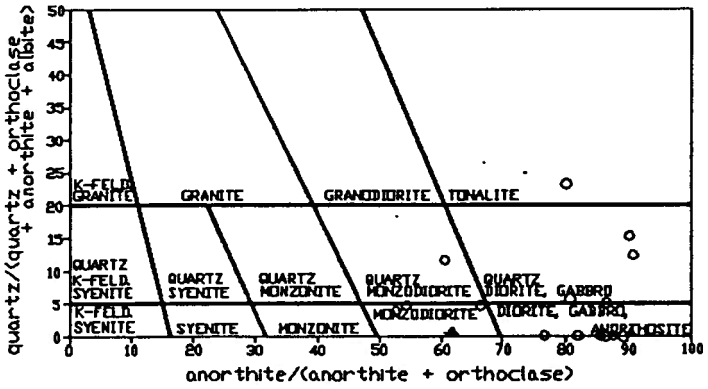

Figure 4.7: Chemical composition of Hedley intrusions (unit 7) French Mine area, south-central British Columbia. Analyses of Table C.3 are plotted on a normative diagram (Streckeisen and LeMaitre, 1979). Open squares = aphyric basalt; crosses = hornblende phyric basalt; circles = quartz diorite; triangles = Copper Mountain stock.

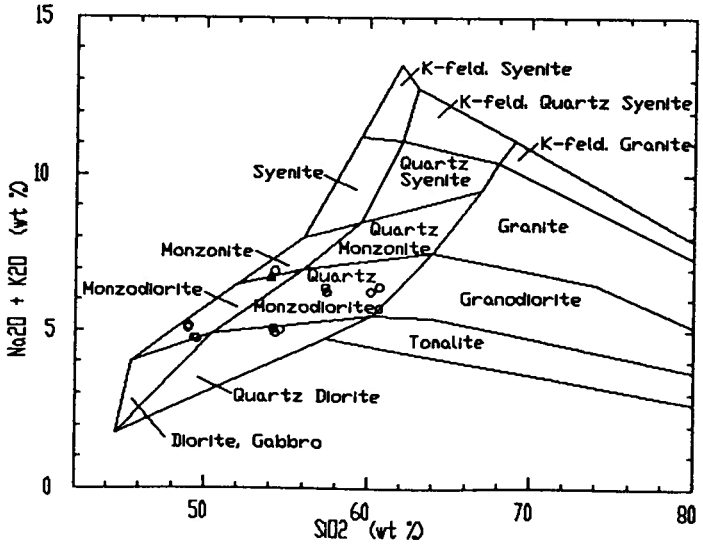

Figure 4.8: Total alkali *vs.* silica plot (compositional fields defined by Middlemost, 1985) of phyric Hedley intrusions from the French mine area, south-central British Columbia. Analyses from Table C.3 suggest that compositions vary from monzodiorite to quartz diorite and quartz monzodiorite. Circles = quartz diorite; triangle = Copper Mountain stock. However, addition of Na_2O from alteration is suspected (see text).

samples collected from sills and stocks west of the French - Good Hope mine area, which plot in the quartz diorite field (average of 27 analysis = 3.2%). This elevation in Na_2O likely reflects albitization associated with skarn alteration and does not necessarily represent a change in magma chemistry within the district.

Hornblende phyric and aphyric basalt intrusions (field names) plot mainly in the basalt and andesite fields in Figure 4.9 (Winchester and Floyd, 1977). One sample of aphyric basalt plots on the line separating the subalkaline basalt field from the alkaline basalt field.

Most samples on a TAS diagram are subalkaline (Fig. 4.10: Irvine and Baragar, 1971), however, two samples of hornblende phyric basalt plot in the alkaline field. They are similar to a sample from the Copper Mountain stock, a Late Triassic to Early Jurassic alkalic body spatially associated with porphyry Cu-Au mineralization, approximately 40 km to the west. However, all subalkalic samples in Figure 4.10 are calcalkaline on a total alkali, total iron and magnesium (AFM) diagram (Fig. 4.11: Irvine and Barager, 1985).

Samples were plotted on tectonic discrimination diagrams constructed for volcanic rocks. Most plots indicate the Hedley intrusions are similar to calcalkaline basalts common to arc environments. On the Ti/100 - Zr - Y*3 triangular diagram (Fig. 4.12: Pearce and Cann, 1973) samples plot mainly in the calcalkaline basalt (CAB) and island arc basalt (IAB) field; however, some samples plot in the within plate basalt (WPB) field. On the Ti/100 - Zr - Sr/2 triangular diagram (Fig. 4.13: Pearce and Cann, 1973) samples plot in both the CAB and IAB field.

4.3.3 Discussion

Hedley intrusions form a texturally diverse suite of intermediate to mafic calcalkaline rocks. Age relationships between the quartz diorite and the hornblende phyric and aphyric intrusions is problematic. It is not known whether the quartz diorite represents a magma pulse from a more crystallized portion of

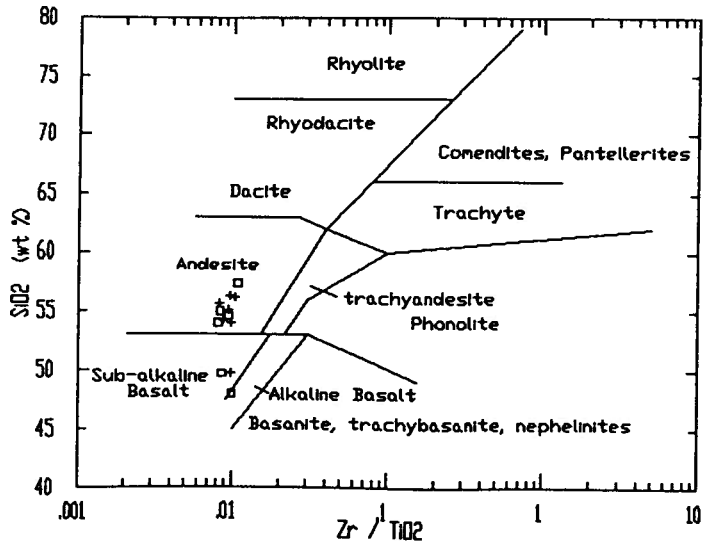

Figure 4.9: SiO_2 *vs.* log (Zr/TiO_2) plot (Winchester and Floyd, 1977) of hornblende phyric and aphyric Hedley intrusion from the French mine area, south-central British Columbia. This plot of analyses from Table C.3 suggest that both these units are andesitic basalt. Open squares = aphyric basalt; crosses = hornblende phyric basalt.

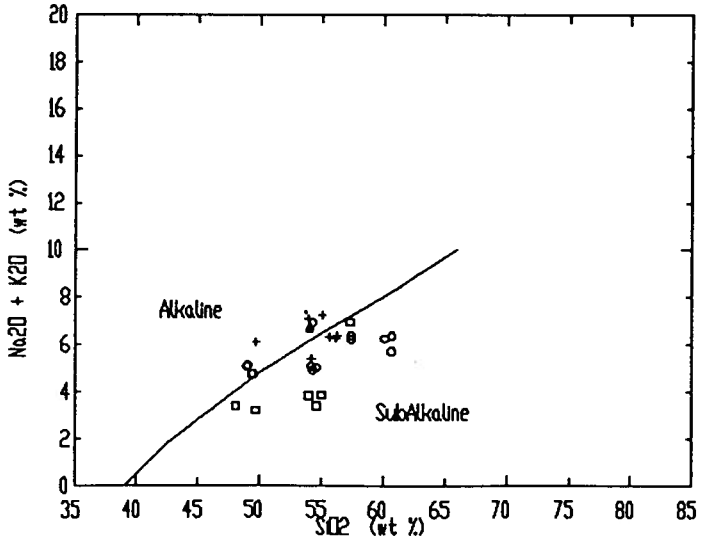

Figure 4.10: Total alkali *vs.* silica plot (TAS: Irvine and Barager, 1971) of phyric and aphyric Hedley intrusions from the French mine area, south-central British Columbia. Analyses from Table C.3 indicate that both these units are generally subalkalic. Some aphyric basalt, hornblende phyric basalt and quartz diorite analyses straddle the alkalic boundary. Open squares = aphyric basalt; crosses = hornblende phyric basalt; circles = quartz diorite; triangle = Copper Mountain stock.

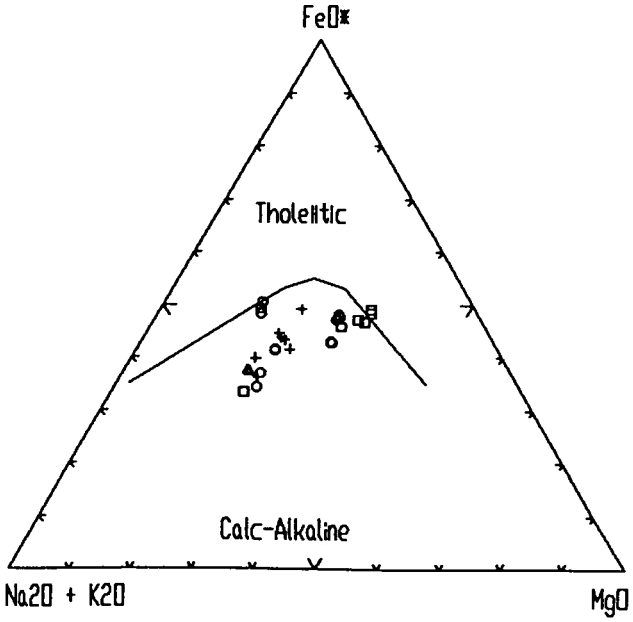

Figure 4.11: AFM diagram (Irvine and Baragar, 1971) of subalkalic phyric and aphyric Hedley intrusions from the French mine area, south-central British Columbia. Analyses from Table C.3 indicate that both units are, overall, calcalkaline (*cf.* Figs 4.10 and 4.11). Open squares = aphyric basalt; crosses = hornblende phyric basalt; circles = quartz diorite; triangles = Copper Mountain stock.

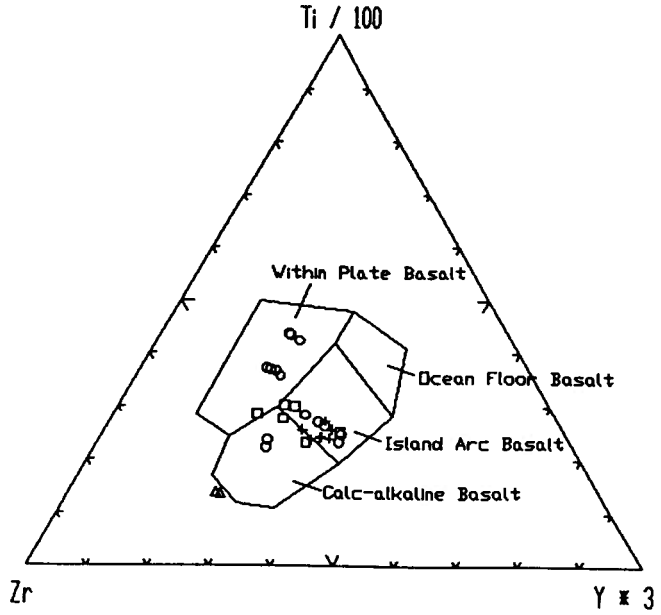

Figure 4.12: Triaxial Ti/100 - Zr - Y*3 plot (Pearce and Cann, 1973) of phyric and aphyric Hedley intrusions from the French Mine area, south-central British Columbia. Analyses from Table C.3 indicate that overall, the units have a calcalkaline signature (*cf.* Fig. 4.9). Open squares = aphyric basalt; crosses = hornblende phyric basalt; circles = quartz diorite; triangles = Copper Mountain stock.

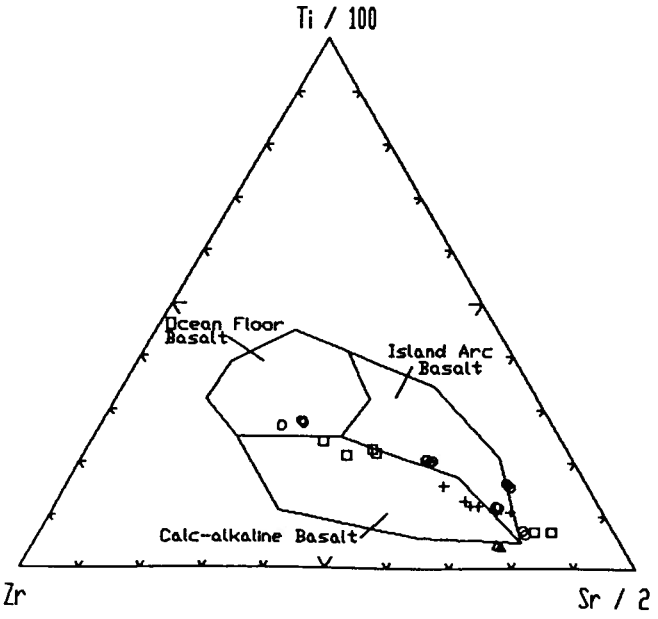

Figure 4.13: Triaxial Ti/100 - Zr - Sr/2 plot (Pearce and Cann, 1973) of phyric and aphyric Hedley intrusions from the French Mine area, south-central British Columbia. Analyses from Table C.3 indicate that overall, the units have a calcalkaline island arc basalt signature (*cf.* Figs. 4.9 to 4.12). Open squares = aphyric basalt; crosses = hornblende phyric basalt; circles = quartz diorite; triangles = Copper Mountain stock.

the same magma chamber as the hornblende phyric and aphyric basalt, or represents a magma pulse from an unrelated magma chamber.

The identification of the aphyric basalt units as intrusive and intimately associated with skarn alteration is significant in that these units were mapped by previous workers as hornfelsed sediment, tuff or flows. Because gold skarn mineralization is intimately related to aphyric basalt sills, and related stocks or dykes, this new interpretation has important implications as to the timing and depth of skarn formation at the French mine and at other skarn deposits in the Hedley camp. Additionally, this interpretation may be important in regional skarn exploration programs where a mineralizing intrusion has not been identified.

Aphyric basalt sills at the French mine exhibit a number of features that support intrusion of wet unconsolidated to poorly consolidated Hedley formation sediment. Features described in Section 4.3.1 include: (i) destruction of sedimentary structures, (ii) wavy sill contacts, (iii) globular peperite, (iv) quench textures, and (v) sedimentary dykes. Experimental studies documenting these phenomena are lacking. However theoretical studies (Kokelaar, 1982 and 1986) and magma-water experiments (Sheridan and Wohletz, 1983; Wohletz, 1983 and 1986; Wohletz and M^{c}Queen, 1984a and 1984b) involving different water to melt ratios, explain different types of interactions, contact configurations and clast types. It is assumed here that wet sediment with a high water content behaves in a manner similar to the magma-water experiments.

Intrusion into wet sediment is accomplished by local fluidization of sediment and subsequent removal of pore water as steam (Kokelaar, 1982). Fluidization is "the mixing of gas and loose fine grained material so that the whole flows like a fluid" (Reynolds, 1954; Bates and Jackson, 1987). It requires a certain minimum vapor flow velocity and is dependent on vapour density, sediment particle size and particle size distribution (Kokelaar, 1982). Precise conditions under which fluidization takes place are difficult to determine; however, expansion of the liquid responsible for fluidization decreases towards the critical point for water. For seawater, the critical point is 312 bars (assuming 3.45% solutes that are 100% NaCl). This is equivalent to 3.1 km of seawater or 1.6 km of wet sediment (assuming a density of 2 g/cm^3; Kokelaar, 1982). At a pressure greater than the critical point for seawater, expansion to dense

supercritical vapour is only moderate. In such a case, there would be no fluidization, because the vapour pressure would be insufficient to overcome the ambient hydrostatic pressure caused by the overlying sediment and water column. Vapour flow as a result of temperature and pressure gradients entrains and moves sediment laterally along the sill contact until the vapour condenses, at which point the sediment is deposited. Room for the sill is made by transport of sediment along the sill margin and by water removed as steam (Kokelaar, 1982).

Magma that comes into contact with wet sediment, therefore, can form steam bubbles that coalesce along the contact to form a thin vapour film. This vapour film is metastable, expanding and contracting on a millisecond or microsecond scale. Such an oscillating film may remain hydrodynamically stable and insulate the magma from the wet sediment, thus preventing hydroclastic fragmentation by thermal shocking caused by rapid contraction upon cooling. However, if enough heat energy is transferred to the vapour film, differences in density between the wet sediment, vapour film and magma can produce a number of instabilities. Three recognized instabilities have been termed: (i) Landua, (ii) Taylor, and (iii) Kelvin-Helmholtz (*cf.* Wohletz, 1986). Instabilities lead to the bulk mixing of magma and wet sediment. If the distortion of the magma surface is sufficiently violent, the magma may detach from the sill to form clasts (globular peperite) in the surrounding sediment (Fig. 4.16a). Continued oscillation can produce clasts that are mixed with the fluidized sediment by "oscillation pumping" (Busby-Spera and White, 1986). The drop like shape of the globular peperite is a result of surface tension effects; they are best developed in fine grained, well sorted loosely packed sediment where grain by grain entrainment of the enclosing sediment can occur within the vapour film. Globular peperites are more often basalt in composition because they have a low viscosity, and are more easily detached and mixed with the fluidized sediment than higher viscosity magmas such as rhyolite.

Globular peperite, similar to the interpreted exposure in the French mine workings (Plate 4.18), are interpreted by Busby-Spera and White (1987) to be an example of a fuel-coolant interaction (FCI); fine grained sedimentary particles are viewed as accidental components of the fluid. Fuel coolant interactions result from hot fluid (fuel) coming into contact with a cooler liquid (coolant) whose vaporization temperature is less that the fuel temperature. FCI's range from nonexplosive vapourization of coolant

along the coolant - fuel interface, to highly explosive interactions. In the later case rapid mixing of the fuel and coolant is accompanied by rapid exchange of heat between the fuel and coolant. This causes sudden vaporization of the coolant and explosive disruption of the system. Most research on FCI's has focused on developing fluid instability and detonation theories for rapid boiling processes that lead to hazardous conditions in nuclear reactors, liquid natural gas, and pulp and metal smelter industries (Wohletz, 1986).

The complex, irregular, wavy and bulbous sill-sediment contacts observed at the French mine (Plate 4.18) are thought to be caused by the above instabilities and by the low viscosity of the basaltic magma. The highly fluidized Hedley formation sediment allowed protrusions of the magma in any direction into the sediment (Plate 4.17). Lack of intimate intermixing of magma and wet sediment along most sill contacts suggest one or more of the following: (i) the sediment contained insufficient water, (ii) the overlying hydrostatic and/or lithostatic pressure was too high, or (iii) the magma solidified before globular peperite could form. What is interpreted as globular peperite can be observed at the French mine along one sill contact (Plate 4.18) and along the Princeton Portal road (1 km west) where Hedley quartz diorite forms a sill complex that is exposed over a distance of 1 000 m (Plate 3.8). Sediment reconstitution by fluidization surrounding the aphyric basalt sills may have caused the normally thinly laminated Hedley formation siltstone to be structureless (white rims in Plates 4.17 and 4.24).

Thin centimeter-scale sills or dykes up to 0.5 m long are extruded from larger metre-scale bodies underground at the French mine (Plate 4.24). Steam moving away from the larger sill or dyke contact into sediment allows thin stringers of magma within the outward rushing fluidized sediment to form these thin intrusions. In such cases, steam does not leave the sill-sediment interface until the host being penetrated is near the boiling temperature appropriate for that depth; when boiling in the host occurs the vapour immediately condenses (Kokelaar, 1982).

Flow banding was observed at thin section scale at the margins of some sills (Plate 4.19). It is likely a result of continued movement accompanied by addition of magma within the sill interior during solidification of the sill margin.

Microveinlets and vesicles of quartz cutting the sills are interpreted to be fluidized Hedley formation siltstone dykelets injected along fractures formed when the protective vapour film was disrupted (Plate 4.23). Quenching combined with continued magma movement in the sill interior resulted in fracturing of the sill margin. Injection of fluidized siltstone into low pressure fractures may be responsible for these sedimentary dykelets.

Quench, skeletal plagioclase textures (Plates 4.21 and 4.22) are common in rift environments such as mid-oceanic ridges or marginal basins where magma is intruded along fractures into water or unconsolidated wet sediment (Wilson, 1989; Busby-Spera and White, 1987). Crystals develop surface to volume ratios that are dependent on the growth and diffusion rate allowed by the physical conditions accompanying crystallization (Bryan, 1972). Growth of plagioclase in quench glass (aphyric basalt sills) occurs under supercooled conditions in which the high viscosity of the melt significantly reduces the diffusion rate. Under these conditions, the ratio of the diffusion rate of the solute atoms in the liquid to the growth rate of the crystal is significantly less than unity. According to the theory of spherulite growth (Keith and Padden, 1963) as applied to silicate systems (Lofgren, 1971b), the most efficient growth form is one in which the surface to volume ratio is a maximum; which results in the skeletal plagioclase crystals observed in some sills. These observations agree with experimental work by Lofgren (1974) and Lofgren and Donaldson (1975) where plagioclase morphology is described as a function of diffusion and growth rates.

4.4 Alteration and mineralization at the French mine

4.4.1 Skarn association with sills and dykes

Gold skarn mineralization is spatially and temporally associated with phyric and aphyric Hedley intrusions hosted within limestone and siltstone of the Hedley formation. Skarn alteration is zoned outward at the centimetre to metre scale from aphyric and hornblende phyric basalt sill or dyke contacts and is strongly dependent on protolith composition. Except for some pillars in the lower stope, most of the

economic gold skarn was removed during mining. Therefore, the overall mineralogical zonation across the deposit is unknown. Individual skarn zones appear to be contained within box like zones formed between sills, and close to sill and intersections with dykes (Fig. 4.16b). Sulphide mineralization is generally <1%, however along the French fault and in skarn zones up to 50 m east of the fault, sulphide mineralization is >5% and comprises mainly bornite and chalcopyrite. Historically, this higher sulphide mineralization--called the 'West Copper Zone'--was not mined because it consumed cyanide, which lowered precious metal recoveries in the milling process (Sharp, 1976).

Hedley formation in the vicinity of the French mine (Fig. 4.4) strikes east and dips gently north. Mine workings (Figs. 4.4 and 4.5) consist of two bedding parallel stopes that are open to surface and accessed by three haulage adits (Kelowna, Cariboo and Granby). Stopes up to 225 m long and 2-15 m high extend from surface to 90 m down dip. They generally dip shallowly to the north. However, where sills apparently step-up stratigraphy the stopes are steeper. The two main stopes are separated by 2-8 m of biotite-rich aphyric Hedley sills and unmineralized Hedley formation sediment. Copperfield breccia commonly forms the back of the upper stope. Mineralization is terminated against the steep French fault on the west, and bottoms on, or is cut off on the east, by the moderate (40^{o}) west dipping Cariboo fault (Fig. 4.4). Other northeast faults identified underground have displaced mineralization by <3 m.

Skarn in the French mine can be classified as: (i) endoskarn, formed within the aphyric or phyric intrusions, or (ii) exoskarn, formed in the carbonate rich sediments adjacent to the sills. The features of these types of skarn are detailed below.

4.4.2 Endoskarn

Phyric and aphyric Hedley intrusions exhibit varying degrees of endoskarn replacement. Endoskarn occurs as: (i) pervasive biotitization, and as successive mineralogical envelopes formed around (ii) microveinlets, and (iii) margins of aphyric intrusions.

Pervasive biotitization occurs in a stock like body of quartz diorite that crops out at the Cariboo adit and in hornblende phyric and aphyric basalt sills and dykes in and around the French mine (Fig. 4.4). Alteration in the quartz diorite ranges from fine grained brown biotite replacement along hornblende crystal margins to complete pseudomorphing of the crystal. Associated with this potassic alteration is variable replacement of the matrix by fine grained albitic plagioclase, orthoclase and quartz resulting in a 'bleached' appearance to the intrusion. Hornblende phyric and aphyric basalt intrusions are overprinted by fine grained brown biotite that gives these rocks a dark purplish brown colour (Plate 4.15), which is common to many hornfelsic rocks.

Microveinlets with successive mineralogical envelopes cross-cut the pervasive biotite alteration in the hornblende phyric and aphyric basalt intrusions. The microveinlets (<3 mm) are randomly oriented and consist of chlorite, epidote, clinozoisite, titanite and opaque minerals. Successive mineralogical envelopes (<5 cm) around these microveinlets consists of grossular garnet (Ad_{20}-Ad_{50}: Fig. 4.14, Table D.2), clinopyroxene (Hd_{65}-Hd_{100}: Fig. 4.15, Table D.3) and orthoclase (Plate 4.25). The succession of mineralogical envelopes record changing fluid conditions and interactions through time and space. Consequently, some microveinlets have only partially developed mineralogical envelopes. In such examples, envelopes about the microveinlet can consist of 1 envelope (orthoclase) or 2 envelopes (orthoclase: outer envelope and clinopyroxene: inner envelope). Locally, where the frequency of microveinlets is high and alteration envelopes encroach on each other, massive orthoclase + clinopyroxene skarn makes protolith identification difficult. The microveinlets, interpreted to have formed during quenching and fracturing of the intrusion, were subsequently infiltrated by hydrothermal fluids and/or unconsolidated sediments. Garnet skarn is locally developed where fluidized limestone is injected into microfractures (see Section 4.3.1) or where adjacent limestone was affected by the magma during sill intrusion.

Margins of the aphyric intrusions record a mineralogical zoning that is similar to zoning around microveinlets. Fine grained pink orthoclase and pale green clinopyroxene form thin parallel envelopes (<3 cm) along the margins of the biotitic intrusions. Sills intruding limestone commonly develop a first envelope of pale reddish brown garnet parallel to the intrusion margin. Where sills intrude siltstones the

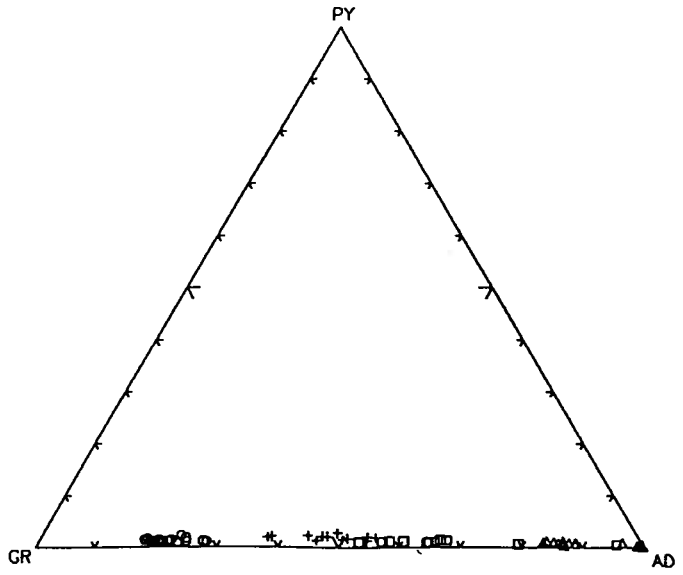

Figure 4.14: Ternary diagram showing the composition of garnet from skarn at the French mine, south-central British Columbia. Data are from Table D.2. Garnets in samples HD170 (circles) and GD6.8 (crosses) have an aphyric basalt (unit 7) protolith and samples HD267 (triangles) and 8969B (squares) have a limestone (unit 2) protolith. Garnets with the aphyric basalt protolith tend to be more grossular.

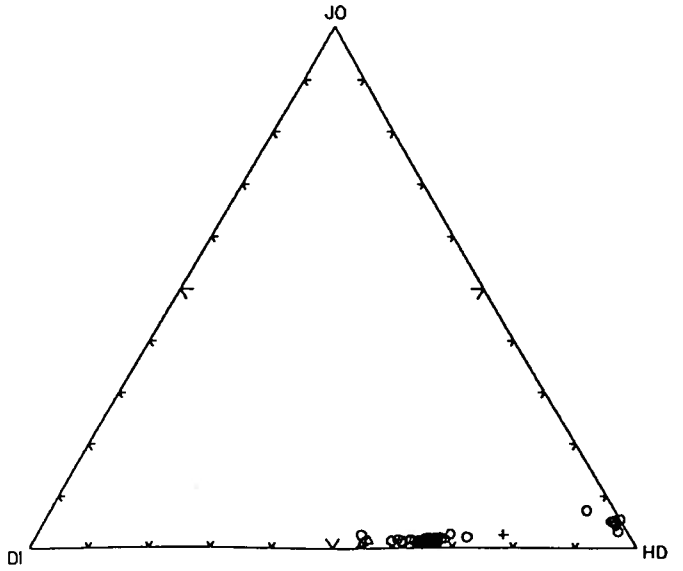

Figure 4.15: Ternary diagram showing the composition of clinopyroxene from skarn at the French mine, south-central British Columbia. Data are from Table D.3. Pyroxenes in samples HD170 (circles) and GD10.4 (triangles) have an aphyric basalt (unit 7) protolith, and sample 8969A (crosses) has a limestone (unit 2) protolith.

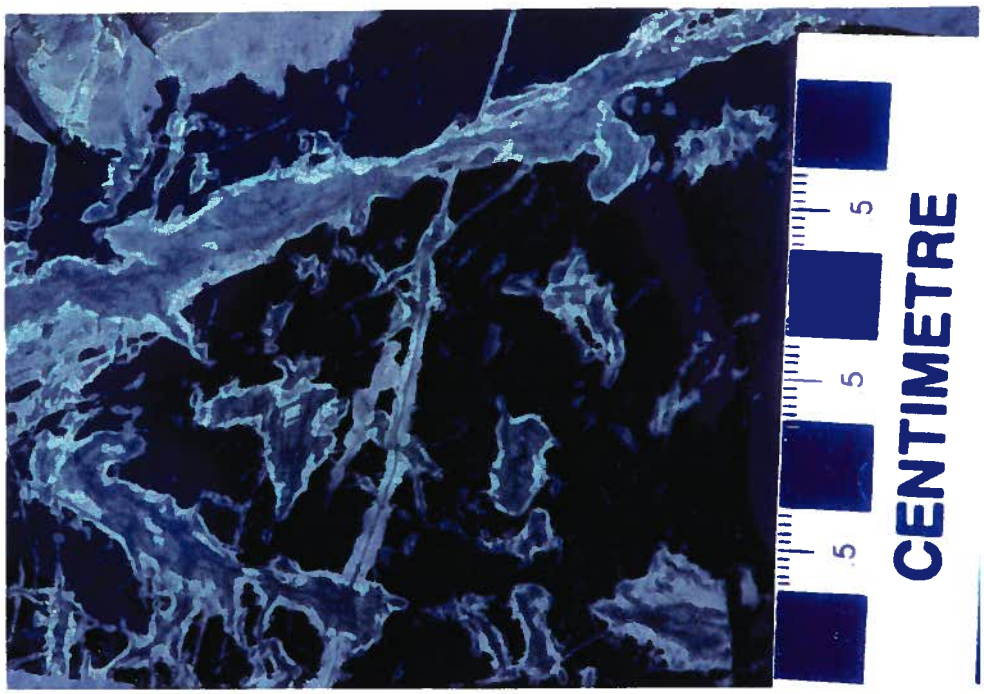

Plate 4.25: Microveinlets with successive mineralogical envelopes of pale green clinopyroxene and pink orthoclase cross-cutting brown biotite altered aphyric Hedley intrusion (unit 7: Fig. 4.4). Note where fracture density is high, individual envelopes encroach on each other to form massive orthoclase + clinopyroxene endoskarn. Sample is from waste dump, French mine.

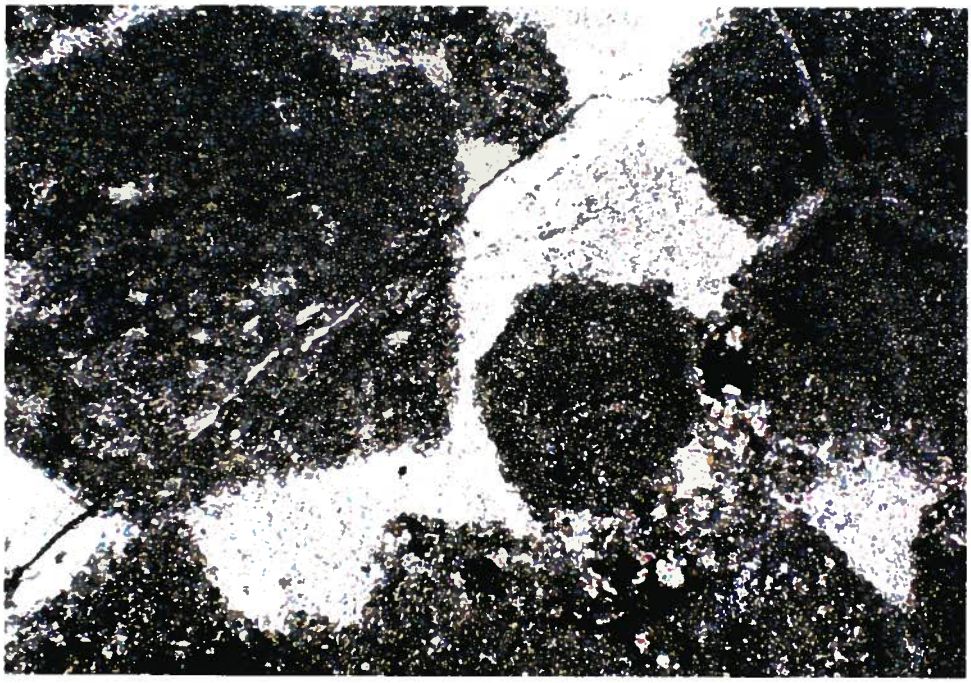

Plate 4.26: Photomicrograph (transmitted light, crossed polars, field of view = 5.0 mm) of isotropic euhedral garnet overprinting clinopyroxene skarned Hedley formation siltstone (unit 2: Fig. 4.4). Sample is from lower stope, French mine.

first envelope along the intrusion margin is clinopyroxene that expands outward into the sediment; this makes definition of the contact difficult. However, the mineralogical envelopes formed along the intrusion margin generally mimic the intrusion contact exactly. In some exposures, the sill contact is highly irregular and so are the corresponding mineralogical envelopes.

4.4.3 Exoskarn

Exoskarn formed by hydrothermal fluids associated with the Hedley intrusions is confined mainly to the Hedley formation at the French mine and forms a continuum from (i) recrystallization and reaction (bimetasomatic diffusional) skarn developed next to sill margins, and (ii) infiltrational skarn developed along sill contacts, sill-dyke intersections, fold hinges, and bedding and fracture planes. Reaction skarns operate on the centimetre scale and are mainly isochemical in nature (Korzhiniskii, 1965; Thompson, 1959; Rose and Burt, 1979; Vidale, 1969). They form by diffusional processes within a pore fluid in response to thermal and chemical gradients between different lithological units. Reaction skarns are characterized by: (i) pale calc-silicates, (ii) form over a few centimetres to 10's of centimetres, and (iii) original sedimentary structures are recognizable. Metasomatic infiltrational skarns form by the addition (Fe, Mg, Si, Al and other cations) and removal (Ca) of constituents by a hydrothermal fluid in response to pressure and thermal gradients, such that, the original bulk composition of the rock is changed. They are characterized by: (i) dark calc-silicates, (ii) form over 10's of centimetres to metres, and (iii) original textures and sedimentary structures are destroyed.

Recrystallization and reaction skarn varies from: (i) recrystallization of siltstone and marble a few centimetres from the sill contact, where the sills are thin and uncommon, to (ii) complete recrystallization of siltstone and limestone beds to fine grained mosaic quartz and coarse grained marble, respectively, where the sills are thick or abundant (Plate 4.24). In some exposures, pale, fine grained orthoclase + clinopyroxene + garnet skarn forms in impure siliciclastics and limestone laminae or at the

contacts of different lithologic units. In these examples, primary textures such as bedding, clasts, *etc.*, are generally preserved.

Infiltrational skarn forms the majority of calc-silicate alteration associated with gold skarn mineralization at the French mine. Fractures and contacts of sills and dykes acted as conduits or impermeable barriers along which hydrothermal fluids--responding to chemical, temperature and pressure gradients--were directed (Fig. 4.16b, Table 4.1). Pale to medium green, fine grained clinopyroxene (Hd_{65}-Hd_{100}: Fig. 4.15, Table D.3) forms along the contact of biotitic aphyric basalt intrusions and in siltstones adjacent to the intrusion contact. Reaction between the fluids responsible for clinopyroxene deposition and the biotite rich aphyric sills produced a thin envelope of pale pink orthoclase, as previously described in Section 4.2.2. With time and changing fluid conditions, the outward expanding clinopyroxene zone commonly changes to darker and presumably more iron rich hedenbergitic pyroxene and dark brown andraditic garnet (Ad_{50}-Ad_{100}: Fig. 4.14, Table D.2). Andraditic garnet (<3 mm) is generally isotropic, subhedral to euhedral and clear to reddish brown in thin section (Plate 4.26). Rare, sector twinned, optically zoned anisotropic andraditic garnets (<2 mm) may be a result of small amounts of water in the crystal structure (Plate 4.27; Meagher, 1980). In some garnet skarn, calcite + silica + vesuvianite + opaque minerals replaces and/or infills growth zones along the margin of the crystal and in vugs between crystals (Plate 4.28). Other minor minerals identified infilling or replacing these open spaces include: actinolite, titanite, wollastonite, clinozoisite, epidote, chlorite, axinite and scapolite (this study and Lamb, 1957). Vesuvianite (<3 mm) occurs as subhedral to euhedral grains replacing garnet crystals (Plate 4.28) and as zoned crystals in veinlets cutting garnet $\pm$ clinopyroxene skarn (Plate 4.29). Space between garnet crystals is apparently created by a volume reduction association with the replacement of limestone by garnet. Except for minor replacement of clinopyroxene and garnet by actinolite + chlorite + titanite + epidote, most of these hydrous-hydroxyl minerals are confined to vugs or fractures with little or no destruction of earlier mineral assemblages (Plate 4.31).

Opaque minerals generally make up <1% of the gold skarn mineralization, except along or 50 m east of the French fault where sulphides (mainly bornite and chalcopyrite) are >5% of the skarn (West Copper zone). Gold mineralization in most of the mine is intimately associated with arsenopyrite and

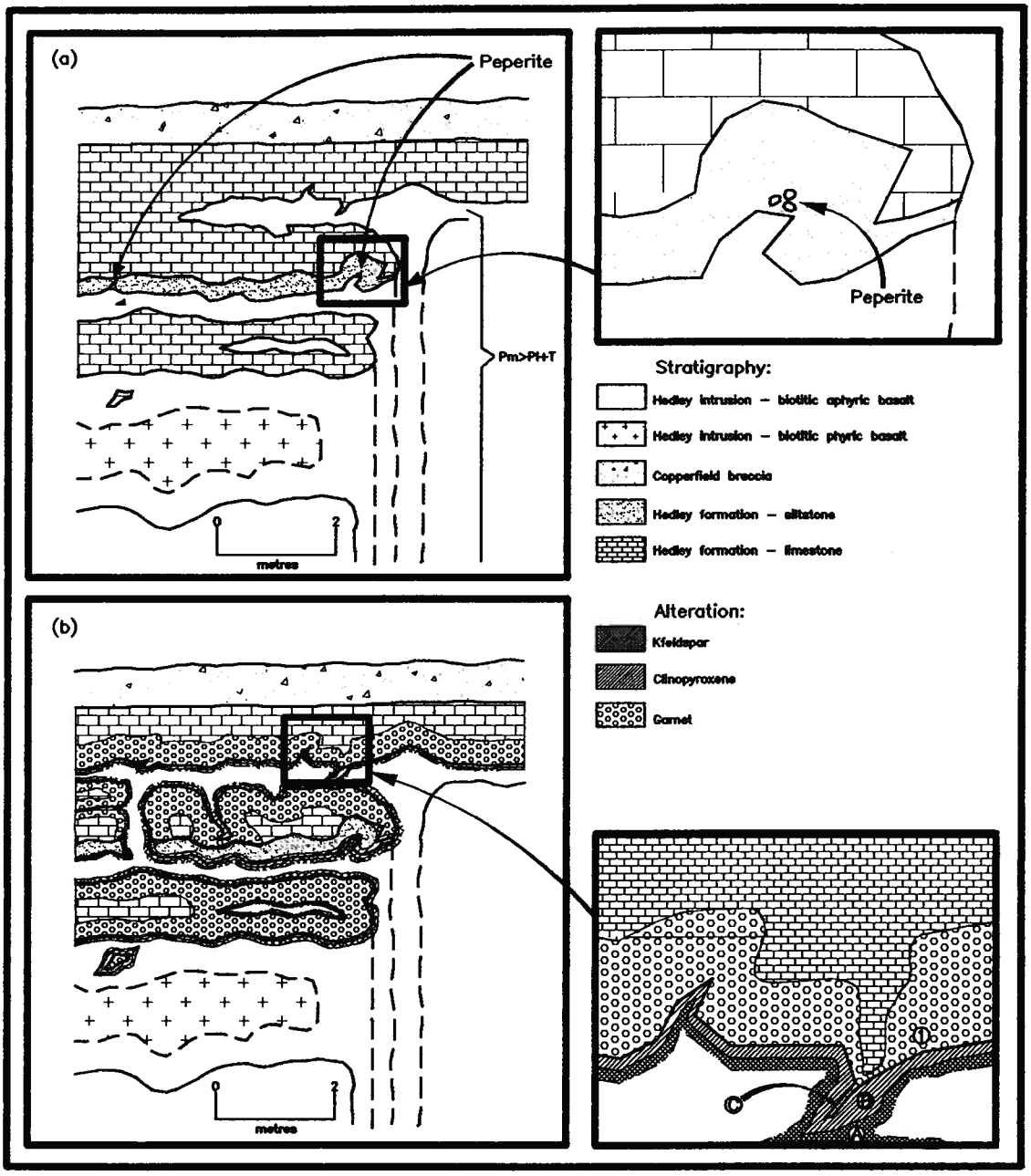

Figure 4.16: Schematic section showing skarn alteration within (endoskarn), and adjacent (exoskarn) to phyric and aphyric biotitic Hedley intrusions, French mine, south-central British Columbia. Line types are: solid line = protolith contact, dashed line = interpreted contact, dash-dot line = alteration contact. (a) Intrusion of sills into wet unconsolidated to poorly consolidated sediment. Note the wavy sill contacts and peperite formed along some sill contacts. Abbreviations are: Pm = magma pressure, Pl = overlying load of sediment and hydrostatic pressure, and T = tensile strength of sediment. (b) Alteration envelopes within and adjacent to intrusion contacts formed by hydrothermal fluids moving through calcareous sediments within box like zones between sills and dykes. Table 4.1 describes the mineralogical envelopes from the enlarged area across the sediment - sill contact (*cf.* Plate 4.25).

Table 4.1: Mineralogy of infiltrational skarn within (endoskarn), and adjacent to (exoskarn) biotitic phyric and aphyric Hedley intrusions, French mine, south-central British Columbia.

Envelope[1]	Description
A	Pale pink, fine grained K-feldspar endoskarn replacement of biotitic aphyric basalt intrusion.
B	Pale green, fine grained, iron poor clinopyroxene endoskarn replacement of biotitic aphyric basalt intrusion.
C	Pale brown, fine grained iron poor grossular garnet ($Ad_{<50}$) endoskarn replacement of biotitic aphyric basalt intrusion.
1	Dark brown, coarse grained iron rich garnet (Ad_{50-100}) and lesser dark green, iron-rich clinopyroxene exoskarn replacement of limestone; garnet crystals commonly are euhedral, sector twinned and anisotropic.

1. See Figure 4.16 and Plate 4.25 for location and character of envelopes.

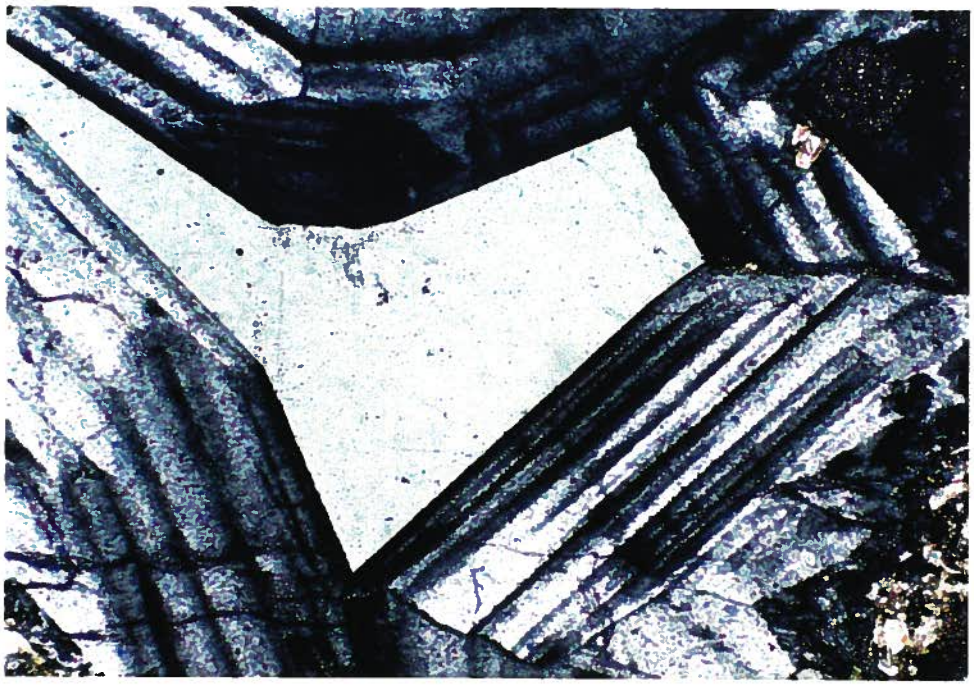

Plate 4.27: Photomicrograph (transmitted light, crossed polars, field of view = 1.25 mm) of sector twinned, optically zoned anisotropic garnet (<2 mm). The anisotropic nature of these garnets may be caused by minute amounts of water in their crystal structure. Protolith of this sample is uncertain, but is likely Hedley formation limestone (unit 2: Fig. 4.4). Sample is from lower stope, French mine.

Plate 4.28: Photomicrograph (transmitted light, field of view = 1.25 mm) of isotropic subhedral to euhedral garnet with calcite + silica + vesuvianite infilling growth zones parallel to the crystal margin. Protolith of this sample is likely Hedley formation limestone (unit 2: Fig. 4.4). Sample is from the lower stope, French mine.

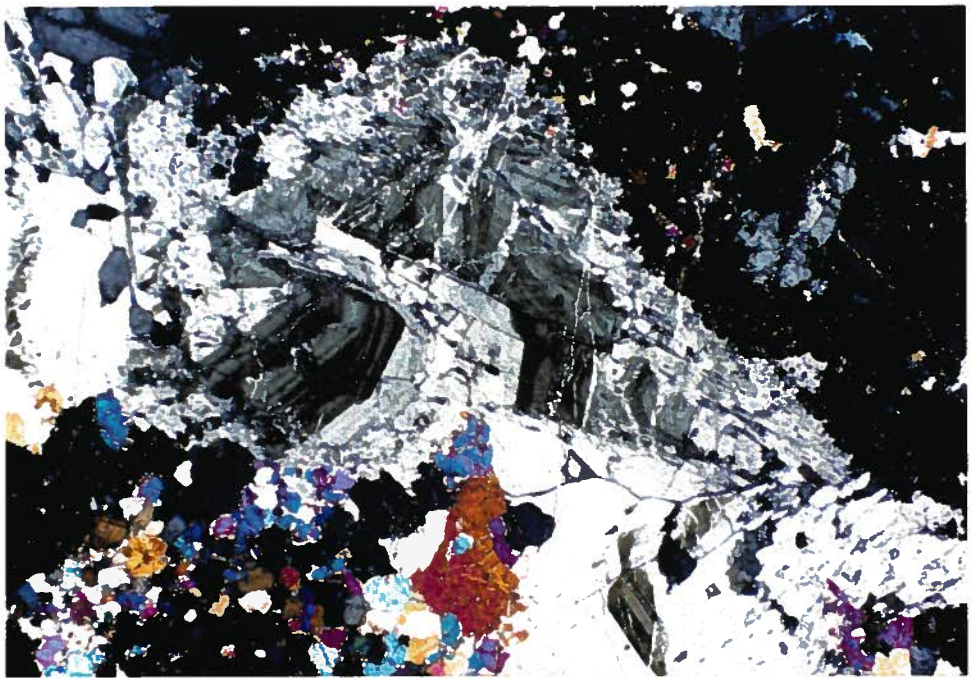

Plate 4.29: Photomicrograph (transmitted light, crossed polars, field of view = 5.0 mm) of optically zoned vesuvianite crystals in a vein cross-cutting garnet ± clinopyroxene skarn. Protolith of this sample is likely Hedley formation limestone (unit 2: Fig. 4.4). Sample is from the lower stope, French mine.

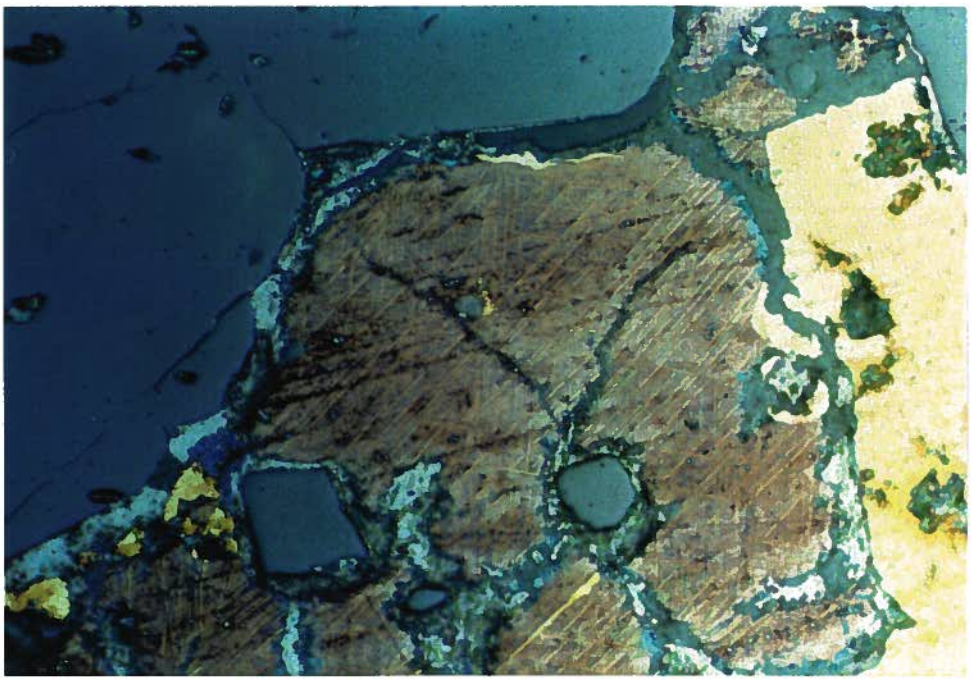

Plate 4.30: Photomicrograph (reflected light, field of view = 0.300 mm) of chalcopyrite exsolution lamellae in bornite infilling vugs between garnet crystals. Protolith of the sample is likely Hedley formation limestone (unit 2: Fig. 4.4). Sample is from the waste dump, French mine.

minor amounts of bismuth tellurides. Limited polished section examination and electon microprobe analysis of opaque minerals identified the following minerals in decreasing order of abundance: chalcopyrite, bornite, arsenopyrite, pyrrhotite, pyrite, magnetite, covellite, cobaltite, erythrite, malachite, azurite, joseite$_b$ ($Bi_{4+x}Te_{2-x}S$ where x = 0-0.3 and may contain some Se and Pb), bismuthinite, native bismuth and native gold. Minerals not identified in this study, but identified by previous workers include: maldonite, wittichenite, klaprothite, calcocite, loellingite-safflorite, hedleyite, gersdorfite, scheelite and molybdenite (Lamb, 1957; Hogan, 1953; Wober, 1990). Bornite (Table D.4) occurs interstitial to and in veins cutting garnet skarn in the West Copper zone. Chalcopyrite occurs as exsolution lamellae in or as margins to the bornite (Plate 4.30). Arsenopyrite is subhedral to euhedral and commonly contains very fine grained inclusions. Visible gold (Au_{79-93}: Table D.5), joseite$_b$ and bismuthinite (Table 4.6), actinolite and calcite infills vugs between iron-rich andraditic garnet (Ad_{50-100}: Table D.3, Plate 4.31). Gold with trace Cu and/or Hg appears to have a higher Au:Ag ratio than where these elements are absent [Table 4.5: 10.4 $\pm$ 1.0 (standard deviation) *vs.* 4.0]. At least two populations of gold fineness are indicated. Note that gold is from the same sample but that the two grains analyzed are different.

4.4.4 Discussion

Hydrothermal fluids moved through box like zones between impermeable dykes and sills or along fractures and bedding planes. As a result of temperature and pressure gradients a number of expanding contemporaneous alteration fronts responsible for the observed mineralogical zoning were produced (Fig.4.16b, Table 4.1). Infiltrational skarns (Korzhiniskii, 1965, Thompson, 1959) are defined below, as (i) endoskarn where formed in an aphyric basalt protolith, and (ii) exoskarn where formed in the sedimentary units.

Gradients in the composition of the hydrothermal fluid at each zonal front in the infiltrational skarn is reflected in a distinct mineralogical zonation. At the French mine, the skarn displays a consistent

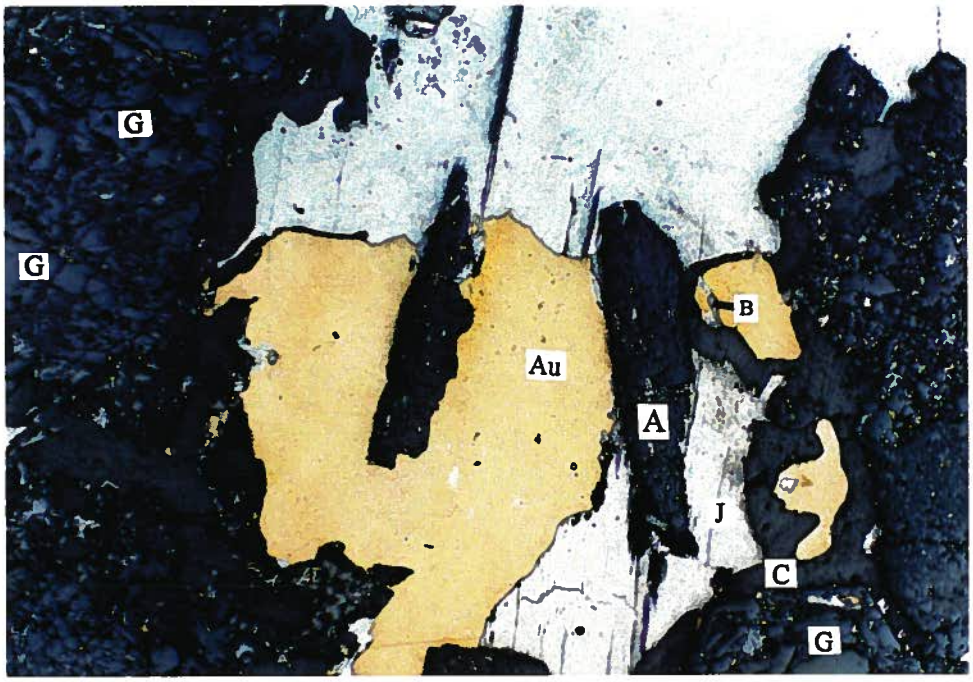

Plate 4.31: Photomicrograph (reflected light, field of view = 5.0 mm) of gold (Au: Au_{79-93}, $joseite_b$ (J), bismuthinite (B), actinolite (A), and calcite (C) infilling vugs between garnet (G) crystals. Protolith of the sample is Hedley formation limestone (unit 2: Fig. 4.4). Sample is from lower stope, French mine.

mineralogical zoning from aphyric basalt to orthoclase endoskarn, Mg-rich clinopyroxene endoskarn, Fe-rich clinopyroxene endoskarn and exoskarn (spans the aphyric basalt - limestone contact) and Fe-rich garnet exoskarn. Minerals within each zone have nearly constant compositions because chemical gradients in the fluid within each zone are weak or absent (mosaic equilibrium of Thompson, 1959). Initial hydrothermal fluids moving along microfractures or intrusion margins remove iron and magnesium from biotite to form orthoclase. As the concentration of iron and magnesium increases in the hydrothermal fluid, diopsidic pyroxene is deposited to form the next mineralogical envelope because magnesium is more strongly partitioned into the silicate phase than iron at higher temperatures (Eugster and Ilton, 1983). With time, the fluid becomes cooler and more iron-rich, and hedenbergitic pyroxene and/or andraditic garnet are deposited to form the innermost envelope of the microfracture, or the outermost envelope from the intrusion margin. In addition to fluid conditions (composition, temperature and pressure), the protolith has an important influence on mineral composition. Early, pale brown garnets replacing aphyric basalt intrusion are typically aluminum-rich grossular (Ad_{20-50}: Fig. 4.14, Table D.2), whereas later, darker brown garnets replacing marble are iron-rich andradite (Ad_{50-100}: Fig. 4.14, Table D.2).

As the hydrothermal fluids cooled, quartz, calcite, hydrous-hydroxyl minerals, sulphides, tellurides and associated gold were deposited in microfractures to form microveinlets or to infill vugs between the Fe-rich garnet $\pm$ pyroxene skarn. Vugs, probably created by volume reduction associated with formation of the infiltrational skarn, are greatest in limestone. Volume changes associated with metasomatic processes at the Nickel Plate deposit (Wagner, 1989) suggest that the siliciclastic and limestone units underwent volume reductions of 30-65% and 80%, respectively. Studies to verify these substantial volume reductions during skarn alteration are currently in progress (1991) at the University of Waterloo (Dr. E.C. Appleyard, personal communication to G.E. Ray). This may be largely responsible for the lithological control to sulphide and associated gold mineralization. Additionally, the more reduced hedenbergite skarn would locally buffer hydrothermal fluids causing the precipitation of these lower temperature minerals. Iron depleted hydrothermal fluids caused by precipitation of iron-rich pyroxene and garnet may be responsible for the low sulphur content minerals such as bornite and pyrrhotite. There is a

close spatial association between arsenopyrite, tellurides, vesuvianite, scapolite and gold. This suggests that arsenic, tellurium and chlorine may be important complex forming elements in the transportation of gold in the French skarn system. The above mineralogical zoning is complicated locally by cross-cutting hydrothermal overprinting.

Retrograde alteration is negligible. This may indicate that the hydrothermal system cooled relatively quickly through the temperature range that these minerals crystallized at, allowing insufficient time for replacement of surrounding skarn assemblages. The rapid cooling of the hydrothermal system is consistent with the shallow environment envision for the intrusion of Hedley sills into wet unconsolidated to poorly consolidated sediment.

Relevant modern day analogies to the French mine skarn occur in the Atlantic II Deep, Red Sea (Zierenberg and Shanks, 1983), and the Guaymas Basin, Gulf of California (Einsele *et al.*, 1980). In the Atlantis II Deep, an assemblage of hematite + magnetite + pyroxene (solid solution between acmite, diopside and hedenbergite) with minor amounts of actinolite, ilvaite, albite (An_{0-40}), quartz, chalcopyrite, anhydrite, smectite, talc, chlorite, sphene and andraditic garnet occur in unconsolidated sediments close to basalt sills. Minor amounts of actinolite form overgrowths on the surface of the pyroxene grains, and apparently precipitated late in the paragenetic sequence. In the Guaymas Basin, an assemblage of epidote, albite and chlorite occurs near sills but is thought to be related to a longer lived heat source at depth.

CHAPTER 5.0 CONCLUSIONS

The Hedley camp in south-central British Columbia contains a number of economically significant gold skarns. Although gold skarns have been mined in the Hedley camp since the early 1900's, little was published on them and they were not recognized as a distinct class of ore deposit in the review of skarns by Einaudi *et al.*, 1981. However, since that time a number of discoveries such as Fortitude (Myers and Meinert, 1991), M^{c}Coy (Brooks *et al.*, 1991), Crown Jewel (Hickey, 1990), and the reopening of Nickel Plate (Ray *et al.*, 1986) has resulted in these deposits being recognized as important sources of gold and viable exploration targets.

In this study, the geological setting of the Hedley camp has been outlined and the lithologic, stratigraphic and structural controls to gold skarns in the camp have been discussed (Section 5.1). Alteration and mineralization around one of these skarns--French Mine--is described (Sections 5.2 and 5.3). Finally, a model for Hedley-type gold skarns is presented (Section 5.4) that links skarn generation to formation of a sill sediment complex.

5.1 Geological setting of the Hedley gold skarn camp

The Hedley gold skarn camp in south-central B.C. occurs along the eastern rifted margin of a marginal basin east of the main Nicola arc in Quesnellia. Rocks in this basin are predominantly sedimentary facies of the Late Triassic Nicola Group (Figs. 1.1 and 3.18: units 2-6) and synsedimentary intrusions (unit 7). These unconformably overlie more deformed oceanic rocks of the Middle to Late Paleozoic Apex Mountain complex (unit 1). West of Hedley, much of this basin is obscured by Jurassic (units 8-12) and Cretaceous intrusions.

The Nicola Group is subdivided into four sedimentary and one volcaniclastic formation. The three youngest sedimentary formations, based on Late Triassic conodonts (Carnian to Norian: M.J. Orchard, written communication, 1988) and paleocurrent indicators, are facies equivalents representing

deposition across a north trending, westward deepening, fault controlled basin margin. They are represented by: (i) siltstones and thick limestones as the shallow water Hedley formation (Fig. 3.17: unit 2), (ii) siltstones and thin limestones as the intermediate depth Chuchuwayha formation (unit 3), and (iii) argillite and rare limestone as the deeper water Stemwinder formation (unit 4). Collapse of this basin is marked by the deposition of the Copperfield breccia (unit 5) which separates the Hedley, Chuchuwayha and Stemwinder formations from the overlying volcaniclastics of the Whistle formation (unit 6). The Copperfield breccia is a limestone breccia that appears to represent a catastrophic massive gravity slide deposit derived from uplifted and faulted reef material with a provenance to the east. Seismic shock related to earthquakes associated with the start of volcanism may have been responsible for the generation of this unit. The overlying Whistle formation forms an extensive unit that grades from thinly laminated tuffaceous siltstones at its base, to massive intermediate to mafic ash and lapilli tuffs. The tuffs are subalkalic and alkalic, and have an island arc trace element signature. Absence of facies changes and limestone units, and the change from thinly laminated turbiditic sediments to thick bedded airfall volcanics in the Whistle formation suggests that sea floor topography varied from a fault bounded basin to a relatively smooth featureless surface after deposition of the Copperfield breccia.

Three intrusive episodes recognized in the Hedley area are: (i) Late Triassic Hedley intrusions (Fig. 1.1: unit 7), (ii) Early Jurassic Bromley batholith (unit 8) and Mount Riordan stock (unit 9), and (iii) Middle Jurassic Cahill Creek pluton (unit 10), Lookout Ridge pluton (unit 11), rhyolite porphyry dykes (unit 12) and their extrusive equivalent, Skwel Peken formation (unit 13).

Hedley intrusions (Fig. 1.1: unit 7) occur as quartz diorite to gabbro dykes, sills and stocks. Chemically they overall are calcalkaline and have an island arc trace element signature. Stocks and dykes occur throughout the Nicola Group; however sills are best developed in the shallow water Hedley formation where they form a sill complex centered about the Toronto stock. It is uncertain if the Toronto stock represents a composite body consisting of numerous dykes that fed the adjacent sills or if the stock was intruded as one large body with numerous apophyses that form sills in the adjacent sediments; however, the former interpretation is preferred. The sills, exposed over a vertical distance of 1 000 m, make up to 40% of the stratigraphy, and are spatially and temporally associated with gold skarn

mineralization. The sills are commonly thin (<2 m) where they intrude thinly bedded limestone and siltstone, but are thick (75 m) where they intrude thick bedded limestone. Individual sill contacts vary from planar to highly irregular, and rarely, are brecciated. The indicated Late Triassic age of the sills (maximum age of 217.5 $\pm$ 4.2 Ma, J. Gabites, written communication, 1993; minimum age of 193 $\pm$ 1 Ma based on cross-cutting relationships with the Bromley batholith), and the above morphological features, suggest they were emplaced into unconsolidated siltstone units that occur between limestones that diagenetically lithified quickly after deposition. Lack of sills in the Stemwinder formation may have been a function of the increased lithostatic and hydrostatic pressure associated with a thicker sedimentary pile and deeper water.

The Early Jurassic Bromley batholith (Fig. 1.1, unit 8: 193 $\pm$ 1 Ma, Parrish and Monger, 1991) and a satellite body called the Mount Riordan stock (Fig. 1.1, unit 9: 194.4 $\pm$ 3.8 Ma, J. Gabites, written communication, 1993) are calcalkaline granodiorite to tonalite. The Mount Riordan stock is spatially and temporally related to Cu-W mineralization and industrial garnet skarn on Mount Riordan.

The Middle Jurassic Cahill Creek pluton (Fig. 1.1, unit 10: 170.0 $\pm$ 9 Ma, J. Gabites, written communication, 1993) is calcalkaline, quartz monzonite to granodiorite and commonly separates the Nicola Group from the underlying Apex Mountain complex. The lacolith like shape in cross-section suggests that the intrusion rose diapirically to the Nicola Group - Apex Mountain complex unconformity where it intruded laterally. Aplite phases at the top of the stock and dykes in the surrounding country rocks formed as the main body crystallized. Minor W-Mo porphyry style mineralization is spatially and temporally associated with the aplite. Rhyolite porphyry dykes (unit 12: 155 $\pm$ 10 Ma, J. Gabites, written communication, 1993) presumably represent feeders between the deeper level Cahill Creek pluton and the Skwel Peken formation. The Skwel Peken formation consists of a lower unit of massive to bedded dacitic tuff (unit 13a: maximum age of 186 $\pm$ 11 Ma, J. Gabites, written communication, 1993) and an upper unit of massive feldspar phyric andesite tuff (unit 13b) that unconformably overlies the Nicola Group. The formation is interpreted to have been deposited in a non-marine, shallow water to subaerial environment.

Nicola Group rocks record Late Triassic extensional and Lower Jurassic to Cretaceous compressional histories. Northeasterly striking normal faults and west-northwesterly striking fracture

zones are products of Late Triassic extension. The major normal faults from east to west are the Cahill Creek, Bradshaw and Chuchuwayha faults. Displacement on these faults during Late Triassic (Carnian to Norian) time formed a stepped seafloor of successively westward down dropped blocks. This is reflected by the successively deepening facies changes represented in the Hedley, Chuchuwayha and Stemwinder formations. West-northwesterly striking fracture zones may reflect transform faults along which some dykes and stocks of Hedley intrusion were emplaced.

Structures associate with Lower Jurassic to Cretaceous compression include a district wide anticline called the Hedley anticline, asymetric minor folds, reverse faults, and possibly, easterly directed thrust faults. The axial plane of the Hedley anticline strikes northeast and dips steeply west; its trace lies along Cahill Creek just east of Nickel Plate mine. Asymetric minor folds on the Hedley anticline occur throughout the district. Reverse faults mark compressional reactivation of many of the Late Triassic normal faults. Duplex like structures observed northwest of Hedley township, and west dipping low angle faults mapped underground at the Nickel Plate and French mine may reflect easterly directed thrust faults.

Galena lead isotope ratios from the Nickel Plate gold skarn mine were compared with the Copper Mountain copper - gold porphyry deposit. In general, the galena lead isotopes from both deposits are very similar and plot between upper crustal lead characterized by the shale curve and mantle lead. This is indicative of lead mixed between reservoirs in an orogene or island arc setting. Present framework models do not appear to characterize the lead, and therefore, the age of the deposits cannot be determined from galena lead isotopes. Copper Mountain lead is slightly more primitive than Nickel Plate lead suggesting it, comparatively, had less access to upper crustal components.

5.2 Geological setting of the French mine gold skarn

The French mine occurs east of the Cahill Creek fault along the eastern rifted margin of the north trending elongate Nicola back-arc basin. In this area, the Late Triassic Nicola Group (Fig. 4.1: units

2, 5 and 6) forms a northeast striking, shallow dipping sequence that unconformably overlays strongly deformed oceanic rocks of the Middle to Late Paleozoic Apex Mountain complex (unit 1).

Apex Mountain complex (Fig. 4.1: unit 1) consists of siliciclastics, andesite to basalt volcanics and subvolcanic intrusions, and minor chert pebble conglomerate, chert, limestone and ultramafic rock. Bedding in these units strikes northeast and dips steeply east and west; the best fit girdle of poles to bedding strikes 313^{o} and dips 82^{o} southwest suggesting shallowly northeast plunging folds.

Nicola Group consists of the Hedley formation (Fig 4.1: unit 2), Copperfield breccia (unit 5) and Whistle formation (unit 6). Bedding in these units strikes 226^{o} and dips shallowly west; locally at the French mine, bedding strikes east-northeast and dips shallowly (30^{o}) north. The Hedley formation forms a thin (<50 m) discontinuous unit of interbedded siltstone, limestone and minor argillite preserved in paleotopographic lows along the westerly sloping basin edge. West of the Cahill Creek fault, this unit dramatically thickens to over 500 m where it hosts gold skarn mineralization at the Nickel Plate deposit. Copperfield breccia is 10 - 100 m thick and overlies the Hedley formation and Apex Mountain complex. It consists of massive to bedded limestone breccia and conglomerate with minor interbeds of thinly laminated limestone. Whistle formation forms a 200 m thick unit that conformably overlays the Copperfield breccia. It consists of interbedded tuffaceous siltstone that grade into massive andesite to basaltic ash and lapilli tuff.

Two intrusive episodes are recognized in the French mine area. These are: (i) Late Triassic Hedley intrusions (Fig. 4.1: unit 7), and (ii) Middle Jurassic Cahill Creek pluton (unit 10) and rhyolite porphyry dykes (unit 12).

Hedley intrusions (Fig. 4.1: unit 7) form a texturally diverse suite of intermediate to mafic calcalkaline dykes, sills and stock like bodies that are spatially and temporally associated with gold skarn mineralization. Phyric intrusions consist of quartz diorite and hornblende basalt porphyries. The aphyric intrusions, previously mapped as hornfelsed tuffaceous sediments, form thin basalt sills, dykes or margins to hornblende phyric basalt porphyries. The hornblende phyric and aphyric intrusions are unique to the French mine area. It is uncertain if the quartz diorite represents a magma pulse from a more crystallized portion of the same magma chamber as the hornblende phyric and aphyric basalt, or represents a magma

pulse from an unrelated magma chamber. Features such as wavy sill contacts, destruction of sedimentary structures, globular peperite, quench textures and sedimentary dykes suggest that the aphyric basalt sills intruded wet unconsolidated to poorly consolidated siltstone and limestone of the Hedley formation. This interpretation implies that the Hedley formation, Hedley intrusions and associated gold skarn are essentially contemporaneous and form at relatively shallow depths.

Cahill Creek pluton (Fig. 4.1: unit 10) forms a sheet like body in the French mine area that intrudes at or near the Nicola Group - Apex Mountain complex unconformity. Contact metamorphism has altered the siliciclastics in the Apex Mountain complex, below and east of the pluton, to biotite + cordierite + garnet. The limestone breccia (Copperfield breccia) and tuffaceous siltstone (Whistle formation) of the Nicola Group above the pluton have been altered to calc-silicate reaction skarn. The pluton is medium grained, equigranular, biotite-hornblende granodiorite to monzodiorite; minor aplite phases form along the upper contact and as dykes in the surrounding country rocks. W-Mo mineralization associated with this intrusion forms disseminations and veins of quartz $\pm$ actinolite, epidote, molybdenite and scheelite in the aplite and adjacent country rocks. The close proximity of the French and Good Hope mines to the upper contact of the Cahill Creek pluton apparently caused the earlier gold skarn to be overprinted by this W-Mo mineralization.

Rhyolite porphyry dykes (Fig. 4.1: unit 12) are isolated and thin (<3 m thick). They are interpreted to be feeders between the deeper level Cahill Creek pluton and the overlying Skwel Peken formation volcanics that crop out on Lookout Mountain, which is 7 km north of the French mine.

5.3 Gold skarn mineralization of the French mine

Gold skarn mineralization at the French mine is hosted in siliciclastics and limestone of the Hedley formation (Fig. 4.3: unit 2). Skarn can be classified as endoskarn and exoskarn. Most gold occurs in infiltrational exoskarn. Mine workings consist of two bedding-parallel stopes that are separated by biotite rich aphyric Hedley sills or unaltered Hedley formation (Fig. 4.4). Copperfield breccia commonly

forms the back of the upper stope. Mineralization is terminated against the steep French fault on the west, and bottoms on, or is cut off on the east by the shallowly west dipping Cariboo fault.

Endoskarn consists of: (i) pervasive biotitization and successive mineralogical envelopes formed around (ii) microveinlets and (iii) intrusion margins. The microveinlets are randomly oriented and consist of: chlorite, epidote, clinozoisite, titanite and opaque minerals. Successive mineralogical envelopes around these microveinlets consist of iron-poor grossular garnet, clinopyroxene and orthoclase. The microveinlets are interpreted to have formed along fractures that were generated by quenching during intrusion and that were subsequently infiltrated by hydrothermal fluids and/or fluidized sediment. Garnet skarn is best developed where fluidized limestone is injected into microfractures or where limestone was ingested by the magma during sill intrusion. Margins of the aphyric intrusions have a similar mineralogical zoning as the microveinlets. Fine grained orthoclase and clinopyroxene form thin (<10 cm) parallel envelopes along the margins of the biotitic intrusions. Sills intruding limestone commonly develop garnet envelopes (<50 cm). However, where sills intrude siltstone the clinopyroxene envelope along the intrusion margin expanded outwards (<10 cm) into the sediment making identification of the contact difficult.

Exoskarn forms a continuum from: (i) recrystallization and reaction (bimetasomatic diffusional) skarn along intrusion margins, to (ii) metasomatic infiltrational skarn formed along sill contacts, sill-dyke intersections, fold hinges, and bedding and fracture planes. Diffusional skarn varies from: (i) recrystallization a few centimetres from the intrusion margin where the bodies are thin and infrequent, to (ii) complete recrystallization of siltstone and limestone beds forming fine grained mosaic quartz and coarse grained marble adjacent to thick or abundant sills.

Infiltrational exoskarn forms the majority of calc-silicate alteration associated with gold skarn mineralization at the French mine (Fig. 4.16b, Table 4.1). The skarn displays consistent mineralogical zoning outward from aphyric basalt to orthoclase endoskarn, Mg-rich clinopyroxene endoskarn, Fe-rich clinopyroxene endoskarn and exoskarn (spans the aphyric basalt - limestone contact) and Fe-rich garnet exoskarn. Hydrothermal fluids moving through box like zones between impermeable dykes and sills, or along fractures and bedding planes as a result of temperature and pressure gradients. A a number of expanding contemporaneous alteration fronts produced the observed mineralogical zoning. This

mineralogical zoning is interpreted to be the result of initial hydrothermal fluids removing iron and magnesium from biotite to form orthoclase from the remaining potassium. As the iron and magnesium increase in the hydrothermal fluid, diopsidic pyroxene is deposited to form the next mineralogical envelope. This is likely because magnesium is more strongly partitioned into the silicate phase than iron at higher temperatures (Eugster and Ilton, 1983). With time and distance, the iron rich fluids become cooler and iron-rich hedenbergitic pyroxene and/or andraditic garnet were deposited to form the envelope outermost from the intrusion margin. Quartz, calcite, hydrous-hydroxyl minerals, arsenopyrite, copper and iron sulphides, tellurides and associated gold are deposited in microfractures and vugs between iron-rich garnet $\pm$ pyroxene skarn as the hydrothermal fluids cooled. Vugs, probably created by volume reduction associated with the infiltrational skarn, are greatest in the limestone and may be responsible for the lithological control to sulphide and associated gold mineralization. This simple mineralogical zoning is commonly only partially developed. Locally, it is overprinted by subsequent hydrothermal fluids, possibly related to multiple magma pulses associated with sill formation.

5.4 Model for Hedley-type gold skarns

Regional mapping in the Hedley camp (Ray and Dawson, 1994) and more detailed studies at the Nickel Plate (Ettlinger *et al*., 1992) and French mine (this study) has identified a number of features that characterize Hedley-type gold skarns. These features are:

1. The back arc or marginal basin setting is marked by rift related faults along the basin edge that influence sedimentation and guide intrusions into siliciclastics and carbonates.
2. Calcalkaline, intermediate to mafic, synsedimentary intrusions directed along these faults into shallow water siliciclastics and carbonates, formed small stock like bodies, sill complexes and minor dykes. The stock like bodies may be composite in nature and consist of numerous dykes that fed the adjacent sills. Sill complexes are confined to shallow water environments (<3 km) because in deeper water environments the overlying hydrostatic and lithostatic pressure is greater

than the pressure of the magma; in such cases, magma is confined to fractures as dykes or small stocks. The sills are commonly thin and numerous in thinly bedded siltstone and limestone, and thick and infrequent in thickly bedded limestone; this suggests that some of the limestones may have lithified quickly after deposition, and thus, excluded intrusion of the sills. The structural, lithological and stratigraphic control of skarns documented in the Hedley camp is a function of features outlined above.

3. Economic gold skarns apparently are related to the stocks and adjacent sills. Individual sills acted as impermeable barriers along which hydrothermal fluids moved. However, sill complexes, such as that exposed on Nickel Plate Mountain, indicate areas of high heat flow and proximity to a large heat source that may have added components to skarn formation. Thus, features such as sill-dyke intersections, abrupt changes in sill orientation, fractures, small 'crumples' related to sill intrusion and close proximity to the marble line (outer boundary of the exoskarn envelope) are secondary controls to skarn formation.

4. Thermal diffusional skarn (hornfels) is characterized by biotite, K-feldspar, quartz, diopsidic pyroxene and grossular garnet; mineralogy is highly dependent on protolith composition.

5. Infiltrational skarn consists dominantly of hedenbergitic pyroxene, andraditic garnet and lesser amounts of vesuvianite, scapolite, axinite, calcite, quartz, wollastonite, epidote, actinolite, apatite, titanite, rutile and other trace minerals. Sulphides are typically reduced, low sulphur assemblages of arsenopyrite, pyrrhotite, bornite, chalcopyrite, bismuth tellurides, native gold and bismuth. Sulphides in general make up <10% of the skarn.

6. Retrograde alteration is negligible in the Hedley gold skarns, which is consistent with the shallow environment of formation envisioned for these skarns.

REFERENCES

Allan, J.F., Gorton, M.P., Cousens, B.L., and Leg 127 Shipboard Party (1990): Geochemistry and character of rocks collected by ODP Leg 127 from the Yamato Basin, eastern Japan Sea: implications for back-arc spreading processes. GAC-MAC Annual Meeting, Programs with Abstracts, Geological Association of Canada, Vol. 15, p. A2.

Andrew, A., Godwin, C.I., and Sinclair, A.J. (1984): Mixing line isochrons: a new interpretation of galena lead isotope data from southeastern British Columbia. Economic Geology, Vol. 79, pp. 919-932.

Andrew, K.P. (1988): Geology and Genesis of the Wolf Precious Metal Epithermal Prospect and the Capoose Base and Precious Metal Porphyry-Style Prospect, Capoose Lake area, central British Columbia. Unpublished M.Sc thesis, The University of British Columbia, p. 334.

Billingsley, P., and Hume, C.G. (1941): The ore deposits of Nickel Plate Mountain, Hedley, British Columbia. Canadian Institute of Mining and Metallurgy, Bulletin, Vol. XLIV, pp. 524-590.

Billingsley, P., Mayo, E.B., and Lea, E.R. (1949): Oregon Prospect - Preliminary Estimate. Kelowna Exploration Company Limited, unpublished report, Sept. 24, 1949..

Bostock, H.S. (1930): Geology and ore deposits of Nickel Plate Mountain, Hedley, British Columbia. Geological Survey of Canada, Summary Report, 1929, Part A.

---------- (1940a): Map of the Hedley area. Geological Survey of Canada, Map 568A.

---------- (1940b): Map of the Wolfe Creek area. Geological Survey of Canada, Map 569A.

Brooks, J.W., Meinert, L.D., Kuyper, B.A., and Lane, M.L. (1991): Petrology and geochemistry of the McCoy gold skarn, Lander County, NV, In:"Geology and Ore Deposits of the Great Basin", Raines, G.L., Lisle, R.E., Schafer, R.W. and Wilkinson, W.H., eds, Geological Society of Nevada, Reno, Vol. 1, pp. 419-442.

Bryan, W.B. (1972): Morphology of quenched crystals in submarine basalts. Journal Geophysical Research, Vol. 777, pp. 5812-5819.

Busby-Spera, C.J., and White, J.D.L. (1987): Variation in peperite textures associated with differing host sediment properties. Bulletin of Volcanology, Vol. 49, pp.765-775.

Camsell, C. (1910): The geology and ore deposits of Hedley Mining District, British Columbia. Geological Survey of Canada, Memoir 2, 218 p.

Cas, R.A.F., and Wright, J.V. (1987): Volcanic successions, modern and ancient. Chapman and Hall, 528 p.

Choquette, P.W., and James, N.P. (1987): Diagenesis in limestone--the deep burial environment. Geoscience Canada, Vol. 14, No. 1, pp. 3-33.

Cox, K.G., Bell, J.D., and Pankhurst, R.J. (1979): The interpretation of igneous rocks. George Allen and Unwin, London, 450 p.

Dawson, G.L., Godwin, C.I., Ray, G.E., Hammack, J., and Bordin, D. (1990a): Geology of the Good Hope - French Mine area, south-central British Columbia. B.C. Energy, Mines and Petroleum Resources, Geological Fieldwork, Paper 1990-1, pp. 271-277.

Dawson, G.L., Godwin, C.I., and Ray, G.E. (1990b): Gold skarn mineralization associated with a sediment sill complex, French Mine, south-central British Columbia. Geological Association of Canada, Annual Meeting, Program with Abstracts, Vol. 15, p.A30, Annual Meeting May 16-18, 1990, Vancouver, B.C. .

Dawson, G.M. (1877): Report of Progress, 1877-1878. Geological Survey of Canada. Part B, pp. 84 and 156.

Debon, F., and Le Fort, P. (1983): A chemical - mineralogical classification of common plutonic rocks. ?

Doe, B.R., and Zartman, R.E. (1979): Chapter 2. Plumbo-tectonics I, the Phanerozoic. In: "Geochemistry of Hydrothermal Ore Deposits, 2nd Edition", Wiley Interscience, New York, N.Y., pp. 22-70.

Dolmage, V., and Brown, C.E. (1945): Contact metamorphism at Nickel Plate Mountain, Hedley, British Columbia. Canadian Institute of Mining and Metallurgy, Bulletin, Vol. XLVIII, pp. 27-68.

Duke, N.A. (1988): The metallogeny of sill-sediment complexes. *In:* "North American Conference on Tectonic Control of Ore Deposits and the Vertical and Horizontal Extent of Ore Systems", (ed.) University of Missouri, pp. 245-251.

Einaudi, M.T., Meinert, L.D. and Newberry, R.J. (1981): Skarn deposits, Economic Geology, 75th Anniversary Volume, pp. 317-391.

Einsele, G., and numerous others (1980): Intrusion of basaltic sills into highly porous sediments, and resulting hydrothermal activity. Nature, Vol. 283, pp. 441-445.

Einsele, G. (1982): Mechanism of sill intrusion into soft sediment and expulsion of pore water. *In* "Initial Reports of the Deep Sea Drilling Project", Curray, J.R., Moore, D.G., et al., eds., Vol. 64, Part 2: Washington, D.C., U.S. Government Printing Office, pp. 1169-1176.

Einsele, G. (1985): Basaltic sill-sediment complexes in young spreading centers: genesis and significance. Geology, Vol. 13, pp. 249-252.

Ettlinger, A.D., Meinert, L.D., and Ray, G.E. (1992): Skarn evolution and hydrothermal fluid characteristics in the Nickel Plate deposit, Hedley District, British Columbia. Economic Geology, Vol. 87, pp. 1541-1566.

Ghosh, D.K. (1991): Nd and Sr isotopic constraints on the timing of abduction of Quesnellia onto the western edge of North America. Project Lithoprobe, Workshop, March 16-17, 1991.

Gill, J.B. (1981): Orogenic andesites and plate tectonics. Springer-Verlag, New York, 390p.

Godfrey, J.S. (1983): Production from French Mine, Hedley, B.C. George Cross Newsletter, Number 97, May 19, 1983.

Godwin, C.I., and Sinclair, A.J. (1982): Average Lead Isotope Growth Curves for Shale -Hosted Zinc Lead Deposits, Canadian Cordillera, Economic Geology, Volume 77, pp. 675-690.

Godwin, C.I., Gabites, J.E., and Andrew, A. (1988): Leadtable: A Galena Lead Isotope Data Base for the Canadian Cordillera. B.C. Ministry of Energy, Mines and Petroleum Resources, Paper 1988-4, pp. 1-188.

Godwin, C.I., and Sinclair, A.J. (1981): Preliminary Interpretations of Lead Isotopes in Galena-Lead from Shale-Hosted Deposits in British Columbia and Yukon Territory. B.C. Ministry of Energy Mines and Petroleum Resources, Geological Fieldwork 1980, Paper 1981-1, pages 185-194.

Green, T.H. (1977): Garnet in Silicic Liquids and its possible use as a P-T Indicator. Contributions to Mineralogy and Petrology, Vol. 65, pp. 163-174.

Hammack, J. (1988): Geological Map of the Good Hope - French Area. Corona Corporation, Unpublished Map (1:6000), October, 1988.

Hedley, M.S. (1955): French (Oregon Mine), Hedley, British Columbia: Notes on Essential Geology. Kelowna Exploration Company Limited, unpublished report, Sept. 26, 1955.

Hickey, R.J. (1990): The geology of the Buckhorn mountain gold skarn, Okanagan County, Washington. Unpublished M.sc. thesis, Washington State University, pp. 1-171.

Hine, A.C., Locker, S.D., Tedesco, L.P., Mullins, H.T., Hallock, P., Belknap, D.F., Gonzales, J.L., Neumann, A.C., and Snyder, S.W. (1992): Megabreccia shedding from modern, low-relief carbonate platforms, Nicaraguan Rise. Geological Society of America Bulletin, Vol. 104, pp. 928-943.

Hogan, J.W. (1953): A mineralogical study of the Oregon Mineral Claim, Hedley, B.C. A Report submitted for partial fulfillment of Geology 409, The University of British Columbia, April, 1953.

Irvine, T.N., and Baragar, W.R.A. (1971): A guide to the chemical classification of the common volcanic rocks. Canadian Journal of Earth Sciences, Vol. 8, pp. 523-548.

Kanmera, K., and Sano, H. (1991): Limestone breccias record seamount collapse. Episodes, Vol. 14, pp. 219-223.

Kokelaar, B.P. (1982): Fluidization of wet sediments during the emplacement and cooling of various igneous bodies. Journal of the Geological Society, London, Vol.139, pp. 21-33.

Kokelaar, B.P. (1986): Magma-water interactions in subaqueous and emergent basaltic volcanism. Bulletin of Volcanology, Vol. 48, pp. 275-289.

Korzhinskii, D.S. (1965): The theory of systems with perfectly mobil components and processes of mineral formation. American Journal of Science, Vol. 263, pp. 193-205.

Krogh, T.E. (1973): A low contamination method for hydrothermal decomposition of zircon and extraction of U and Pb for isotopic age determinations. Geochimica et Cosmochimica Acta, Vol. 37, pp. 485-494.

Lamb, J. (1957): French Mine, Hedley, B.C. In: Gilbert, G., ed., Structural Geology of Canadian Ore Deposits, A Symposium arranged by the Geological Division of the CIMM.

Lamb, J., Bush, J.B., and Williams, C.T. (1957): Nickel Plate Mine, Hedley, B.C.In: Gilbert, G., ed., Structural Geology of Canadian Ore Deposits, A Symposium arranged by the Geological Division of the CIMM.

Lee, J.W. (1951): The geology of Nickel Plate Mountain, B.C. Unpublished Ph.D. Thesis, Stanford University, 89 p.

Lofgren, G. (1974): An experimental study of plagioclase crystal morphology: isothermal crystallization. American Journal of Science, Vol. 274, pp. 243-273.

Lofgren, G.E. and Donaldson, C.H. (1975): Curved branching crystals and differentiation in comb-layered rocks. Contributions to Mineralogy and Petrology, Vol. ?, pp. 509-519.

Ludwig, K.R. (1980): Calculation of uncertainties of U-Pb isotope data. Earth and Planetary Science Letters, Vol. 46, pp. 212-220.

Meschede, M. (1986): A method of discriminating between different types of mid-ocean ridge basalts and continental tholeiites with the NB-Zr-Y diagram. Chemical Geology, Vol. 56, pp. 207-218.

Meagher, E.P. (1980): Silicate garnets. In: Ribbe, P.H., eds., Orthosilicates. Reviews in Mineralogy, Vol. 5, pp. 25-58.

Middlemost, E.A.K. (1985): Magmas and magmatic rocks. Longman Group Limited, Essex, p.

Milford, J.C. (1984): Geology of the Apex Mountain Group, north and east of the Similkameen River, south-central B.C. Unpublished M.Sc thesis, The University of British Columbia, p. 108.

Miller, C.F. and Stoddard, E.F. (1981): The Role of Manganese in the Paragenesis of Magmatic Garnet: An example from the Old Woman-Piute Range, California. Journal of Geology, Vol. 89, pp. 233-246.

Molnar, P., and Atwater, T. (1978): Interarc spreading and cordilleran tectonics as alternates to the age of subducted ocean lithosphere. Earth and Planetary Science Letters, Vol. 46, pp. 46-67.

Monger, J.W.H., Price, R.A., and Tempelman-Kluit, D.J. (1982): Tectonic accretion and the origin of the two major metamorphic and plutonic welts in the Canadian Cordillera. Geology, Vol. 10, pp. 70-75.

Monger, J.W.H. (1985): Structural evolution of the southwestern Intermontane Belt, Ashcroft and Hope map areas, British Columbia. *In* Current Research, Part A, Geological Survey of Canada, Paper 85-1A, pp. 349-358.

Monger, J.W.H. (1989): Geology of Hope and Ashcroft map areas, British Columbia. Geological Survey of Canada, Map 42-1989.

Mortimer, N. (1987): The Nicola Group: Late Triassic and Early Jurassic subduction-related volcanism in British Columbia. Canadian Journal of Earth Science, Vol. 24, pp. 2521-2536.

Myers, G.L. and Meinert, L.D. (1991): Alteration, mineralization, and gold distribution in the Fortitude gold skarn. In: ""Geology and Ore Deposits of the Great Basin", Raines, G.L., Lisle, R.E., Schafer, R.W. and Wilkinson, W.H., eds, Geological Society of Nevada, Reno, Vol. 1, pp. 407-418.

Parrish, R.A. (1987): An improved micro-capsule for zircon dissolution in U-Pb geochronology. Chemical Geology: Isotope Geoscience Section, Vol. 66, pp. 99-102.

Parrish, R.A. and Krogh, T.E. (1987): Synthesis and purification of ^{205}Pb for U-Pb geochronology. Chemical Geology: Isotope Geoscience Section, Vol. 66, pp. 103-110.

Parrish, R.A., and Monger, J.W.H. (1991): New U-Pb dates from southwestern British Columbia. Geological Survey of Canada, Paper 91-2, pp. 87-108.

Pearce, J.A. (1983): The role of sub-continental lithosphere in magma genesis at destructive plate margins. *In* "Continental basalts and mantle xenoliths", C.J. Hawkesworth and M.J. Norry (eds.), pp. 230-249.

Pearce, J.A., and Cann, J.R. (1973): Tectonic setting of basic volcanic rocks determined using trace element analysis. Earth and Planetary Science Letters, Vol. 19, pp. 290-300.

Preto, V.A. (1979): Geology of the Nicola Group between Merrit and Princeton, British Columbia Ministry of Energy, Mines and Petroleum Resources, Bulletin 69, 90 p.

Ray, G.E., and Dawson, G.L. (1994): Geology of the Hedley Gold Camp, south-central British Columbia. B.C. Ministry of Energy, Mines and Petroleum Resources, Geological Survey Branch, Bulletin 89.

Ray, G.E., Dawson, G.L., and Simpson, R. (1988): Geology, geochemistry and metallogenic zoning in the Hedley gold-skarn camp (92H/08; 82E/05). B.C. Ministry of Energy, Mines and Petroleum Resources, "Geological Fieldwork, 1987", Paper 1988-1, pp. 59-80.

---------- (1987): The geology and controls of skarn mineralization in the Hedley gold camp, southern British Columbia. B.C. Ministry of Energy, Mines and Petroleum Resources, "Geological Fieldwork, 1986", Paper 1987-1, pp. 65-79.

Ray, G.E., Grond, H.C., Dawson, G.L., and Webster, I.W.L (1992): The Mount Riordan industrial skarn deposit, Hedley district, southern British Columbia. Economic Geology.

Ray, G.E., Simpson R., Wilkinson, W., and Thomas P. (1986): Preliminary report on the Hedley mapping project. B.C. Ministry of Energy, Mines and Petroleum Resources, "Geological Fieldwork", 1985, Paper 1986-1, pp. 101-105.

Ray, G.E., Webster, I.C.L., Dawson, G.L., and Ettlinger, A.D. (1993): A Geological Overview of the Hedley Gold Skarn District, Southern British Columbia (92H). Ministry of Energy, Mines and Petroleum Resources, Geological Fieldwork 1992, Paper 1993-1, pp. 269-279.

Reynolds, D.L. (1954): Fluidization as a geological process, and its bearing on the problems of intrusive granites. American Journal of Science, Vol. 252, pp. 577-614.

Rejebian, V.A., Harris, A.G., and Huebner, J.S. (1987): Conodont color and textural alteration: An index to regional metamorphism, contact metamorphism and hydrothermal alteration. Geological Society of America Bulletin, Vol. 99, pp. 471-479.

Roddick, J.C. (1987): Generalized numerical error analysis with applications to geochronology and thermodynamics. Geochemica et Cosmochemica Acta, Vol. 51, pp. 2129-2135.

Roddick, J.C., Farrar, E., and Procyshyn, E.L. (1972): Potassium-argon ages of igneous rocks from the area near Hedley, southern British Columbia. Canadian Journal of Earth Science, Vol. 9, pp. 1632-1639.

Rose, A.W., and Burt, D.M. (1979): Chapter 5. Hydrothermal alteration. In: "Geochemistry of Hydrothermal Ore Deposits, 2nd Edition" Wiley Interscience, New York, N.Y., pp. 173-235.

Sharp, W.M. (1976): Geology and Ore Potential of the French Mine Property, Hedley, B.C. Grove Explorations Ltd., unpublished report, July, 1976.

Sheridan, M.F., and Wohletz, K.H. (1983): Hydrovolcanism: basic considerations and review. Journal of Volcanology and Geothermal Research, Vol. 17, pp. 1-29.

Simpson, R.G., and Ray, G.E. (1986): Nickel Plate Gold Mine. Canadian Institute of Mining and Metallurgy, District 6 Meeting, Paper 30, p. 19, Victoria, British Columbia, October 1986.

Stacey, N.W., and Goldsmith, L.B. (1980): Geological Investigations of the French Mine Property. Grove Explorations Ltd., unpublished report.

Stacey, N.W., and Goldsmith, L.B. (1981): Geological Report on Underground Drilling of the French Mine. Grove Explorations Ltd. unpublished report, Feb., 1981.

Steiger, R.H. and Jager, E. (1977): Subcomission on Geochronology: Convention on the use of decay constants in geo- and comochronology. Earth and Planetary Science Letters, Vol. 36, pp. 359-362.

Streckeisen, A., and Lemaitre, R.W.L. (1979): A chemical approximation to the modal QAPF classification of the Igneous Rocks, N. Jb Miner. Abh., Stuttgart, Vol. 136, pp. 169-206.

Sun, S.S. (1980): Lead isotopic study of young volcanic rocks from mid-ocean ridges and island arcs. Phil. Trans. R.Society of London, Vol. A297, pp. 409-445.

Tempelman-Kluit, D., and Parkinson, D. (1986): Extension across the Eocene Okanagan crustal shear in southern British Columbia. Geology, Vol. 14, pp. 318-321.

Thompson, J.B. (1959): Local Equilibrium in Metasomatic Processes. Researches in Geochemistry. In: Abelson, P.H., ed., Researches in Geochemistry. Wiley, New York, Vol. 1, pp. 427-457.

Thompson, R.N., Morrison, M.A., Hendry, G.L., and Parry, S.J. (1984): An assessment of the relative roles of crust and mantle in magma genesis: an elemental approach. Phil. Trans. Royal Society of London, Vol. A310, pp. 549-590.

Vidale, R.J. (1969): Metasomatism in a chemical gradient and the formation of calc-silicate bands. American Journal of Sciences, Vol. 58, pp. 991-997.

Wagner, D.W. (1989): Mass balance relationships and their influences on the mineralization of the auriferous skarns of the Nickel Plate mine, Hedley, British Columbia. Unpublished B.Sc. thesis, University of Waterloo, p. 77.

Warren, H.V., and Cummings, J.V. (1936): Mineralogy at the Nickel Plate mine. Miner, Vol. 9, pp. 27-28.

Warren, H.V., and Peacock, M.A. (1945): Hedleyite, a new bismuth telluride from British Columbia, with notes on wehrlite and some bismuth-tellurium alloys. University of Toronto studies, Geological Series, No 49, pp. 55-69.

Westervelt, R.D. (1978a): Exploration of the French Mine Property, Hedley. B.C. Grove Explorations Ltd., unpublished report by Westervelt Engineering Ltd., Jan. 12, 1978.

Westervelt, R.D. (1978b): Exploration of the French Mine Property, Hedley. B.C. Grove Explorations Ltd., unpublished report by Westervelt Engineering Ltd., Jan. 12, 1978.

White, G.E. (1976): Geophysical Report of the French Mine Property. Grove Explorations Ltd., unpublished report by White Geophysical Ltd.

Wilson, M.B. (1989): Chapter 2: Geochemical characteristics of igneous rocks as petrogenetic indicators. In: Igneous Petrogenesis, Unwin Hyman Ltd., UK, pp. 13-34.

Winchester, J.A., and Floyd, P.A. (1977): Geochemical discrimination of different magma series and their differentiation products using immobile elements. Chemical Geology, Vol. 20, pp. 325-343.

Wober, G. (1990): A petrographic study of samples from the French Mine, Hedley, B.C. A Report submitted in partial fulfillment of the requirements for Geology 428, The University of British Columbia, Dec. 13, 1990.

Wohletz, K.H. (1986): Explosive magma-water interactions: thermodynamics, explosion mechanisms, and field studies. Bulletin of Volcanology, Vol. 48, pp. 245-246.

Wohletz, K.H., and M^{c}Queen, R.G. (1984): Experimental studies of hydromagmatic volcanism. *In* "Explosive Volcanism: Inception, Evolution and Hazards", eds. Studies in Geophysics. National Academy Press, Washington DC, Vol. , pp. 158-169.

Wood, D.A., Joron, J.L., and Treuil, M. (1979): A re-appraisal of the use of trace elements to classify and discriminate between magma series erupted in different tectonic settings. Earth and Planetary Science Letters, Vol. 45, pp. 326-336.

York, D. (1969): Least-squares fitting of a straight line with correlated errors: Earth and Planetary Science Letters, Vol. 5, pp. 320-324.

Zartman, R.E., and Doe, B.R. (1981): Plumbotectonics--The Model. *In* "Evolution of the Upper Mantle", R.E. Zartman and S.R. Taylor (eds.) Tectonophysics, Vol. 75, pp. 135-162.

Zeirenberg, R.A., and Shanks, W.C. (1983): Mineralogy and geochemistry of Epigenetic Features in Metalliferous Sediment, Atlantis II Deep, Red Sea. Economic Geology, Vol. 78, pp. 57-73.

APPENDIX A: Fossil descriptions and ages of microfossils from the Hedley area, south-central British.

Appendix A contains information on sampling procedures and a table of fossil descriptions, ages and colour index (Ray and Dawson, 1994; Table A.1). Sample locations are on Figure 3.1.

Sampling Procedure

Samples, approximately 1.5 kg in size, were collected from limestones, calcareous siliciclastics and limestone breccia units in the Apex Mountain complex (unit 1), Hedley formation (unit 2), Chuchuwayha formation (unit 3), Stemwinder formation (unit 4) and Copperfield breccia (unit 5) for possible microfossils. Samples were dissolved in acetic acid in the field and the residues were sent to the Geological Survey of Canada for separation, picking and identification. Conodonts and other microfossils were recovered from all major stratigraphic units (Table A.1). Samples collected east of the Cahill Creek fault, in the Good Hope - French mine area, are highly altered and no recognizable microfossils were recovered from units in this area. Determinations (written communication, 1988) were by M.J. Orchard (Nicola Group - units 2-5) and E.C. Prosh (Apex Mountain complex), Geological Survey of Canada, Vancouver, British Columbia.

Table A.1: Fossil descriptions and ages of microfossils from the Apex Mountain complex and the Nicola Group, Hedley area, south-central British Columbia. Number of species identified are in brackets at end of name. All determinations (written communications, 1988) were by M.J. Orchard (Nicola Group - units 2-5) and E.C. Prosh (Apex Mountain complex - unit 1), Geological Survey of Canada, Vancouver, British Columbia.

FIELD NO. MAP NO.[1]	GSC NO.	UTM COORDINATES: EAST	NORTH	UNIT[2]	FOSSIL	AGE	DATE[3] (Ma)	CAI[4]
HD-45 F_1	C-103300	707900	5470500	5	Bryozoans ?, ichthyoliths Conodonts: *Metapolygnathus* polygnathiformis (Burdurov & Stefanov) (4)	Late Triassic: Carnian	227	5
HD-47 F_2	C-143398	707800	5470410	5	Ichthyoliths, shell material Conodonts: *Metapolygnathus* nodusus Hayashi (2)	Late Triassic: probably Late Carnian	229	5
HD-48 F_3	C-103724	707800	5470400	5	Pelecypods Conodonts: *Epigndolella* triangularis (Burdurov) (3)	Late Triassic: late Early Norian	220	5
HD-112 F_4	C-103735	708950	5472750	4	Conodonts: *Epigondolella* triangularis (Budurov) *Neogondolella* navicula	Late Triassic late Early Norian	220	5
HD-135 F_5	C-103739	708230	5466075	4	Conodonts: *Epigondolella* triagularis (Burdurov) (4); *Neogondella?* sp. (1)	Late Triassic: late Early Norian	220	~5
HD-49 F_6	C-103725	707900	5470250	4	Ramiform elements Conodonts: *Epigondolella* bidentata (Mosher) (5); *Neogondolella* sp. (25)	Late Triassic Late Norian	211	5

1. Map number is plotted on Figure 3.1.
2. Unit is identified in Table 3.1 and on Figure 1.1.
3. Time scale used is after Armstrom *et al.*, 1988. Date is assigned age used in Figure 3.17.
4. CAI is colour index that reflects metamorphic grade (Rejebian *et al.*, 1987). 5 = 300 - 480°C; 6 = 360 - 550°C; 7 = 490 - 720°C; 8 = >600°C.

Table A.1: Fossil descriptions and ages of microfossils from the Apex Mountain complex and the Nicola Group, Hedley area, south-central British Columbia (continued)...

FIELD NO. MAP NO.[1]	GSC NO.	UTM COORDINATES: EAST	NORTH	UNIT[2]	FOSSIL	AGE	DATE[3] (Ma)	CAI[4]
HD-57 F_7	C-103727	709500	5469695	4	Conodonts: *Metapolygnathus* nodosus (Hayashi) (4)	Late Triassic: Late Carnian	228	5.5
HD-51 F_8	C-143399	708000	5469540	4	Ramiform elements, ichthyoliths spicules, shell material Conodonts: *Epigondolella* sp. (1)	Late Triassic Middle-Late Norian	213	5
HD-56 F_9	C-103726	708830	5469510	4	Conodonts: *Metapolygnathus* [cf. M. communisti (Hayashi) (2)]	Late Triassic: probably Late Carnian	228	5
HD-8 F_{10}	C-103728	710370	5471480	4	Conodonts: *Metapolygnathus?* sp. (1)	Late Triassic: probably Carnian	227	5
HD-28 F_{11}	C-103729	709180	5471995	4	Ramiform elements (1) Conodonts: *Metapolygnathus* primutus (Mosher) (3)	Late Triassic: Late Carnian-Early Norian	225	5
HD-20 F_{12}	C-103723	711202	5472811	3	Pelecypods, ramiform elements (1) Conodont: *Epigondolella* sp. (3)	Late Triassic: Early - Middle Norian	220	5
HD-19 F_{13}	C-103722	711500	5472520	3	Ramiform elements (8) Conodont: *Epigondolella* triagularis (Budvrov) (42)	Late Triassic: late Early Norian	220	5

Table A.1: Fossil descriptions and ages of microfossils from the Apex Mountain complex and the Nicola Group, Hedley area, south-central British Columbia (continued)...

FIELD NO. MAP NO.[1]	GSC NO.	UTM COORDINATES: EAST	NORTH	UNIT[2]	FOSSIL	AGE	DATE[3] (Ma)	CAI[4]
HD-12 F_{14}	C-143397	711200	5471770	3	Spicules Conodonts: *Epigondolella* abneptis (1)	Late Triassic: Early Norian	222	5
HD-106 F_{15}	C-103732	713570	5470270	2	Conodonts: *Epigondolella* sp. (3)	Late Triassic: Early-Middle Norian	219	7-8
HD-260 F_{16}	C-103746	715030	5471350	2	Ichthyoliths Conodonts: *Epigondolella* abneptis subsp. A Orchard (4)	Late Triassic: late Early Norian	220	5
HD-118 F_{17}	C-103736	714810	5471500	2	Ichthyoliths Conodonts: *Epigondolella* abneptis subsp. A. Orchard (4); *Epigondolella* triangularis (Budurov) (5)	Late Triassic	214	5.5-6
HD-120 F_{18}	C-103737	714350	5471165	2	Ichthyoliths Conodonts: *Epigondolella* sp.	Late Triassic: Early-Middle Norian	219	6?
HD-305 F_{19}	C-103750	715710	5473300	2	Sponge spicules Conodonts: *Epigondolella* abneptis subsp. A. Orchard (6); *Epigondolella* triangularis (Budurov) (11); *Metapolygnathus* sp. (2)	Late Triassic: Early Norian	222	5-7

Table A.1: Fossil descriptions and ages of microfossils from the Apex Mountain complex and the Nicola Group, Hedley area, south-central British Columbia (continued)....

FIELD NO. MAP NO.[1]	GSC NO.	UTM COORDINATES: EAST	NORTH	UNIT[2]	FOSSIL	AGE	DATE[3] (Ma)	CAI[4]
F_{20}	C-102996	711827	5470238	2	Ichthyoliths, ramiform elements (1) Conodonts: *Epigondolellas* abneptis Huckriede (18)	Late Triassic Early Norian	222	6-7
HD-651 F_{21}	C-153760	717950	5462220	1	Brachiopods, tentaculitids, phosphatic tubes (?)	Devonian	465	
HD-652 F_{22}	C-153761	717950	5462220	1	Tentaculitids (?)	Cambrian-Devonian	465	
HD-653 F_{23}	C-153762	717950	5462220	1	Brachiopods, tentaculitids (?), phosphatic tubes	Devonian	465	
HD-186 F_{24}	C-103299	714400	5461550	1	Ichthyolith (recrystallized)	Indeterminate		
HD-46 F_{25}	C-143400	707800	5470410	1	Ichthyoliths	Indeterminate		

APPENDIX B: Isotopic analyses (U-Pb zircon, K-Ar biotite hornblende and amphibole, and galena lead) from the Hedley area, south-central British Columbia.

Appendix B contains information on sampling procedures, analytical methods, and tables of U-Pb zircon analyses of intrusive (units 7, 9, 10 and 12) and tuffaceous (unit 13) rocks from the Hedley area (Ray and Dawson, 1994; Table B.1) and galena lead analyses of mineralization from the Nickel Plate and Copper Mountain mines (this study, Table B.3). Previously published K-Ar (biotite, hornblende and amphibole) and U-Pb (zircon) analyses of intrusive (units 7, 8, 11 and 12) rocks from the Hedley area are in Table B.2. Sample locations are on Figure 3.1.

U-Pb Zircon Analyses

Sampling Procedure

Five samples, each approximately 50 kg, were collected from intrusive and extrusive rocks in the Hedley area, south-central British Columbia. Samples were sent to Fipke Laboratories in Kelowna where they were crushed and split into various size fractions and magnetic susceptibilities. Zircons from these samples were hand picked under a binocular microscope by G.E. Ray and G.L. Dawson. Two additional samples of Hedley quartz diorite (unit 7) were collected from the Toronto stock and a stock like body near the French mine. These samples were processed at The University of British Columbia similar to the method described above; however they contained insufficient zircon for analysis.

Analytical Methods

Analysis of zircons were completed at The University of British Columbia by P. Van der Heyden, D. Murphy and J. Gabites. Some fractions were abraded using air abrasion techniques (Krogh, 1973) to improve concordance. Chemical dissolution and mass spectrometry are modified from procedures described by Parrish and Krogh (1987), and employed a mixed ^{205}Pb - ^{233}U - ^{235}U spike. Zircons were dissolved in small volume teflon capsules contained in a large Parr bomb (Parrish, 1987). Both U and Pb were eluted into the same beaker, and loaded and run together on the same Re filament with silica gel and phosphoric acid. The mass spectrometer used is a Vacuums Generator Isomass 54R solid source with a Daly collector to improve the quality of measurement of the low intensity ^{204}PB signals. Error in U-Pb ages were obtained by individually propagating all the calibration and measurement uncertainties through the entire age calculation and summing the individual contributions to the total variance (Roddick, 1987). The decay constants used for the age calculation are those recommended by IUGS Subcomission on Geochronology (Steiger and Jager, 1977). Concordia intercepts are based on a York (1969) regression model and the Ludwig (1980) error logarithm. Errors reported for the raw U-Pb data are one sigma; those for final ages and those shown on concordia plots for two sigma (95% confidence limits).

Galena Pb Analyses

Sampling Procedure

Two samples of galena were collected from skarn mineralization in the northern and central pit at the Nickel Plate mine. Clean cubes of galena were handpicked under a binocular microscope, rinsed in ultrapure water to minimize contamination from other lead bearing sources and placed in small beaker for dissolution.

Analytical Methods

Analysis of galena was completed at The University of British Columbia by A. Pickering and J. Gabites using mass spectrometry and the silica gel-phosphoric acid method described by Cameron *et al.* (1969). Galena is dissolved in high purity 2-normal hydrochloric acid and evaporated to dryness to obtain lead chloride. The lead chloride crystals are washed several times in 4-normal hydrochloric acid and then redissolved in ultrapure water. One microgram of lead from the lead chloride solution is combined with phosphoric acid and silica gel and loaded onto a clean, single, rhenium filament. The loaded filament is run in a Vacuum Generators Ltd. Isomass 54R solid source mass spectrometer interfaced with a Hewlett Packard-85 computer. Ratios of the various lead isotopes, *i.e.* $^{207}Pb/^{206}Pb$, $^{208}Pb/^{206}Pb$ and $^{204}Pb/^{207}Pb$, are measured at least five times for each data block. A minimum of six data blocks are taken for each sample run. At the end of the run, the raw data is converted to ratios of: $^{206}Pb/^{204}Pb$, $^{207}Pb/^{204}Pb$, $^{208}Pb/^{204}Pb$, $^{207}PB/^{206}Pb$ and $^{208}Pb/^{206}Pb$. Reported results represent the normalized means of the calculated ratios. Within-run precision is usually better than 0.01 percent standard deviation. Absolute variation in duplicate analyses is generally less than 0.10 percent. Errors associated with mass spectrometry of lead isotopes (run instability, ^{204}Pb error and fractionation error) are monitored by repeated measurement of standards and duplicate analysis. For a complete description of these errors and of standards used the reader is referred to Godwin *et al.* (1988).

Table B.1: U-Pb analyses of zircon fractions from intrusive and tuffaceous rocks in the Hedley area, south-central British Columbia. Sample locations are on Figure 3.1. U-Pb analysis of each rock unit are plotted on concordia diagrams (Fig. 3.10). Analyses are by P. Van der Heyden, D. Murphy and J. Gabites (written communications, 1989 to 1990), Geochronometry Laboratory, The University of British Columbia, Vancouver, B.C.

Fraction[1] (Magnetic properties) (Mesh Size)	Wt (mg)	Concentration[2] U (ppm)	Pb (ppm)	Pb Isotope Abundance ^{207}Pb ^{208}Pb ^{204}Pb ^{206}Pb=100 Picograms of blank Pb[3]			Measured $^{206}Pb/^{204}Pb$	$^{206}Pb/^{238}U$ Date ± 1 SD	Atomic Ratios (dates Ma)[4] $^{207}Pb/^{235}U$ Date ± 1 SD	$^{207}Pb/^{206}Pb$ Date ± 1 SD
SKWEL PEKEN FORMATION (HD-271; Z_1, Fig. 3.1; unit 13; 5461080 N, 707800 E):										
NM2A/1° -100+200m ABR	0.4	229	5.1	5.5689	9.9861	0.0253	1538 50	0.02227 ± 0.00022 142.0 ± 1.4	0.1596 ± 0.0008 150.3 ± 0.7	0.05198 ± 0.00051 284.3 ± 22
M1.5A/3° -200+325m	0.4	372	9.5	6.1330	13.591	0.0782	1055 37	0.02445 ± 0.00006 155.7 ± 0.4	0.1680 + 0.0007 157.7 ± 0.6	0.04984 ± 0.00012 187.5 ± 5.6
NM2A/1° -100+200m ABR	0.2	283	8.1	7.696	16.1789	0.1842	260 200	0.02593 ± 0.00006 165.0 ± 0.4	0.1783 ± 0.0021 166.6 ± 1.8	0.04989 ± 0.00056 189.9 ± 26.5
RHYOLITE PORPHYRY (HD-272; Z_2, Fig. 3.1; unit 12; 5463220 N, 705720 E):										
NM2A/1° -100+200m ABR	1.6	1042	26.3	6.7361	14.0228	0.1075	865 200	0.02381 ± 0.00012 151.7 ± 0.8	0.1694 ± 0.0009 158.9 ± 0.8	0.05159 ± 0.00010 267.9 ± 4.4

1. M, NM = magnetic and nonmagnetic fractions separated on Franz isodynamic separator at indicated amperage and angle of side tilt. ABR = abraded fraction.
2. U and Pb concentrations are corrected for blank Pb.
3. Isotopic composition of variable blank is 206:207:208:204 = 17.75:15.50:37.30:1.00. Common Pb assumed to be Stacey and Kramers (1975) model Pb of 190+80 Ma age.
4. IUGS conventional decay constants (Steiger and Jager, 1977) are: $^{238}U = 1.55125*10^{-10}a^{-1}$, $^{235}U = 9.8485*10^{-10}a^{-1}$, $^{238}U/^{235}U = 137.88$ atom ratio.

Table B.1: U-Pb analyses of zircon fractions from intrusive and tuffaceous rocks in the Hedley area, south-central British Columbia (continued)...

Fraction[1] (Magnetic properties) (Mesh Size)	Wt (mg)	Concentration[2] U (ppm)	Pb (ppm)	Pb Isotope Abundance ^{207}Pb ^{208}Pb ^{204}Pb ^{206}Pb=100 Picograms of blank Pb[3]	Measured $^{206}Pb/^{204}Pb$	$^{206}Pb/^{238}U$ Date ± 1 SD	Atomic Ratios (dates Ma)[4] $^{207}Pb/^{235}U$ Date ± 1 SD	$^{207}Pb/^{206}Pb$ Date ± 1 SD
RHYOLITE PORPHYRY (HD-272; Z_2, Fig. 3.1; unit 12; 5463220 N, 705720 E):								
M2A/1° -200 ABR	2.1	1251	31.3	5.9025 12.516 0.0689	1417 80	0.02425 ± 0.00015 154.5 ± 0.9	0.1641 ± 0.0011 154.2 ± 1.0	0.04907 ± 0.00012 151.0 ± 5.8
M2A/1° -200m	2.1	1567	44.3	7.9137 17.3352 0.2006	484 200	0.02523 ± 0.00013 160.6 ± 0.6	0.1727 ± 0.0012 161.8 ± 1.0	0.04965 ± 0.00020 178.7 ± 9.2
NM2A/1° -100+200m	3.9	1097	31.7	6.6546 14.3302 0.1131	854 200	0.02717 ± 0.00030 172.8 ± 1.9	0.1870 ± 0.0021 174.1 ± 1.8	0.04992 ± 0.00026 191.3 ± 12.0
CAHILL CREEK PLUTON (HD-80; Z_3, Fig. 3.1; unit 10; 5469140 N, 715050 E):								
M2A/3° -200+325m	3.2	785	18.4	8.014719.1720 0.2051	478 120	0.02060 ± 0.00008 131.4 ± 0.5	0.1420 ± 0.0018 134.9 ± 1.6	0.05002 ± 0.00056 195.7 ± 26.4
NM2A/1° -100+200m	3.2	513	11.6	5.291611.8788 0.0193	4056 120	0.02238 ± 0.00006 142.7 ± 0.4	0.1546 ± 0.0045 145.9 ± 3.9	0.05008 ± 0.00138 198.8 ± 65
NM2A/1° -200+325m ABR	2.5	546	12.7	5.106612.2332 0.0128	5871 80	0.02303 ± 0.00020 146.8 ± 1.3	0.1562 ± 0.0015 147.4 ± 1.3	0.04919 ± 0.00016 156.7 ± 7.8
NM2A/1° -100+200 ABR	4.8	404	10.5	5.141412.4544 0.0132	5018 200	0.02554 ± 0.00022 162.6 ± 1.4	0.1742 ± 0.0013 163.1 ± 1.4	0.04947 ± 0.00017 170.2 ± 8.0

Table B.1: U-Pb analyses of zircon fractions from intrusive and tuffaceous rocks in the Hedley area, south-central British Columbia (continued)...

Fraction[1] (Magnetic properties) (Mesh Size)	Wt (mg)	Concentration[2] U (ppm)	Pb (ppm)	Pb Isotope Abundance ^{207}Pb ^{208}Pb ^{204}Pb ^{206}Pb=100 Picograms of blank Pb[3]	Measured $^{206}Pb/^{204}Pb$	$^{206}Pb/^{238}U$ Date ± 1 SD	Atomic Ratios (dates Ma)[4] $^{207}Pb/^{235}U$ Date ± 1 SD	$^{207}Pb/^{206}Pb$ Date ± 1 SD
MOUNT RIORDAN STOCK (HD-406; Z_4, Fig. 3.1; unit 9; 54761119 N, 288478 E):								
NM2A/1° +200m ABR	0.9	191	6.5	6.5872 12.063 0.0817	1078 37	0.03274 ± 0.00009 207.7 ± 0.6	0.2435 ± 0.001 221.2 ± 0.8	0.05392 ± 0.00011 367.8 ± 4.7
M1.5A/3° -200m ABR	0.4	250	8.5	7.6780 14.735 0.1742	517 37	0.03127 ± 0.00008 198.5 ± 0.5	0.2209 ± 0.0011 202.6 ± 0.9	0.05123 ± 0.00018 251.1± 7.9
BANBURY STOCK (HD-273; Z_5; Fig. 3.1; unit 7; 5470950 N, 708310 E):								
M2A/1° -200m	1.0	1524	39.0	5.9840 16.6106 0.0568	1521 200	0.02387 ± 0.00004 152.1 ± 0.2	0.1695 ± 0.0003 159.0 ± 0.3	0.05150 ± 0.00004 263.4 ± 1.6
M2A/1° -200 ABR	0.4	1124	31.7	5.6641 15.889 0.0262	3173 37	0.02678 ± 0.00017 170.4 ± 1.0	0.1937 ± 0.0008 180.9 ± 2.0	0.05262 ± 0.00012 320.5 ± 15
NM2A/1° -200m	2.0	926	27.0	5.2167 14.1710 0.0110	5774 200	0.02833 ± 0.00009 180.1 ± 0.6	0.1975 ± 0.0007 183.0 ± 0.6	0.05056 ± 0.00007 220.6 ± 3.2
NM2A/1° -100+200m	0.4	1174	34.9	5.2106 15.7711 0.0114	2794 200	0.02847 ± 0.00006 181.0 ± 0.4	0.1980 ± 0.0005 183.4 ± 0.4	0.05043 ± 0.00006 214.9 ± 2.9

Table B.1: U-Pb analyses of zircon fractions from intrusive and tuffaceous rocks in the Hedley area, south-central British Columbia (continued)....

Fraction[1] (Magnetic properties) (Mesh Size)	Wt (mg)	Concentration[2] U (ppm)	Pb (ppm)	Pb Isotope Abundance ^{207}Pb ^{208}Pb ^{204}Pb ^{206}Pb=100 Picograms of blank Pb[3]	Measured $^{206}Pb/^{204}Pb$	$^{206}Pb/^{238}U$ Date ± 1 SD	Atomic Ratios (dates Ma)[4] $^{207}Pb/^{235}U$ Date ± 1 SD	$^{207}Pb/^{206}Pb$ Date ± 1 SD
STEMWINDER STOCK (HD-81; Z_6, Fig. 3.1; unit 7; 5472310 N, 711500 E):								
NM2A/3° -100+200m	2.0	440	12.6	5.4758 14.3983 0.0204	3515 120	0.02758 ± 0.00007 175.4 ± 0.5	0.1969 ± 0.0008 182.5 ± 0.7	0.05177 ± 0.00016 275.3 ± 6.9
NM2A/.5 -200+325m	0.4	893	27.6	6.6251 19.9095 0.1072	721 200	0.02778 ± 0.00009 176.6 ± 0.6	0.1935 ± 0.0008 179.6 ± 0.7	0.05051 ± 0.00012 218.6 ± 5.4
M2A/3° -200+325m	1.6	879	26.1	5.7486 17.4002 0.0426	2099 120	0.02782 ± 0.00010 176.9 ± 0.6	0.1965 ± 0.0010 182.2 ± 0.6	0.05124 ± 0.00018 251.5 ± 8.2
M2A/0.5° -100+200m	0.4	421	13.4	6.6426 18.1366 0.1035	600 200	0.02898 ± 0.00008 184.2 + 0.5	0.2047 ± 0.0017 189.1 + 1.5	0.05124 ± 0.00039 251.7 + 17.5

Table B.2: Other K-Ar (biotite, hornblende and amphibole) and U-Pb (zircon) analyses of intrusive rocks in the Hedley area, south-central British Columbia. Data are incorporated with data from Table B.1 in Figure 3.18.

Sample No.	Map No.[1]	UTM Coordinates Northing	Easting	Unit	Mineral	Date and error (Ma)[2]	Reference
Hedley intrusions:							
21a	A_1	5471750	714625	7	amphibole	175.2 ± 5.2	Roddick *et al.*, 1972
21b	A_2	5471750	714625	7	amphibole	180.7 ± 5.8	Roddick *et al.*, 1972
22	A_3	5471850	714450	7	amphibole	193.0 ± 6.0	Roddick *et al.*, 1972
24	A_4	5471825	714100	7	amphibole	195.0 ± 6.0	Roddick *et al.*, 1972
26a	A_5	5471900	715225	7	amphibole	175.0 ± 5.4	Roddick *et al.*, 1972
26b	A_6	5471900	715225	7	amphibole	184.0 ± 7.4	Roddick *et al.*, 1972
28	A_7	5473175	712525	7	amphibole	187.8 ± 5.8	Roddick *et al.*, 1972
Bromley batholith:							
8	H_1	5473500	706525	8	hornblende	186.1 ± 5.6	Roddick *et al.*, 1972
9	B_1	5474500	708575	8	biotite	180.9 ± 5.4	Roddick *et al.*, 1972
9	H_2	5474500	708575	8	hornblende	188.1 ± 5.8	Roddick *et al.*, 1972
8-2	Z_7	5473850	705300	8	zircon	193.0 ± 1.0	Parrish and Monger, 1991
8-2	H_3	5473850	705300	8	hornblende	185.7 ± 2.8	Monger, 1989
8-2	B_2	5473850	705300	8	biotite	173.4 ± 4.7	Monger, 1989
Cahill Creek pluton:							
1	B_3	5469600	713825	11	biotite	158.4 ± 4.8	Roddick *et al.*, 1972
1a	B_4	5469600	713825	11	biotite	153.4 ± 4.6	Roddick *et al.*, 1972
1b	B_5	5469600	713825	11	biotite	154.4 ± 4.6	Roddick *et al.*, 1972

1. Map number is plotted on Figure 3.1.
2. All analyses have been corrected to modern day constants.

Table B.2: Other K-Ar (biotite, hornblende and amphibole) and U-Pb (zircon) analyses of intrusive rocks in the Hedley area, south-central British Columbia (continued)....

Sample No.	Map No.[1]	UTM Coordinates Northing	Easting	Unit	Mineral	Date and error (Ma)[2]	Reference
Cahill Creek pluton:							
2	H_4	5469450	714300	11	hornblende	159.9 ± 2.9	Roddick *et al.*, 1972
3	B_6	5469625	714800	11	biotite	160.9 ± 4.8	Roddick *et al.*, 1972
4	B_7	5470200	715825	11	biotite	160.4 ± 4.8	Roddick *et al.*, 1972
5	B_8	5472075	713450	11	biotite	161.3 ± 3.4	Roddick *et al.*, 1972
5	H_5	5472075	713450	11	hornblende	162.8 ± 5.0	Roddick *et al.*, 1972
6	B_9	5470025	715150	11	biotite	158.6 ± 4.8	Roddick *et al.*, 1972
7	H_6	5468750	709150	11	hornblende	174.5 ± 5.2	Roddick *et al.*, 1972
10	B_{10}	5468000	709825	11	biotite	155.9 ± 4.8	Roddick *et al.*, 1972
Lookout Ridge pluton:							
13	B_{11}	5476025	712575	12	biotite	164.5 ± 4.8	Roddick *et al.*, 1972

Table B.3: Galena lead isotope data[1] for the Nickel Plate gold skarn and the Copper Mountain copper-gold porphyry deposit, south-central British Columbia. Data are plotted on Figure 3.16.

Sample	206Pb/204Pb	207Pb/204Pb	208Pb/204Pb	207Pb/206Pb*100	208Pb/206Pb*10
Nickel Plate (L1)[2]					
30302-001	18.759	15.631	38.441	83.329	20.493
30302-002	18.724	15.605	38.354	83.343	20.486
30302-003	18.731	15.607	38.368	83.321	20.484
30302-AVG3[3]	18.738	15.614	38.388	83.331	20.488
Copper Mountain					
30445-001	18.674	15.571	38.184	83.383	20.449
30445-002	18.678	15.564	38.183	83.328	20.444
30445-003	18.663	15.564	38.161	83.395	20.448
30445-AVG3[3]	18.672	15.566	38.176	83.369	20.447
MEAN±STD DEV[4]	18.70±0.03	15.59±0.00	38.28±0.11	83.35±0.03	20.47+0.02

1. Samples were analyzed by Anne Pickering and Janet Gabites, Geochronometry Laboratory, Department of Geological Sciences, The University of British Columbia, Vancouver, B.C., Canada. A vacuum Generators Ltd. Isomass 54R solid source, single filament (silica gel method), mass spectrometer was used. Errors at two sigma are less than 0.01%.
2. Sample number L1 is plotted on Figure 3.1.
3. AVG3 is the average of the three analyses tabulated immediately above.
4. MEAN±STD DEV is the mean and standard deviation of the 6 analyses above.

APPENDIX C: Lithogeochemical analyses from the Hedley area, south-central British Columbia.

Appendix C contains information on sampling procedure, analytical method, and tables of major and minor element analyses with their calculated CIPW normative mineralogy for intrusive (units 7, 9 and 10) and extrusive (units 6, 13a and 13b) units in the Hedley area (Ray and Dawson, 1994; Tables C.1.and C.2), and from phyric and aphyric Hedley intrusions (unit 7) in the French mine area (this study; Tables C.3 and C.4), south-central British Columbia. Sample locations are on Figures 3.1 and 4.6, respectively.

Sampling Procedure

One to two kg samples were collected from unaltered intrusive and extrusive rocks in the Hedley area (Tables C.1 and C.2), and from phyric and aphyric Hedley intrusions in the French mine area (Tables C.3 and C.4). Samples in Tables C.1 and C.2 were prepared at the B.C. Energy, Mines and Petroleum Resources Laboratory where they were crushed to chip size in a jaw crusher, and split and pulverized in a tungsten carbide ring mill.

Samples in Tables C.3 and C.4 were prepared at The University of British Columbia where they were crushed to chip size in a jaw crusher, pulverized in a tungsten carbide ring mill for two minutes and reduced to a 100-200 gm sample by repetitive splitting. The jaw crusher was cleaned with a wire brush and compressed air, the ring mill was cleaned with water and compressed air, and the splitter and sampling trays were cleaned with paper towels and compressed air between each sample run.

Analytical Methods

Major oxides in Table C.1 were determined by fused disk X-ray fluorescence (XRF) at B.C. Energy, Mines and Petroleum Resources Laboratory. Loss on ignition (LOI) was calculated after heating predried samples to 1050°C for four hours. Precision for major elements averages 5% relative error.

Trace elements in Table C.2 were determined by fused disk XRF (Co, Cr, Hg, Sb, Ba, Sr, Te, Rb, Y, Zr, Nb, Ta, U and Th), flame atomic spectroscopy absorption (ASS; Ag, Cu, Pb, Zn, Ni, Mo, As and Bi) and fire assay - atomic absorption spectroscopy (AAS) finish (Au) at the B.C. Energy, Mines and Petroleum Resources Laboratory. Precision for trace elements averages 5% relative error.

Major oxides in Table C.3 were determined by fused disk XRF at the Cominco Laboratory. LOI was calculated after heating predried samples to 1050°C for four hours.

Trace elements in Table C.4 were determined by fused disk XRF at the Cominco Laboratory (Rb, Sr, Nb, Zr, Y and Ba) and the B.C. Energy, Mines and Petroleum Resources Laboratory (Cr, Ti, V, La, Ce), by atomic absorption spectrometry at the B.C. Energy, Mines and Petroleum Resources Laboratory (Ni, Co, Cu, Pb, Zn, Mo and As), and by induced coupled plasma (ICP) at the Acme Labs Ltd. (Bi, Te).

Table C.1: Major element analyses and CIPW normative mineralogy of volcanic and intrusive rocks from the Hedley area, south-central British Columbia. Major element values are in weight percent. Analyses were by fused disk XRF completed at the B.C. Ministry of Energy, Mines and Petroleum Resources Laboratory, Victoria, B.C. Loss on ignition (LOI) was calculated after heating predried samples to 1050° C for four hours. Fe_2O_3 is expressed as total iron. Symbols "<", "-" and "*" denote below detection limit, not analysed and lab duplicate, respectively.

FIELD NO.	521	522	523	525	526	50	52	60	60*
MAP NO. [1]	W1	W2	W3	W4	W5	W6	W7	W8	W8
LAB NO.	34188	34175	34176	34178	34179	30825	30826	30827	30843
NORTHING	5454200	5470132	5469954	5469562	5469332	5469906	5469964	5472322	5472322
EASTING	700385	706060	705870	704891	704753	707907	707558	711537	711537
UNIT [2]	6	6	6	6	6	7	7	7	7
SiO_2	48.27	45.56	50.29	55.89	49.55	54.21	54.29	56.81	57.24
TiO_2	0.72	0.79	0.77	0.66	0.94	0.79	0.83	0.60	0.62
Al_2O_3	15.51	16.62	17.86	15.38	15.72	19.20	19.53	17.50	18.01
$Fe_2O_{3(T)}$	10.94	10.11	9.00	7.04	10.34	9.25	8.11	7.03	7.13
MnO	0.19	0.21	0.18	0.16	0.19	0.17	0.15	0.12	0.13
MgO	8.51	4.67	3.85	3.58	5.57	4.49	3.24	3.81	3.86
CaO	11.58	10.91	8.00	7.04	6.86	9.90	9.16	7.98	8.04
Na_2O	2.04	2.80	4.16	3.91	3.51	2.69	3.12	3.03	3.04
K_2O	0.53	2.05	1.16	1.52	2.21	0.83	0.93	1.64	1.65
P_2O_5	0.14	0.26	0.16	0.30	0.27	0.23	0.26	0.15	0.15
LOI	1.20	5.55	3.81	4.52	4.47	1.68	1.25	0.97	0.96
SUM	99.63	99.53	99.24	100.00	99.63	103.44	100.87	99.64	100.83
CIPW Normative Minerals[3]									
Q	0.00	0.00	0.00	8.85	0.00	10.08	10.47	12.75	12.50
C	0.00	0.00	0.00	0.00	0.00	0.00	0.00	0.00	0.00
Z	0.01	0.01	0.01	0.02	0.01	0.01	0.01	0.01	0.01
OR	3.20	12.98	7.23	9.45	13.82	4.84	5.53	9.86	9.80
AB	17.61	17.14	37.11	34.82	31.43	22.43	26.56	26.04	25.81
AN	32.24	28.64	28.09	20.98	21.82	37.31	36.77	29.76	30.73
NE	0.00	4.47	0.00	0.00	0.00	0.00	0.00	0.00	0.00
DI	21.65	22.42	10.32	11.13	9.99	7.48	5.64	7.36	6.47
HY	14.79	0.00	7.73	8.96	8.71	7.55	5.50	6.23	6.65
OL	3.10	6.59	2.77	0.00	6.11	0.00	0.00	0.00	0.00
MT	5.66	5.50	4.81	3.76	5.55	6.22	5.17	4.83	4.83
CM	0.06	0.01	0.00	0.01	0.03	0.00	0.00	0.01	0.01
HM	0.00	0.00	0.00	0.00	0.00	2.09	2.15	1.67	1.68
IL	1.39	1.61	1.54	1.32	1.89	1.48	1.59	1.16	1.18
AP	0.34	0.66	0.40	0.75	0.68	0.54	0.62	0.36	0.36
SUM	100.06	100.02	100.02	100.04	100.04	100.02	100.02	100.03	100.03

1. Map number is plotted on Figure 3.1.
2. Unit is identified in Table 3.1 and on Figure 1.1.
3. CIPW Normative Minerals are Q-quartz, C- corundum, Z-zircon, OR-orthoclase, AB-albite, AN-anorthite, NE-nepheline, DI-diopside, HY-hypersthene, OL-olivine, MT-magnetite, CM-chromite, HM-hematite, IL-ilimenite, AP-apatite.

Table C.1: Major element analyses and CIPW normative mineralogy of volcanic and intrusive rocks from the Hedley area, south-central British Columbia (continued)...

FIELD NO.	62	64	65	66	67	68	69	70	71
MAP NO.[1]	W9	W10	W11	W12	W13	W14	W15	W16	W17
LAB NO.	30829	30831	30832	30833	30834	30835	30836	30837	30838
NORTHING	5472771	5473042	5473143	5473242	5473346	5473415	5473809	5473907	5473410
EASTING	711930	711770	711562	711419	711319	711212	711096	710966	711060
UNIT[2]	7	7	7	7	7	7	7	7	7
SiO_2	54.08	52.94	59.48	53.27	50.82	59.46	54.27	49.13	55.92
TiO_2	0.68	0.65	0.53	0.72	0.65	0.51	0.64	0.80	0.58
Al_2O_3	18.35	19.89	17.86	19.02	20.24	17.99	19.33	20.18	18.41
$Fe_2O_{3(T)}$	8.77	7.93	6.41	8.75	8.39	5.83	7.66	9.07	7.27
MnO	0.17	0.15	0.11	0.16	0.17	0.13	0.17	0.16	0.14
MgO	4.03	4.04	2.51	3.93	4.18	2.88	3.27	5.09	3.13
CaO	9.25	10.15	6.66	9.12	10.30	7.24	9.19	11.46	8.14
Na_2O	2.91	3.40	3.28	3.10	2.90	3.72	3.20	2.55	3.22
K_2O	1.11	1.24	2.00	1.35	0.75	2.01	1.55	1.17	1.66
P_2O_5	0.16	0.19	0.14	0.17	0.20	0.15	0.20	0.18	0.17
LOI	1.03	1.10	1.00	1.32	1.24	0.87	1.12	1.51	1.26
SUM	100.54	101.68	99.98	100.91	99.84	100.79	100.60	101.30	99.90
CIPW Normative Minerals[3]									
Q	9.99	4.13	16.18	7.38	5.54	12.60	8.04	1.53	11.18
C	0.00	0.00	0.00	0.00	0.00	0.00	0.00	0.00	0.00
Z	0.01	0.01	0.02	0.01	0.01	0.01	0.01	0.01	0.01
OR	6.62	7.31	11.98	8.04	4.51	11.92	9.24	6.96	9.98
AB	24.81	28.67	28.09	26.41	24.95	31.56	27.28	21.68	27.68
AN	33.99	35.23	28.45	34.23	40.67	26.52	34.06	40.36	31.37
NE	0.00	0.00	0.00	0.00	0.00	0.00	0.00	0.00	0.00
DI	8.72	10.68	3.17	7.95	7.75	6.62	8.22	12.14	6.64
HY	6.07	5.08	4.86	6.17	6.99	4.12	4.39	7.11	4.84
OL	0.00	0.00	0.00	0.00	0.00	0.00	0.00	0.00	0.00
MT	6.26	5.48	4.45	6.09	6.07	4.03	5.40	6.11	5.17
CM	0.00	0.00	0.00	0.00	0.00	0.00	0.00	0.01	0.01
HM	1.87	1.75	1.47	1.97	1.78	1.31	1.68	2.16	1.60
IL	1.30	1.23	1.02	1.38	1.25	0.97	1.22	1.53	1.12
AP	0.38	0.45	0.34	0.41	0.48	0.36	0.48	0.43	0.41
SUM	100.02	100.02	100.02	100.02	100.02	100.02	100.02	100.03	100.03

Table C.1: Major element analyses and CIPW normative mineralogy of volcanic and intrusive rocks from the Hedley area, south-central British Columbia (continued)...

FIELD NO.	72	73	73*	156	157	158	159	161	162
MAP NO.[1]	W18	W19	W19	W20	W21	W22	W23	W24	W25
LAB NO.	30839	30840	30844	31849	31850	31851	31852	31854	31855
NORTHING	5473200	5473215	5473215	5470521	5470666	5471625	5472167	5471068	5471111
EASTING	710980	711065	711537	712967	712905	712191	712424	714497	713668
UNIT[2]	7	7	7	7	7	7	7	7	7
SiO_2	54.85	57.68	55.38	54.83	55.56	53.33	55.61	54.12	53.36
TiO_2	0.65	0.67	0.66	0.67	0.66	0.56	0.61	0.65	0.68
Al_2O_3	18.72	18.60	18.61	18.81	18.71	19.24	18.38	18.22	18.57
$Fe_2O_{3(T)}$	8.08	7.91	8.05	7.98	7.53	8.19	7.35	8.32	7.31
MnO	0.15	0.15	0.15	0.14	0.16	0.14	0.12	0.14	0.12
MgO	3.54	3.10	3.06	4.83	4.16	4.45	3.69	4.10	4.23
CaO	8.73	8.23	8.00	8.00	7.13	9.47	8.12	8.32	8.32
Na_2O	3.06	3.22	3.21	3.20	3.28	2.77	2.91	2.72	2.77
K_2O	1.65	1.80	1.78	0.64	1.37	1.17	1.00	1.01	1.10
P_2O_5	0.18	0.21	0.21	0.14	0.17	0.17	0.15	0.16	0.16
LOI	1.17	1.26	1.15	1.42	1.82	1.36	1.35	1.11	2.69
SUM	100.78	102.83	100.26	100.66	100.55	100.85	99.29	98.87	99.31
CIPW Normative Minerals[3]									
Q	9.40	12.05	10.45	10.72	10.82	8.35	13.80	12.48	10.87
C	0.00	0.00	0.00	0.00	0.00	0.00	0.00	0.00	0.00
Z	0.01	0.01	0.01	0.01	0.01	0.01	0.01	0.01	0.01
OR	9.82	10.51	10.65	3.83	8.23	6.98	6.06	6.13	6.76
AB	26.06	26.89	27.47	27.35	28.17	23.62	25.20	23.60	24.31
AN	32.68	30.58	31.47	35.43	32.77	36.89	34.93	35.41	36.29
NE	0.00	0.00	0.00	0.00	0.00	0.00	0.00	0.00	0.00
DI	7.57	6.51	5.67	2.91	1.56	7.27	4.12	4.56	4.24
HY	5.36	4.60	5.08	0.80	9.79	7.80	7.50	8.36	8.96
OL	0.00	0.00	0.00	0.00	0.00	0.00	0.00	0.00	0.00
MT	5.67	5.36	5.64	5.50	5.23	6.00	5.13	5.95	4.95
CM	0.00	0.00	0.00	0.01	0.01	0.01	0.01	0.01	0.01
HM	1.78	1.77	1.81	1.85	1.74	1.64	1.73	1.87	1.89
IL	1.24	1.26	1.27	1.28	1.27	1.07	1.19	1.27	1.34
AP	0.43	0.49	0.50	0.33	0.41	0.41	0.36	0.39	0.39
SUM	100.02	100.02	100.02	100.02	100.03	100.02	100.02	100.02	100.02

Table C.1: Major element analyses and CIPW normative mineralogy of volcanic and intrusive rocks from the Hedley area, south-central British Columbia (continued)...

FIELD NO.	163	164	218	334	767	381	406	77	78
MAP NO.[1]	W26	W27	W28	W29	W30	W31	W32	W33	W34
LAB NO.	31856	31857	31858	33914	34198	34197	33916	30845	30846
NORTHING	5471489	5472219	5471860	5473601	5474500	5475550	5476119	5468971	5469056
EASTING	713725	712174	715260	282307	711050	287800	288478	715093	715086
UNIT[2]	7	7	7	7	7	9	9	10	10
SiO_2	54.13	56.38	54.31	54.25	53.68	64.02	63.27	61.29	61.13
TiO_2	0.62	0.58	0.61	0.65	1.04	0.48	0.48	0.66	0.65
Al_2O_3	17.55	18.37	18.29	17.92	16.72	16.60	16.88	18.34	18.17
$Fe_2O_3(T)$	6.64	6.29	6.01	7.59	10.11	5.53	5.51	5.46	5.34
MnO	0.09	0.10	0.07	0.16	0.17	0.10	0.09	0.11	0.12
MgO	3.99	3.41	3.83	3.71	4.84	2.15	2.23	1.83	1.84
CaO	6.48	7.10	7.45	7.83	8.00	5.25	5.31	4.81	4.86
Na_2O	4.79	4.06	3.34	3.87	3.26	3.13	3.53	4.39	4.39
K_2O	2.13	1.01	2.08	2.54	1.36	2.09	1.56	2.44	2.48
P_2O_5	0.16	0.17	0.18	0.19	0.20	0.11	0.12	0.13	0.13
LOI	1.75	1.28	2.43	0.62	0.56	0.72	0.75	0.99	0.79
SUM	98.33	98.75	98.60	99.33	99.94	100.18	99.73	100.45	99.90
CIPW Normative Minerals[3]									
Q	1.14	10.48	7.56	3.88	8.26	22.53	21.32	12.59	12.37
C	0.00	0.00	0.00	0.00	0.00	0.00	0.02	0.04	0.00
Z	0.01	0.01	0.01	0.00	0.00	0.00	0.00	0.04	0.04
OR	13.08	6.15	12.83	15.17	8.11	12.46	9.35	14.57	14.86
AB	42.05	35.31	29.44	33.09	27.84	26.72	30.28	37.47	37.60
AN	20.85	29.73	29.97	24.28	27.23	25.30	25.91	23.22	22.82
NE	0.00	0.00	0.00	0.00	0.00	0.00	0.00	0.00	0.00
DI	8.89	4.16	5.69	8.27	8.96	0.21	0.00	0.00	0.59
HY	6.19	6.80	7.30	5.51	8.01	8.38	8.69	7.34	7.06
OL	0.00	0.00	0.00	0.00	0.00	0.00	0.00	0.00	0.00
MT	4.43	4.23	3.84	5.30	6.39	3.24	3.24	3.19	3.13
CM	0.01	0.00	0.00	0.00	0.00	0.00	0.00	0.00	0.00
HM	1.77	1.61	1.74	1.72	2.73	0.00	0.00	0.00	0.00
IL	1.22	1.13	1.21	1.25	1.99	0.92	0.92	1.26	1.25
AP	0.39	0.41	0.44	1.58	0.48	0.26	0.29	0.31	0.31
SUM	100.03	100.02	100.03	100.03	100.01	100.01	100.01	100.04	100.04

Table C.1: Major element analyses and CIPW normative mineralogy of volcanic and intrusive rocks from the Hedley area, south-central British Columbia (continued)...

FIELD NO.	79	80	717	514.15	514.6	151	152	171	172
MAP NO.[1]	W35	W36	W37	W38	W39	W40	W41	W42	W43
LAB NO.	30847	30848	34181	35229	35234	31860	31861	31863	31864
NORTHING	5469056	5469196	5470427	5469300	5469300	5461980	5461900	5461155	5461223
EASTING	715086	715086	715746	717700	717700	708800	708770	707726	707744
UNIT[2]	10	10	10	10	10	13a	13a	13a	13a
SiO_2	60.00	60.54	64.72	63.82	63.01	62.51	62.45	62.77	65.21
TiO_2	0.71	0.66	0.50	0.50	0.53	0.51	0.49	0.54	0.48
Al_2O_3	18.12	18.67	16.33	18.06	17.80	18.14	19.15	18.61	18.17
$Fe_2O_{3(T)}$	5.70	5.23	4.80	4.06	4.32	5.33	3.60	5.06	5.30
MnO	0.13	0.11	0.11	0.08	0.09	0.10	0.12	0.11	0.11
MgO	2.09	1.80	1.56	1.08	1.25	0.69	0.55	0.93	0.89
CaO	5.24	4.96	3.95	3.85	4.01	3.93	3.88	4.71	4.17
Na_2O	4.26	4.25	3.80	4.32	4.35	3.73	4.72	3.73	3.65
K_2O	2.43	2.59	2.87	2.89	2.89	1.39	1.59	1.49	1.49
P_2O_5	0.17	0.10	0.13	0.12	0.13	0.16	0.17	0.15	–
LOI	1.08	0.80	1.35	1.31	1.53	1.62	1.06	0.98	1.03
SUM	99.93	99.71	100.12	100.09	99.91	98.11	97.78	99.08	100.50
CIPW Normative Minerals[3]									
Q	11.28	11.85	20.36	17.45	15.88	26.18	20.13	23.61	27.29
C	0.00	0.10	0.10	1.13	0.55	3.89	3.13	2.72	3.35
Z	0.04	0.04	0.00	0.00	0.00	0.02	0.03	0.02	0.02
OR	14.60	15.55	17.22	17.34	17.41	8.56	9.75	9.02	8.88
AB	36.59	36.47	32.65	37.09	37.51	32.82	41.38	32.27	31.10
AN	23.49	24.30	19.04	18.59	19.41	19.19	18.80	22.89	19.85
NE	0.00	0.00	0.00	0.00	0.00	0.00	0.00	0.00	0.00
DI	1.44	0.00	0.00	0.00	0.00	0.00	0.00	0.00	0.00
HY	7.46	7.15	6.54	4.77	5.36	4.77	3.28	5.08	5.17
OL	0.00	0.00	0.00	0.00	0.00	0.00	0.00	0.00	0.00
MT	3.36	3.08	2.83	2.39	2.55	3.21	2.16	3.00	3.09
CM	0.00	0.00	0.00	0.00	0.00	0.00	0.00	0.00	0.00
HM	0.00	0.00	0.00	0.00	0.00	0.00	0.00	0.00	0.00
IL	1.37	1.27	0.96	0.96	1.03	1.01	0.96	1.05	0.92
AP	0.41	0.24	0.31	0.29	0.31	0.39	0.42	0.36	0.36
SUM	100.05	100.04	100.01	100.01	100.01	100.03	100.03	100.03	100.03

Table C.1: Major element analyses and CIPW normative mineralogy of volcanic and intrusive rocks from the Hedley area, south-central British Columbia (continued)....

FIELD NO.	173	309	527	528	529	530	531	532
MAP NO.[1]	W44	W45	W46	W47	W48	W49	W50	W51
LAB NO.	31865	32194	34189	34190	34191	34192	34193	34194
NORTHING	5461355	5475072	5460444	5460808	5460913	5459828	5462426	5462517
EASTING	707602	716367	703502	703772	703834	703409	706268	706356
UNIT[2]	13a	13a	13b	13b	13b	13b	13b	13b
SiO_2	64.99	62.08	61.11	60.67	59.03	58.56	60.69	60.80
TiO_2	0.49	0.47	0.65	0.63	0.65	0.75	0.61	0.58
Al_2O_3	18.13	17.25	17.16	16.00	16.48	17.18	17.18	16.83
$Fe_2O_{3(T)}$	4.28	5.13	6.69	6.71	6.95	7.73	6.93	6.45
MnO	0.13	0.14	0.12	0.12	0.19	0.17	0.17	0.19
MgO	0.94	1.44	1.46	2.32	2.40	2.58	2.38	2.37
CaO	3.95	5.74	5.82	5.18	5.58	6.39	5.65	5.93
Na_2O	3.79	4.02	3.21	3.15	3.12	3.25	3.45	3.53
K_2O	1.57	1.47	1.78	1.96	2.02	1.94	1.90	1.92
P_2O_5	0.15	0.12	0.17	0.16	0.17	0.18	0.16	0.16
LOI	1.52	1.16	1.68	2.04	2.47	0.75	1.04	1.26
SUM	99.94	99.02	99.85	98.94	99.06	99.48	100.16	100.02
CIPW Normative Minerals[3]								
Q	26.94	18.75	20.03	19.60	16.92	13.95	16.46	16.22
C	3.44	0.00	0.00	0.00	0.00	0.00	0.00	0.00
Z	0.02	0.02	0.02	0.02	0.03	0.02	0.02	0.02
OR	9.47	8.91	10.76	12.01	12.42	11.67	11.38	11.54
AB	32.67	34.87	27.79	27.63	27.46	27.99	29.58	30.37
AN	18.97	25.30	27.79	24.60	26.01	27.04	26.13	24.82
NE	0.00	0.00	0.00	0.00	0.00	0.00	0.00	0.00
DI	0.00	2.53	0.51	0.78	1.34	3.31	1.00	3.30
HY	4.69	5.38	7.96	10.22	10.48	10.15	10.32	8.91
OL	0.00	0.00	0.00	0.00	0.00	0.00	0.00	0.00
MT	2.53	3.05	3.47	3.53	3.67	3.99	3.56	3.33
CM	0.00	0.00	0.00	0.00	0.00	0.00	0.00	0.01
HM	0.00	0.00	0.00	0.00	0.00	0.00	0.00	0.00
IL	0.95	0.91	1.26	1.24	1.28	1.45	1.17	1.12
AP	0.36	0.29	0.41	0.39	0.42	0.43	0.38	0.39
SUM	100.03	100.02	100.03	100.03	100.03	100.02	100.03	100.03

Table C.2: Trace element analyses of volcanic and intrusive rocks from the Hedley area, south-central British Columbia. Analyses were completed at the B.C. Ministry of Energy, Mines, and Petroleum Resources Laboratory, Victoria, B.C. Values are in parts per million. Symbols "<", "--" and "*" denote below detection limit, not analysed and lab duplicate, respectively.

FIELD NO.	521	522	523	525	526	50	52	60	60*
MAP NO.[1]	W1	W2	W3	W4	W5	W6	W7	W8	W8
LAB NO.	34188	34175	34176	34178	34179	30825	30826	30827	30843
NORTHING	5454200	5470132	5469954	5469562	5469332	5469906	5469964	5472322	5472322
EASTING	700385	706060	705870	704891	704753	707907	707558	711537	711537
UNIT[2]	6	6	6	6	6	6	7	7	7
Au	--	--	--	--	<5	21	6	6	49
Ag	--	--	--	--	400	<300	<300	<300	<300
Cu	120	69	104	103	12	7	28	25	30
Pb	23	7	5	5	<3	4	4	5	3
Zn	90	90	90	103	93	82	59	58	71
Co	32	23	22	33	34	30	36	37	37
Ni	14	2	23	38	10	7	16	12	4
Mo	<8	<8	<8	<8	<3	<3	<3	<3	<3
Cr	--	--	--	--	<3	<25	58	64	<25
Hg	--	--	--	--	<25	<25	25	40	<25
As	7.4	6.2	4.7	5.9	<10.0	<10.0	<10.0	<10.0	<10.0
Sb	0.6	1.0	0.8	0.8	<10.0	<10.0	<10.0	<10.0	<10.0
Ba	1067	715	1391	2136	940	962	1140	1160	862
Sr	--	--	--	--	575	614	450	438	546
Bi	<3	<3	<3	<3	<3	<3	<3	<3	<3
Te	--	--	--	--	--	--	--	--	--
Rb	--	--	--	--	5	3	35	41	22
Y	19	19	26	23	12	14	13	10	12
Zr	46	48	80	64	48	55	61	64	52
Nb	1	1	7	1	<3	<3	<3	<3	<3
Ta	--	--	--	--	<4	<4	<4	--	<4
U	--	--	--	--	<2	<2	<2	<2	<2
Th	--	--	--	--	29	23	30	24	25

1. Map number is plotted on Figure 3.1.
2. Unit is identified in Table 3.1 and on Figure 1.1.

Table C.2: Trace element analyses of volcanic and intrusive rocks from the Hedley area, south-central British Columbia (continued)...

FIELD NO.	62	64	65	66	67	68	69	70	71
MAP NO.[1]	W9	W10	W11	W12	W13	W14	W15	W16	W17
LAB NO.	30829	30831	30832	30833	30834	30835	30836	30837	30838
NORTHING	5472771	5473042	5473143	5473242	5473346	5473415	5473809	5473907	5473410
EASTING	711930	711770	711562	711419	711319	711212	711096	710966	711060
UNIT[2]	7	7	7	7	7	7	7	7	7
Au	49	5	22	9	16	15	19	11	6
Ag	<300	<300	<300	<300	<300	<300	<300	<300	<300
Cu	30	7	5	9	15	8	28	60	8
Pb	3	3	6	9	4	3	3	3	3
Zn	71	59	50	74	62	42	57	60	51
Co	37	35	32	32	30	29	30	31	31
Ni	4	4	2	4	7	4	3	6	4
Mo	<3	<3	<3	<3	<3	<3	<3	<3	<3
Cr	<25	<25	<25	<25	<25	<25	<25	42	32
Hg	<25	<25	30	30	25	<25	25	50	30
As	<10	<10	<10.0	<10.0	<10.0	<10.0	<10.0	<10.0	<10.0
Sb	<10	<10	<10.0	<10.0	<10.0	15.0	<10.0	<10.0	<10.0
Ba	862	1307	1300	918	606	1154	1232	1088	<40
Sr	546	810	333	494	653	380	520	466	708
Bi	<3	<3	<3	<3	<3	<3	<3	<3	<3
Te	–	–	–	–	–	–	–	–	–
Rb	22	17	29	22	18	27	21	35	39
Y	12	13	18	14	12	14	15	13	12
Zr	52	47	81	53	40	68	50	44	66
Nb	<3	<3	<3	<3	<3	<3	<3	<3	<3
Ta	<4	<4	<4	<4	<4	<4	<4	<4	<4
U	<2	2	<2	<2	<2	<2	<2	1	<2
Th	25	28	23	32	23	25	19	35	23

Table C.2: Trace element analyses of volcanic and intrusive rocks from the Hedley area, south-central British Columbia (continued)...

FIELD NO.	72	73	73*	156	157	158	159	161	162
MAP NO.[1]	W18	W19	W19	W20	W21	W22	W23	W24	W25
LAB NO.	30839	30840	30844	31849	31850	31851	31852	31854	31855
NORTHING	5473200	5473215	5473215	5470521	5470666	5471625	5472167	5471068	5471111
EASTING	710980	711065	711065	712967	712905	712191	712424	714497	713668
UNIT[2]	7	7	7	7	7	7	7	7	7
Au	8	5	10	<30	<30	<30	<30	<30	<30
Ag	<300	<300	<300	<10	<10	<10	<10	<10	<10
Cu	11	6	5	22	13	30	12	22	46
Pb	<3	5	7	23	9	13	12	14	13
Zn	58	60	61	93	87	92	71	58	58
Co	31	27	28	41	33	35	32	37	38
Ni	3	3	2	25	9	13	8	11	11
Mo	<3	<3	<3	<3	<3	<3	<3	<3	5
Cr	<25	<25	<25	52	31	34	23	35	28
Hg	25	25	40	<10	<10	28	10	23	13
As	<10.0	<10.0	<10.0	93.5	14.0	5.4	1.7	12.6	165.0
Sb	<10.0	<10.0	<10.0	2.5	1.1	<1.0	<1.0	1.0	1.1
Ba	1014	1273	1200	756	811	854	652	653	1040
Sr	519	484	494	841	667	636	654	679	819
Bi	<3	<3	<3	8	<5	<5	<5	<5	<5
Te	--	--	--	<5	<5	<5	<5	<5	<5
Rb	26	29	28	14	32	28	30	23	32
Y	12	16	17	11	14	13	13	13	14
Zr	56	70	70	53	59	51	67	60	59
Nb	<3	<3	<3	<3	<3	<3	<3	<3	<3
Ta	1	<4	<4	<4	<4	<4	<4	<4	<4
U	<2	<2	2	<2	1	<2	1	<2	3
Th	27	27	30	25	22	16	25	18	23

Table C.2: Trace element analyses of volcanic and intrusive rocks from the Hedley area, south-central British Columbia (continued)...

FIELD NO.	163	164	218	334	767	381	406	77	78
MAP NO.[1]	W26	W27	W28	W29	W30	W31	W32	W33	W34
LAB NO.	31856	31857	31858	33914	34198	34197	33916	30845	30846
NORTHING	5471489	5472219	5471860	5473601	5474500	5475550	5476119	5468971	5469056
EASTING	713725	712174	715260	282307	711050	287800	288478	715093	715086
UNIT[2]	7	7	7	7	7	9	9	10	10
Au	191	<30	<30	20	<5	–	<20	–	–
Ag	<10	<10	<10	<300	<300	–	–	–	–
Cu	16	18	73	11	7	12	20	–	–
Pb	21	18	15	10	7	7	10	–	–
Zn	57	48	76	60	70	44	61	–	–
Co	29	30	29	37	24	11	–	33	29
Ni	9	10	8	22	2	8	5	48	4
Mo	<3	<3	<3	8	<10	<10	<2	–	–
Cr	23	19	21	35	–	17	–	10	4
Hg	21	12	11	<10	–	–	–	–	–
As	9.0	11.1	120.0	21.3	7.5	2.7	11	–	–
Sb	1.7	<1.0	2.0	1.2	1.1	<0.5	0.5	–	–
Ba	1441	1022	1520	978	–	1360	–	1297	1333
Sr	920	837	676	678	–	–	–	432	421
Bi	12	11	9	<5	<3	<3	<10	–	–
Te	<5	<5	<5	<5	–	–	–	–	–
Rb	50	30	50	22	–	–	–	57	61
Y	14	12	14	–	23	20	–	21	25
Zr	59	63	59	–	–	98	–	209	217
Nb	<3	<3	<3	–	–	7	–	<1	4
Ta	<4	<4	–	–	–	–	–	<4	<4
U	<2	<2	<2	–	–	–	–	<2	<2
Th	21	22	17	–	–	–	–	20	23

Table C.2: Trace element analyses of volcanic and intrusive rocks from the Hedley area, south-central British Columbia (continued)...

FIELD NO.	79	80	717			151	152	171	172
MAP NO.[1]	W35	W36	W37	W38	W39	W40	W41	W42	W43
LAB NO.	30847	30848	34181	35229	35234	31860	31861	31863	31864
NORTHING	5469056	5469196	5470427	5469300	5469300	5461980	5461900	5461155	5461223
EASTING	715086	715086	715746	717700	717700	708800	708770	707726	707744
UNIT[2]	10	10	10	10	10	13a	13a	13a	13a
Au	--	--	--	--	--	<30	<30	<30	<30
Ag	--	--	--	--	--	<10	<10	<10	<10
Cu	--	--	6	10	8	18	12	14	9
Pb	--	--	15	17	9	16	16	13	13
Zn	--	--	65	46	46	105	72	83	74
Co	30	26	8	7	9	28	28	37	24
Ni	1	5	3	<3	<3	6	6	7	4
Mo	--	--	1	<10	<10	<3	<3	<3	<3
Cr	20	1	4	--	--	<10	<10	11	11
Hg	--	--	--	--	--	<10	<10	18	<10
As	--	--	--	7	5	3.2	1.7	1.7	1.0
Sb	--	--	0.5	0.5	2	<1.0	<1.0	<1.0	<1.0
Ba	1319	1390	1510	--	--	937	946	926	1028
Sr	423	425	329	--	--	632	596	532	543
Bi	--	--	<3	<5	<5	<5	<5	<5	5
Te	--	--	--	--	--	<5	<5	<5	<5
Rb	56	49	73	--	--	33	24	30	30
Y	24	22	22	--	--	19	23	22	17
Zr	218	216	172	--	--	110	133	113	93
Nb	<1	1	6	--	--	1	<3	<3	<3
Ta	<4	<4	--	--	--	<4	<4	<4	6
U	<2	<2	10	--	--	<2	2	3	6
Th	23	26	13	--	--	22	22	26	24

Table C.2: Trace element analyses of volcanic and intrusive rocks from the Hedley area, south-central British Columbia (continued)....

FIELD NO.	173	309	527	528	529	530	531	532
MAP NO.[1]	W44	W45	W46	W47	W48	W49	W50	W51
LAB NO.	31865	32194	34189	34190	34191	34192	34193	34194
NORTHING	5461355	5475072	5460444	5460808	5460913	5459828	5462426	5462517
EASTING	707602	716367	703502	703772	703834	703409	706268	706356
UNIT[2]	13a	13a	13b	13b	13b	13b	13b	13b
Au	35	--	--	--	--	--	--	--
Ag	<10	--	--	--	--	--	--	--
Cu	6	--	26	36	38	20	12	25
Pb	12	--	36	15	18	14	20	17
Zn	73	--	75	77	83	93	99	88
Co	24	--	14	14	14	16	12	12
Ni	6	--	2	2	<2	<2	5	12
Mo	<3	--	<10	<10	<10	35	10	40
Cr	<10	--	18	12	16	6	19	28
Hg	12	--	--	--	--	--	--	--
As	2.5	--	2.4	2.6	3.0	2.3	2.7	5.0
Sb	1.0	--	<0.5	0.6	0.6	0.6	0.7	1.1
Ba	1211	--	--	--	--	--	--	--
Sr	538	--	--	--	--	--	--	--
Bi	<5	--	3	<3	4	4	3	<3
Te	<5	--	--	--	--	--	--	--
Rb	34	20	--	--	--	--	--	--
Y	17	16	23	21	30	24	22	26
Zr	106	96	121	116	123	105	105	113
Nb	<3	<3	4	1	15	2	5	12
Ta	<4	<4	--	--	--	--	--	--
U	2	<2	--	--	--	--	--	--
Th	20	21	--	--	--	--	--	--

Table C.3: Major element analyses and CIPW normative mineralogy of phyric and aphyric Hedley intrusions from the French Mine area, south-central British Columbia. Major element values are in weight percent. Analyses were by fused disk XRF completed at the Cominco Laboratory, Vancouver, B.C. Loss on ignition (LOI) was calculated after heating predried samples to 1050°C for four hours. Fe_2O_3 is expressed as total iron. Symbols "<", "–", "$", "#" and "*" denote below detection limit, not analysed, field duplicate , field duplicate - chrome grinder and lab duplicate, respectively.

FIELD NO.	2-2	12-1	12-2	12-5	12-15	12-15$	12-4	12-4$
MAP NO.[1]	W1	W2	W3	W4	W5	W5	W6	W6
LAB NO.	40412	40413	40414	40425	40429	40424	40423	40420
NORTHING	5467915	5467755	5467755	5467740	5468025	5468025	5467690	5467690
EASTING	716890	716435	716435	716350	716455	716455	716385	716385
UNIT[2]	7	7	7	7	7	7	7	7
ROCK TYPE[3]	Bin	Bin	Bin	Bin	Bin	Bin	hBin	hBin
SiO_2	49.73	57.36	54.61	48.08	55.01	53.97	56.14	56.30
TiO_2	0.66	0.52	1.30	1.59	1.53	1.42	0.87	0.89
Al_2O_3	15.03	18.12	14.73	15.59	14.63	14.72	17.87	18.23
Fe_2O_3(T)	7.05	5.75	10.75	11.08	10.29	10.50	9.14	9.22
MnO	0.15	0.09	0.20	0.19	0.18	0.17	0.21	0.21
MgO	4.27	3.31	6.88	6.94	6.52	6.97	3.98	4.21
CaO	18.10	6.66	7.46	12.05	7.42	7.55	4.92	4.39
Na_2O	2.72	4.54	2.96	2.83	3.21	3.27	5.69	5.63
K_2O	0.50	2.42	0.44	0.57	0.67	0.57	0.57	0.77
P_2O_5	0.29	0.15	0.18	0.16	0.19	0.17	0.19	0.21
LOI	0.86	0.75	0.45	0.34	0.37	0.30	0.26	0.27
SUM	99.36	99.67	99.96	99.42	100.02	99.61	99.84	100.33
CIPW Normative Mineralogy[4]								
Q	0.00	2.17	6.89	0.00	6.44	4.35	0.36	0.52
C	0.00	0.00	0.00	0.00	0.00	0.00	0.00	0.57
Z	0.01	0.01	0.02	0.03	0.03	0.02	0.02	0.02
OR	2.96	14.32	2.60	3.38	3.97	3.37	3.37	4.56
AB	17.69	38.41	25.04	23.33	27.16	27.67	48.14	47.63
AN	27.35	22.00	25.62	28.17	23.56	23.83	21.59	20.70
NE	2.88	0.00	0.00	0.33	0.00	0.00	0.00	0.00
DI	38.43	7.90	7.68	24.39	9.22	9.60	1.56	0.00
WO	4.65	0.00	0.00	0.00	0.00	0.00	0.00	0.00
HY	0.00	11.06	25.37	0.00	22.72	24.09	19.80	21.21
OL	0.00	0.00	0.00	12.61	0.00	0.00	0.00	0.00
MT	1.53	1.25	2.34	2.41	2.24	2.28	1.99	2.01
CM	0.01	0.00	0.04	0.07	0.04	0.04	0.01	0.01
IL	1.25	0.99	2.47	3.02	2.91	2.70	1.65	1.69
AP	0.69	0.36	0.43	0.38	0.45	0.40	0.45	0.50
CC	1.07	0.39	0.34	0.34	0.34	0.34	0.00	0.00
SUM	98.54	98.86	98.86	98.46	99.08	98.71	98.94	99.41

1. Map number is plotted on Figure 4.6.
2. Unit is identified in Table 3.1 and on Figure 4.1.
3. Field classification of rock types are: Bin=aphyric basalt intrusion, hBin=hornblende phyric intrusion, qDi=quartz diorite.
4. CIPW Normative Minerals are: Q=quartz, Z=zircon, OR=orthoclase, AB=albite, AN=anorthite, NE=nepheline, DI=diopside, WO=wollastonite, HY=hypersthene, OL=olivine, MT=magnetite, CM=chromite, IL=ilimenite, AP=apatite, CC=calcite.

Table C.3: Major element analysis and CIPW normative mineralogy of phyric and aphyric Hedley intrusions from the French Mine area, south-central British Columbia (continued)...

FIELD NO.	12-11	12-16	89-36	89-37	89-37$	2-3	2-3#	2-3#
MAP NO.[1]	W7	W8	W9	W10	W10	W11	W11	W11
LAB NO.	40428	40432	40435	40436	40442	40415	40418	40443
NORTHING	5468325	5467765	5468000	5468000	5468000	5468068	5468068	5468068
EASTING	716340	716395	716875	716875	716875	717320	717320	717320
UNIT[2]	7	7	7	7	7	7	7	7
ROCK TYPE[3]	hBin	hBin	hBin	hBin	hBin	qDi	qDi	qDi
SiO_2	54.22	55.59	49.74	54.01	55.08	60.68	60.70	60.15
TiO_2	0.98	0.94	0.95	0.84	0.84	1.16	1.24	1.25
Al_2O_3	16.75	17.04	17.68	17.00	17.20	14.58	14.75	14.52
Fe_2O_3(T)	10.61	9.12	8.43	7.86	7.05	9.56	9.85	9.92
MnO	0.23	0.19	0.13	0.11	0.10	0.19	0.18	0.18
MgO	4.46	4.38	4.52	3.58	3.93	2.72	3.07	2.95
CaO	6.45	5.09	9.30	7.61	7.56	4.88	3.66	3.68
Na_2O	4.23	5.57	4.11	4.23	4.71	5.34	5.93	5.77
K_2O	1.20	0.78	2.03	2.88	2.57	0.39	0.48	0.49
P_2O_5	0.21	0.16	0.21	0.17	0.18	0.19	0.20	0.18
LOI	0.28	0.39	2.33	0.68	0.55	0.28	0.10	0.23
SUM	99.62	99.25	99.43	98.97	99.77	99.97	100.16	99.32
CIPW Normative Minerals[4]								
Q	1.03	0.00	0.00	0.00	0.00	11.05	8.52	8.95
C	0.00	0.00	0.00	0.00	0.00	0.00	0.00	0.00
Z	0.02	0.02	0.02	0.02	0.02	0.02	0.02	0.02
OR	7.11	4.61	12.03	17.05	15.22	2.31	2.85	2.90
AB	35.79	47.13	24.47	34.96	38.19	45.18	50.17	48.82
AN	23.23	19.26	23.86	18.95	18.25	14.68	12.23	12.29
NE	0.00	0.00	5.58	0.45	0.90	0.00	0.00	0.00
DI	6.47	4.47	17.73	15.10	15.31	7.04	3.97	4.12
WO	0.00	0.00	0.00	0.00	0.00	0.00	0.00	0.00
HY	20.29	17.07	0.00	0.00	0.00	13.92	16.56	16.25
OL	0.00	1.55	8.82	7.62	7.41	0.00	0.00	0.00
MT	2.31	1.98	1.83	1.71	1.53	2.08	2.14	2.16
CM	0.01	0.01	0.01	0.01	0.01	0.00	0.00	0.02
IL	1.86	1.79	1.80	1.60	1.60	2.20	2.35	2.37
AP	0.50	0.38	0.50	0.41	0.43	0.45	0.48	0.43
CC	0.00	0.00	0.00	0.00	0.00	0.00	0.00	0.00
SUM	98.62	98.28	96.66	97.86	98.86	98.94	99.30	98.33

Table C.3: Major element analysis and CIPW normative mineralogy of phyric and aphyric Hedley intrusions from the French Mine area, south-central British Columbia (continued)...

FIELD NO.	6-5	6-5$	6-5#	6-5*	6-7	6-7$	8-1	8-1$
MAP NO.[1]	W12	W12	W12	W12	W13	W13	W14	W14
LAB NO.	40417	40416	40444	40411	40419	40422	40421	40427
NORTHING	5467735	5467735	5467735	5467735	5467750	5467750	5467675	5467675
EASTING	716385	716385	716385	716385	716360	716360	716375	716375
UNIT[2]	7	7	7	7	7	7	7	7
ROCK TYPE[3]	qDi	qDi	qDi	qDi	qDi	qDi	qDi	qDi
SiO_2	49.03	49.54	49.35	48.98	54.31	54.31	54.32	54.61
TiO_2	2.08	2.08	2.08	2.10	0.92	0.92	1.75	1.76
Al_2O_3	15.60	15.21	15.04	15.50	17.54	17.58	15.83	15.62
Fe_2O_3(T)	11.56	11.27	11.34	11.62	8.91	8.85	9.07	9.18
MnO	0.15	0.15	0.14	0.14	0.15	0.15	0.12	0.12
MgO	6.55	6.35	6.27	6.51	4.36	4.38	5.81	6.00
CaO	8.54	9.07	9.21	8.47	5.65	5.45	6.48	6.64
Na_2O	3.60	3.61	3.65	3.55	4.89	4.92	3.81	3.95
K_2O	1.55	1.14	1.12	1.54	2.04	2.02	1.12	1.08
P_2O_5	0.44	0.46	0.42	0.46	0.17	0.17	0.31	0.31
LOI	0.86	0.92	0.84	0.70	0.79	0.86	0.87	0.79
SUM	99.96	99.80	99.46	99.57	99.73	99.61	99.49	100.06
CIPW Normative Minerals[4]								
Q	0.00	0.00	0.00	0.00	0.00	0.00	3.61	2.97
C	0.00	0.00	0.00	0.00	0.00	0.00	0.00	0.00
Z	0.03	0.03	0.03	0.03	0.02	0.02	0.02	0.02
OR	9.18	6.75	6.64	9.12	12.07	11.95	6.62	6.39
AB	29.00	30.54	30.88	29.59	41.37	41.63	32.24	33.42
AN	21.87	21.97	21.38	21.85	20.03	20.06	22.85	21.76
NE	0.79	0.00	0.00	0.24	0.00	0.00	0.00	0.00
DI	14.79	16.72	17.99	14.41	6.43	5.56	6.34	7.86
WO	0.00	0.00	0.00	0.00	0.00	0.00	0.00	0.00
HY	0.00	2.89	0.85	0.00	5.26	6.11	20.33	20.19
OL	15.16	11.72	12.66	15.24	9.28	8.94	0.00	0.00
MT	2.51	2.45	2.47	2.53	1.94	1.92	1.97	2.00
CM	0.01	0.01	0.02	0.01	0.01	0.01	0.05	0.05
IL	3.95	3.95	3.95	3.99	1.75	1.75	3.32	3.34
AP	1.05	1.09	1.00	1.10	0.41	0.41	0.74	0.74
CC	0.00	0.00	0.00	0.00	0.00	0.00	0.00	0.00
SUM	98.34	98.13	97.87	98.11	98.55	98.36	98.10	98.74

Table C.3: Major element analysis and CIPW normative mineralogy of phyric and aphyric Hedley intrusions from the French Mine area, south-central British Columbia (continued)....

FIELD NO.	8-1*	89-35	89-35$	89-136	89-136$
MAP NO.[1]	W14	W15	W15	W16	W16
LAB NO.	40431	40433	40437	40434	40434
NORTHING	5467675	5468000	5468000		
EASTING	716375	716875	716875		
UNIT[2]	7	7	7		
ROCK TYPE[3]	qDi	qDi	qDi		
SiO_2	54.19	57.45	57.38	54.09	54.04
TiO_2	1.79	0.52	0.52	0.52	0.52
Al_2O_3	15.59	18.27	18.01	18.73	18.56
Fe_2O_3(T)	9.22	6.35	5.73	6.79	6.70
MnO	0.13	0.07	0.08	0.19	0.20
MgO	5.93	3.47	3.49	3.22	3.26
CaO	6.63	6.59	6.59	7.86	7.87
Na_2O	4.00	4.67	4.44	3.86	3.98
K_2O	1.09	1.57	1.95	2.98	2.75
P_2O_5	0.31	0.15	0.14	0.32	0.33
LOI	0.87	1.03	1.04	1.53	1.50
SUM	99.75	100.14	99.37	100.09	99.71
CIPW Normative Minerals[4]					
Q	2.39	3.53	3.82	0.00	0.00
C	0.00	0.00	0.00	0.00	0.03
Z	0.02	0.01	0.01	0.03	16.27
OR	6.45	9.30	11.54	17.63	33.67
AB	33.84	39.51	37.57	32.66	24.72
AN	21.42	24.33	23.54	25.05	0.00
NE	0.00	0.00	0.00	0.00	10.58
DI	8.10	6.53	7.28	10.34	0.00
WO	0.00	0.00	0.00	0.00	4.91
HY	19.92	12.84	11.77	4.29	4.48
OL	0.00	0.00	0.00	5.02	1.46
MT	2.01	1.38	1.25	1.48	0.00
CM	0.05	0.00	0.00	0.00	0.00
IL	3.40	0.99	0.99	0.99	0.99
AP	0.74	0.36	0.34	0.76	0.79
CC	0.00	0.00	0.00	0.00	0.00
SUM	98.35	98.80	98.10	98.25	97.90

Table C.4: Trace element analyses of phyric and aphyric Hedley intrusions from the French Mine area, south-central British Columbia. Values are in parts per million. Analyses were by Cominco Laboratory (Rb, Sr, Nb, Y, Ba, Sn), B.C. Ministry of Energy, Mines and Petroleum Resources Laboratory (Cr, Ni, Co, Cu, Pb, Zn, Mo, As, Zr, Ti, V, La, Ce) and Acme Labs Ltd. (Bi, Te). Symbols "<", "--", "$", "#" and "*" denote below detection limit, not analysed, field duplicate, field duplicate - chrome grinder and lab duplicate, respectively.

FIELD NO.	2-2	12-1	12-2	12-5	12-15	12-15$	12-4	12-4$
MAP NO.[1]	W1	W2	W3	W4	W5	W5	W6	W6
LAB NO.	40412	40413	40414	40425	40429	40424	40423	40420
NORTHING	5467915	5467755	5467755	5467740	5468025	5468025	5467690	5467690
EASTING	716890	716435	716435	716350	716455	716455	716385	716385
UNIT[2]	7	7	7	7	7	7	7	7
ROCK TYPE[3]	Bin	Bin	Bin	Bin	Bin	Bin	hBin	hBin
Cr	59	19	206	318	195	202	33	30
Ni	17	3	82	106	67	84	<3	<3
Co	46	36	43	44	39	43	26	20
Cu	17	49	6	114	42	64	17	14
Pb	8	13	5	<3	8	8	10	6
Zn	97	38	89	80	83	83	75	85
Bi	0.1	0.2	0.1	0.1	0.2	0.1	0.3	0.1
Mo	<10	<10	<10	<10	<10	<10	<10	<10
As	368	28	28	64	5	5	2	2
Te	0.1	0.2	0.4	0.1	0.4	0.1	0.3	0.1
Rb	16	51	11	25	37	10	15	16
Sr	939	712	244	379	394	350	590	547
Nb	<10	<10	12	17	11	15	<10	<10
Zr	57	64	124	159	129	117	91	87
Ti	3957	3117	7793	9532	9172	8513	5216	5336
Y	20	15	26	26	27	27	25	26
Ba	131	1309	120	256	286	245	288	322
Sn	<10	<10	<10	<10	<10	<10	<10	<10
V	263	164	225	234	237	240	252	252
La	17	<15	27	23	15	<15	<15	<15
Ce	39	<15	24	42	28	23	28	23

1. Map number is plotted on Figure 4.6.
2. Unit is identified in Table 3.1 and on Figure 4.1.
3. Field classification of rock types are: Bin=aphyric basalt intrusion, hBin=hornblende phyric basalt intrusion, qDi=quartz diorite.

Table C.4: Trace element analysis of phyric and aphyric Hedley intrusions from the French Mine area, south-central British Columbia (continued)...

FIELD NO.	12-11	12-16	89-36	89-37	89-37$	2-3	2-3#	2-3#
MAP NO.[1]	W7	W8	W9	W10	W10	W11	W11	W11
LAB NO.	40428	40432	40435	40436	40442	40415	40418	40443
NORTHING	5468325	5467765	5468000	5468000	5468000	5468068	5468068	5468068
EASTING	716340	716395	716875	716875	716875	717320	717320	717320
UNIT[2]	7	7	7	7	7	7	7	7
ROCK TYPE[3]	hBin	hBin	hBin	hBin	hBin	qDi	qDi	qDi
Cr	37	41	35	31	29	17	17	80
Ni	<3	<3	<3	<3	<3	<3	<3	<3
Co	26	23	21	20	17	30	24	16
Cu	28	37	78	172	76	17	7	10
Pb	10	8	11	8	18	<3	<3	5
Zn	122	68	120	81	66	74	60	61
Bi	0.2	0.2	0.1	0.2	0.1	0.1	0.1	0.1
Mo	<10	<10	<10	<10	<10	<10	<10	<10
As	1	4	8	19	11	1	1	1
Te	0.4	0.4	0.1	0.2	0.1	0.3	0.1	0.4
Rb	35	<10	80	67	81	<10	21	<10
Sr	456	782	789	583	674	151	172	179
Nb	<10	<10	<10	<10	<10	<10	<10	<10
Zr	86	78	94	83	81	112	107	109
Ti	5875	5635	5695	5036	5036	6954	7434	7494
Y	28	24	28	21	26	39	33	39
Ba	844	647	1260	1195	1085	120	230	225
Sn	<10	<10	<10	<10	15	<10	<10	<10
V	300	280	276	245	241	154	160	158
La	20	<15	17	<15	15	16	<15	<15
Ce	30	21	29	27	18	<15	<15	20

Table C.4: Trace element analysis of phyric and aphyric Hedley intrusions from the French Mine area, south-central British Columbia (continued)...

FIELD NO.	6-5	6-5$	6-5#	6-5*	6-7	6-7$	8-1	8-1$
MAP NO.[1]	W12	W12	W12	W12	W13	W13	W14	W14
LAB NO.	40417	40416	40444	40411	40419	40422	40421	40427
NORTHING	5467735	5467735	5467735	5467735	5467750	5467750	5467675	5467675
EASTING	716385	716385	716385	716385	716360	716360	716375	716375
UNIT[2]	7	7	7	7	7	7	7	7
ROCK TYPE[3]	qDi	qDi	qDi	qDi	qDi	qDi	qDi	qDi
Cr	54	52	83	52	40	40	247	239
Ni	61	58	61	60	<3	<3	87	83
Co	43	45	42	40	21	18	32	32
Cu	65	89	84	64	18	19	33	25
Pb	6	8	10	5	3	15	8	6
Zn	86	75	79	83	65	70	123	114
Bi	0.2	0.3	0.2	0.3	0.2	0.2	0.1	0.2
Mo	<10	<10	<10	<10	<10	<10	<10	<10
As	3	3	3	3	5	11	2	2
Te	0.2	0.1	0.1	0.1	0.1	0.2	0.1	0.1
Rb	50	28	54	35	30	24	<10	15
Sr	677	695	699	674	672	690	974	949
Nb	28	28	29	35	<10	<10	<10	<10
Zr	141	141	138	142	78	79	85	85
Ti	12470	12470	12470	12589	5515	5515	10491	10551
Y	23	27	25	24	20	23	19	17
Ba	717	534	513	711	2326	2260	544	528
Sn	<10	<10	<10	<10	<10	<10	<10	<10
V	213	203	224	213	284	279	104	110
La	34	35	41	38	<15	16	<15	<15
Ce	58	67	66	67	16	25	24	30

Table C.4: Trace element analysis of phyric and aphyric Hedley intrusions from the French Mine area, south-central British Columbia (continued)....

FIELD NO.	8-1*	89-35	89-35$	89-136	89-136$
MAP NO.[1]	W14	W15	W15		
LAB NO.	40431	40433	40437	40441	40434
NORTHING	5467675	5468000	5468000		
EASTING	716375	716875	716875		
UNIT[2]	7	7	7		
ROCK TYPE[3]	qDi	qDi	qDi		
Cr	239	19	19	19	17
Ni	82	<3	<3	3	3
Co	33	22	24	19	21
Cu	26	57	47	72	115
Pb	5	3	8	53	11
Zn	116	31	32	76	68
Bi	0.2	0.1	0.1	0.2	0.1
Mo	<10	<10	<10	<10	<10
As	2	7	5	2	3
Te	0.3	0.1	0.2	0.1	0.1
Rb	24	54	51	43	54
Sr	952	689	754	1043	1076
Nb	<10	<10	<10	<10	<10
Zr	87	64	69	140	139
Ti	10731	3117	3117	3117	3117
Y	17	12	13	19	18
Ba	535	1087	1294	848	796
Sn	<10	<10	<10	<10	<10
V	98	164	163	215	204
La	<15	<15	<15	15	<15
Ce	15	21	20	23	22

APPENDIX D: Electron microprobe analyses from the Hedley area, south-central British Columbia.

Appendix D contains information on the sampling procedure, analytical method and tables of electron microprobe data (Ray and Dawson, 1994 and this study) for igneous garnet (Table D.1), skarn garnet (Table D.2), skarn clinopyroxene (Table D.3), sulphide minerals(Table D.4), native gold (Table D.5) and telluride minerals (Table D.4).

Sampling Procedure

This study incorporates analyses (HD prefix) from a regional mapping program (Ray and Dawson, 1994) and additional analyses (without HD prefix) from this study. Garnets from a minor intrusion (Table D.1) were chosen to determine their composition and to compare with garnet compositions from other geological environments. Samples from the French mine were chosen to determine the composition of skarn related garnet (Table D.2), clinopyroxene (Table D.3), sulphides (Table D.4), gold (Table D.5) and unknown telluride (Table D.6) minerals. Samples containing minerals of interest were prepared as polished thin sections and carbon coated. Prior to carbon coating, the sections were examined under a petrographic microscope and minerals of interest were marked to assist in locating the minerals when the section was loaded into the probe.

Analytical Method

Quantitative and semi-quantitative analyses were done on a fully automated CAMECA SX-50 microprobe operating in wavelength-dispersive (WDS) mode. Garnet and clinopyroxene were analyzed with an accelerating potential of 15 kV, a beam current of 20 nA and a beam width of 2 μ. Suphides, tellurides and gold were analyzed with an accelerating potential of 20 kV, a beam current of 30 nA and a beam width of 5 μ. UBC standards of similar composition to the mineral of interest were used. Microprobe data from samples prefixed with 'HD' were reduced using the CAMECA Georef Program. Raw data from the remainder of the samples were reduced using a spreadsheet program developed at Washington State University.

Table D.1: Microprobe analysis of igneous garnet from minor intrusion near Skwel Peken Ridge , Hedley area, south-central British Columbia. Three part analytical number indicates sample number (first number), grain number (second number) and beam position (third number; letter c = core, m = margin and absent = not identified).

Analytical No.	HD329-1-1	HD329-1-2	HD329-1-3	HD329-1-4	HD329-1-5m	HD328-1-1c
Weight percent:						
FeO	29.29	28.94	29.41	13.66	13.71	29.19
Fe_2O_3	0.62	0.76	0.89	0.14	0.36	0.90
SiO_2	36.31	36.51	36.35	35.97	35.62	36.58
CaO	3.22	3.26	3.33	2.25	2.20	3.19
Al_2O_3	20.23	20.14	20.17	20.23	20.07	20.11
TiO_2	0.28	0.20	0.24	0.05	0.04	0.24
MgO	2.72	2.66	2.78	0.15	0.17	2.75
MnO	6.21	6.14	6.14	5.90	6.22	6.11
Total	98.88	98.61	99.31	78.35	78.39	99.07
Cations based on 12 oxygens:						
Fe2+	2.003	1.980	2.005	1.079	1.087	1.990
Fe3+	0.038	0.047	0.055	0.010	0.026	0.055
Si4+	2.969	2.988	2.963	3.399	3.378	2.982
Ca2+	0.282	0.286	0.291	0.228	0.224	0.279
Al3+	1.949	1.942	1.938	2.253	2.243	1.932
Ti4+	0.017	0.012	0.015	0.004	0.003	0.015
Mg2+	0.332	0.324	0.338	0.021	0.024	0.334
Mn2+	0.430	0.426	0.424	0.472	0.500	0.422
Sum	8.020	8.005	8.027	7.466	7.485	8.009
Mole percent[1]:						
AD	2.39	2.70	3.11	0.54	1.20	3.18
GR	6.56	6.56	6.14	6.12	5.21	5.76
PY	10.92	10.77	11.08	0.62	0.69	11.07
SP	14.17	14.15	13.90	60.98	61.26	13.98
AL	65.96	65.82	65.77	31.75	31.63	66.00

1. Abbreviations are: AD = andradite, GR = grossular, PY = pyrope, SP = spessartine, AL = almandite.

Table D.1: Microprobe analysis of igneous garnet from minor intrusion near Skwel Peken Ridge , Hedley area, south-central British Columbia (continued)...

Analytical No.	HD328-1-2	HD328-1-3	HD328-1-4	HD328-1-5m	HD328-2-1c	HD328-2-2
Weight percent:						
FeO	28.97	29.37	29.47	14.49	28.25	29.10
Fe_2O_3	0.35	0.72	0.84	0.14	0.67	0.47
SiO_2	36.33	36.67	36.72	36.03	36.70	36.18
CaO	3.10	3.38	3.34	0.24	3.20	3.08
Al_2O_3	20.11	20.29	20.24	20.45	20.17	20.17
TiO_2	0.21	0.25	0.30	0.04	0.22	0.22
MgO	2.79	2.80	2.83	0.26	2.67	2.67
MnO	6.07	5.78	5.79	5.69	6.45	6.02
Total	97.93	99.26	99.53	77.34	98.33	97.91
Cations based on 12 oxygens:						
Fe2+	1.994	1.996	1.999	1.154	1.933	2.006
Fe3+	0.022	0.044	0.051	0.010	0.041	0.029
Si4+	2.991	2.980	2.978	3.431	3.003	2.982
Ca2+	0.273	0.294	0.290	0.024	0.281	0.272
Al3+	1.951	1.943	1.935	2.295	1.945	1.959
Ti4+	0.013	0.015	0.018	0.003	0.014	0.014
Mg2+	0.342	0.339	0.342	0.037	0.326	0.328
Mn2+	0.423	0.398	0.398	0.459	0.447	0.420
Sum	8.010	8.011	8.011	7.414	7.990	8.010
Mole percent[1]:						
AD	2.98	2.65	3.09	0.50	2.47	1.86
GR	6.59	6.81	6.30	6.01	7.00	6.89
PY	11.21	11.23	11.33	1.04	10.89	10.85
SP	13.87	13.18	13.16	59.39	14.95	13.93
AL	65.36	66.13	66.11	33.06	64.69	66.47

Table D.1: Microprobe analysis of igneous garnet from minor intrusion near Skwel Peken Ridge , Hedley area, south-central British Columbia (continued)...

Analytical No.	HD328-2-3	HD328-2-4	HD328-2-5m	HD328-3-1c	HD328-3-2	HD328-3-3
Weight percent:						
FeO	28.92	29.18	13.98	28.73	29.18	29.00
Fe_2O_3	0.68	0.71	0.23	0.59	0.51	0.58
SiO_2	36.43	36.34	35.80	36.72	37.00	36.62
CaO	3.28	3.40	2.05	3.07	3.02	2.97
Al_2O_3	20.06	20.23	20.14	20.25	20.52	20.22
TiO_2	0.33	0.25	0.08	0.26	0.21	0.23
MgO	2.78	2.82	0.16	2.77	2.70	2.74
MnO	5.82	6.05	5.95	6.31	6.53	6.12
Total	98.30	98.98	78.39	98.70	99.67	98.48
Cations based on 12 oxygens:						
Fe2+	1.983	1.992	1.107	1.960	1.974	1.984
Fe3+	0.042	0.044	0.016	0.036	0.031	0.036
Si4+	2.987	2.967	3.389	2.996	2.993	2.996
Ca2+	0.288	0.297	0.208	0.268	0.262	0.260
Al3+	1.938	1.946	2.247	1.947	1.956	1.949
Ti4+	0.020	0.015	0.006	0.016	0.013	0.014
Mg2+	0.340	0.343	0.023	0.337	0.326	0.334
Mn2+	0.404	0.418	0.477	0.436	0.447	0.424
Sum	8.003	8.023	7.473	7.997	8.001	7.998
Mole percent[1]:						
AD	2.70	2.61	0.88	2.30	1.93	2.21
GR	6.50	6.87	5.11	6.35	6.55	6.20
PY	11.31	11.27	0.67	11.27	10.83	11.17
SP	13.45	13.75	60.94	14.59	14.92	14.17
AL	66.03	65.49	32.40	65.50	65.78	66.25

Table D.1: Microprobe analysis of igneous garnet from minor intrusion near Skwel Peken Ridge , Hedley area, south-central British Columbia (continued)...

Analytical No.	HD328-3-4	HD328-3-5m	HD328-4-1c	HD328-4-2	HD328-4-3	HD328-4-4
Weight percent:						
FeO	28.88	29.01	29.14	29.21	29.00	13.83
Fe_2O_3	0.66	0.70	0.54	0.67	0.62	0.33
SiO_2	36.60	36.60	36.71	36.60	36.73	35.83
CaO	3.36	3.36	3.09	3.36	3.33	2.10
Al_2O_3	20.19	20.24	21.45	20.23	20.31	20.20
TiO_2	0.24	0.27	0.16	0.24	0.18	0.12
MgO	2.83	2.78	2.72	2.70	2.77	0.14
MnO	5.70	6.06	6.42	5.80	5.63	6.65
Total	98.46	99.02	100.23	98.81	98.57	79.20
Cations based on 12 oxygens:						
Fe2+	1.974	1.976	1.958	1.994	1.979	1.088
Fe3+	0.041	0.043	0.033	0.041	0.038	0.023
Si4+	2.992	2.981	2.949	2.987	2.997	3.370
Ca2+	0.294	0.293	0.266	0.294	0.291	0.212
Al3+	1.945	1.943	2.031	1.946	1.953	2.239
Ti4+	0.015	0.017	0.010	0.015	0.011	0.008
Mg2+	0.345	0.338	0.326	0.328	0.337	0.020
Mn2+	0.395	0.418	0.437	0.401	0.389	0.530
Sum	8.001	8.009	8.009	8.005	7.996	7.490
Mole percent[1]:						
AD	2.46	2.61	1.93	2.48	2.24	1.24
GR	7.05	6.78	6.79	6.99	7.24	4.78
PY	11.48	11.18	10.94	10.93	11.22	0.57
SP	13.15	13.87	14.65	13.34	13.42	61.76
AL	65.85	65.55	65.69	66.26	65.89	31.64

Table D.1: Microprobe analysis of igneous garnet from minor intrusion near Skwel Peken Ridge , Hedley area, south-central British Columbia (continued)...

Analytical No.	HD328-4-5m	HD328-5-1c	HD328-5-2	HD328-5-3	HD328-5-4	HD328-5-5m
Weight percent:						
FeO	14.57	29.00	28.77	29.27	28.71	12.46
Fe_2O_3	0.00	0.78	0.55	0.72	0.34	0.20
SiO_2	36.16	36.50	36.39	36.46	36.48	35.84
CaO	1.71	3.40	3.40	3.36	3.42	2.42
Al_2O_3	20.48	20.19	20.25	20.30	20.32	20.21
TiO_2	0.21	0.26	0.24	0.28	0.25	0.07
MgO	0.22	2.67	2.74	2.83	2.69	0.14
MnO	5.64	6.32	6.16	6.22	5.90	7.15
Total	78.99	99.12	98.50	99.44	98.11	78.49
Cations based on 12 oxygens:						
Fe2+	1.143	1.977	1.970	1.990	1.969	0.984
Fe3+	0.000	0.048	0.034	0.044	0.021	0.014
Si4+	3.391	2.976	2.979	2.964	2.992	3.386
Ca2+	0.172	0.297	0.298	0.293	0.301	0.245
Al3+	2.263	1.940	1.954	1.945	1.964	2.250
Ti4+	0.015	0.016	0.015	0.017	0.015	0.005
Mg2+	0.031	0.325	0.334	0.343	0.329	0.020
Mn2+	0.448	0.436	0.427	0.428	0.410	0.572
Sum	7.463	8.014	8.012	8.024	8.000	7.477
Mole percent[1]:						
AD	0.39	2.84	2.14	2.68	1.51	0.75
GR	4.45	6.65	7.43	6.61	8.20	6.32
PY	0.92	10.73	11.06	11.27	10.97	0.56
SP	60.37	14.43	14.14	14.06	13.66	63.57
AL	33.87	65.35	65.24	65.38	65.65	28.80

Table D.1: Microprobe analysis of igneous garnet from minor intrusion near Skwel Peken Ridge , Hedley area, south-central British Columbia (continued)...

Analytical No.	HD328-6-1c	HD328-6-2	HD328-6-3	HD328-6-4	HD328-6-5m	HD328-7-1c
Weight percent:						
FeO	29.12	28.38	29.14	29.27	29.22	29.07
Fe_2O_3	0.51	0.72	0.94	0.82	0.80	0.88
SiO_2	36.28	36.52	36.91	36.54	36.38	36.55
CaO	3.31	3.39	3.32	3.27	3.35	3.30
Al_2O_3	20.34	20.11	20.12	20.09	20.04	20.07
TiO_2	0.20	0.24	0.22	0.28	0.26	0.24
MgO	2.80	2.74	2.78	2.83	2.77	2.82
MnO	6.10	6.23	5.62	5.65	5.56	5.76
Total	98.66	98.33	99.05	98.75	98.38	98.69
Cations based on 12 oxygens:						
Fe2+	1.993	1.944	1.981	1.999	2.004	1.986
Fe3+	0.031	0.044	0.058	0.050	0.049	0.054
Si4+	2.969	2.992	3.001	2.984	2.983	2.986
Ca2+	0.290	0.298	0.289	0.286	0.294	0.289
Al3+	1.962	1.941	1.928	1.934	1.937	1.933
Ti4+	0.012	0.015	0.013	0.017	0.016	0.015
Mg2+	0.342	0.335	0.337	0.345	0.339	0.343
Mn2+	0.423	0.432	0.387	0.391	0.386	0.399
Sum	8.022	8.001	7.993	8.006	8.008	8.005
Mole percent[1]:						
AD	1.91	2.65	3.28	3.02	2.93	3.13
GR	7.38	6.98	6.15	6.16	6.51	6.18
PY	11.22	11.16	11.29	11.44	11.25	11.41
SP	13.92	14.40	12.95	12.97	12.82	13.24
AL	65.57	64.81	66.33	66.42	66.49	66.04

Table D.1: Microprobe analysis of igneous garnet from minor intrusion near Skwel Peken Ridge , Hedley area, south-central British Columbia (continued)...

Analytical No.	HD328-7-2	HD328-7-3	HD328-7-4	HD328-7-5m	HD328-8-1c	HD328-8-2
Weight percent:						
FeO	12.09	13.64	14.35	14.71	28.98	29.69
Fe_2O_3	0.35	0.16	0.40	0.14	0.41	0.74
SiO_2	36.06	35.68	36.32	35.64	36.52	36.64
CaO	2.46	2.25	1.86	1.80	3.26	3.25
Al_2O_3	20.23	20.11	20.12	20.14	20.35	20.27
TiO_2	0.06	0.07	0.21	0.15	0.24	0.32
MgO	0.13	0.17	0.18	0.19	2.79	2.86
MnO	6.88	5.84	5.91	5.63	5.90	5.71
Total	78.26	77.92	79.35	78.40	98.45	99.48
Cations based on 12 oxygens:						
Fe2+	0.954	1.085	1.123	1.166	1.982	2.015
Fe3+	0.025	0.011	0.028	0.010	0.025	0.045
Si4+	3.403	3.392	3.398	3.379	2.987	2.974
Ca2+	0.249	0.229	0.186	0.183	0.286	0.283
Al3+	2.250	2.253	2.219	2.251	1.962	1.939
Ti4+	0.004	0.005	0.015	0.011	0.015	0.020
Mg2+	0.019	0.024	0.025	0.027	0.340	0.346
Mn2+	0.550	0.470	0.468	0.452	0.409	0.393
Sum	7.455	7.470	7.463	7.480	8.005	8.014
Mole percent[1]:						
AD	1.19	0.65	1.65	0.73	1.69	2.81
GR	5.99	5.96	3.60	4.41	7.52	6.15
PY	0.51	0.71	0.74	0.79	11.29	11.42
SP	62.63	60.93	60.78	60.06	13.60	12.98
AL	29.68	31.75	33.22	34.02	65.91	66.64

Table D.1: Microprobe analysis of igneous garnet from minor intrusion near Skwel Peken Ridge , Hedley area, south-central British Columbia (continued)...

Analytical No.	HD328-8-3	HD328-8-4	HD328-8-5m	HD328-9-1c	HD328-9-2	HD328-9-3
Weight percent:						
FeO	29.46	29.17	29.37	28.88	28.89	28.85
Fe_2O_3	0.89	0.49	0.73	0.58	0.90	0.58
SiO_2	36.78	36.71	36.60	36.63	36.68	36.57
CaO	3.34	3.36	3.44	3.23	3.28	3.40
Al_2O_3	20.23	20.27	20.26	20.25	20.11	20.37
TiO_2	0.35	0.27	0.18	0.26	0.24	0.25
MgO	2.79	2.76	2.77	2.76	2.72	2.64
MnO	6.08	5.42	5.55	6.06	6.24	6.62
Total	99.92	98.45	98.90	98.65	99.06	99.28
Cations based on 12 oxygens:						
Fe2+	1.993	1.993	2.002	1.972	1.968	1.963
Fe3+	0.054	0.030	0.045	0.036	0.055	0.036
Si4+	2.975	2.998	2.984	2.991	2.988	2.975
Ca2+	0.289	0.294	0.300	0.283	0.286	0.296
Al3+	1.928	1.951	1.947	1.949	1.931	1.953
Ti4+	0.021	0.017	0.011	0.016	0.015	0.015
Mg2+	0.336	0.336	0.337	0.336	0.330	0.320
Mn2+	0.416	0.375	0.383	0.419	0.431	0.456
Sum	8.013	7.994	8.009	8.001	8.004	8.015
Mole percent[1]:						
AD	3.32	2.03	2.55	2.25	3.20	2.19
GR	5.83	7.47	7.17	6.85	6.02	7.30
PY	11.13	11.24	11.17	11.18	10.99	10.59
SP	13.78	12.55	12.71	13.97	14.31	15.07
AL	65.93	66.71	66.39	65.75	65.47	64.85

Table D.1: Microprobe analysis of igneous garnet from minor intrusion near Skwel Peken Ridge , Hedley area, south-central British Columbia (continued)...

Analytical No.	HD328-9-4	HD328-9-5m	HD328-10-1c	HD328-10-2	HD328-10-3	HD328-10-4
Weight percent:						
FeO	14.09	14.54	29.52	29.54	27.27	29.67
Fe_2O_3	0.46	0.07	0.50	0.41	1.17	0.77
SiO_2	35.80	36.18	36.40	36.53	36.56	36.59
CaO	2.13	1.72	3.18	3.14	3.25	3.55
Al_2O_3	20.04	20.32	20.35	20.38	19.33	20.28
TiO_2	0.18	0.18	0.23	0.23	0.22	0.27
MgO	0.17	0.22	2.73	2.76	2.71	2.68
MnO	6.20	5.85	5.98	5.65	5.44	5.69
Total	79.07	79.08	98.89	98.64	95.95	99.50
Cations based on 12 oxygens:						
Fe2+	1.110	1.141	2.016	2.019	1.902	2.015
Fe3+	0.033	0.005	0.031	0.025	0.073	0.047
Si4+	3.372	3.394	2.973	2.985	3.049	2.972
Ca2+	0.215	0.173	0.278	0.275	0.290	0.309
Al3+	2.225	2.247	1.959	1.963	1.900	1.941
Ti4+	0.013	0.013	0.014	0.014	0.014	0.016
Mg2+	0.024	0.031	0.332	0.336	0.337	0.325
Mn2+	0.495	0.465	0.414	0.391	0.384	0.391
Sum	7.486	7.468	8.018	8.007	7.950	8.017
Mole percent[1]:						
AD	1.77	0.57	1.94	1.68	4.23	2.80
GR	4.28	4.32	6.95	7.17	5.48	7.07
PY	0.69	0.91	10.94	11.15	11.60	10.69
SP	60.93	60.56	13.65	12.98	13.23	12.91
AL	32.34	33.64	66.52	67.03	65.46	66.52

Table D.1: Microprobe analysis of igneous garnet from minor intrusion near Skwel Peken Ridge , Hedley area, south-central British Columbia (continued)....

Analytical No.	HD328-10-5m	HD328-11-1c	HD328-11-2	HD328-11-3	HD328-11-4	HD328-11-5m
Weight percent:						
FeO	14.33	28.92	28.88	28.93	12.52	14.95
Fe_2O_3	0.23	0.50	0.91	1.02	0.09	0.00
SiO_2	35.91	36.57	36.52	36.74	35.92	35.76
CaO	2.00	3.13	3.27	3.25	2.48	1.66
Al_2O_3	20.15	20.34	20.08	19.91	20.26	20.25
TiO_2	0.17	0.20	0.26	0.30	0.06	0.15
MgO	0.14	2.75	2.78	2.73	0.12	0.21
MnO	5.98	6.25	6.26	5.75	6.85	5.36
Total	78.91	98.66	98.96	98.63	78.30	78.34
Cations based on 12 oxygens:						
Fe2+	1.129	1.976	1.971	1.976	0.990	1.184
Fe3+	0.016	0.031	0.056	0.063	0.006	0.000
Si4+	3.383	2.987	2.980	3.001	3.395	3.387
Ca2+	0.202	0.274	0.286	0.284	0.251	0.168
Al3+	2.238	1.958	1.931	1.917	2.257	2.261
Ti4+	0.012	0.012	0.016	0.018	0.004	0.011
Mg2+	0.020	0.335	0.338	0.332	0.017	0.030
Mn2+	0.477	0.432	0.433	0.398	0.548	0.430
Sum	7.478	8.006	8.011	7.990	7.469	7.472
Mole percent[1]:						
AD	1.04	1.92	3.24	3.71	0.38	0.28
GR	4.37	6.94	5.92	5.47	6.91	4.47
PY	0.59	11.13	11.19	11.17	0.51	0.36
SP	60.36	14.37	14.35	13.36	68.14	59.65
AL	33.14	65.64	65.31	66.30	29.06	34.74

Table D.2: Electron microscope analysis of garnet from the French mine, south-central British Columbia. Data are plotted in Figure 4.14. Three part analytical number indicates sample number (first number), grain number (second number) and beam position (third number: letter c = core, m = margin and absent = not defined).

Analytical No.	HD170-2A-1c	HD170-2A-2	HD170-2A-3	HD170-2A-4	HD170-2A-5	HD170-2A-6
Weight percent:						
SiO_2	37.89	37.69	37.84	37.70	38.12	38.09
TiO_2	0.20	0.17	0.32	0.44	0.53	0.48
Al_2O_3	17.51	17.85	17.65	18.16	18.45	18.38
Fe_2O_3	6.26	5.80	6.09	5.10	4.76	4.93
MgO	0.12	0.12	0.16	0.20	0.21	0.18
CaO	35.08	35.03	34.74	34.74	35.02	35.14
MnO	0.18	0.35	0.42	0.27	0.31	0.27
FeO	0.82	1.08	1.45	1.53	1.22	1.14
Total	98.06	98.09	98.67	98.14	98.62	98.61
Cations based on 12 oxygens:						
Si	2.9706	2.9539	2.9508	2.9453	2.9576	2.9575
Ti	0.0118	0.0100	0.0188	0.0259	0.0309	0.0280
Al	1.6184	1.6493	1.6226	1.6726	1.6876	1.6825
Fe[1]	0.4231	0.4128	0.4519	0.3998	0.3571	0.3621
Mg	0.0140	0.0140	0.0186	0.0233	0.0243	0.0208
Ca	2.9470	2.9417	2.9028	2.9081	2.9113	2.9235
Mn	0.0120	0.0232	0.0277	0.0179	0.0204	0.0178
Sum	7.9968	8.0050	7.9932	7.9927	7.9892	7.9922
Mole percent[2]:						
PY	0.85	1.20	1.49	1.32	1.46	1.26
GR	78.43	78.78	76.73	79.39	81.08	81.03
AD	20.72	20.02	21.78	19.29	17.46	17.71

1. All iron is reported as Fe_2O_3.
2. Abbreviations are: PY = pyralspite (pyrope + almandite + spessartine), GR = grossular, AD = andradite.

Table D.2: Electron microscope analysis of garnet from the French mine, south-central British Columbia (continued)...

Analytical No.	HD170-2A-7	HD170-2A-8	HD170-2A-9	HD170-2A-10m	HD170-2B-1c	HD170-2B-2
Weight percent:						
SiO_2	37.88	37.77	37.89	37.54	37.91	38.06
TiO_2	0.48	0.31	0.49	0.40	0.41	0.33
Al_2O_3	18.31	17.41	16.81	16.56	18.27	18.04
Fe_2O_3	4.92	6.27	7.09	7.34	5.12	5.63
MgO	0.21	0.15	0.08	0.09	0.17	0.16
CaO	34.94	33.73	33.69	33.63	35.05	35.14
MnO	0.37	0.59	0.41	0.37	0.34	0.26
FeO	1.20	2.14	2.49	2.38	1.28	1.25
Total	98.31	98.37	98.95	98.31	98.54	98.87
Cations based on 12 oxygens:						
Si	2.9520	2.9542	2.9537	2.9497	2.9497	2.9551
Ti	0.0281	0.0182	0.0287	0.0236	0.0241	0.0194
Al	1.6822	1.6054	1.5449	1.5340	1.6756	1.6510
Fe^1	0.3667	0.5090	0.5782	0.5904	0.3833	0.4102
Mg	0.0244	0.0175	0.0093	0.0105	0.0193	0.0187
Ca	2.9176	2.8269	2.8141	2.8315	2.9223	2.9237
Mn	0.0244	0.0391	0.0271	0.0246	0.0226	0.0169
Sum	7.9954	7.9703	7.9560	7.9644	7.9968	7.9949
Mole percent[2]:						
PY	1.59	1.78	1.14	1.10	1.36	1.15
GR	80.51	74.14	71.62	71.11	80.03	78.95
AD	17.90	24.07	27.24	27.79	18.61	19.90

Table D.2: Electron microscope analysis of garnet from the French mine, south-central British Columbia (continued)...

Analytical No.	HD170-2B-3	HD170-2B-4	HD170-2B-5	HD170-2B-6	HD170-2B-7	HD170-2B-8
Weight percent:						
SiO_2	37.80	38.13	37.77	37.65	37.73	37.75
TiO_2	0.23	0.20	0.21	0.43	0.62	0.63
Al_2O_3	18.04	17.47	17.32	16.85	17.48	17.67
Fe_2O_3	5.59	6.41	6.39	6.81	5.78	5.61
MgO	0.12	0.11	0.11	0.09	0.09	0.08
CaO	34.93	35.04	34.67	34.11	34.33	34.72
MnO	0.30	0.37	0.26	0.37	0.30	0.32
FeO	1.50	0.67	1.01	1.54	1.62	1.48
Total	98.52	98.40	97.74	97.84	97.95	98.27
Cations based on 12 oxygens:						
Si	2.9473	2.9798	2.9719	2.9656	2.9588	2.9516
Ti	0.0134	0.0119	0.0125	0.0253	0.0368	0.0373
Al	1.6583	1.6098	1.6068	1.5648	1.6157	1.6286
Fe^1	0.4260	0.4208	0.4450	0.5050	0.4471	0.4269
Mg	0.0144	0.0124	0.0129	0.0102	0.0103	0.0094
Ca	2.9177	2.9343	2.9229	2.8786	2.8842	2.9082
Mn	0.0200	0.0242	0.0175	0.0248	0.0201	0.0214
Sum	7.9971	7.9931	7.9896	7.9742	7.9730	7.9833
Mole percent[2]:						
PY	1.10	1.20	0.99	1.13	0.98	1.00
GR	78.46	78.08	77.32	74.48	77.34	78.23
AD	20.44	20.72	21.69	24.40	21.67	20.77

Table D.2: Electron microscope analysis of garnet from the French mine, south-central British Columbia (continued)...

Analytical No.	HD170-2B-9	HD170-2B-10m	HD170-2C-1c	HD170-2C-2	HD170-2C-3	HD170-2C-4
Weight percent:						
SiO_2	38.16	37.95	37.75	37.77	37.81	37.53
TiO_2	0.54	0.49	0.26	0.31	0.38	0.43
Al_2O_3	18.14	18.54	17.07	17.21	17.57	17.93
Fe_2O_3	5.15	4.55	6.85	6.62	6.01	5.60
MgO	0.11	0.13	0.08	0.07	0.10	0.10
CaO	34.64	34.52	34.90	34.78	34.64	35.03
MnO	0.37	0.37	0.30	0.34	0.34	0.43
FeO	1.46	1.79	1.11	1.26	1.41	1.71
Total	98.56	98.34	98.32	98.36	98.26	98.75
Cations based on 12 oxygens:						
Si	2.9653	2.9516	2.9610	2.9594	2.9582	2.9261
Ti	0.0314	0.0286	0.0155	0.0181	0.0224	0.0252
Al	1.6617	1.6998	1.5790	1.5895	1.6206	1.6479
Fe[1]	0.3955	0.3827	0.4774	0.4732	0.4461	0.4399
Mg	0.0128	0.0146	0.0092	0.0087	0.0118	0.0114
Ca	2.8839	2.8769	2.9333	2.9200	2.9045	2.9264
Mn	0.0241	0.0242	0.0197	0.0223	0.0225	0.0281
Sum	7.9747	7.9785	7.9952	7.9912	7.9861	8.0049
Mole percent[2]:						
PY	1.20	1.24	0.94	1.00	1.11	1.26
GR	79.58	80.38	75.85	76.05	77.31	77.67
AD	19.22	18.38	23.22	22.94	21.58	21.07

Table D.2: Electron microscope analysis of garnet from the French mine, south-central British Columbia (continued)...

Analytical No.	HD170-2C-5	HD170-2C-6	HD170-2C-7	HD170-2C-8	HD170-2C-9	HD170-2C-10m
Weight percent:						
SiO_2	37.82	37.92	37.96	37.81	37.86	37.04
TiO_2	0.42	0.39	0.27	0.31	0.41	0.30
Al_2O_3	18.05	17.48	17.44	17.99	18.38	18.11
Fe_2O_3	5.42	6.09	6.33	5.38	4.90	5.00
MgO	0.12	0.12	0.10	0.10	0.08	0.39
CaO	34.93	34.45	34.87	34.73	34.89	33.01
MnO	0.50	0.35	0.39	0.30	0.28	0.42
FeO	1.38	1.33	0.94	1.25	1.66	3.16
Total	98.63	98.11	98.30	97.88	98.47	97.42
Cations based on 12 oxygens:						
Si	2.9457	2.9690	2.9706	2.9625	2.9459	2.9152
Ti	0.0244	0.0228	0.0160	0.0184	0.0240	0.0178
Al	1.6573	1.6135	1.6092	1.6616	1.6864	1.6802
Fe[1]	0.4079	0.4457	0.4342	0.3996	0.3950	0.5041
Mg	0.0138	0.0141	0.0119	0.0112	0.0098	0.0458
Ca	2.9151	2.8903	2.9242	2.9154	2.9094	2.7839
Mn	0.0330	0.0233	0.0256	0.0197	0.0186	0.0279
Sum	7.9972	7.9787	7.9917	7.9885	7.9893	7.9749
Mole percent[2]:						
PY	1.51	1.21	1.22	1.00	0.91	2.25
GR	78.74	77.15	77.53	79.61	80.11	74.67
AD	19.75	21.64	21.25	19.39	18.98	23.08

Table D.2: Electron microscope analysis of garnet from the French mine, south-central British Columbia (continued)...

Analytical No.	HD267-2A-1c	HD267-2A-2	HD267-2A-3	HD267-2A-4	HD267-2A-5	HD267-2A-6
Weight percent:						
SiO_2	34.78	34.95	34.79	34.98	34.61	34.33
TiO_2	0.02	0.03	0.01	0.05	0.01	0.02
Al_2O_3	2.37	2.76	3.33	2.90	0.76	0.00
Fe_2O_3	27.47	26.90	25.97	26.67	29.35	30.18
MgO	0.01	0.02	0.05	0.02	0.01	0.01
CaO	32.67	32.66	32.57	32.81	32.35	32.80
MnO	0.30	0.30	0.44	0.32	0.30	0.10
FeO	0.43	0.42	0.34	0.15	0.00	0.00
Total	98.06	98.04	97.50	97.91	97.40	97.43
Cations based on 12 oxygens:						
Si	2.9683	2.9746	2.9699	2.9791	2.9957	2.9854
Ti	0.0010	0.0022	0.0003	0.0031	0.0006	0.0011
Al	0.2383	0.2774	0.3353	0.2909	0.0778	0.0000
Fe[1]	1.7950	1.7528	1.6926	1.7199	1.9115	1.9747
Mg	0.0018	0.0021	0.0067	0.0026	0.0011	0.0008
Ca	2.9878	2.9779	2.9788	2.9939	3.0002	3.0566
Mn	0.0220	0.0214	0.0322	0.0230	0.0221	0.0077
Sum	8.0141	8.0082	8.0158	8.0124	8.0091	8.0262
Mole percent[2]:						
PY	0.78	0.77	1.28	0.85	0.78	0.29
GR	10.94	12.89	15.25	13.62	3.13	0.00
AD	88.28	86.34	83.47	85.53	96.09	99.71

Table D.2: Electron microscope analysis of garnet from the French mine, south-central British Columbia (continued)...

Analytical No.	HD267-2A-7	HD267-2A-8m	HD267-2B-1c	HD267-2B-2	HD267-2B-3	HD267-2B-4
Weight percent:						
SiO_2	33.98	34.07	35.14	35.09	75.01	35.19
TiO_2	0.03	0.00	0.08	0.02	0.00	0.00
Al_2O_3	0.00	0.03	3.06	2.75	0.50	2.36
Fe_2O_3	29.75	30.01	26.43	26.79	5.45	27.80
MgO	0.00	0.01	0.07	0.07	0.00	0.00
CaO	32.76	32.77	32.74	32.94	0.47	32.74
MnO	0.10	0.05	0.34	0.36	0.07	0.35
FeO	0.00	0.00	0.06	0.00	0.00	0.62
Total	96.62	96.93	97.93	98.01	81.50	99.05
Cations based on 12 oxygens:						
Si	2.9811	2.9793	2.9865	2.9863	5.7105	2.9721
Ti	0.0017	0.0000	0.0050	0.0010	0.0000	0.0000
Al	0.0001	0.0032	0.3070	0.2758	0.0452	0.2346
Fe^1	1.9642	1.9746	1.6945	1.7157	0.3123	1.8105
Mg	0.0000	0.0012	0.0086	0.0086	0.0000	0.0000
Ca	3.0802	3.0701	2.9816	3.0035	0.0386	2.9628
Mn	0.0077	0.0035	0.0246	0.0262	0.0043	0.0251
Sum	8.0351	8.0318	8.0078	8.0170	6.1108	8.0053
Mole percent[2]:						
PY	0.26	0.16	1.11	1.16	0.80	0.82
GR	0.01	0.00	14.23	12.69	11.84	10.65
AD	99.73	99.84	84.66	86.15	87.37	88.53

Table D.2: Electron microscope analysis of garnet from the French mine, south-central British Columbia (continued)...

Analytical No.	HD267-2B-5	HD267-2B-6	HD267-2B-7	HD267-2B-8	HD267-2B-9	HD267-2B-10m
Weight percent:						
SiO_2	34.98	34.87	35.13	34.39	34.42	34.60
TiO_2	0.09	0.05	0.03	0.00	0.03	0.00
Al_2O_3	2.74	2.69	3.40	0.01	0.01	0.03
Fe_2O_3	27.20	27.12	26.07	30.91	30.62	30.09
MgO	0.05	0.00	0.04	0.00	0.01	0.00
CaO	33.47	33.16	33.25	33.17	33.07	33.07
MnO	0.33	0.17	0.35	0.13	0.15	0.00
FeO	0.14	0.34	0.00	0.00	0.00	0.00
Total	99.02	98.41	98.28	98.61	98.30	97.80
Cations based on 12 oxygens:						
Si	2.9547	2.9619	2.9746	2.9616	2.9707	2.9947
Ti	0.0057	0.0031	0.0018	0.0000	0.0022	0.0000
Al	0.2733	0.2689	0.3393	0.0014	0.0005	0.0032
Fe[1]	1.7393	1.7578	1.6607	2.0030	1.9888	1.9597
Mg	0.0069	0.0000	0.0050	0.0003	0.0017	0.0001
Ca	3.0295	3.0176	3.0168	3.0604	3.0580	3.0662
Mn	0.0236	0.0125	0.0254	0.0096	0.0106	0.0000
Sum	8.0332	8.0217	8.0236	8.0362	8.0325	8.0238
Mole percent[2]:						
PY	1.01	0.41	1.01	0.33	0.41	0.00
GR	12.57	12.86	15.95	0.06	0.03	0.16
AD	86.42	86.73	83.03	99.61	99.56	99.83

Table D.2: Electron microscope analysis of garnet from the French mine, south-central British Columbia (continued)...

Analytical No.	HD267-1A-1c	HD267-1A-2	HD267-1A-3	HD267-1A-4	HD267-1A-5	HD267-1A-6
Weight percent:						
SiO_2	34.57	34.58	34.76	35.11	35.14	35.08
TiO_2	0.00	0.00	0.00	0.00	0.00	0.00
Al_2O_3	0.05	0.05	0.00	0.24	0.12	0.11
Fe_2O_3	29.77	30.75	30.60	30.72	30.71	30.81
MgO	0.00	0.00	0.00	0.02	0.01	0.01
CaO	32.71	32.88	32.95	33.17	33.01	32.99
MnO	0.16	0.11	0.22	0.07	0.13	0.09
FeO	0.00	0.00	0.00	0.00	0.00	0.00
Total	97.27	98.36	98.53	99.32	99.12	99.11
Cations based on 12 oxygens:						
Si	3.0056	2.9794	2.9890	2.9892	2.9984	2.9944
Ti	0.0000	0.0000	0.0000	0.0000	0.0000	0.0000
Al	0.0055	0.0046	0.0001	0.0239	0.0119	0.0115
Fe[1]	1.9476	1.9940	1.9798	1.9681	1.9717	1.9790
Mg	0.0000	0.0000	0.0001	0.0021	0.0008	0.0013
Ca	3.0474	3.0353	3.0361	3.0266	3.0178	3.0173
Mn	0.0119	0.0078	0.0159	0.0049	0.0093	0.0067
Sum	8.0179	8.0212	8.0210	8.0148	8.0099	8.0103
Mole percent[2]:						
PY	0.41	0.26	0.54	0.23	0.34	0.27
GR	0.28	0.23	0.00	0.97	0.26	0.31
AD	99.31	99.51	99.46	98.80	99.40	99.42

Table D.2: Electron microscope analysis of garnet from the French mine, south-central British Columbia (continued)...

Analytical No.	HD267-1A-7	HD267-1A-8m
Weight percent:		
SiO_2	34.89	35.10
TiO_2	0.02	0.02
Al_2O_3	0.05	0.00
Fe_2O_3	30.70	30.41
MgO	0.01	0.00
CaO	32.89	33.00
MnO	0.10	0.09
FeO	0.00	0.00
Total	98.65	98.63
Cations based on 12 oxygens:		
Si	2.9931	3.0087
Ti	0.0010	0.0015
Al	0.0050	0.0000
Fe[1]	1.9819	1.9611
Mg	0.0011	0.0006
Ca	3.0234	3.0310
Mn	0.0070	0.0066
Sum	8.0125	8.0093
Mole percent[2]:		
PY	0.27	0.24
GR	0.22	0.00
AD	99.51	99.76

Table D.2: Electron microscope analysis of garnet from the French mine, south-central British Columbia (continued)...

Analytical No.	8969B-1-1	8969B-1-2	8969B-2-1	8969B-2-2	8969B-2-3	8969B-2-4
Weight percent:						
Na_2O	0.01	0.01	0.00	0.00	0.02	0.01
FeO	19.43	18.54	19.31	18.81	17.44	18.93
SiO_2	33.35	35.93	36.12	35.86	36.30	35.72
CaO	32.43	31.94	33.03	33.10	32.89	33.00
Al_2O_3	7.71	8.70	7.28	7.45	9.03	7.45
TiO_2	0.94	1.13	0.83	0.90	0.79	1.14
MgO	0.02	0.02	0.05	0.02	0.02	0.04
MnO	0.36	0.50	0.39	0.37	0.50	0.39
Cl	0.00	0.00	0.00	0.01	0.01	0.00
F	0.00	0.15	0.13	0.16	0.28	0.13
Cr_2O_3	0.02	0.05	0.00	0.04	0.00	0.07
Total	94.28	96.96	97.15	96.72	97.27	96.89
Cations based on 12 oxygens:						
Na	0.0012	0.0011	0.0000	0.0000	0.0027	0.0022
Fe^1	1.3808	1.2669	1.3237	1.2961	1.1881	1.3025
Si	2.8340	2.9351	2.9610	2.9538	2.9561	2.9391
Ca	2.9522	2.7961	2.9015	2.9217	2.8703	2.9094
Al	0.7726	0.8382	0.7035	0.7239	0.8669	0.7225
Ti	0.0602	0.0692	0.0510	0.0559	0.0485	0.0708
Mg	0.0024	0.0026	0.0064	0.0029	0.0023	0.0050
Mn	0.0261	0.0345	0.0271	0.0257	0.0346	0.0273
Sum	8.0296	7.9436	7.9743	7.9802	7.9693	7.9788
Mole percent[2]:						
PY	0.88	1.17	1.10	0.95	1.20	1.06
GR	35.00	38.64	33.60	34.89	40.99	34.62
AD	64.12	60.18	65.30	64.17	57.82	64.32

Table D.2: Electron microscope analysis of garnet from the French mine, south-central British Columbia (continued)...

Analytical No.	8969B-5-1	8969B-6-1	8969B-7-1	8969B-8-1	8969B-9-1	8969B-10-1
Weight percent:						
Na_2O	0.00	0.01	0.02	0.01	0.00	0.01
FeO	16.65	19.15	17.75	19.57	26.60	23.10
SiO_2	36.31	36.07	36.42	36.11	34.85	35.03
CaO	32.31	33.24	32.23	33.05	32.76	32.59
Al_2O_3	10.50	6.98	9.61	6.79	0.92	4.32
TiO_2	0.75	0.88	0.82	0.73	0.00	0.07
MgO	0.00	0.07	0.01	0.10	0.01	0.02
MnO	0.48	0.47	0.50	0.41	0.15	0.27
Cl	0.00	0.00	0.00	0.01	0.00	0.00
F	0.20	0.23	0.30	0.11	0.00	0.00
Cr_2O_3	0.12	0.01	0.03	0.00	0.00	0.06
Total	97.32	97.12	97.66	96.87	95.29	95.45
Cations based on 12 oxygens:						
Na	0.0000	0.0022	0.0025	0.0013	0.0000	0.0013
Fe^1	1.1275	1.3162	1.2012	1.3471	1.9075	1.6329
Si	2.9393	2.9655	2.9470	2.9721	2.9885	2.9617
Ca	2.8026	2.9282	2.7941	2.9151	3.0100	2.9521
Al	1.0024	0.6766	0.9163	0.6593	0.0929	0.4302
Ti	0.0454	0.0545	0.0496	0.0449	0.0000	0.0041
Mg	0.0002	0.0083	0.0008	0.0117	0.0017	0.0020
Mn	0.0328	0.0330	0.0342	0.0289	0.0107	0.0190
Sum	7.9503	7.9847	7.9459	7.9804	8.0113	8.0033
Mole percent[2]:						
PY	1.04	1.38	1.10	1.35	0.41	0.68
GR	46.03	32.57	42.17	31.51	4.23	20.17
AD	52.94	66.05	56.73	67.14	95.36	79.15

Table D.2: Electron microscope analysis of garnet from the French mine, south-central British Columbia (continued)...

Analytical No.	GD6.8-1-1c	GD6.8-2-1	GD6.8-3-1	GD6.8-4-1	GD6.8-5-1	GD6.8-6-1
Weight percent:						
Na_2O	0.02	0.00	0.01	0.00	0.02	0.00
FeO	15.88	16.24	14.08	14.48	15.19	15.00
SiO_2	35.84	36.46	36.45	35.80	36.25	36.04
CaO	33.08	32.99	33.13	32.41	32.82	33.12
Al_2O_3	9.67	9.36	10.60	12.20	10.81	10.34
TiO_2	0.51	0.49	1.09	0.50	0.46	1.11
MgO	0.12	0.08	0.17	0.06	0.05	0.05
MnO	0.65	0.67	0.88	0.51	0.60	0.69
C	0.00	0.00	0.00	0.00	0.00	0.01
F	0.18	0.00	0.16	0.15	0.16	0.19
Cr_2O_3	0.00	0.02	0.00	0.05	0.00	0.00
Total	95.95	96.31	96.56	96.17	96.35	96.55
Cations based on 12 oxygens:						
Na	0.0024	0.0000	0.0011	0.0000	0.0027	0.0002
Fe[1]	1.0937	1.1118	0.9585	0.9860	1.0363	1.0242
Si	2.9528	2.9839	2.9664	2.9157	2.9567	2.9421
Ca	2.9200	2.8935	2.8891	2.8284	2.8685	2.8973
Al	0.9389	0.9029	1.0170	1.1716	1.0393	0.9948
Ti	0.0318	0.0300	0.0664	0.0304	0.0282	0.0680
Mg	0.0150	0.0102	0.0206	0.0075	0.0060	0.0064
Mn	0.0455	0.0462	0.0609	0.0353	0.0411	0.0474
Sum	8.0002	7.9786	7.9800	7.9751	7.9787	7.9805
Mole percent[2]:						
Pyral	1.98	1.87	2.75	1.32	1.51	1.78
Gross	44.21	42.95	48.73	52.98	48.56	47.49
And	53.81	55.18	48.52	45.70	49.93	50.73

Table D.2: Electron microscope analysis of garnet from the French mine, south-central British Columbia (continued)....

Analytical No.	GD6.8-7-1	GD6.8-8-1	GD6.8-9-1	GD6.8-10-1	GD6.8-11-1	GD6.8-121
Weight percent:						
Na_2O	0.02	0.03	0.00	0.00	0.01	0.01
FeO	16.33	11.82	12.06	12.89	13.94	14.20
SiO_2	36.27	37.05	36.96	36.72	36.43	36.77
CaO	33.24	32.78	32.72	33.22	33.13	33.26
Al_2O_3	9.83	14.04	13.96	11.72	11.51	11.28
TiO_2	0.55	0.67	0.49	0.86	0.62	0.35
MgO	0.06	0.06	0.05	0.11	0.06	0.08
MnO	0.45	0.77	0.85	0.79	0.86	0.82
C	0.02	0.00	0.00	0.00	0.01	0.03
F	0.11	0.13	0.00	0.01	0.44	0.28
Cr_2O_3	0.00	0.00	0.21	0.01	0.02	0.08
Total	96.87	97.34	97.31	96.32	97.02	97.15
Cations based on 12 oxygens:						
Na	0.0032	0.0039	0.0000	0.0000	0.0009	0.0014
Fe^1	1.1122	0.7871	0.8051	0.8736	0.9455	0.9611
Si	2.9543	2.9515	2.9504	2.9761	2.9548	2.9754
Ca	2.9004	2.7975	2.7982	2.8854	2.8795	2.8840
Al	0.9436	1.3189	1.3140	1.1201	1.1002	1.0762
Ti	0.0337	0.0400	0.0295	0.0524	0.0378	0.0214
Mg	0.0073	0.0065	0.0057	0.0128	0.0075	0.0098
Mn	0.0309	0.0522	0.0575	0.0542	0.0589	0.0561
Sum	7.9856	7.9575	7.9605	7.9746	7.9851	7.9853
Mole percent[2]:						
PY	1.24	1.86	1.99	2.24	2.16	2.15
GR	44.66	60.77	60.02	53.94	51.62	50.67
AD	54.10	37.37	37.99	43.82	46.22	47.18

Table D.3: Electron microscope analysis of pyroxene from the French mine, south-central British Columbia. Data are plotted in Figure 4.15. Three part analytical number indicates sample number (first number), grain number (second number) and beam position (third number: letter c = core, m = margin and absent = not defined). Symbol "--" denotes not analyzed for.

Analytical No.	HD170-1A-1c	HD170-1A-2	HD170-1A-3	HD170-1A-4	HD170-1A-5	HD170-1A-6
Weight percent:						
Na_2O	0.06	0.07	0.05	0.04	0.04	0.05
Fe_2O_3	2.29	2.76	2.84	2.16	1.60	2.16
SiO_2	48.66	48.33	48.16	48.24	48.69	48.46
CaO	23.13	23.14	23.20	23.08	23.28	23.13
Al_2O_3	0.49	0.54	0.35	0.21	0.22	0.25
TiO_2	0.05	0.05	0.04	0.02	0.00	0.02
MgO	5.73	5.71	5.41	5.32	5.27	5.38
MnO	0.54	0.49	0.56	0.62	0.56	0.64
Cr_2O_3	0.00	0.02	0.00	0.00	0.03	0.03
FeO	17.56	17.17	17.48	17.83	18.25	17.85
Total	98.52	98.28	98.08	97.52	97.93	97.96
Cations based on 6 oxygens:						
Na	0.0047	0.0059	0.0037	0.0035	0.0034	0.0042
Fe[1]	0.6631	0.6669	0.6831	0.6765	0.6694	0.6742
Si	1.9659	1.9604	1.9633	1.9739	1.9802	1.9736
Ca	1.0011	1.0058	1.0133	1.0117	1.0143	1.0091
Al	0.0233	0.0260	0.0167	0.0103	0.0105	0.0118
Ti	0.0016	0.0014	0.0011	0.0005	0.0000	0.0006
Mg	0.3452	0.3451	0.3285	0.3243	0.3192	0.3265
Mn	0.0184	0.0167	0.0193	0.0216	0.0194	0.0221
Sum	4.0232	4.0281	4.0291	4.0222	4.0163	4.0221
Mole percent[2]:						
JO	1.80	1.62	1.87	2.11	1.93	2.16
DI	33.62	33.55	31.87	31.72	31.66	31.92
HD	64.58	64.83	66.26	66.17	66.41	65.92

1. All iron is reported as Fe_2O_3.
2. Abbreviations are: JO = johannsenite, DI = diopside, HD = hedenbergite.

Table D.3: Electron microscope analysis of pyroxene from the French mine, south-central British Columbia (continued)...

Anaytical No.	HD170-1A-7	HD170-1A-8	HD170-1A-9m	HD170-1B-1c	HD170-1B-2	HD170-1B-3
Weight percent:						
Na_2O	0.04	0.04	0.05	0.09	0.09	0.08
Fe_2O_3	2.10	2.94	1.80	2.87	1.49	2.99
SiO_2	48.47	48.02	48.46	48.19	48.16	47.31
CaO	23.31	23.29	22.96	23.17	23.06	22.78
Al_2O_3	0.27	0.27	0.32	0.69	0.61	0.54
TiO_2	0.01	0.03	0.03	0.08	0.08	0.03
MgO	5.19	5.40	5.28	5.64	5.31	5.38
MnO	0.53	0.55	0.63	0.46	0.37	0.52
Cr_2O_3	0.00	0.00	0.00	0.01	0.01	0.01
FeO	18.12	17.21	18.25	17.10	17.85	16.96
Total	98.05	97.76	97.78	98.29	97.03	96.59
Cations based on 6 oxygens:						
Na	0.0034	0.0035	0.0043	0.0070	0.0073	0.0061
Fe[1]	0.6813	0.6793	0.6773	0.6677	0.6568	0.6799
Si	1.9734	1.9643	1.9753	1.9553	1.9713	1.9579
Ca	1.0168	1.0209	1.0029	1.0072	1.0114	1.0099
Al	0.0129	0.0130	0.0152	0.0331	0.0296	0.0263
Ti	0.0004	0.0008	0.0008	0.0024	0.0023	0.0010
Mg	0.3150	0.3294	0.3208	0.3408	0.3237	0.3318
Mn	0.0182	0.0191	0.0218	0.0157	0.0128	0.0182
Sum	4.0214	4.0302	4.0184	4.0292	4.0153	4.0310
Mole percent[2]:						
JO	1.79	1.85	2.14	1.54	1.29	1.77
DI	31.05	32.05	31.46	33.27	32.59	32.22
HD	67.16	66.10	66.41	65.19	66.12	66.02

Table D.3: Electron microscope analysis of pyroxene from the French mine, south-central British Columbia (continued)...

Analytical No.	HD170-1B-4	HD170-1B-5	HD170-1B-6	HD170-1B-7	HD170-1B-8	HD170-1B-9
Weight percent:						
Na_2O	0.07	0.09	0.07	0.07	0.07	0.08
Fe_2O_3	2.43	2.45	3.01	3.07	1.93	3.02
SiO_2	48.25	48.41	48.11	47.94	48.23	48.26
CaO	23.21	23.25	23.29	23.22	23.02	23.41
Al_2O_3	0.57	0.58	0.53	0.53	0.43	0.32
TiO_2	0.05	0.06	0.04	0.05	0.05	0.03
MgO	5.46	5.53	5.55	5.54	5.44	5.20
MnO	0.42	0.45	0.44	0.45	0.47	0.57
Cr_2O_3	0.01	0.00	0.00	0.00	0.00	0.07
FeO	17.53	17.42	17.03	16.96	17.70	17.51
Total	97.99	98.24	98.08	97.82	97.34	98.47
Cations based on 6 oxygens:						
Na	0.0054	0.0071	0.0058	0.0056	0.0058	0.0065
Fe[1]	0.6707	0.6655	0.6719	0.6731	0.6644	0.6886
Si	1.9628	1.9629	1.9583	1.9571	1.9714	1.9640
Ca	1.0115	1.0102	1.0160	1.0160	1.0085	1.0207
Al	0.0272	0.0279	0.0256	0.0255	0.0206	0.0151
Ti	0.0015	0.0017	0.0011	0.0016	0.0015	0.0009
Mg	0.3310	0.3340	0.3370	0.3371	0.3312	0.3154
Mn	0.0146	0.0156	0.0151	0.0155	0.0164	0.0196
Sum	4.0248	4.0250	4.0307	4.0314	4.0197	4.0309
Mole percent[2]:						
JO	1.44	1.54	1.48	1.51	1.62	1.92
DI	32.57	32.90	32.91	32.86	32.73	30.81
HD	65.99	65.56	65.62	65.62	65.65	67.27

Table D.3: Electron microscope analysis of pyroxene from the French mine, south-central British Columbia (continued)...

Analytical No.	HD170-1B-10m	HD170-1C-1	HD170-1C-2	HD170-3A-1c	HD170-3A-2	HD170-3A-3
Weight percent:						
Na_2O	0.06	0.06	0.07	0.07	0.04	0.02
Fe_2O_3	2.53	3.76	2.47	0.00	0.00	0.00
SiO_2	48.55	48.34	48.35	42.94	41.37	35.93
CaO	23.31	23.60	23.29	22.90	22.88	22.82
Al_2O_3	0.31	0.32	0.27	12.59	16.64	26.14
TiO_2	0.02	0.06	0.00	0.06	0.00	0.01
MgO	5.28	5.25	5.55	4.10	3.54	1.79
MnO	0.61	0.53	0.61	0.32	0.17	0.19
Cr_2O_3	0.01	0.03	0.02	0.01	0.01	0.01
FeO	17.89	17.46	17.16	12.64	10.19	3.89
Total	98.57	99.41	97.79	95.62	97.84	90.81
Cations based on 6 oxygens:						
Na	0.0046	0.0044	0.0055	0.0053	0.0034	0.0018
Fe[1]	0.6838	0.7048	0.6606	0.4235	0.3395	0.1314
Si	1.9685	1.9547	1.9710	1.7200	1.6475	1.4501
Ca	1.0130	1.0225	1.0172	0.9829	0.9762	0.9866
Al	0.0148	0.0153	0.0130	0.5946	0.7810	1.2439
Ti	0.0006	0.0017	0.0000	0.0019	0.0000	0.0003
Mg	0.3193	0.3166	0.3369	0.2446	0.2102	0.1079
Mn	0.0211	0.0183	0.0212	0.0107	0.0059	0.0066
Sum	4.0257	4.0382	4.0253	3.9835	3.9637	3.9286
Mole percent[2]:						
JO	2.06	1.76	2.08	1.58	1.06	2.69
DI	31.17	30.45	33.07	36.03	37.83	43.87
HD	66.77	67.79	64.85	62.39	61.12	53.44

Table D.3: Electron microscope analysis of pyroxene from the French mine, south-central British Columbia (Continued)...

Analytical No.	HD170-3A-4	HD170-3A-5	HD170-3A-6	HD170-3A-7	HD170-3A-8	HD170-3A-9
Weight percent:						
Na_2O	0.05	0.07	0.09	0.07	0.08	0.09
Fe_2O_3	1.09	2.43	2.16	2.41	1.73	2.01
SiO_2	46.99	48.43	48.35	48.37	48.50	48.48
CaO	23.17	23.13	23.38	23.21	23.19	23.32
Al_2O_3	3.91	0.55	0.53	0.47	0.65	0.56
TiO_2	0.05	0.03	0.06	0.03	0.05	0.04
MgO	5.24	5.53	5.43	5.41	5.27	5.33
MnO	0.42	0.44	0.39	0.42	0.35	0.46
Cr_2O_3	0.00	0.03	0.02	0.00	0.01	0.00
FeO	16.54	17.67	17.40	17.74	18.22	17.73
Total	97.45	98.31	97.83	98.13	98.05	98.02
Cations based on 6 oxygens:						
Na	0.0037	0.0057	0.0075	0.0056	0.0063	0.0073
Fe[1]	0.5913	0.6734	0.6581	0.6767	0.6711	0.6634
Si	1.8965	1.9641	1.9671	1.9660	1.9685	1.9685
Ca	1.0022	1.0052	1.0192	1.0110	1.0085	1.0149
Al	0.1859	0.0262	0.0256	0.0225	0.0310	0.0270
Ti	0.0014	0.0009	0.0017	0.0009	0.0016	0.0012
Mg	0.3155	0.3341	0.3293	0.3275	0.3186	0.3226
Mn	0.0145	0.0153	0.0136	0.0143	0.0120	0.0157
Sum	4.0110	4.0247	4.0221	4.0246	4.0176	4.0205
Mole percent[2]:						
JO	1.57	1.49	1.36	1.41	1.20	1.56
DI	34.24	32.66	32.90	32.15	31.81	32.21
HD	64.19	65.84	65.75	66.44	67.00	66.23

Table D.3: Electron microscope analysis of pyroxene from the French mine, south-central British Columbia continued...

Analytical No.	HD170-3A-10m	HD170-3B-1c	HD170-3B-2	HD170-3B-3	HD170-3B-4	HD170-3B-5
Weight percent:						
Na_2O	0.09	0.09	0.10	0.09	0.07	0.07
Fe_2O_3	0.00	3.19	3.05	3.30	2.79	3.16
SiO_2	43.75	47.76	47.60	47.61	47.89	47.46
CaO	25.49	23.09	23.13	23.21	23.25	23.30
Al_2O_3	18.49	0.57	0.65	0.64	0.69	0.61
TiO_2	0.01	0.05	0.07	0.05	0.06	0.05
MgO	0.89	5.79	5.84	5.84	5.92	5.88
MnO	0.12	0.39	0.37	0.46	0.30	0.45
Cr_2O_3	0.01	0.04	0.00	0.00	0.00	0.01
FeO	4.24	16.45	16.11	15.95	16.36	15.69
Total	93.10	97.43	96.91	97.15	97.32	96.67
Cations based on 6 oxygens:						
Na	0.0069	0.0068	0.0076	0.0074	0.0057	0.0057
Fe^1	0.1394	0.6614	0.6476	0.6490	0.6445	0.6379
Si	1.7205	1.9553	1.9546	1.9527	1.9557	1.9539
Ca	1.0739	1.0129	1.0176	1.0199	1.0173	1.0277
Al	0.8572	0.0275	0.0314	0.0311	0.0331	0.0297
Ti	0.0002	0.0017	0.0020	0.0015	0.0020	0.0015
Mg	0.0522	0.3534	0.3576	0.3567	0.3601	0.3607
Mn	0.0041	0.0136	0.0130	0.0158	0.0102	0.0156
Sum	3.8543	4.0327	4.0314	4.0340	4.0286	4.0326
Mole percent[2]:						
JO	2.11	1.33	1.28	1.55	1.01	1.54
DI	26.66	34.36	35.12	34.92	35.48	35.57
HD	71.23	64.31	63.60	63.53	63.51	62.90

Table D.3: Electron microscope analysis of pyroxene from the French mine, south-central British Columbia (continued)...

Analytical No.	HD170-3B-6	HD170-3B-7	HD170-3B-8	HD170-3B-9	HD170-3B-10m	HD170-3C-1c
Weight percent:						
Na_2O	0.08	0.05	0.12	0.06	0.04	0.06
Fe_2O_3	3.22	2.83	0.00	1.24	0.00	2.50
SiO_2	47.72	47.80	43.48	46.66	43.20	48.43
CaO	23.29	23.32	24.80	22.52	25.50	23.49
Al_2O_3	0.67	0.72	14.76	2.37	19.29	0.52
TiO_2	0.08	0.06	0.05	0.03	0.00	0.05
MgO	5.68	5.54	1.99	5.11	1.01	5.58
MnO	0.45	0.46	0.15	0.55	0.12	0.38
Cr_2O_3	0.01	0.00	0.01	0.02	0.00	0.00
FeO	16.35	16.75	7.41	17.01	3.83	17.25
Total	97.55	97.54	92.77	95.58	92.98	98.26
Cations based on 6 oxygens:						
Na	0.0062	0.0042	0.0096	0.0051	0.0032	0.0047
Fe[1]	0.6583	0.6596	0.2492	0.6274	0.1260	0.6611
K	0.0000	0.0000	0.0000	0.0000	0.0000	0.0000
Si	1.9514	1.9538	1.7497	1.9310	1.6977	1.9631
Ca	1.0207	1.0212	1.0693	0.9987	1.0738	1.0202
Al	0.0325	0.0347	0.7000	0.1155	0.8936	0.0247
Ti	0.0024	0.0020	0.0015	0.0009	0.0000	0.0015
Mg	0.3459	0.3376	0.1190	0.3149	0.0589	0.3371
Mn	0.0156	0.0158	0.0052	0.0193	0.0039	0.0131
Sum	4.0330	4.0290	3.9036	4.0129	3.8571	4.0254
Mole percent[2]:						
JO	1.53	1.56	1.39	2.01	2.09	1.29
DI	33.92	33.33	31.88	32.75	31.19	33.33
HD	64.55	65.11	66.73	65.24	66.72	65.37

Table D.3: Electron microscope analysis of pyroxene from the French mine, south-central British Columbia continued...

Analytical No.	HD170-3C-2	HD170-3C-3	HD170-3C-4	HD170-3C-5	HD170-3C-6	HD170-3C-7
Weight percent:						
Na_2O	0.07	0.07	0.08	0.07	0.08	0.08
Fe_2O_3	2.15	1.65	2.46	1.95	2.47	2.31
SiO_2	48.26	49.04	48.36	48.31	48.00	48.13
CaO	23.19	23.25	23.42	23.16	23.15	23.29
Al_2O_3	0.57	0.40	0.61	0.66	0.54	0.60
TiO_2	0.07	0.04	0.05	0.03	0.05	0.06
MgO	5.66	6.13	5.59	5.70	5.68	5.72
MnO	0.41	0.48	0.39	0.40	0.37	0.41
Cr_2O_3	0.00	0.00	0.00	0.02	0.00	0.00
FeO	17.21	17.13	17.15	17.22	16.94	16.81
Total	97.60	98.20	98.10	97.54	97.28	97.41
Cations based on 6 oxygens:						
Na	0.0058	0.0057	0.0060	0.0058	0.0060	0.0060
Fe[1]	0.6522	0.6273	0.6569	0.6457	0.6555	0.6445
K	0.0000	0.0000	0.0000	0.0000	0.0000	0.0000
Si	1.9650	1.9756	1.9618	1.9660	1.9630	1.9633
Ca	1.0116	1.0036	1.0183	1.0098	1.0142	1.0177
Al	0.0273	0.0189	0.0291	0.0318	0.0260	0.0287
Ti	0.0022	0.0012	0.0016	0.0011	0.0016	0.0017
Mg	0.3436	0.3680	0.3379	0.3458	0.3463	0.3476
Mn	0.0143	0.0165	0.0135	0.0139	0.0128	0.0142
Sum	4.0220	4.0167	4.0251	4.0199	4.0254	4.0237
Mole percent[2]:						
JO	1.41	1.63	1.33	1.38	1.26	1.42
DI	34.02	36.38	33.51	34.40	34.13	34.54
HD	64.57	62.00	65.16	64.22	64.61	64.04

Table D.3: Electron microscope analysis of pyroxene from the French mine, south-central British Columbia continued...

Analytical No.	HD170-3C-8	HD170-3C-9	HD170-3C-10m	HD170-3D-1	HD170-3D-2	HD170-3D-3
Weight percent:						
Na_2O	0.09	0.07	0.06	0.01	0.00	0.00
Fe_2O_3	1.88	0.00	1.54	7.78	7.70	8.45
SiO_2	47.96	45.13	46.54	37.25	37.17	36.85
CaO	23.53	24.42	22.51	33.34	33.32	33.14
Al_2O_3	1.31	10.04	1.89	17.01	17.04	16.91
TiO_2	0.06	0.02	0.05	0.33	0.39	0.40
MgO	5.65	3.67	6.00	0.07	0.07	0.06
MnO	0.40	0.24	0.49	0.44	0.44	0.45
Cr_2O_3	0.00	0.04	0.00	0.05	0.00	0.01
FeO	16.40	9.82	15.40	1.53	1.54	1.41
Total	97.27	93.46	94.46	97.81	97.67	97.67
Cations based on 6 oxygens:						
Na	0.0068	0.0055	0.0047	0.0004	0.0000	0.0000
Fe^1	0.6154	0.3326	0.5845	0.2884	0.2864	0.3060
K	0.0000	0.0000	0.0000	0.0000	0.0000	0.0000
Si	1.9507	1.8273	1.9383	1.5058	1.5038	1.4967
Ca	1.0256	1.0594	1.0044	1.4442	1.4444	1.4425
Al	0.0630	0.4794	0.0929	0.8109	0.8124	0.8096
Ti	0.0020	0.0007	0.0015	0.0100	0.0119	0.0123
Mg	0.3422	0.2216	0.3726	0.0041	0.0043	0.0034
Mn	0.0136	0.0083	0.0172	0.0152	0.0150	0.0154
Sum	4.0192	3.9350	4.0161	4.0790	4.0781	4.0861
Mole percent[2]:						
JO	1.40	1.48	1.76	4.93	4.91	4.76
DI	35.23	39.39	38.24	1.34	1.41	1.05
HD	63.37	59.12	59.99	93.73	93.69	94.19

Table D.3: Electron microscope analysis of pyroxene from the French mine, south-central British Columbia (continued)...

Analytical No.	HD170-3D-4	HD170-3D-5	HD170-3D-6	HD170-3D-7	HD170-3D-8	HD170-3D-9
Weight percent:						
Na_2O	0.00	0.01	0.02	0.07	0.06	0.08
Fe_2O_3	7.72	7.21	4.55	0.00	0.00	0.00
SiO_2	37.26	37.37	38.03	41.57	42.15	42.21
CaO	33.19	33.03	32.21	27.03	25.71	26.44
Al_2O_3	17.11	17.24	17.93	22.49	23.74	23.57
TiO_2	0.37	0.29	0.32	0.06	0.00	0.02
MgO	0.07	0.08	0.05	0.02	0.01	0.01
MnO	0.40	0.46	0.45	0.10	0.04	0.04
Cr_2O_3	0.02	0.00	0.05	0.00	0.03	0.00
FeO	1.83	1.98	3.86	1.75	0.46	1.12
Total	97.97	97.66	97.45	93.09	97.21	93.48
Cations based on 6 oxygens:						
Na	0.0000	0.0006	0.0015	0.0055	0.0045	0.0061
Fe[1]	0.2963	0.2858	0.2662	0.0571	0.0151	0.0361
K	0.0000	0.0000	0.0000	0.0000	0.0000	0.0000
Si	1.5036	1.5084	1.5224	1.6239	1.6387	1.6284
Ca	1.4352	1.4287	1.3817	1.1312	1.0710	1.0930
Al	0.8140	0.8203	0.8461	1.0356	1.0882	1.0719
Ti	0.0113	0.0087	0.0096	0.0018	0.0000	0.0007
Mg	0.0040	0.0048	0.0031	0.0010	0.0008	0.0006
Mn	0.0138	0.0156	0.0151	0.0032	0.0012	0.0012
Sum	4.0782	4.0731	4.0457	3.8593	3.8194	3.8380
Mole percent[2]						
JO	4.39	5.11	5.33	5.17	7.27	3.26
DI	1.28	1.58	1.08	1.71	4.60	1.49
HD	94.33	93.32	93.60	93.13	88.12	95.25

Table D.3: Electron microscope analysis of pyroxene from the French mine, south-central British Columbia (continued)...

Analytical No.	HD170-3D-10m	HD170-3E-1c	HD170-3E-2	HD170-3E-3	HD170-3E-4	HD170-3E-5m
Weight percent:						
Na_2O	0.08	0.03	0.05	0.06	0.02	0.02
Fe_2O_3	0.00	3.42	2.17	1.90	4.48	5.03
SiO_2	41.95	46.66	47.75	46.92	44.03	41.83
CaO	26.30	25.19	24.25	24.66	27.17	29.31
Al_2O_3	23.05	3.33	2.28	3.61	6.97	10.81
TiO_2	0.01	0.07	0.02	0.04	0.12	0.19
MgO	0.00	5.03	5.62	5.49	4.05	2.79
MnO	0.06	0.50	0.48	0.39	0.41	0.45
Cr_2O_3	0.00	0.02	0.02	0.00	0.00	0.00
FeO	0.96	14.00	15.32	14.09	10.21	7.15
Total	92.41	98.24	97.96	97.16	97.44	97.59
Cations based on 6 oxygens:						
Na	0.0060	0.0020	0.0037	0.0047	0.0016	0.0012
Fe[1]	0.0312	0.5770	0.5825	0.5340	0.4828	0.3937
K	0.0000	0.0000	0.0000	0.0000	0.0000	0.0000
Si	1.6367	1.8848	1.9252	1.8960	1.7849	1.6868
Ca	1.0993	1.0903	1.0475	1.0676	1.1802	1.2664
Al	1.0603	0.1588	0.1083	0.1719	0.3333	0.5141
Ti	0.0004	0.0021	0.0006	0.0011	0.0037	0.0059
Mg	0.0000	0.3028	0.3378	0.3306	0.2449	0.1677
Mn	0.0018	0.0169	0.0163	0.0134	0.0141	0.0152
Sum	3.8357	4.0347	4.0220	4.0192	4.0455	4.0509
Mole percent[2]:						
JO	5.52	1.89	1.74	1.52	1.90	2.64
DI	0.00	33.77	36.07	37.65	33.01	29.09
HD	94.48	64.34	62.19	60.82	65.09	68.28

Table D.3: Electron microscope analysis of pyroxene from the French mine, south-central British Columbia. Symbol "--" denotes not analysed for (continued)....

Analytical No.	GD10.4-1-1	GD10.4-2-1	GD10.4-3-1	GD10.4-4-1	GD10.4-5-1	8969A-1
Weight percent:						
Na_2O	0.08	0.07	0.06	0.08	0.07	0.03
FeO	19.25	19.68	17.00	16.94	16.94	22.51
SiO_2	49.79	49.16	49.96	50.16	49.81	48.18
CaO	23.25	22.91	23.45	23.26	23.36	22.90
Al_2O_3	0.32	0.50	0.85	0.40	0.29	0.23
TiO_2	0.02	0.05	0.08	0.11	0.02	0.04
MgO	5.92	5.96	7.45	7.84	7.71	3.34
MnO	0.52	0.47	0.53	0.35	0.45	0.77
Cr_2O_3	0.00	0.01	0.00	0.00	0.08	0.00
Cl	--	--	--	--	--	0.02
F	--	--	--	--	--	0.00
Total	99.15	98.83	99.38	99.14	98.72	98.00
Cations based on 6 oxygens:						
Na	0.0058	0.0056	0.0047	0.0060	0.0057	0.0020
Fe^1	0.6418	0.6598	0.5593	0.5581	0.5616	0.7744
Si	1.9846	1.9709	1.9657	1.9754	1.9742	1.9821
Ca	0.9931	0.9842	0.9886	0.9816	0.9918	1.0093
Al	0.0150	0.0236	0.0394	0.0184	0.0133	0.0112
Ti	0.0006	0.0016	0.0023	0.0032	0.0006	0.0012
Mg	0.3518	0.3564	0.4370	0.4605	0.4555	0.2047
Mn	0.0177	0.0160	0.0176	0.0118	0.0152	0.0267
Cr	0.0000	0.0003	0.0000	0.0001	0.0024	0.0000
Cl	--	--	--	--	--	0.0009
F	--	--	--	--	--	0.0000
Sum	4.0103	4.0184	4.0146	4.0151	4.0202	4.0125
Mole percent[2]:						
JO	1.75	1.55	1.73	1.14	1.47	2.65
DI	34.79	34.52	43.10	44.69	44.13	20.35
HD	63.47	63.92	55.17	54.16	54.40	77.00

Table D.4: Electron microprobe analysis of sulphide minerals from the French mine, south-central British Columbia. Three part analytical number indicates sample number (first number), grain number (second number) and beam position (third number).

Analytical No.	DUMP-1-1	DUMP-2-1	DUMP-3-1	DUMP-4-1
Mineral	Bornite	Chalcopyrite	Bornite	Bornite
Weight percent:				
Cu	55.10	34.54	60.45	59.47
S	31.00	34.47	27.30	27.88
Fe	13.45	30.54	12.12	12.51
Pb	0.00	0.00	0.00	0.00
Zn	0.00	0.00	0.00	0.00
Au	0.00	0.05	0.04	0.07
As	0.07	0.04	0.00	0.02
Hg	0.00	0.02	0.03	0.00
Mn	0.00	0.01	0.00	0.01
Co	0.00	0.00	0.00	0.01
Ni	0.01	0.02	0.00	0.00
Sb	0.00	0.00	0.01	0.00
Total	99.63	99.69	99.94	99.97

Table D.5: Electron microscope analysis of gold from the French mine, south-central British Columbia. Three part analytical number indicates sample number (first number), grain number (second number) and beam position (third number).

Analytical No.	8969A-1-1	8969A-1-2	8969A-2-1	8969A-2-2	8969A-2-3	8969A-2-4	8969A-2-5	8969A-2-6
Weight percent:								
Au	79.01	79.21	88.54	89.35	92.82	91.50	90.93	89.015
Ag	20.15	19.92	10.35	10.32	7.14	7.28	8.52	10.410
Cu	0.00	0.00	0.07	0.04	0.07	0.02	0.03	0.075
Hg	0.00	0.00	0.08	0.00	0.18	0.18	0.18	0.051
Total	99.16	99.13	99.04	99.71	100.20	98.99	99.67	99.552
Au:Ag	3.9	4.0	8.6	8.7	13.0	12.6	10.78	8.6

Table D.6: Electron microscope analyses of telluride and bismuth minerals from the French mine, south-central British Columbia. Three part analytical number indicates sample number (first number), grain number (second number) and beam position (third number).

Analytical No. Mineral	8969A-1-1 Joeseite$_b$	8969A-1-23 Joeseite$_b$	8969A-1-3 Joeseite$_b$	8969A-1-4 Joeseite$_b$	8969A-1-5 Bismuthinite	8969A-2-1 Bismuthinite	8969A-3-1 Joeseite$_b$	8969A-4-1 Bismuthinite	8969A-5-1 Joeseite$_b$
Weight percent:									
Bi	73.93	73.54	73.85	73.39	81.11	80.85	74.01	79.88	74.06
Te	22.31	22.49	22.44	22.52	0.01	0.00	23.02	0.00	22.36
S	3.17	3.19	3.17	3.07	19.01	19.16	3.02	19.03	3.11
Total	99.40	99.21	99.46	98.99	100.13	100.02	100.05	98.90	99.53

Table D.6: Electron microscope analyses of telluride and bismuth minerals from the French mine, south-central British Columbia (continued)....

Analytical No. Mineral	8969B-1-1	8969B-2-1	8969B-3-1	8969B-4-1 Bismuthinite	8969B-5-1 Bismuthinite
Weight percent					
Bi	77.74	74.03	73.95	78.62	80.01
Te	5.67	22.47	22.45	0.60	0.01
S	14.86	3.03	3.08	18.54	18.74
Total	98.27	99.52	99.47	97.22	98.76